Design of Non-Linear Optical Materials Based on Inorganic Compounds

Curt Lamberth

Thesis submitted in part fulfilment of the

requirements for the degree of

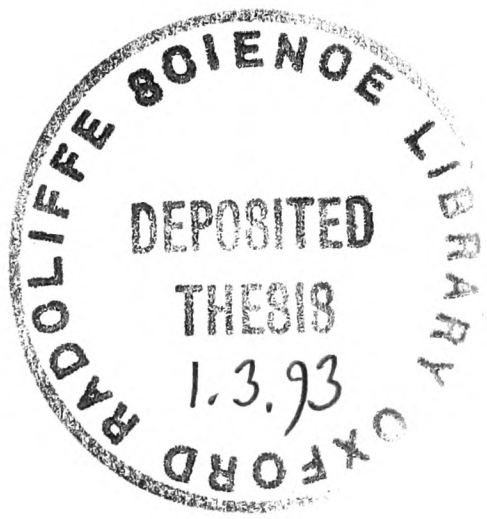
Doctor of Philosophy

at the

University of Oxford

New College

Oxford



September 1992

The work described in this Thesis was carried out in the Inorganic Chemistry Laboratory, Oxford, from September 1988 to September 1991, under the supervision of Dr D.M.P. Mingos.

All the work is my own, unless stated to the contrary, and it has not been previously submitted for a degree at this or any other University.

ABSTRACT

Submitted for the Degree of Doctor of Philosophy, Trinity Term 1992
Curt Lamberth, New College, Oxford.

Design of Non-linear Optical Materials Based on Inorganic Compounds

This Thesis is concerned with the prediction, synthesis, characterization and testing of inorganic materials for Second Harmonic Generation (SHG).

Chapter One describes the fundamentals of non-linear optics, and poses the problems, and some of their solutions which confront the synthetic chemist and the theoretical prediction of the second order hyperpolarizability constant β using CNDOVSB calculations.

Chapter Two describes the design, implementation and calibration of an apparatus for measurements of the second harmonic generating efficiency of solids based on the Kurtz powder technique, and a solvatochromic method for the determination of β.

Novel compounds with potential chirality due to atropisomerism, asymmetric octahedral structures, and asymmetric tetrahedral symmetry of metal centers are discussed in Chapters Three to Five.

Chapter Three surveys the use of pentane-2,4-dionato- ligands and their coordination compounds as possible NLO active materials. The single crystal X-ray structures of bis(triphenylphosphine)(4-nitrobenzoylacetonato)palladium(II) tetrafluoroborate and tris(triphenylphosphine)[3-(2,4-dinitrophenyl)-pentane-2,4-dionato]palladium(II) tetrafluoroborate were determined.

Chapter Four describes the syntheses, characterization and SHG properties of *trans*-β-ionylidenecyanoacetic acid (2-cyano-3-methyl-5-(2,6,6-trimethyl-1-cyclohexen-1-yl)-2,4-pentadienoic acid) and some of its metal and non-metal salts

Chapter Five describes the synthesis, characterization and second harmonic generation properties of some platinum(II) and palladium(II) complexes of β-ionylidenecyanoacetic acid.

Chapter Six describes the use of conventional asymmetric carbon centers to introduce chirality into centrosymmetric compounds. The chiral compound (L)-N-[2-cyano-3-methyl-5-(2,6,6-trimethyl-1-cyclohexene-1-yl)-2,4-pentadiene-1-one]-L-proline and some of its salts were synthesized from β-ionylidenecyanoacetic acid and tested for SHG.

ACKNOWLEDGEMENTS

Now where do I start?

Perhaps it is better to start at the beginning and work forward. Firstly, I am indebted to my supervisor, Dr Mike Mingos, for spawning the project, overseeing its execution and wrapping it up at the end and to my industrial supervisor, Dr John Morley (and The Molecular Modelling Group), for their enthusiasm and support during my brief insight into the workings of ICI.

I would also like to thank my fellow workers; but for this I have to go back into the annals of history; to JJ, Osayi (thanks for the bench), Zhenyang, Tonie, Paul, Jonathan (De Bells), Mike, Don, Roy (fellow Radio 1 listener), Jane, Jenny, Dave, Andy, Gavin (mad as a hatter), Yang and Ian (for the training on the laser) to Dr Robert Denning (for providing the laser), to the support staff of the ICL (who did a great job sorting out both the practical and personal aspects of my life), to Nick, Laura and Steve (for being such good housemates), to the People and Porters of New College (who guided me well, especially when leaving the bar), and, finally, to the members of the "RDX" (may we remain together).

Now where do I finish?

CONTENTS

Design of Non-linear Optical Materials Based on Inorganic Compounds

ABBREVIATIONS - And Units

CHAPTER ONE - Non-linear Optics 1

1.1 The Fundamentals of Optics - From the Molecular level 2

1.1.1 Units

1.2 Factors Influencing of the Second-Order Hyperpolarizability Constant β 5

1.3 Summary of Factors Affecting the Magnitude of β 10

1.4 CNDOVSB Calculations of β and the Theoretical Optimization of β 11

1.4.1 Introduction to the CNDOVSB Model

1.4.2 Calibration

1.5 From Molecular Hyperpolarizability to Material Susceptibility 14

1.5.1 Introduction

1.6 Imposing Non-centrosymmetry on Materials 18

1.6.1 Introduction - Common Strategies

1.7 Further Requirements for Second Harmonic Generating Materials 27

1.7.1 Thermal Stability - Damage Threshold

1.7.2 Light Stability

1.7.3 Phase Matching

1.7.4 Frequency Cut-off

1.8 Aims of this Thesis 28

CHAPTER TWO - The Measurement of Second Order Non-linear Optical Properties

2.1 Introduction 30

2.2 Overview of Experimental SHG Measurement Technique 31

2.2.1 Apparatus Construction

2.2.2 Signal processing

2.2.3 Calibration of the Optical Density Filters

2.2.4 Response of the Photomultiplier Tube

2.2.5 Calibration

2.3 Further Errors Associated with SHG Measurements 40

2.3.1 Pseudo Second Harmonic Signals

2.3.2 Residual Second Harmonic Signals in Centrosymmetric Media

2.4 The Calculation of the Hyperpolarizabilities of Some Organic Compounds from Solvatochromism Measurements 44

2.4.1 Introduction

2.4.2 Errors Within the Solvatochromic Method for the Determination of β

2.4.3 Discussion

2.5 Conclusion 50

CHAPTER THREE - Synthesis, Structure and Non-linear Optical Properties of Co-ordination Compounds Based on Pentadionato- Compounds.

3.1 Introduction 52

3.2 CNDOVSB Calculations on Pentane-2,4-dionato- Ligands 56

3.3 Results and Discussion 60

3.3.1 Palladium compounds (III.13) and (III.14)

3.3.2 Discussion of the crystal structures of (III.13) and (III.14)

3.3.3 Rhodium Compounds (III.15) to (III.20)

3.3.4 Cobalt(III) and Rhodium(III) Tris-pentane-2,4-dionates

3.4 Second-Harmonic Generation (SHG) Properties of Pentane-2,4-dionato- Compounds 75

3.5 Crystal Structure Determination of (III.13) and (III.14) 80

3.5.1 Data Collection

3.5.2 Data Reduction

3.5.3 Structure Solution and Refinement

3.6 Summary and Conclusions of Chapter Three 82

CHAPTER FOUR - Salts of β-Ionylidenecyanoacetic Acid

4.1 Introduction 84

4.2 Choice of Ligand 84

4.2.1 Introduction

4.2.2 CNDOVSB calculations on retinol-like molecules

4.3 Synthetic Strategies 91

4.4 Vibrational Spectra of Metal Carboxylates 92

4.4.1 Ionic Carboxylates (i)

4.4.2 Monodentate Carboxylates (ii)

4.4.3 Bidentate Carboxylates (iii) and (iv)

4.5 Preparation and Properties of β-Ionylidenecyanoacetic Acids 93

4.6 The Synthesis of Salts of trans-β-Ionylidenecyanoacetic Acid 104

4.6.1 Ammonium *trans*-2-cyano-3-methyl-5-(2,6,6-trimethyl-1-cyclohexen-1-yl)-2,4-pentadienate (ammonium *trans*-β-ionylidenecyanoacetate) (IV.1)

4.6.2 Diethylammonium*trans*-2-cyano-3-methyl-5-(2,6,6-trimethyl-1-cyclohexen-1-yl)-2,4-pentadienate (IV.2)

4.6.3 Tetraethyl*trans*-2-cyano-3-methyl-5-(2,6,6-trimethyl-1-cyclohexen- 1-yl)-2,4-pentadienate (IV.3)

4.6.4 Caesium*trans*-2-cyano-3-methyl-5-(2,6,6-trimethyl-1-cyclohexen-1-yl-2,4-pentadienate (IV.4)

4.6.5 *Trans*-[2-cyano-3-methyl-5-(2,6,6-trimethyl-1-cyclohexen-1-yl)-pentadienato]silver(I) (silver *trans*-β−ionylidenecyanoacetate) (IV.5)

4.6.6 Barium*trans*-2-cyano-3-methyl-5-(2,6,6-trimethyl-1-cyclohexen-1-yl)-2,4-pentadienate (IV.6)

4.6.7 *Trans*-[2-cyano-3-methyl-5-(2,6,6-trimethyl-1-cyclohexen-1-yl)-2,4-pentadienato]zinc(II) (IV.7)

4.6.8 *Trans*-[2-cyano-3-methyl-5-(2,6,6-trimethyl-1-cyclohexen-1-yl)-2,4 -pentadienato]copper(II) (IV.8)

4.8 The Synthesis of Salts of *Cis*-β-Ionylidenecyanoacetic Acid **119**

4.8.1 Ammonium*cis*-2-cyano-3-methyl-5-(2,6,6-trimethyl-1-cyclohexen- 1-yl)-2,4-pentadienate (IV.10)

4.8.2 Barium*cis*-2-cyano-3-methyl-5-(2,6,6-trimethyl-1-cyclohexen-1-yl)-2,4-pentadienate (IV.11)

4.8.3 *Cis*-[2-cyano-3-methyl-5-(2,6,6-trimethyl-1-cyclohexen-1-yl)-2,4-pentadienato]copper(II) Dihydrate (IV.12)

4.8.4 *Cis*-[2-cyano-3-methyl-5-(2,6,6-trimethyl-1-cyclohexen-1-yl)-2,4-pentadienato]zinc.cyclohexane dihydrate (IV.13)

4.8.5 Other Metal Salts of β-Ionylidenecyanoacetic Acid

4.8.6 Summary

4.9 Second Harmonic Generation Properties of Salts Derived from β-Ionylidenecyanoacetic Acid **125**

4.10 Summary and Conclusion **126**

CHAPTER FIVE - Palladium and Platinum Complexes of β-Ionylidenecyanoacetic Acid

5.1 Synthesis of Palladium and Platinum Carboxylates **129**

5.1.1 Introduction

5.1.2 The Vibrational Analysis of Platinum and Palladium Halides

5.2 The Syntheses and Characterization of Platinum and Palladium - β-Ionylidenecyanoacetate Complexes 134

5.2.1 Introduction and Synthetic Strategies

5.2.2 The Synthesis of Monochloro-[bis(triphenylphosphine)-*cis*-{2-cyano-3-methyl-5-(2,6,6-trimethyl-1-cyclohexen-1-yl)-2,4- pentadienato}]platinum(II), PtCl(β-ionylidenecyanoacetate)$(PPh_3)_2$ (V.4)

5.2.3 The Synthesis of Di{*cis*-2-cyano-3-methyl-5-(2,6,6-trimethyl-1-cyclohexen-1-yl)-2,4-pentadienato]-bis(triphenylphosphine)}palladium(II), Pd(β-ionylidenecyanoacetate)$_2(PPh_3)_2$ (V.5)

5.2.4 The Synthesis of Di-{*cis*[2-cyano-3-methyl-5-(2,6,6-trimethyl-1-cyclohexen-1-yl)-2,4-pentadienato]-(diphenylphosphinoethane}platinum(II), Pt(β-ionylidenecyanoacetate)$_2$(diphos) (V.6)

5.2.5 The Attempted Synthesis of Monochloro-[*cis*-{2-cyano- 3-methyl-5-(2,6,6-trimethyl-1-cyclohexen-1-yl)-2,4-pentadienato}-(diphenylphosphinoethane)] platinum(II), PtCl(β-ionylidenecyanoacetate)(diphos) (V.7)

5.2.6 The Attempted Synthesis of {*Cis*[2-cyano-3-methyl-5-(2,6,6-trimethyl-1-cyclohexen-1-yl)-2,4-pentadienato]$_2$-bis(triphenylphosphine)}-platinum(II), Pt(β-ionylidenecyanoacetate)$_2(PPh_3)_2$ (V.8)

5.3 Possible Evidence for η2-Pt/Pd Bonding in Platinum or Palladium(II) Complexes of β-Ionylidenecyanoacetic Acid and Summary of their Chemical Properties 152

5.4 Second Harmonic Generation Properties of Platinum(II) and Palladium(II) Complexes of β-Ionylidenecyanoacetic Acid 153

5.5 Conclusion 154

CHAPTER SIX - The Introduction of Chirality Into β-Ionylidenecyanoacetic Acid

6.1 Introduction 155

6.1.1 Metal Salts of L-Proline

6.1.2 Optical Activity in the Non-linear Susceptibility

6.2 Synthesis of N-Bonded Amino Acid Compounds - The Strategy 159

6.3 The Synthesis and Characterization of N-[2-Cyano-3-methyl-5-(2,6,6 -trimethyl-1-cyclohexene-1-yl)-2,4-pentadiene-1-one]-L-proline (VI.11) 161

6.4 The Synthesis and Characterization of Metal Salts of N-[2- Cyano-3-methyl-5-(2,6,6-trimethyl-1-cyclohexene-1-yl)-2,4- pentadiene-1-one]-L-proline 164

6.4.1 The Synthesis and Characterization of [N-{2-Cyano-3- methyl-5-(2,6,6-trimethyl-1-cyclohexene-1-yl)-2,4-pentadiene-1-one}-L- prolinato]lithium (VI.12)

6.4.2 The Synthesis and Characterization of [N-{2-Cyano-3-methyl-5-(2,6,6-trimethyl-1-cyclohexene-1-yl)-2,4-pentadiene-1-one}-L-prolinato]barium (VI.13)

6.4.3 The Attempted Syntheses of Other [N-(2-Cyano-3-methyl-5-(2,6,6-trimethyl-1-cyclohexene-1-yl)-2,4-pentadiene-1-one)-amino Acids and Related Compounds

6.5 Summary 167

6.6 Second Harmonic Generation (SHG) Studies on N-[2-Cyano-3-methyl-5-(2,6,6-trimethyl-1-cyclohexene-1-yl)-2,4-pentadiene-1-one]-L-proline and its Metal Salts. 168

6.7 Conclusion 170

CHAPTER SEVEN - Experimental

7.1 General Details 172

Starting Materials 172

7.2 Experimental Details Relevant to Chapter Three 173

7.3 Experimental Details Relevant to Chapter Four 180

7.4 Experimental Details Relevant to Chapter Five 186

7.5 Experimental Details Relevant to Chapter Six 190

REFERENCES 193

APPENDIX ONE - Second Harmonic Generation Data of Powdered Samples

Introduction and Discussion 206

APPENDIX TWO - FORTRAN program for the calculation of β. 216

ABSTRACT 219

ABBREVIATIONS

α	Polarizability.
a	Molecular cavity radius.
A	Acceptor.
A_1	The area of a laser beam.
Ac	Acetate.
ADP	Ammonium Dihydrogen Phosphate.
AESOP	An Energy and Structural Optimizational Programme.
asym	Asymmetric.
$\beta_{(x)}$	Molecular Hyperpolarizability - the subscript shows the vector direction to be in the x direction in m^4V^{-1}. The subscript can be relative to bond type e.g. σ, π, to charge transfer, CT, mol, or to the band, Q.

Conversions

β Molecular Hyperpolarizability in m^4V^{-1}

For β: $1 \times 10^{-40}\ \beta\left(\text{MKS in } m^4V^{-1}\right) = 4.189 \times 10^{-10}\ \beta\ (\text{CGS in esu})$

$$\beta\left(\text{SI in } m^4V^{-1}\right) = \frac{4}{3}\pi \times 10^{-10}\ \beta\left(\text{CGS in } cm^5\,esu^{-1}\right)$$

$$\beta\left(C^3J^{-2}m^3\right) = 3.7 \times 10^{-21}\ \beta\left(cm^5\,esu^{-1}\right)$$

For $\mu_0\beta$ values: $$\beta\left(\text{MKS in } 10^{-40}\ m^4V^{-1}\right) = \frac{4.189 \times 10^8 \times \mu_0\beta\,(\text{Dulcic})}{\mu_0(\text{In Debye Units})}$$

bipy	2,2'-dipyridyl.
$\chi^{(n)}$	Macroscopic coefficients of the projection of the microscopic molecular tensors on the unit cell.
$\chi^{(2)}$	Second order susceptibility constant.
C	Speed of light (3×10^8 mS^{-1}).

CNDOVSB	Complete (Computer) Neglect of Differential Overlap Valence Shell Bonding model.
CT	Charge Transfer.
d	Doublet.
D	Donor.
d_{ij}	SHG coefficient or second-order non-linear dielectric susceptibility in pmV^{-1}

$$d_{ij}: \quad 1\ pm\ V^{-1} = \frac{3 \times 10^{-8}}{3\pi}\ esu\ (erg\ cm^{-3})^{-1/2} = 2.38 \times 10^{-9}\ esu$$

DCSHG	Direct current SHG.
DCM	Dichloromethane.
ε	Extinction coefficient.
ε_0	Permittivity of free space, $8.85 \times 10^{-12}\ Fm^{-1}$.
ε_s	Solvent dielectric constant.
$\int \varepsilon\, d\nu$	Integral over an electronic transition, in Hz.
$\Delta\varepsilon_{eff}$	The change in the effective dielectric constant.
e	The charge of an electron (1.602×10^{-19} C).
E	Molecular electronic cloud or applied electric field.
E_0	Electric Field.
EFISH	Electric Field Induced Second Harmonic generation (direct current SHG, DCSHG).
EIF model	The Equivalent Internal Field Model.
esu	2.998×10^9e.
f	Oscillator strength.
FAB	Fast atom bombardment mass spectroscopy.
γ	Third order hyperpolarizability constant.
GHz	Hertz Frequency x 10^9.
η	Index of refraction.
$\hbar\omega$	The fundamental (LASER) photon energy (in J or eV).

HEX	Hexane.
I_i	Incident light.
I_i	Transmitted light.
i.r.	Infra-red.
KDP	Potassium Dihydrogen Phosphate.
λ_{max}	Wavelength at maximum absorption.
LB	Langmuir-Blodgett films.
lu	Luminescence.
μ_{ex}	The excited state dipole moment, Cm.
μ_g	The ground state dipole, Cm. Note: 1Debye = 3.33×10^{-30} Cm.
μ_i	Induced dipole.
μ_0	Molecular ground state dipole.
μ_π	The dipole moment induced by the field E as a result of a substituent group.
The (M)	subscripts M, RX and ArX are the types of substituents making up the total induced dipole moment.
$\Delta\mu_{ex}$	The change in the dipole moment on excitation to a specified energy level, Cm.
m	Electron mass (9.109×10^{-31} Kg), medium if used as a prefix, and multiplet.
mNA	*m*-Nitroaniline (3-nitroaniline).
MNA	2-Methyl-4-nitroaniline.
m.u.	Mass units.
m/z	Atomic mass of particle / charge on particle.
ν	The frequency of the transition in Hz of the λ_{max} of an electronic transition.
$\Delta\nu$	Difference between $\nu(COO)_{asym}$ and $\nu(COO)_{sym}$.
N	Avogadro's number (6.02×10^{23}).
NLO	Non-linear Optics. or Non-linear Optical ~.
Nd/YAG	Neodymium / Yttrium Aluminium Garnet.

n.m.r.	Nuclear magnetic resonance.
P	Macroscopic medium's induced polarization.
P_1	Laser Power.
P_0	Macroscopic medium's ground state polarization.
P^*	The calibration factor for the solvatochromism calculations, and for 4-nitroaniline, is equal to 1.55×10^{22}.
POE	Poly(oxyethylene).
p.p.m.	Parts per million.
θ	The angle of incidence to the surface.
R	The repetition rate.
s	Strong, or singlet.
sh	Shoulder.
SH	Second Harmonic ~.
SHG	Second Harmonic Generation.
sym	Symmetric.
τ	Excited state.
t	Time period, or triplet depending on context.
T	Pulse duration.
u.g.	Ungraded powder.
v	Very.
ω	Fundamental frequency.
ω_0	Natural resonances of the electronic cloud.
2ω	Second Harmonic.
w	Weak.
W	The energy of the transition in joules.

CHAPTER ONE

Non-linear Optics

When laser radiation passes through a medium, the intense electromagnetic fields of the laser light interact with the medium to give rise to new fields which have been altered in frequency, phase or amplitude relative to the incident radiation - this effect is termed "non-linear optics" or NLO. This Thesis is concerned with the prediction, synthesis, characterization and testing of materials based on 'inorganic' compounds for the non-linear optical phenomena called second harmonic generation (SHG).

The field of non-linear optics has great financial possibilities. The market breakdown for non-linear optics in 1988 was as follows:[219] Inorganic crystals, $52M; compound semiconductors, $15M; organic and polymeric materials, nil; Total = $67M. The commercial market is expected to double by 1995, and double again by the turn of the century. The non-linear optical market is directed at the opto-electronic interfaces and optical data storage required in the communications and electronics industries.[6] As demand for faster and more efficient data handling, transfer and storage increases, so does the need for advances in the electro-optics industry.[181]

At present, the micro-chips making up most of the computing hardware ranging from washing machines, children's toys all the way to satellites, are based on conventional semiconducting devices (transistors of several kinds). Each device is a low level switch, which can modulate the electronic fields carried by a conducting cable or radio wave which allows transfer of data from one place to another. This method is limited by the rate of diffusion of electrons and in turn the switching speeds of the transistors, which are now approaching the GHz range (10^9 Hz). However, light is an oscillating wave with a frequency in the order of 10^{14} Hz, and thus allows the data transfer rate to be increased by 10,000 times. Molecular dipoles can provide the switches required to modulate light and are able to operate at speeds vastly greater than those of the conventional semiconductors.

Furthermore, the laser beam can be modulated in two ways; firstly as a simple on/off switch and secondly, the frequency of the light can be varied, that is the fundamental frequency (ω) can be doubled (2ω) on application of a modulating voltage. As well as the important increase in speed, the minimum size of the devices are only limited by the wavelength of the light used, which allows the packing of more switches per unit area, and therefore the miniaturization of the electro-optic devices.[129] Current research is far from the realization of a working and practical electro-optic "chip". Non-linear optics is part of electro-optics which is in turn a part of molecular electronics, all involve some form of molecular manipulation. The study of molecular electronics brings together a variety of disciplines such as synthetic chemistry, physics, biology and electrical engineering, consequently, this Thesis covers an equally varied range of disciplines.[73] The work of Ivanov *et al* suggest that atoms held in strong electromagnetic fields and excited in a non-linear manner, generate shortwave radiation, so perhaps non-linear processes will be used in the new generation of radio communications.[109]

1.1 The Fundamentals of Optics - From the Molecular level

Light can be considered from both a wave and a particle view point. In optics, light is made up of photons, considered as periodic electric fields, originating from an oscillating electric dipole. The periodic oscillations are described by eq. (1.1):

$$E_0 \cos 2\pi\omega_0 t \qquad (1.1)$$

The interaction of light with matter can be divided into three electromagnetic interactions depending on their response times; n photon absorption (luminescence, fluorescence) is slower than magnetic effects (and quadrupolar) which are in turn slower than electronic effects (SHG, Pockels, Kerr).

The electron cloud surrounding molecular units interacts with the applied (or incident) field and deformations result. This interaction is almost purely electronic, and does not affect the nucleii of the molecules in any significant way. The electron clouds of

molecules have natural resonant frequencies which are observed in ultra violet and visible spectra. If the incident field has a frequency equal to one of the natural resonances of the electron cloud then the photon is absorbed. However, if the incident field has a frequency which is not near a resonant frequency of the electron cloud then the electron cloud will be forced to oscillate at the frequency of the incident radiation.

If the incident radiation has a frequency which does not coincide with the natural resonant frequency of an electron cloud on a molecule then the induced dipole μ_i, is then given by:

$$\mu_i = \alpha E \tag{1.2}$$

Where α is the polarizability of the molecular electron cloud, E the applied electronic field.

The polarizability, α, is frequency dependent and as mentioned earlier, there are two special situations which must be considered. Firstly, when the incident radiation ω has a frequency far away from any natural resonances of the electron cloud ω_0, the amplitude of the forced vibration is given by:

$$\alpha(\omega) \approx \frac{f}{\omega_0^2 - \omega^2} \tag{1.3}$$

f is the oscillator strength of the transition. Secondly, as the frequency of the incident radiation approaches the natural resonance of the electron cloud the term $(\omega - \omega_0)$ approaches zero as $\omega \approx \omega_0$, thus another term is necessary which is equivalent to the energy required to maintain the dipolar oscillation since energy is lost through relaxation processes. The polarizability $\alpha(\omega_0)$ is then related to the lifetime of the excited state, τ:

$$\alpha(\omega_0) \approx \omega_0 f \tau^2 \tag{1.4}$$

All the interactions described so far are on the molecular scale, and are linear. The

dipoles of molecules (the electron clouds referred to previously) are in the order of 10^{11} Vm^{-1}, while bright sunlight creates a field of around 600 Vm^{-1}, and all the interactions between molecular dipoles and sunlight are therefore linear.

The energy of a photon is proportional to its frequency whereas light occurs as a stream of photons and the energy of this flux of photons is proportional to the time average square of the amplitude of the electric field. If the flux of photons is increased (i.e. the power), the polarization induced on the electron cloud of a molecule is no longer linear with the incident field, and the effect can be described by a Taylor series:

$$\mu_i = \alpha E + \beta E^2 + \gamma E^3 + ... \qquad (1.5)$$

Where the term β is the second-order hyperpolarizability constant, and γ is the third-order hyperpolarizability constant. This Thesis is concerned with the magnitude of β, which is responsible for the size of the second-order process called second harmonic generation (SHG).

If the molecule possesses a ground state dipole, μ_0, then eq. (1.5) must be modified to include this total dipolar change:

$$\mu = \mu_0 + \alpha E + \beta E^2 + \gamma E^3 + ... \qquad (1.6)$$

All the terms in eq. (1.6) are vectors, and μ is the resultant dipole of the molecule under the influence of the incident radiation. The next section describes what molecular properties are required to optimize the magnitude of β.

1.1.1 Units

All units for β in this Thesis will be in m^4V^{-1}.

Conversions

β Molecular Hyperpolarizability in m^4V^{-1}

d_{ij} SHG coefficient or second-order non-linear dielectric susceptibility in pmV^{-1}

$$d_{ij}: \qquad 1 \text{ pm V}^{-1} = \frac{3 \times 10^{-8}}{3\pi} \text{ esu (erg cm}^{-3})^{-1/2} = 2.38 \times 10^{-9} \text{ esu}$$

$$\text{For } \beta: \qquad 1 \times 10^{-40} \beta\left(\text{MKS in m}^4\text{V}^{-1}\right) = 4.189 \times 10^{-10} \beta \text{ (CGS in esu)}$$

$$\beta\left(\text{SI in m}^4\text{V}^{-1}\right) = \frac{4}{3}\pi \times 10^{-10} \beta\left(\text{CGS in cm}^5\text{esu}^{-1}\right)$$

$$\beta\left(\text{C}^3\text{J}^{-2}\text{m}^3\right) = 3.7 \times 10^{-21} \beta\left(\text{cm}^5\text{esu}^{-1}\right)$$

$$\text{For } \mu_0\beta \text{ values: } \beta\left(\text{MKS in } 10^{-40}\text{ m}^4\text{V}^{-1}\right) = \frac{4.189 \times 10^8 \times \mu_0 \beta\,(\text{Dulcic})}{\mu_0(\text{In Debye Units})}$$

1.2 Factors Influencing the Second-Order Hyperpolarizability Constant β

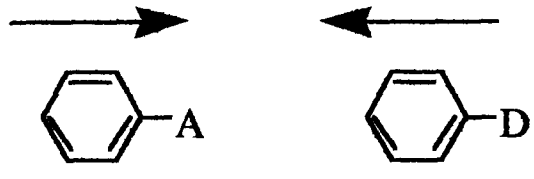
The research described in this Thesis is concerned with the search for new materials which possess significant second harmonic generation efficiencies and the magnitude of this effect is dependent on the magnitude of β. The next section describes the important factors on which the magnitude of β is dependent.

Several attempts have been made to compute additively the polarizability of a molecular unit from its constituent bonds.[38,86,207,208] From these results it was found that

the more easily polarized π bonds had more effect on the polarizability of molecules than σ bonds because the electrons in π bonds are more effectively delocalized. It was proposed that β could be separated into its constituent parts:[124,125,144,161]

$$\beta_{mol} = \beta_{\sigma} + \beta_{\pi} + \beta_{CT} \tag{1.7}$$

The equivalent internal field model (EIF model) has been applied to substituted benzene compounds and resulted in good correlations of the magnitude of β_{π} and β_{σ} between experiment and calculated β_n values.[160] It was found that monosubstituted benzene derivatives had a larger β than similar saturated molecules.[125,126] Furthermore, the magnitude of β was found to be related to the donor or acceptor nature of the substituent. β was found to be negative for acceptor groups (NO_2, CN, etc.) and positive for donor groups (O^-, NMe_2, NH_2, etc.):



β is negative β is positive

The EIF model considers the distortion of the static π electronic field, as a polarization induced by an applied electric field E, so taking a slight modification of equation (1.5):

$$\mu_{\pi} = \alpha E + \beta_{\pi} E^2 + \gamma_{\pi} E^3 + \ldots. \tag{1.8}$$

Where μ_{π} is the dipole moment induced by the field E as a result of the substituent group. The mesomeric moment is defined by the difference between the dipole moment of alkyl and aryl derivatives:

$$\mu_M = \mu_{RX} - \mu_{ArX}$$

Benzene is symmetric, and the response with E and -E is equivalent but of opposite sign and therefore β is zero.

$$\mu_{\pi} = \alpha E + \gamma_{\pi} E^3 + \ldots. \tag{1.9}$$

If this mesomeric dipole caused by a substituent in the ring is considered as equivalent to a static "internal" field, E_0, and the interaction between substituent and the π electron cloud is small then:

$$\mu_M = \alpha_\pi E_0 \approx \mu_\pi \tag{1.10}$$

If an external field is applied, E_{ext} (such as that generated by a laser beam) then:

$$E = E_0 + E_{ext} \tag{1.11}$$

Taking equation (1.9) and substituting for E:

$$\mu_\pi = \alpha_\pi (E_{ext}+E_0) + \gamma_\pi (E_{ext}+E_0)^3 + ... \tag{1.12}$$

Expanding, and summing equation (1.12):

$$\mu_\pi = \alpha_\pi E_0 + \alpha E_{ext} + 3\gamma_\pi E_{ext} E_0^2 + ... \tag{1.13}$$

Equating terms in E_0^2;

$$\beta = 3\,\gamma_\pi E_{ext} \tag{1.14}$$

then using equation (1.10), and making the assumptions already mentioned:

$$\beta_\pi = 3\left(\frac{\gamma_\pi}{\alpha_\pi}\right)\mu_\pi \tag{1.15}$$

So β depends on the sign of μ_M (note that this is $= \mu_\pi$), and the magnitude of μ_M which in turn is dependent on the donor or acceptor strength of the substituent and on the length of conjugation within the molecule. For monosubstituted benzenes:

$$\frac{\gamma_\pi}{\alpha_\pi} \approx (\text{Length})^2$$

The EIF model using additive polarizabilities is only applicable to simple molecules where donor-acceptor interactions are weak (see equation (1.10)). If the donor-acceptor interactions are strong, and the degree of conjugation between the donor and acceptor groups is increased then the model underestimates the size of β. The model does not take into account the charge transfer component of β. Table 1.1 shows values of β derived from various sources, and the values of $\beta_{\sigma+\pi}$ calculated by the EIF model described above are seen to vary considerably from experimental values when electron transfer between the donor and acceptor groups is extensive. This deviation from experimental values is most pronounced for 2- and 4-nitroanilines.

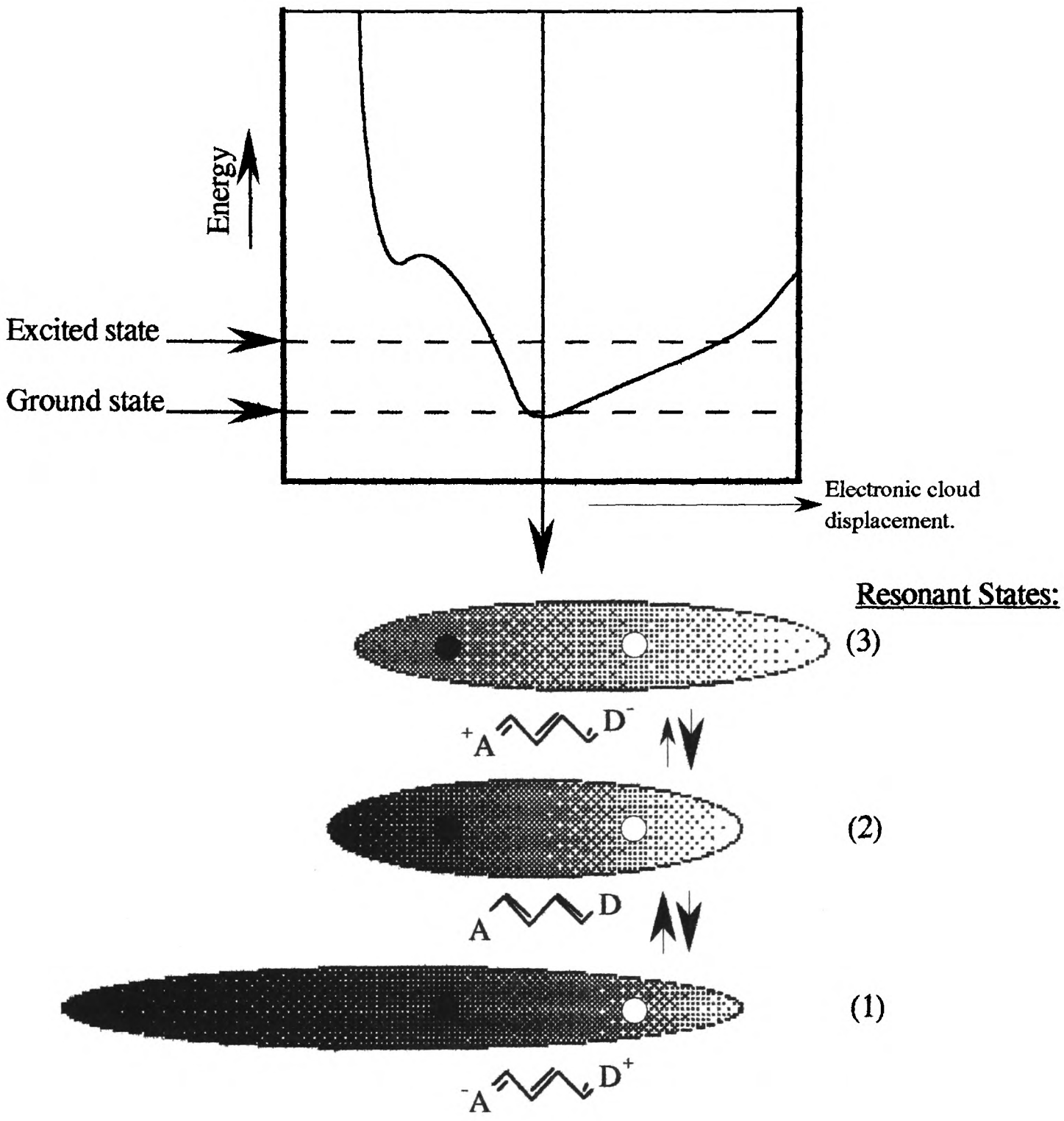
If a molecule can undergo electronic charge transfer from donor- to acceptor-substituents then the component of β associated with the charge transfer is about an order of magnitude larger than contributions from sigma and pi polarizations. Fig. 1.1 shows pictorially why an asymmetric molecule has a non-zero response to an electric field, and therefore a non-zero β.

Table 1.1 A Comparison of the calculated and theoretical second-order hyperpolarizability constant, β, for the disubstituted nitroanilines. All values of β are in m^4V^{-1}.[47]

Compound	$\beta_{\sigma+\pi}$	β_{CT}	β_{T}	$\beta_{x,exp}$
2-Nitroaniline	8.4	46	53	43
3-Nitroaniline	13	17	29	25
4-Nitroaniline	15	82	96	145

β_n where n signifies component or source of β, i.e. σ and π are sigma and pi contributions; CT is charge transfer; T is theoretical and x,exp is the component of β measured experimentally in the direction of the ground state dipole (the x direction).

Fig. 1.1 Pictorial representation of the effect of an electric field on an asymmetric molecule with donor and acceptor functions.



Consider a simple molecule with a donor- and acceptor- group connected by a conjugated π system (Fig. 1.1, resonant state (2)). On exposure to an external oscillating electric field, the electronic part of the molecule will start to vibrate, and will enter the two excited states (1) and (3). State (3) is unfavourable because of the polarizing action of the donor- and acceptor- groups, but state (1) is favourable. Thus the response oscillation has an undisplaced node but whose electron cloud is polarized in an asymmetric manner towards the acceptor- substituent (see Excited state label on graph of Fig. 1.1). This model

of the effect of donor- and acceptor- substituents has been compared to the effect of a diode in an electronic circuit.

A simple two-level system has been applied to the theoretical description of the charge transfer component of the second-order hyperpolarizability constant, β_{CT}. If the component of β is considered in the direction of the ground state dipole (this is an approximation, but the contribution from other components of the tensor are smaller) then the inexact relationship for β is given by: [161,226, 229]

$$\beta_{CT} = \left(\frac{3e^2 \hbar^2}{2m} \right) \frac{W}{\left[W^2 - (2\hbar\omega)^2 \right] \left[W^2 - (\hbar\omega)^2 \right]} f \Delta\mu_{ex} \qquad (1.12)$$

Terms: W is the energy of the transition in joules. $\hbar\omega$ is the fundamental (LASER) photon energy. f is the oscillator strength and is the fraction of electrons involved in the transition. $\Delta\mu_{ex}$ is the change in the dipole moment on excitation to a specified energy level, and is in Cm. For further discussion of terms see Chapter 2.

Equation (1.12) has been used as the basis for determining the magnitude of β using data obtained from shifts in electronic spectra with different polarities of solvent. This effect is called solvatochromism.[225]

1.3 Summary of Factors Affecting the Magnitude of β

1) The molecule must have asymmetric electronic delocalization. For centrosymmetric compounds such as benzene, β is zero for symmetry reasons.

2) The interaction between the donor and acceptor groups at each end of the conjugated system which creates the dipole must be high.[144] The common functional groups have been assigned the following approximate order; for donors CH_3 < OH < MeO < NH_2 < NMe_2 < O^- and for acceptors COMe < Br < Cl < F < CO_2H < CN < NO_2.

3) The charge transfer component of β is usually much greater than the π and σ

components, when charge transfer can occur. Therefore, molecules that have an easily accessible charge transfer band, will have a greater β than those without.

4) The size of β depends on the difference between the excited state and ground state dipole moments, $\Delta\mu_{ex}$. The greater the difference, the larger the β (see Chapter Two, Section 2.3).

5) β generally increases as the conjugated length between the donor and acceptor groups is increased. [72,144,160,227] For example, polyphenols show a marked increase in β, as the number of aromatic rings approaches 6, and then the size of β drops. The drop in the magnitude of β in the polyphenols case is probably due to the increase in molecular size which has the effect of diluting the gain achieved for β from the presence of additional groups. However, as the conjugation length increases the transparency of the molecule decreases, this is the inevitable trade-off when using length of conjugation as a synthetic method of increasing β. Oudar *et al*[163] have shown that β is proportional to the cube of the length of the π system.

6) The size of the molecular unit. The size of β will depend on the amount of space the active electro-optic parts of the molecule take up, compared to the entire size of the molecule. This dilution effect has been discussed with reference to CNDOVSB calculations of β. [144,145]

7) It has already been shown that as the frequency of the incident radiation approaches a natural electronic resonance of the molecule,W, the magnitude of β is expected to reach infinity. However, other absorption terms take over, which reduces the size of β as the electronic dipole starts to resonate (see eq. 1.12).

1.4 CNDOVSB Calculations of β and the Theoretical Optimization of β

Factors affecting the magnitude of β can be illustrated using the CNDOVSB model (complete neglect of differential overlap of valence shell bonding). The calculations were performed by me on a VAX mainframe computer at ICI, Manchester, under the supervision of Dr John O. Morley. The model has been calibrated specifically for dye-like organic

molecules and shows a good correlation with experimental electric field induced second harmonic generation (EFISH) values of the size of β .[69] The EFISH method of measuring the magnitude of β is the most accurate, general determination. EFISH uses the SHG generated by statistical orientation of a solution of the molecules under test when an intense electric field is applied to that solution. The EFISH technique is described in Chapter Two.

1.4.1 Introduction to the CNDOVSB Model

The calculations are based on actual or proposed molecular structures of compounds taken or derived from crystal structure data obtained from the Chemical Crystallography Database, Cambridge.[41] Structures which were incomplete were modified using Viking Molecular Modelling software run on an Evans and Southerland computer. The input data consists of atom coordinates and atom type for the chosen molecule and the energy of the exciting field (taken to be 1.17 eV for 1064 nm laser radiation).

The calculation involves a well defined series of steps:

- The molecular volume is calculated from covalent radii and bond length data.

-The ground state molecular dipole is calculated using a STO-3G level program.

- 50 excited states are estimated from knowledge of the structure, and the charge densities on each atom of each excited state are determined. All excited states which have an oscillator strength, f, less than 0.05 are rejected.

- The dipole moment of each significant excited state is calculated. An unrotated tensor for β is then built up with an applied frequency (ω=1064 nm, 1.17 eV) and at DC (ω=0).

- The β tensor is rotated so that y is the molecular plane, and x corresponds to the ground state dipole moment vector. This rotation is necessary because in EFISH experiments, the component of β along the ground state dipole direction is the quantity that is measured.

- Final determination of the x component of β at zero field and at 1.17 eV.

1.4.2 Calibration

The model was tested using data on molecules which have had their second-order non-linear optical properties fully investigated by the EFISH determination of β. The model has been optimized with respect to the absorption spectra and the CNDOVSB calculations have shown a good correlation between experimental and theoretical spectra and ground state dipoles for an extended set of conjugated aromatic compounds. The model tends to overestimate $\beta_{(x)}$ for the smaller molecules. CNDOVSB calculations provide a means of selecting molecules with the potential to show large non-linear optical effects, prior to synthesis.

Table 1.2 A Summary of data obtained from CNDOVSB calculations for three compounds. Calculations were performed using a VAX mainframe using a program developed by Dr John O. Morley *et al* at ICI, Manchester.

Compound	Molecular Volume, $Å^3$	Ground-state dipole moment, Debyes	Calculated electronic Transitions and oscillator strengths		Literature cited electronic spectra and extinction coefficients
			nm	f	
4-Nitroaniline	109	8.1	306 288 217 205	0.63 0.13 0.66 0.65	320 (4.2) HEX 226 (4.0)
3-Nitroaniline	111	6.6	314 270 234 220 210	0.13 0.22 0.63 0.22 0.67	265 (3.7) HEX 247 (3.2)
2-Chloro-4-nitroaniline	128	6.9	304 301 240 234	0.40 0.24 0.16 0.11	353 DCM 360 (4.2) ALC

Literature cited values for λ_{max} and extinction coefficients taken from; "Organic Electronic Spectral Data", various volumes, Interscience, John Wiley and Sons, New York and measured in the laboratory.

Table 1.2 B Comparison of β coefficients for three compounds derived from CNDOVSB and EFISH experiments.

	$\beta_{(x)}$ x 10^{-40} m^4V^{-1}		
	CNDOVSB		Literature[ref]
Compound	At ω = 0	At ω = 1.17 eV = 1064 nm	At ω = 1.17 eV = 1064 nm
4-Nitroaniline	32	56	49 - 151[47]
3-Nitroaniline	13	19	25[47]
2-Chloro-4-nitroaniline	26	46	142[127]

Table 1.2 B compares the magnitude of β for three example compounds calculated by the CNDOVSB method to the accepted literature values. Unless otherwise stated all CNDOVSB calculations in this Thesis were done at ICI, Manchester. For more examples see references 47 and 69.

CNDOVSB calculations have been used as a "predictive" tool in Chapters Three and Four to pre-select molecules with a high second order hyperpolarizability constant, β.

1.5 From Molecular Hyperpolarizability to Material Susceptibility

1.5.1 Introduction

Non-linear optical interactions with matter are on a molecular scale, but non-linear effects are mostly observed on the macro-molecular scale. Thus molecules can be synthesized with the required properties but the usefulness of the material depends eventually on the macroscopic structure of the material. The second-order hyperpolarizability coefficient β has been described in terms of the molecular dipole change μ from the ground-state dipole μ_0 induced by an external field E:

$$\mu = \mu_0 + \alpha E + \beta E^2 + \gamma E^3 + \ldots.$$

(1.6)

In the case of a macroscopic medium with a ground state polarization P_0, the induced polarization P is created by an electric field E, and the $\chi^{(n)}$ are the macroscopic coefficients that measure the projection of the microscopic molecular tensors on the unit cell, correspondingly: [22, 89]

$$P = P_0 + \chi^{(1)} E + \chi^{(2)} EE + \chi^{(3)} EEE + \ldots.$$

(1.13)

Equation (1.13) does not explain simply the problems associated with the synthesis of non-linear materials. Consider, first, the linear situation:

$$P(\omega) = \varepsilon_0 \chi^{(1)} E(\omega)$$

(1.14)

The polarization $P(\omega)$ induced by the electric field $E(\omega)$, where $\varepsilon_0 \chi^{(1)}$ is the size of the dipole moment. The linear optical effect of refraction is derived from equation (1.15):

$$P(\omega) = \eta^2 E(\omega)$$

(1.15)

The linear equation (1.15) can be extended to include the non-linear coefficients:

$$P(\omega) = \varepsilon_0 \left[\chi^{(1)} E + \chi^{(2)} E^2 + \chi^{(3)} E^3 + \ldots. \right]$$

(1.16)

Equation (1.16) describes the response of matter to an electric field E. The second-order susceptibility is symmetry dependent. In non-centrosymmetric media $\chi^{(2)}$ is finite, but in centrosymmetric media $\chi^{(2)}$ is zero. Equation (1.16) can be expanded in terms of an oscillating electric field such that:

$$E_x = E_0 \cos \omega_0 t$$

(1.17)

so

$$P(\omega)_{(x)} = \varepsilon_0 \left[\chi^{(1)} E_0 \cos \omega_0 t + \chi^{(2)} E_0^2 \cos^2 \omega_0 t + \chi^{(3)} E_0^3 \cos^3 \omega_0 t + ... \right]$$

$$= \varepsilon_0 \left[\chi^{(1)} E_0 \cos \omega_0 t + \frac{1}{2} \chi^{(2)} E_0^2 \left(1 + \cos 2\omega_0 t\right) + ... \right]$$

(1.18)

The polarization $P(\omega)$ is a vector, as are the electric fields so if the polarization in the x direction is considered then under the influence of a $+E_0$ field the corresponding equation is:

$$P(\omega)_{(+x)} = \varepsilon_0 \left[\chi^{(1)} E_0 \cos \omega_0 t + \frac{1}{2} \chi^{(2)} E_0^2 \left(1 + \cos 2\omega_0 t\right) + ... \right]$$

(1.19)

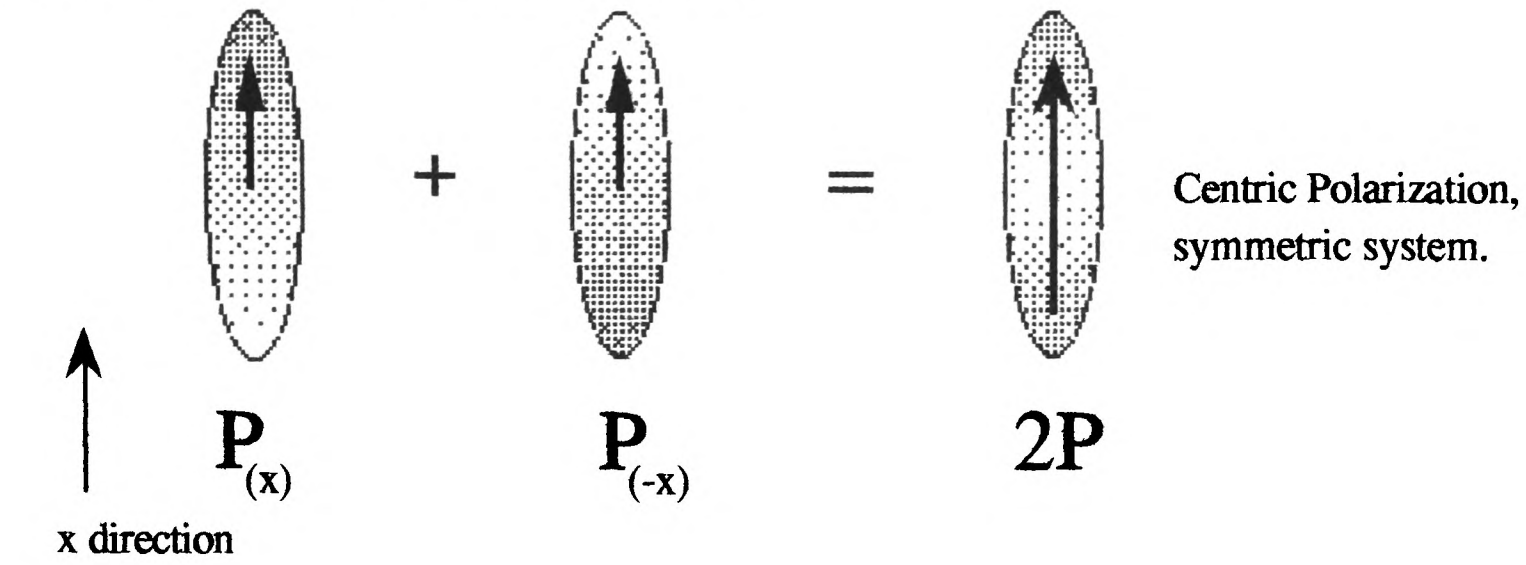
Since the electric field is oscillating, there is a corresponding $-E_0$ relationship:

$$P(\omega)_{(-x)} = \varepsilon_0 \left[- \chi^{(1)} E_0 \cos \omega_0 t + \frac{1}{2} \chi^{(2)} E_0^2 \left(1 + \cos 2\omega_0 t\right) + ... \right]$$

(1.20)

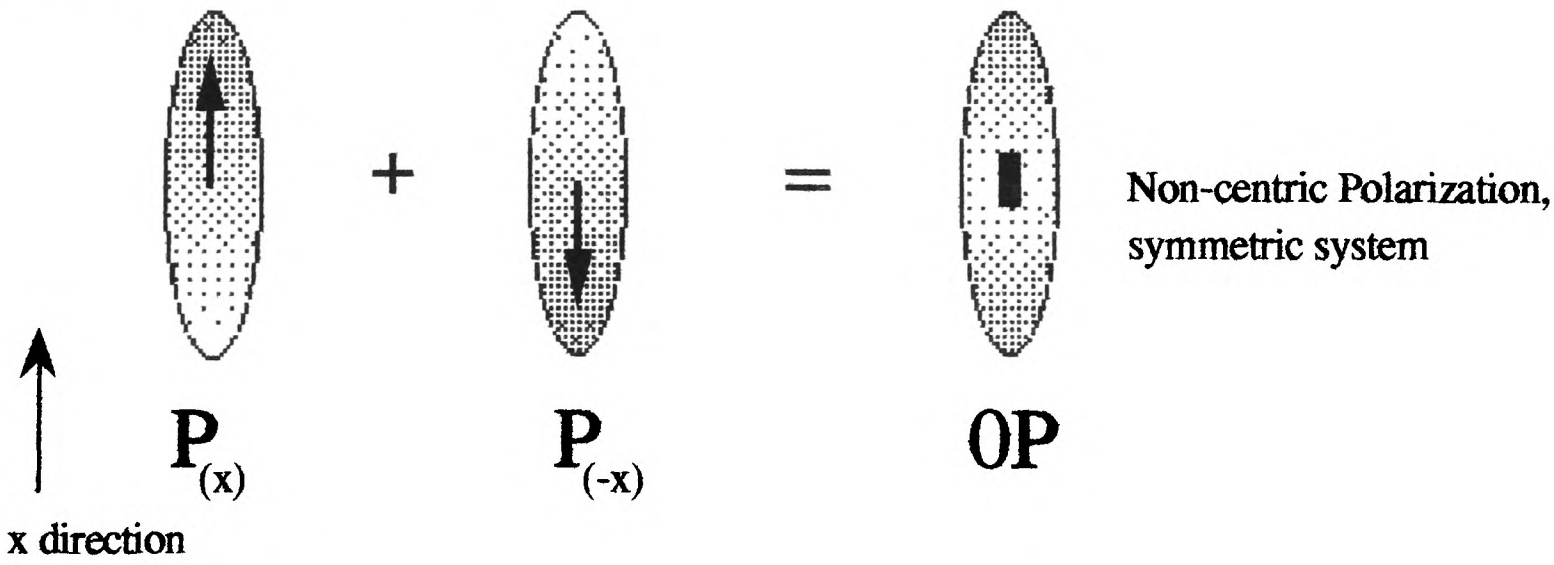
For a centrosymmetric system, the response to $+E_0$ is identical to that of a $-E_0$ field, and for odd terms in equation (1.18), the response follows the same sign i.e. $(+/-E_0)^{\text{odd powers}} = (+/-P(\omega))$. Figure 1.2 shows a pictorial representation of the response of an odd term in the power series of equation (1.18) to an oscillating electronic field. The response is equivalent to vectorially adding equation (1.19) to (1.20), the result is twice the magnitude of either of the components.

Fig. 1.2 Pictorial representation of the polarizations induced in odd terms in equation (1.18) for a centrosymmetric system. The vector addition is equivalent to eqn. (1.19) + (1.20), see text. The resultant is non-zero.



The response to an oscillating field (+/-E_0) on even terms in the power series of equation (1.18) for a centrosymmetric system results in a complete cancellation of effects such that $\chi^{(2)} = 0$.

Fig. 1.3 Pictorial representation of the polarizations induced in even terms in equation (1.18) for a centrosymmetric system. The vector addition is equivalent to eqn. (1.19) + (1.20). The resultant is zero.

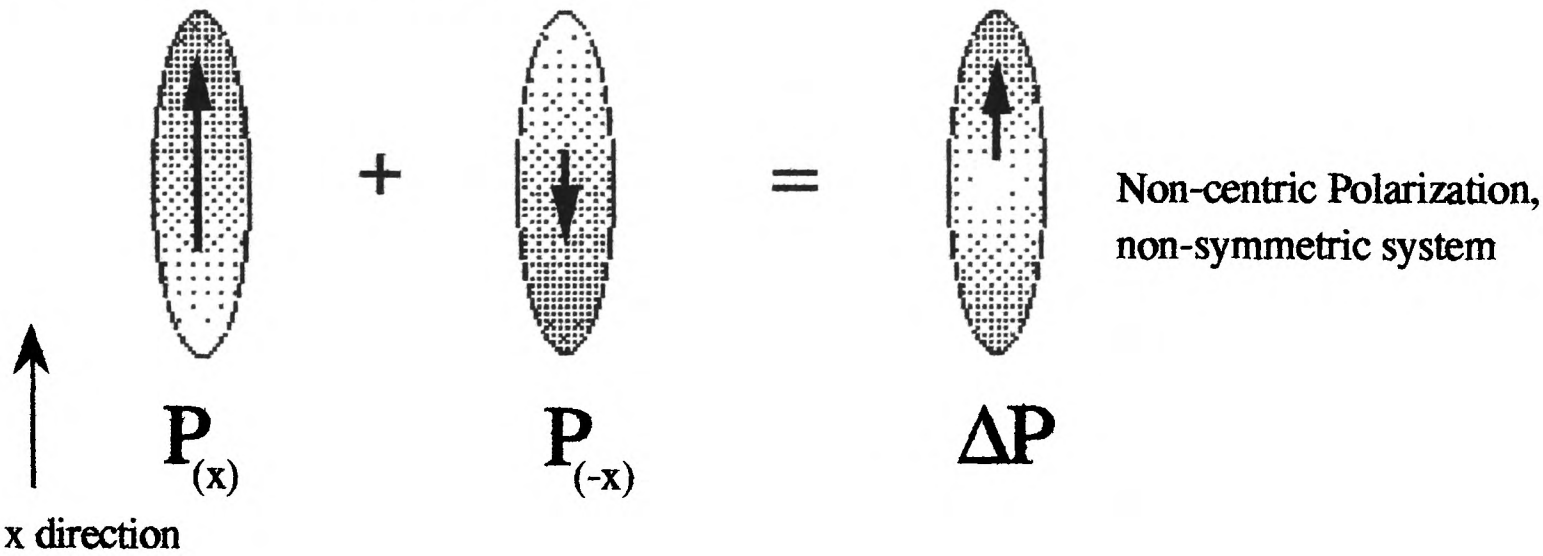


The response for such a system to +E_0 is identical in magnitude and sign to the response to -E_0 , and so if the responses are added, then the resultant is zero, e.g.

$(+/E_0)^{\text{even powers}} = (+P(\omega))$. Figure 1.3 shows pictorially the response of even terms in the power series for a centrosymmetric electron cloud.

If the electron cloud is non-centrosymmetric then the response to $+E_0$ is not equal in magnitude or direction to the response to $-E_0$ and so even terms in the power series of equation (1.18) do not vanish. Figure 1.4 is a pictorial representation of the effect of a sine wave on a non-centrosymmetric electron cloud.

Fig. 1.4 Pictorial representation of the polarizations induced in even terms in equation (1.18) for a non-centrosymmetric system. The vector addition is equivalent to eqn. (1.19) + (1.20). The resultant is non-zero.



It has been shown that for second-order non-linear optical effects to be observed in bulk media there must be an absence of a centre of symmetry.

1.6 Imposing Non-centrosymmetry on Materials

1.6.1 Introduction - Common Strategies

Non-centrosymmetry is the most difficult requirement for second-order non-linear optical processes to induce in media. Centrosymmetric materials have been observed to possess slight non-centrosymmetry (see Chapter 2), but this gives rise to non-linear effects of an order of magnitude lower than the required for the less efficient commercial devices. The methods available to induce the required non-symmetry can be divided up into three categories; within gases, liquids and solids:

Gases

Only centrosymmetric related coefficients are observed.

Liquids

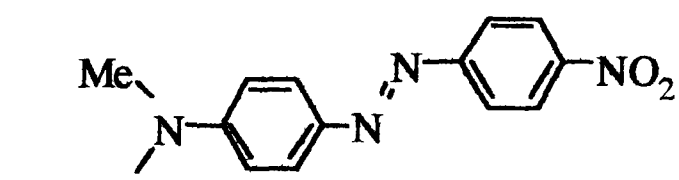
Solutions of compounds, like gases, can rotate freely, and any molecule which possesses the second-order coefficient β, will have a susceptibility coefficient, $\chi^{(2)}$, equal to zero. Thus solutions will not display second-order processes.

If a solution of a compound, with a non-zero β, is subjected to an intense electric field (up to 1 MVm^{-1}) then partial alignment of the molecular dipoles is achieved. The induced asymmetry is observed by passing a laser beam (of suitable frequency) through the poled solution. This is the basis of electric field induced second harmonic generation (EFISH generation, or direct current SHG, DCSHG).[182,217] This method is also the basis of many electro-optic devices now in every-day use. If optically perfect crystals of the compound cannot be grown, then the EFISH determination of β is the most accurate to date. It is interesting to note that literature cited measurements of β determined, using the EFISH method, for various compounds tend to vary up to ±50% (see Chapter Two, Table 2.4). Errors of ±15 to ±20% have been quoted for the EFISH technique of measurements of β.[182, Appendix of Ref.47, Vol II.] The EFISH method requires that the compound under test must have a dipole (i.e. be an asymmetric molecule, otherwise β will be zero), and that it dissolves in a non-conducting, non-polar solvent to a reasonable degree (such as hexane). It is possible to use polar aprotic solvents (such as dimethylsulphoxide), but it is then necessary to take into account the local field of the solvent, which tends to reduce the effect of the applied field, and as β is concentration dependent, to extrapolate to infinite dilution.[123, 128] EFISH values are commonly expressed in terms of $\mu_0 \beta$, determination of the ground state dipole, μ_0, of the compound will allow β to be calculated.

The ability to orientate molecular dipoles with an intense electric field has been extended to a process by which the correct symmetry can be engineered into polymers, and other composite materials.[141] It is included in the "liquid" category as some molecular

rotation is necessary to achieve the alignment, and the alignment is therefore done in a liquid, or semi-liquid phase.

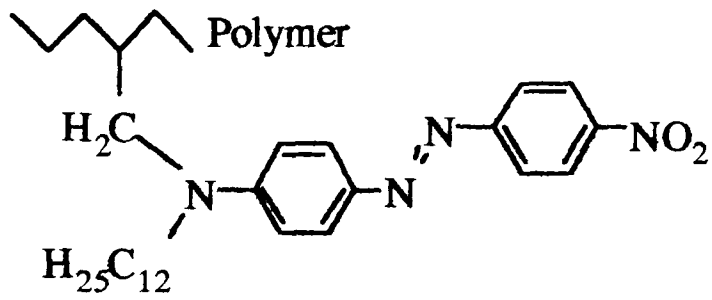
Guest-host polymers: Guest-host systems can be prepared by mixing an active material with a monomer, prior to polymerization. The principle will be illustrated by two examples. First an azo dye:



Disperse Red 1

may be dissolved in poly(methyl methacrylate), the doped polymer then heated, poled at 0.8 MVm^{-1}, then cooled which "freezes" the asymmetry into the matrix.[34] By this method the polymer gave a d_{33} coefficient of 15 pmV^{-1}. The matrix serves only to separate the active dopant molecules and has no non-linear effects of its own.[10] Secondly, the host can be a nematic liquid-crystalline thermoplastic into which the dopant is dissolved. On application of an external field the liquid-crystalline domains orientate themselves to the field (above the glass temperature), the dopant molecules are then held in an anisotropic environment.[14,82] Such poled polymers tend to undergo a conversion from being anisotropic to isotropic, due to thermal rotation. Watanabe *et al*[210] fabricated a polymer from 4-nitroaniline and poly(oxyethylene) (POE), which, after poling, gave an SHG efficiency of 20 to 30 times urea. Unfortunately the SHG efficiency of the 4-nitroaniline-POE polymer had a half life of only 10 hours.[210]

Co-polymers: The active electro-optic molecular unit is tagged onto a monomer, and then the new monomer is polymerized, and poled. For example a monomer can be synthesized from Disperse Red 1, and methacryloyl chloride:



Then polymerized and poled in the usual manner. The measured SHG coefficient (second-order non-linear dielectric susceptibility) for a typical co-polymer made from Disperse Red 1 was measured as 57 pmV^{-1} an improvement over the guest host mixture, using the same chromophore, of almost three times (for comparison of values to reference compounds, see Table 1.3).[34]

Table 1.3 Typical second-order non-linear dielectric susceptibilities for common reference materials. Literature values taken from reference 47.

Compound	$d\left[pmV^{-1}\right]$	SHG x urea	
		Literature Values	Measured as part of this Thesis
Urea	$d_{14}=2.3$	1	1
KDP	$d_{14}=0.67$	0.33	0.34
Lithium niobate	$d_{31}=-5.95$	2.5	--
ADP	$d_{36}=0.76$	0.37	0.37
Quartz	$d_{11}=0.50$	0.01-0.05	0.29 ugr
3-Nitroaniline	$d_{333}=17.6$	2.5	--
2-Methyl-4-nitroaniline	$d_{12}=38$ $d_{11}=250$	6.6-17.6	8.55

Solids:

Ground-state dipoles and *inter*molecular forces govern the orientation of molecules within a structure. Large ground-state dipoles favour large second-order hyperpolarizabilities, but also favour the crystallization of the molecules in centrosymmetric structures which orientate the dipoles in opposite directions, thus creating a centre of

dipolar inversion, and zero β. For solid materials to show second harmonic generation the molecules must crystallize in a non-centrosymmetric manner.[154,155,156] This is the most difficult requirement to impose on molecular solids. The same solids will also show other effects such as pyroelectric, piezoelectric, ferroelectric and optical rotation properties.

Non-centrosymmetric Crystallization: There is a small chance that a compound will crystallize in a non-centric space group. There are 230 predicted unique ways to organize objects. These 230 **space groups** have been collected into 32 unique **point groups**. Of the 32 point groups only 21 have the required non-centrosymmetric operators. From that 21, three groups have vanishing optical tensor coefficients (422, 432 and 622).[114] This leaves 18 useful point groups (see Table 1.4).

It is not sufficient for compounds to merely belong to one of these 18 point groups, the compound must also be able to be phase matched (see Section 1.7.3). Phase matching is a process by which the second harmonic efficiency of a material can be improved. For a material to be phased matched, the incident laser beam or field must be at an angle to the crystal such that the refractive indices at the incident and doubled frequencies are equal. This process uses the constructive interference of waves to increase the electric fields in the molecular domains. Furthermore, each point group has an optimum arrangement of molecules to the crystal axis, this is not always realized in the crystal structure and an "optimal % efficiency" can thus be calculated.[226, 229] The space group 19, $P2_12_12_1$ is the most efficient group and has an optimal efficiency about 39.5%, while 4, $P2_1$ is only 23.3% efficient. Zyss and Oudar calculated the maximum SHG efficiency for certain compounds and compared the result to that measured. They found that it was theoretically possible to improve the efficiencies of SHG materials if the crystal packing could be altered. The NLO reference material, urea could be be made 2.5 times more efficient, and POM (3-methyl-4-nitropyridine-1-oxide) 3.7 times more efficient.[226,229] It has been observed that organic compounds tend to crystallize in space groups that are useful for SHG, while inorganic compounds do not.[Nicoud *et al* in Ref. 47.]

Table 1.4 Non-centrosymmetric space groups and typical examples (in Schoenflies notation), taken from ref. 91.

System	Crystal Class	Space Group	Examples
Triclinic	1	1	P1
Monoclinic	2	3-5	$P2_1$
	m	6-9	Cc
Orthorhombic	222	16-24	$P2_12_12_1$
	mm2	25-46	$Pna2_1$
Tetragonal	4	75-80	P4, I4
	$\bar{4}$	81-82	$P\bar{4}$
	422		
	4mm	99-110	P4bm
	$\bar{4}$2m	111-122	$P\bar{4}2_1c$
Trigonal	3	143-146	P3
	32	149-155	R32
	3m	156-161	P3c1
Hexagonal	6	168-173	P6
	$\bar{6}$	174	$P\bar{6}$
	622		
	6mm	183-186	P6cc
	$\bar{6}$2m	187-190	$P\bar{6}2m$
Cubic	23	195-199	P23
	$\bar{4}$3m	215-220	$P\bar{4}3n$

There are several methods by which non-centrosymmetry using chirality can be achieved:[68]

Chirality, using an asymmetric tetrahedral carbon atom: The readily available

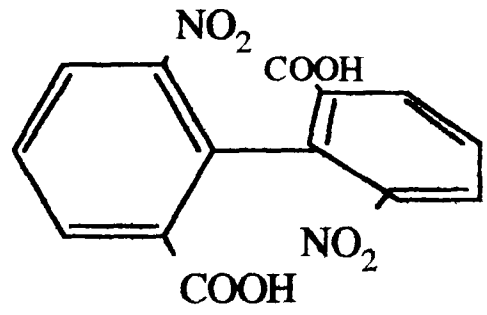
chiral amino acids provide a diverse series of molecular templates which may be modified to incorporate a suitable donor-acceptor conjugated system. The incorporation of amino acid side groups to molecules has been by far the most successful approach especially in the case of R/L-proline and its derivatives. This technique forms the basic synthetic technique followed in Chapter Four.

Chirality, using other quadrivalent asymmetric atoms: A tetrahedral carbon atom, with four differing groups attached is chiral, and in the same way any quadrivalent element with tetrahedral geometry will also be optically active. For instance asymmetric compounds formed from Si, Ge and NR_4^+, Zn, Mn, Cu, and Be have been shown to be chiral.[17,35,185] The synthesis of metal compounds which possess chirality is attempted in Chapter Four.

Chirality, using compounds with tervalent asymmetric atoms: Tervalent atoms with three different groups and a lone pair as the 'fourth' group will show optical activity, only if the molecule is restrained from 'flipping' (pyramidal inversion, the umbrella effect). This method of forming chiral compounds was not used in this Thesis.[33]

Chirality, using compounds with asymmetric octahedral atoms: Compounds with octahedral geometry can form propeller-like molecules which have a right or left handed screw. Chiral compounds of Cr(III), Co(III) and Pt(IV) have been synthesized[214]. The use of octahedral compounds for non-linear optics has been discussed at length in Chapter Three.

Chirality, using restricted rotation to give rise to perpendicular dissymmetric planes: Chiral compounds that have a 'pseudo asymmetric tetrahedron' formed by the restricted rotation of a group are said to show atropisomerism. The well known class of asymmetrically substituted bi-phenyls are chiral because the rings are prevented from rotating round the central bond by the *ortho-* substituents on both rings:[92]



The introduction of atropisomerism into a compound has been attempted and described in Chapter Three.

Chirality, using helices and knots: Compounds with a helical geometry can show chirality such as the helicene heptahelicene.[135] The as yet hypothetical knot system may also show chirality.[84] Neither of these unusual methods of imposing chirality have been attempted as part of this Thesis.

The natural tendency for compounds to favour centrosymmetric space groups is problematic in the research into new materials for SHG. However, new methods of molecular engineering are being devised which, to some degree, control the molecular symmetry:

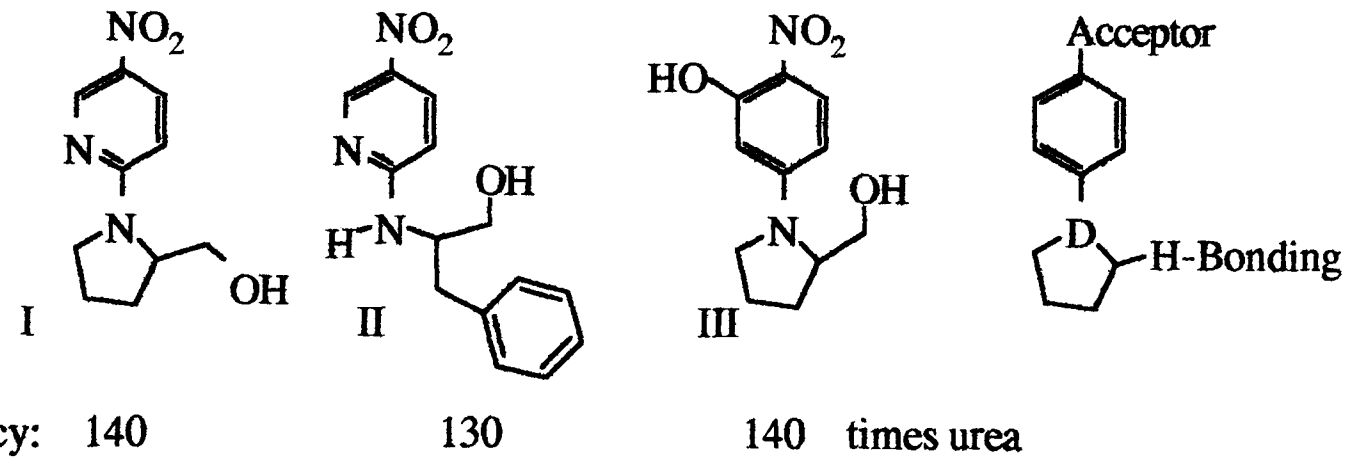
Molecular Engineering - By Directed Crystallization: Crystallization of a compound from a solution is a process which involves nucleation at a surface. If the surface at which crystallization is nucleated has a directed symmetry, then the subsequent molecular layers must interact with the surface. The nucleation of crystals has been investigated at charged or poled surfaces,[118] at surfaces of specially engineered polymers with chiral or highly polar surfaces. There has also been some success at directing the symmetry of crystal growth by using molecular recognition at the crystal/solution interface.[212]

Molecular Engineering - By Dipole and Hydrogen - bonding Interactions: It is possible to influence the magnitude of β by altering structural features of the NLO active molecules e.g. the strength of the donor - acceptor interaction, but this tends to increase the magnitude of the ground-state dipole moment. As the ground-state dipole becomes larger, then the

electrostatic forces between neighbouring molecules tends to favour such an orientation that the dipoles are aligned anti-parallel. The upshot of this is that β may increase, but it becomes more difficult to direct the molecular packing by physical forces, and lowers the probability of the molecules crystallizing in an acentric manner.

Hydrogen bonding has been shown to be responsible for the second harmonic generation effects observed in solid urea. The crystal structure of urea is composed of a lattice of hydrogen bonds which force the molecules to align themselves in head-to-tail columns.[228] The presence of hydrogen bonding within molecular structures appears to be vital for the performance of many SHG active compounds but, so far, only empirical hypotheses have been suggested for the exact nature of the hydrogen bonding contributions to crystal packing. It has been observed that many efficient NLO active organic molecules have a charge-transfer route which is separated, physically and electronically, from a hydrogen bonding group.[183] The hydrogen bonding group serves only to direct the crystal packing, and does not take part in the electronic delocalization (see Fig. 1.5).[202]

Fig.1.5 Examples of efficient organic SHG molecules where the charge transfer (CT) axis is separated from the hydrogen bonding site. From references 203, and Appendix I - Vol. II ref. 47.



Efficiency: 140 130 140 times urea

Molecular Engineering -By Langmuir-Blodgett Films: Second-order non-linear effects are forbidden in a solid which has an center of inversion but are allowed at the surface where the inversion symmetry is broken. The formation of surface layers by Langmuir-Blodgett

(LB) deposition is a special case of orientated surface creation, and eventually the process may be repeated to create a multilayer. LB films have been used in the monolayer second harmonic generation technique to measure the magnitude of β for certain compounds. This approach has been shown to be as effective as EFISH, but far simpler to execute. It is necessary to introduce onto the chromophore a straight alkyl chain (such as docosyl) by synthetic means.[168] LB films suffer from thermal instability[120] and as more layers are deposited, the bulk hyperpolarizability falls off.[168]

1.7 Further Requirements for Second Harmonic Generating Materials

1.7.1 Thermal Stability - Damage Threshold

For SHG applications where high incident powers are used it is necessary to use materials which are not affected by the high pulse temperatures involved. Urea has a damage threshold of 5 $GWcm^{-2}$,[203] while the efficient organic compound 2-methyl-4-nitroaniline has a damage threshold of only 200 $MWcm^{-1}$.[123] In applications where the light intensities are low, the damage threshold is not an important factor.

1.7.2 Light Stability

The intense fields which are required to excite NLO materials must not have a detrimental effect on the NLO material itself. It is possible that the incident photon energy may not be able to degrade the NLO material, but after frequency doubling or tripling, the photons might have sufficient energy for decomposing the material.

1.7.3 Phase Matching

The interaction of electro-magnetic waves travelling through a medium can be 'tuned' to the molecular absorbers by orientating a small crystal such that there is constructive interference of the waves within the crystal or altering the angle at which the molecular dipoles are orientated to the incident radiation. The constructive interference occurs when the refractive indices of the medium at the fundamental and second harmonic

are equal. The maximum SHG is observed as the crystal dimensions approach the coherence length, and if the size of the crystals are increased, the SHG response reaches a constant level (see Chapter Two). The efficiency of SHG for 2-methyl-4-nitroaniline may be increased from 1.3 x 10^6 (times quartz) to 1 x 10^8 if correctly phased matched.[123] It has been demonstrated that sandwich layering a NLO material with an inactive spacer layer at the coherence length of the material, produces a system where additive SHG is observed, and the SHG is proportional to the layer thickness.[202]

1.7.4 Frequency Cut-off

Materials used for SHG must be transparent at the wavelength of the second harmonic. Compounds tested at 1064 nm fundamental, produce green light at 532 nm, and thus red compounds are not suitable for SHG studies at this laser wavelength. However, efficient SHG compounds show considerable SHG even when the materials have considerable absorption at the second harmonic. Furthermore, the hyperpolarizability constant β will increase as the absorption edge of the compound approaches the second harmonic wavelength. This result is due to optical resonance, and has been explained in Section 1.3.

1.8 Aims of this Thesis

This Thesis is concerned with the prediction, synthesis, characterization and testing of materials based on 'inorganic' compounds for the non-linear optical phenomena, second harmonic generation (SHG).

Chapter One has described the fundamentals of non-linear optics, and posed the problems, and some of their solutions, confronting the synthetic chemist in the search for new non-linear optical materials. Theoretical predictions of the second order hyperpolarizability constant β using CNDOVSB calculations have been discussed. For a material to show SHG, it must possess some degree of non-centrosymmetry (as a surface/layer, crystallize in a non-centrosymmetric space group, be poled by and electric

field, or held in an asymmetric host matrix). Furthermore, to have significant NLO effects the compounds must have suitable donor - acceptor functional groups joined by a conjugated molecular system, which must have easily accessible low-lying charge-transfer bands, as well as other less important requirements. The methods by which non-centrosymmetry is introduced into the molecules synthesized in this Thesis are discussed, some of which have not yet been investigated. Novel compounds with potential chirality due to atropisomerism (chirality due to restricted rotation of a group), asymmetric octahedral structures, and asymmetric tetrahedral symmetry of metal centers are discussed in Chapters Three, Four and Five, while conventional asymmetric carbon centers used to introduce chirality are discussed in Chapter Six.

Chapter Two describes the construction, calibration and use of an experimental set-up for the determination of the SHG efficiency of powders. The technique is based on that described by Kurtz and Perry [118] The results of the powder SHG tests are summarized in Appendix 1. A technique by which the magnitude of the molecular constant β can be estimated by a solvatochromic method is also described in Chapter Two.

CHAPTER TWO

The Measurement of Second Order Non-linear Optical Properties

2.1 Introduction

The investigation of second-order non-linear optical properties of materials involves three basic techniques:

(a) The measurement of the magnitude of the hyperpolarizability constant, β.

This can be done using Electric Field Induced Second Harmonic Generation, EFISH (sometimes referred to as Direct Current SHG, DCSHG).[182] This technique does not require the material under test to be non-centrosymmetric. However, EFISH experiments require the compounds under test to be dissolved in non-conducting, non-polar solvents. Furthermore, extra data on molecular properties are required, e.g. dipole moment, and the experimental set-up must have a uniform electric field throughout the cell. EFISH tests are accurate but are time-consuming and not applicable to all materials (see Chapter 1, part 1.6.1). Table 2.4 shows the variation of β measured by the EFISH technique from several literature sources for the compound 4-nitroaniline. Although the EFISH method is accurate the range of cited β values demonstrates that there is a variation of $\pm$ 50%, and errors of $\pm$15-20% to $\pm$25-38% have been quoted.[Appendix in ref. 47 (Vol II), 161,182] EFISH measurements were not performed as part of the research described in this Thesis.

The measurement of β, which is a molecular property unlike the susceptibility constant, $\chi^{(2)}$, can be done without the requirement of non-centrosymmetry in the crystal structure. An approximate magnitude of β can be obtained from the size of the solvatochromic shift observed for a particular compound. This technique does require knowledge of molecular parameters such as molecular volume and dipole moment, but measurements of electronic spectra are far simpler to perform. This Thesis describes a

solvatochromic method of determining the approximate magnitude of β.

(b) The measurement of the efficiency of second harmonic generation.

This is a macroscopic measurement which includes all the factors involved in the magnitude of the SHG. The materials have to be non-centrosymmetric, either naturally (Langmuir-Blodgett films, crystal structure) or induced by external means such as by an external field (DCSHG). The susceptibility constant, χ, which is a bulk property, is non-zero only when the change in the dipole moment on excitation occurs in a non-centrosymmetric manner. Accurate measurements can only be made if the factors involved in SHG are fixed in known ways. The measurement of the SHG response of single crystals, held at a particular known orientation to the exciting laser beam, or using a particular crystal face is one of the most accurate instances of SHG measurement. SHG measurement by corona induced poling, or other poling methods and by powder methods can only be used as a guide to SHG magnitude for although the methods can be made accurate to better than 2%, variations in the sample itself will cause greater inaccuracies. 2-Methyl-4-nitroaniline has an SHG response of 5.7 to 8.6 times urea using recrystallized samples ground to particle sizes of 100 microns, with placement errors (errors within the measurement - using the same sample) in the order of 1.75 to 2.0%. An ungraded sample, gave a relative SHG signal of 2.6 times urea, a variation of 30% from the graded sample.

2.2 Overview of Experimental SHG Measurement Technique

The second harmonic generation properties of the compounds described in this Thesis were measured by a modification of the Kurtz powder method.[118] Samples were ground, but not sieved, and exposed to incident light of 1064nm. The source was a low power Nd/YAG laser (less than 0.05mW), attenuated by a series of calibrated neutral optical density filters, which irradiated a silica cell, containing the sample, see Fig. 2.1A. The cell faces were at right angles to the incident beam, and were located at the centre of a concave mirror, which collected all reflected light. The reflected light was then passed

through an interference filter centered at 532nm (band width 2 nm). The intensity of the second harmonic frequency was detected by a photomultiplier tube. The amplified anode signal was measured with a summing oscilloscope. Each measurement was the average of 64 pulses, and this ensured that the pulse to pulse variation was removed. The sample signals were compared to those from graded (100 micron) reference samples. To avoid any ambiguity, the test was repeated with a different incident laser power, and a new measurement taken. If the relationship between the two measurements was second order with respect to the incident power, then the signal was presumed to be a second harmonic.

2.2.1 Apparatus Construction

The output from a Nd/YAG laser, incident power 7.4mJ/pulse, pulse duration 10-15ns, operating only in oscillator mode was directed through a photo-diode power measuring device, and then attenuated by neutral optical density filters. The attenuated incident light then passed into a series of collimator slits, of 8mm diameter, held within a blackened, light-proof aluminium tube. The collimator was attached to one side of a purpose built light proof box, in which the sample was housed, see Figs. 2.1 and 2.2.

The photomultiplier tube had to be protected from accidental exposure to laboratory light and so a fail-safe sliding lid was incorporated into the design. The sliding lid, when open, locked a shutter in position, covering the photomultiplier tube window. When the lid was closed, the shutter could be opened to allow the second harmonic to enter the photomultiplier tube.

Powdered samples, of 1mm thickness, are almost opaque, and so the apparatus was designed to collect all reflected light from the front surface of the sample. This method is not the most accurate since the multitude of surfaces gives rise to dispersive effects which gives an SHG efficiency slightly higher than that measured by a technique where the dispersive effects are lessened.[118] The simplest method was to place the sample at the focal point of a concave mirror, so that the incident light would pass through an aperture (8mm diameter) drilled in the centre of the mirror, and all reflected would pass parallel to the laser beam, to the detection apparatus.

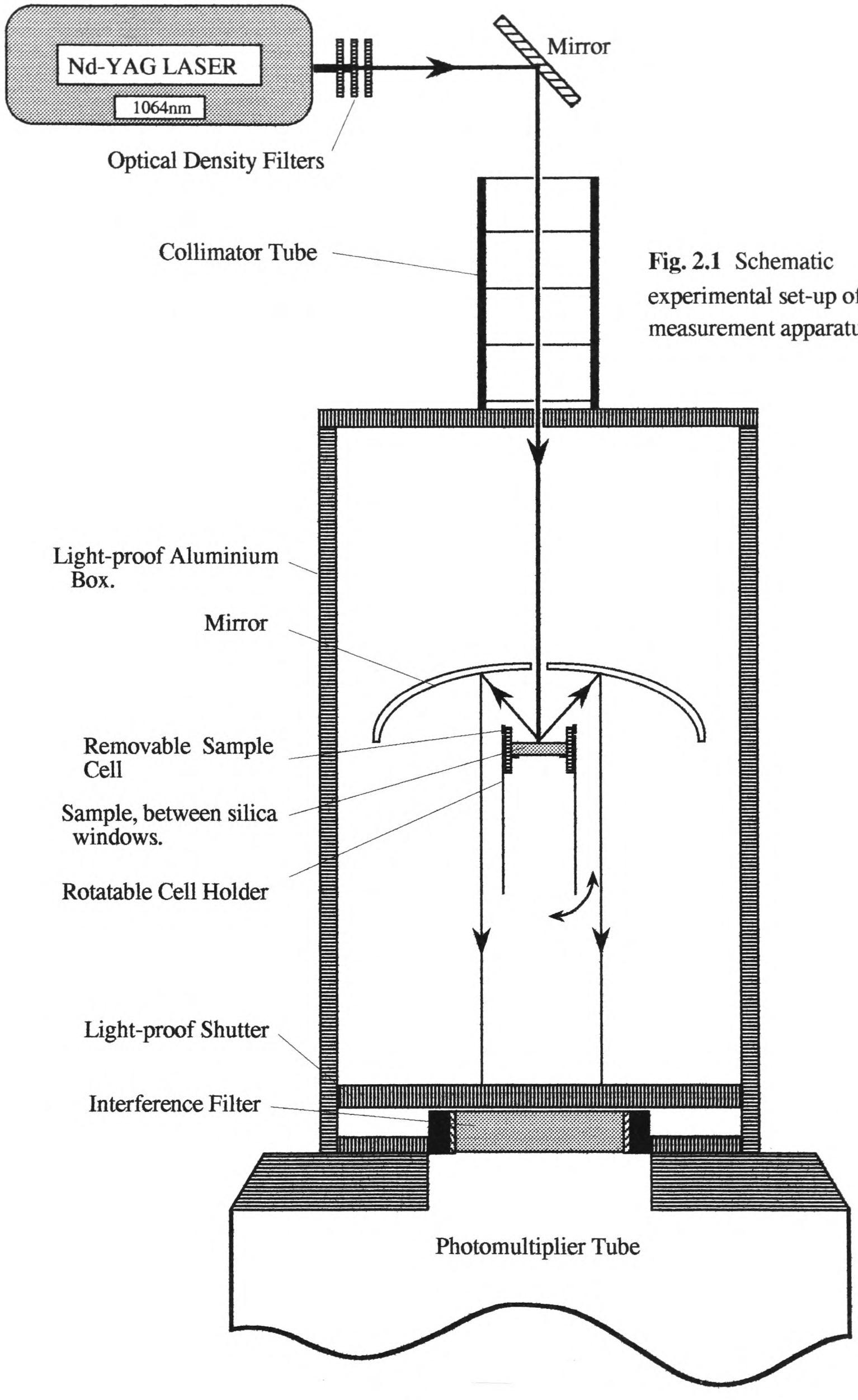
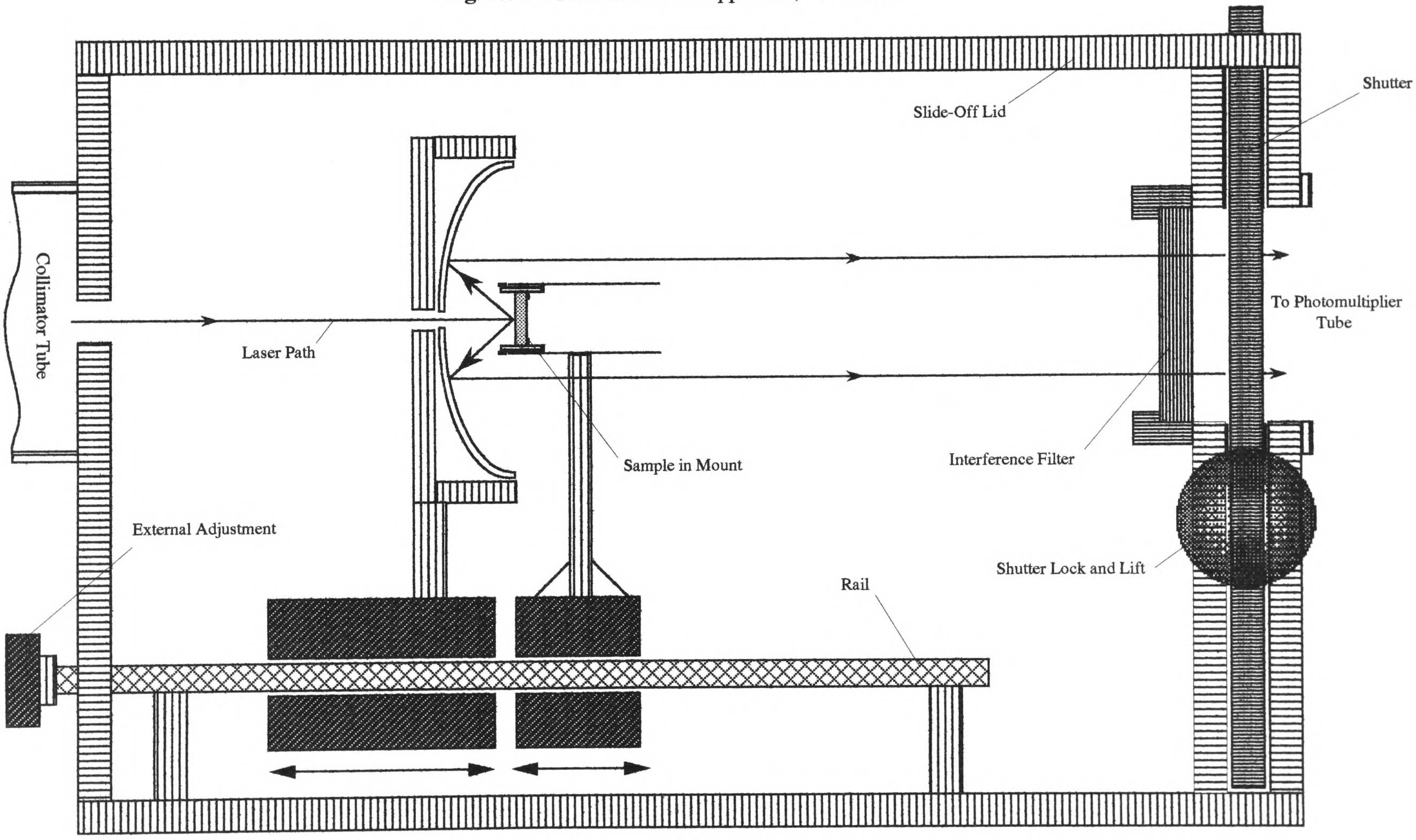


Fig. 2.1 Schematic experimental set-up of SHG measurement apparatus.

Fig. 2.2 SHG Measurement Apparatus, Side View



The apparatus was designed to use a variety of incident frequencies, from 1064 nm to 1900 nm, so in order for the incident light not to be attenuated by the sample holder, a suitable material had to be chosen for the face of the holder cell. At the incident frequencies, soda-lime, pyrex and silica glasses have similar properties, and absorption resonances do not occur at either 1900 or 1064nm. Silica windows would be required if the apparatus were to be used for third harmonic generation measurements and so this was chosen as the material for the cell face.

The sample holder had to be movable, for convenience, and was designed to rotate away from the mirror, so that samples could be removed easily. The sample holder was a tube, supported on a pedestal which was itself mounted on a racked carriage. The carriage could be racked from outside the box, allowing fine adjustments *in situ*. The sample holders had to be small, as they were supported in the main path of the mirror, and would otherwise obstruct the light.

The scattered light from the sample surface was reflected parallel to the incident beam, towards an interference filter. The signal contained much incident light which had to be filtered out before entering the photomultiplier tube, as the intensity of the light would increase the dark current level and damage the amplification circuitry. The reflected light was filtered by an interference filter which was centred on the second harmonic (532nm for 1064nm incident radiation). The filter has a band-width of 1nm providing the incident light was within 1° of the normal to the interference filter surface, so it was vitally important to set the sample at the exact focus of the collecting mirror.

The filtered second harmonic was detected by a photomultiplier tube, operating with an anode voltage in the region of 1.6 kV. Slight modifications were required for the computer interfacing. The amplified signal from the last dynode had the same response time as the laser pulse, and the computer analogue to digital interface settling time (the time that each event takes to record) was several orders of magnitude slower, so the pulse from the last dynode was fed into (without amplification) an Ortec Amplifier. The Ortec Amplifier is a simple capacitor charge/discharge integrator circuit which "slows down" the signal by allowing the charge from the last dynode (formed in 10ns) to be "dumped" into a

capacitor, and then the capacitor allowed to discharge through a resistor; the voltage across the resistor being followed by a high resistance buffer unity gain amplifier circuit, making the discharge time in the order of milliseconds. The area of the peak is directly proportional to the magnitude of the dynode pulse.

2.2.2 Signal processing

Two outputs were available for measurement; the integrated dynode output, as described above, and the amplified anode pulse. Initially, the integrated dynode output was used to check the pulse to pulse variation, by first digitizing the signal, summing a pre-determined number of laser pulses, and comparing these with the power output obtained from the photo-diode. The magnitude of the second harmonic is proportional to the square of the incident laser power, so for a given standard (e.g. 100 μ urea) the relationship should hold. The system was then calibrated for a known standard, the SH signal then recorded, and used for comparison with other standards and samples. It was found that the dynamic range of this set-up was not sufficient for the vast majority of samples since the SH signals of quartz (about 0.007 x urea) and 2-chloro-4-nitroaniline (8 x urea) could not be measured accurately on the same scale. To overcome the problem, the incident laser power was varied to tune the signal into the linear range of the photomultiplier tube, which would necessitate accurate calibration of neutral optical density filters, but would allow a much more accurate determination of the SH signal for a large range of efficiencies.

The use of a computer summing interface was not necessary once the apparatus had been calibrated. Measurements were then taken directly from a 1GHz Hewlett Packard summing oscilloscope. The maximum amplitude of the SH signal on the oscilloscope was proportional to the SH signal, as the duration of each laser pulse was constant. Pulse to pulse variation was reduced by summing continuously 64 individual pulses.

2.2.3 Calibration of the Optical Density Filters

The transmittance of each optical density filter used was measured on a Cary 17

absorption spectrometer, centred at 1064nm. Table 2.1 displays the deviation from the marked values. Equation 2.1 shows the relationship between incident light, I_i, and transmitted light, I_o, to the optical density of the filter.

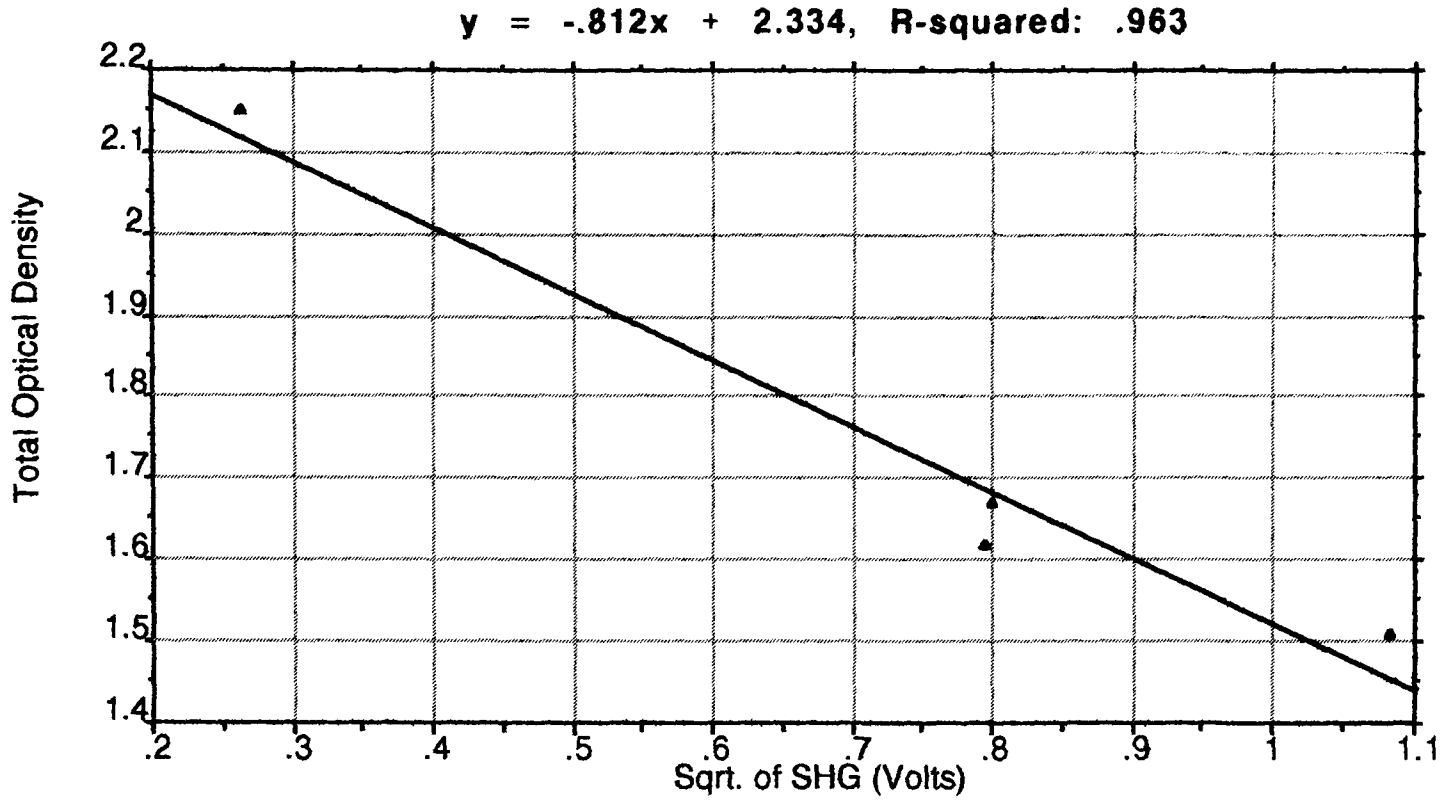
$$\text{Log}\left(\frac{I_o}{I_i}\right) = \text{Optical Density Of Filter} \tag{2.1}$$

Table 2.1 Results of the calibration of optical density filters at 1064 nm, compared to manufacturers specification.

Marked Optical Density:	Measured Optical Density:
0.1	0.11
0.2	0.48
0.3	0.64
0.4	1.03
1.0	1.50

To check the apparatus directly, a series of measurements was taken with urea as the standard, by altering the number of optical density filters in the path of the laser. A plot of the calculated incident light attenuated by the optical density filters versus the square root of the output voltage should show a linear response (see Fig. 2.3). The number of data points were restricted by the maximum amount of light which the P.M.T. could measure, which was set to be equivalent to 5 V output, and the maximum number of permutations of calibrated optical density filters that could be used within the dynamic range of 5 V.

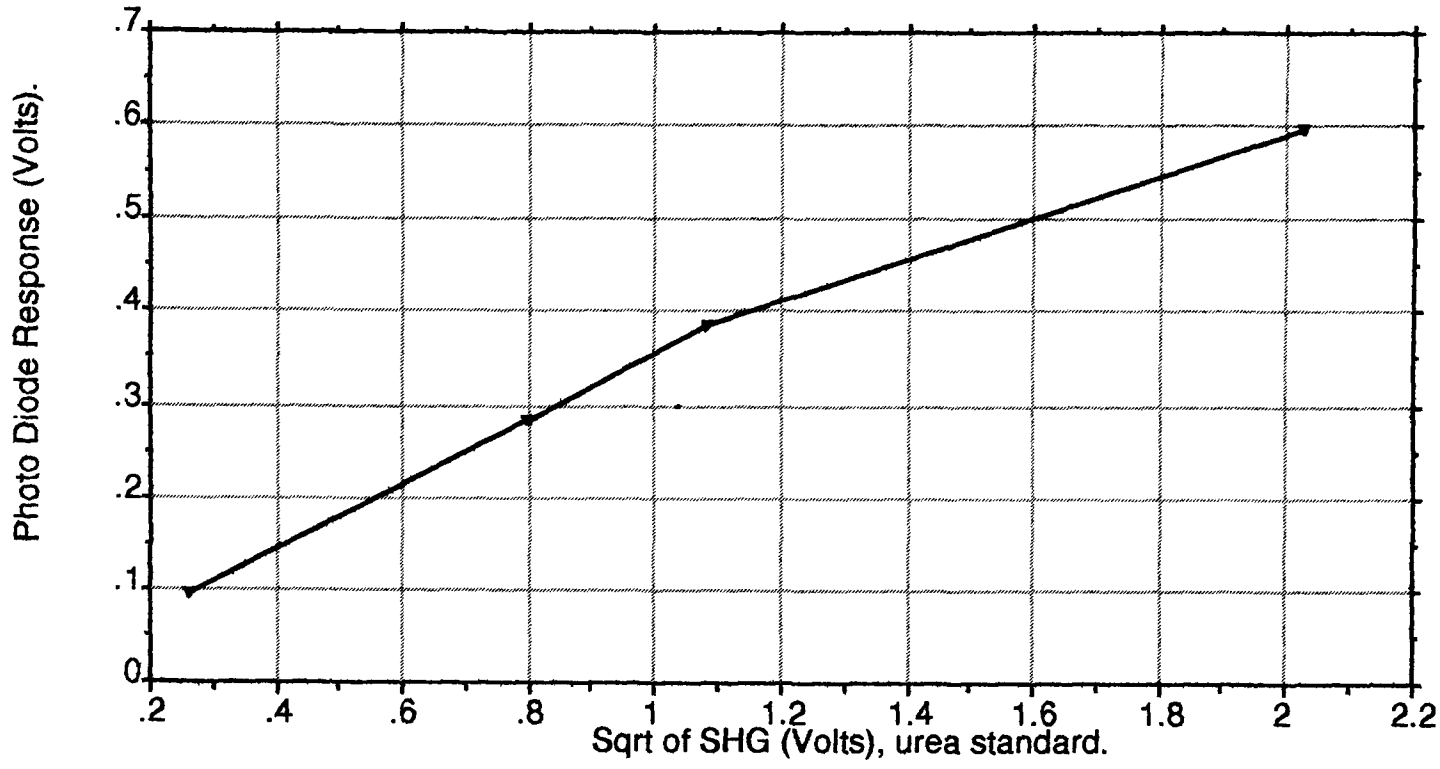
Fig. 2.3 Measured response of photomultiplier tube to the second harmonic generated by a urea standard versus differing attenuation achieved by calibrated optical density filters.



2.2.4 Response of the Photomultiplier Tube

Using the same set-up as for the measurement of the optical density filters above, the incident radiation, after attenuation, was measured using a sensitive photo diode. The SH derived from a urea sample, with various incident powers, was measured, Fig. 2.4 shows the response curve of the photomultiplier tube, which was taken to be linear if the output voltage from the anode (observed SHG) was less than one volt.

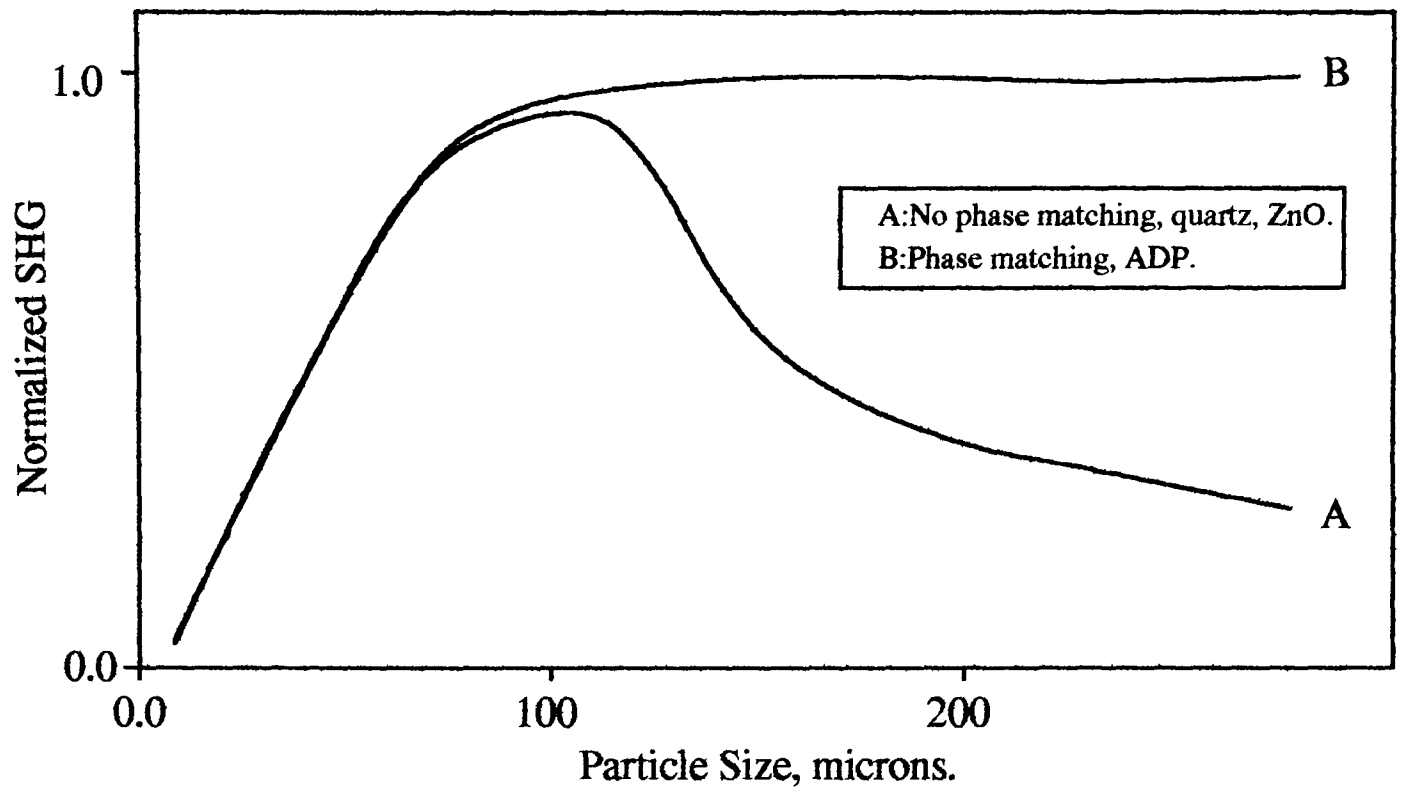
Fig. 2.4 Photo diode response (therefore power) versus the square root of the measured second harmonic generated by a urea standard. Showing that the the linear region for measurement of second harmonic signals occurred when the output from the photomultiplier tube was less than one volt.



2.2.5 Calibration

The dynamic range of the SH measurements required a series of compounds with equally varied efficiencies with which to calibrate the system. Standards had to be ground to the same size as quoted for that particular SH measurement. Those compounds which have phase matching properties were ideal, as the SH becomes independent of the size of particles when the particle size exceeds the coherence length (see Fig. 2.5).[118]

Fig. 2.5 The relationship between the magnitude of the second harmonic and particles size for materials that, A, show no phase matching and B, show phase matching. The coherence length is shown here at about 100 microns.



However, those compounds with SHG larger than about 2 x urea have inherent phase-matching properties, and it was necessary for these compounds to be ground to a standard size. This effect was most noticeable with 2-methyl-4-nitroaniline, and 2-chloro-4-nitroaniline. The SH signal of compounds also varied slightly due to the solvent system they were crystallized from, but this effect was too small to be of significance. Table 2.2 shows the effect of particle size on the efficiency of several standard compounds.

2.3 Further Errors Associated with SHG Measurements

Neglecting the variations between samples caused by differences in morphology, solvent of crystallization, phase matching, and size of particle, errors caused by placement of sample and rotation of sample were examined. Removal and replacement of sample, caused a maximum variation in the relative SHG of urea to be < 1%. The deviation from non-linearity of the optical density filters and the photomultiplier tube gave rise to ± 6% error. Slight rotation of the sample cell away from the central axis caused an error of ±

7%, and this was easily solved by locking the sample cell in position with a sprung-catch. The maximum error due to equipment alone was thus reduced to ± 7% of the SHG signal.

Table 2.2 Comparison of the reported second harmonic generation efficiencies for selected standard compounds and those measured by the apparatus described in this Chapter.

	Efficiency, x Urea		
Compound:	Literature value, 100 μ particle size. From ref. 47	Standard compounds measured by the method described above	Powder size of samples.
Sand (silica)	0.05-0.01	0.2	Unsized
KDP	0.333	0.63	Unsized
	-----	0.34	100μ
ADP	0.366	0.6	Unsized
	-----	0.34	100μ
Urea	1.00 def	1.00	100μ
	-----	0.71	<125μ
	-----	0.89	125-417μ
	-----	0.98	1/2 mm
4-Nitrocatechol	6	1.46	Unsized
2-Chloro-4-nitroaniline	0.4-16.6 *	1.7	Unsized
2-Methyl-4-nitroaniline	6.6-17.6	2.60	Unsized
	-----	8.55	100μ

* The measurements were done on single crystals, where $\chi^{(2)}_{ijk}$ compared to $\chi^{(2)}_{ijk}$ of KDP in references 179 and 187.

2.3.1 Pseudo Second Harmonic Signals

A second harmonic signal can be caused by other processes including luminescence and higher - order non-linear effects. The response times for the three electromagnetic interactions are in the order; 2 photon absorption >> magnetic (and quadrupole)[140] effects >> electronic (SHG, Pockels, Kerr), where >> means longer than. Luminescence or fluorescence occurs with compounds which have a low or zero SHG signal, and when the incident radiation is increased to the maximum level. The oscilloscope trace of the SH shows a tailing, extending long after the laser pulse has stopped. When luminescence occurs, the second harmonic signal is masked by a broader signal due to other processes, and the measurement of the SHG efficiency is then not possible.

The compound, $[PtCO_3(PPh_3)_2]$ was observed to have an SHG response of 0.1 x urea at a laser power of 0.93 mJ, but when the power was reduced by half, the SH signal became effectively zero. This effect was due to a much higher order process. To ascertain that the signal observed was a second harmonic derived from a second-order process, the incident power was varied, and a new measurement taken which should have a second order relationship to the first. This confirmation of second-order processes is often neglected in literature measurements.

2.3.2 Residual Second Harmonic Signals in Centrosymmetric Media

Residual SHG signals have been reported for compounds which have been found to crystallize in a centrosymmetric space groups. Many reasons for these observations have been proposed but not elucidated, they include polymorphism, spontaneous crystallization in a non-centrosymmetric manner, slight rotational alterations within a repeating lattice and surface effects.[13,122,140,209] Undoubtedly, in some cases, the measurements have been done so that luminescence and higher order effects have not been taken into account. The SH efficiency of 4-nitrophenol has been quoted as 0.7 x mNA (= 0.28 x urea),[164] subsequent measurements in this laboratory have shown that the efficiency is almost zero, and the crystal structure is known to be centrosymmetric. The largest

reported anomalous signal was for 2,4,6-trinitro-1,3,5-triaminobenzene which crystallizes in the centric space group $P\bar{1}$, but shows a powder efficiency of 3 x urea.[122] The maximum known centric SHG response measured in this Thesis was 1.33 x urea for a tin catecholate complex (see Appendix 1).

Second harmonic generation is not strictly forbidden in centrosymmetric media,[107] it has been shown that weak, non-local terms are symmetry allowed (see also Chapter Four of this Thesis).[23] In all centrosymmetric media, the surface has non-centric properties, and it can be shown that for a generalized set-up the number of second harmonic photons emitted from a surface per second is given by:

$$S(2\omega) = \left[\frac{(32\pi^4\omega)}{hc^3}\right]\frac{\mathrm{Sec}^2\theta P_1^2}{A_1 TR}\left|\chi^{(2)}_{s,eff}\right|^2 \qquad (2,2)$$

Where P_1 is the laser power, T the pulse duration, R the repetition rate, A_1 the area, θ the angle of incidence to the surface, and for a typical laser P_1 = 1 Watt, T = 10 ns, R = 10 Hz, A_1 = 1 cm^2, $\lambda = 2\pi c/\omega$ = 1μm, and assumed detection limit of 10 photons per second, so the minimum detectable $\chi^{(2)}_{s,eff}$ is in the range of 1 x 10^{-17}esu.[48] This detection level is sufficient to analyze the orientations of monolayers on various surfaces, including metals. For comparison, the d_{11} coefficient is 1.19 x 10^{-9} esu (0.5 pmV^{-1}) for quartz, which gives a powder SHG efficiency of 0.05 to 0.014 x urea.

Langmuir-Blodgett films comprising of head to tail packing of 2 x 20 molecular layers of 4-[N-(4-carboxypentyl)-N-methylamino]-4'-nitrostilbene gave a relative SHG of 0.3 x KDP (= 0.1 x urea, taking KDP = 0.333 x urea), extrapolating from the thickness of the KDP standard, the efficiency was 2.3 x 10^3 times as effective as the standard, KDP (= 766 x urea).[14] From this example, it is easy to see that slight asymmetry in the surface layers of centric compounds with a large hyperpolarizability constant, β, will give rise to trace SHG efficiencies of around 0.1 x urea as observed in some cases.

2.4 The Calculation of the Hyperpolarizabilities of Some Organic Compounds from Solvatochromism Measurements

2.4.1 Introduction

The most reliable method of determining the absolute magnitude of the molecular hyperpolarizability constant, β, for any system, may be done using the EFISH method.[81] This method is experimentally difficult to perform, and requires the compound under investigation to be soluble in a non-conducting, non-polar solvent, to have an appreciable dipole moment and also to have the correct optical transparency at the second harmonic frequency. The solvatochromism method for determining β has not been well described, [34,104,165] but is based on the calculation of the excited state dipole moment from the shifts in λ_{max} of the electronic spectrum as the "polarity" of the solvent is varied. Thus almost any compound which is soluble in organic solvents and has an appreciable dipole, may be investigated. The results are simple to calculate, but do have a larger uncertainty than EFISH measurements.

The hyperpolarizability constant, β_Q, where Q is the stated band, e.g. first or second charge transfer band, is given by the simplified, and therefore inexact equation;

$$\beta_{CT} = \left(\frac{3e^2 \hbar^2}{2m} \right) \frac{W}{\left[W^2 - (2\hbar\omega)^2 \right] \left[W^2 - (\hbar\omega)^2 \right]} f \Delta\mu_{ex} \qquad (2.3)$$

Equation (2.3) has been simplified further by calibration using results derived from 4-nitroaniline as an almost ideal charge-transfer compound. β must be in one series of units, and can be converted using the following factors:[34]

$$\beta \left(\text{SI in } m^4 V^{-1} \right) = \beta \frac{4}{3} \pi \times 10^{-10} \left(\text{CGS in cm}^5 \text{esu}^{-1} \right)$$

$$\text{which} = x \left[4.189 \times 10^{-10} \right]$$

and

$$\beta\left(C^{3}J^{-2}m^{3}\right)=3.7\times10^{-21}\,\beta\left(cm^{5}esu^{-1}\right)$$

$$\beta_{CT}=(P)\frac{W}{\left[W^{2}-(2\hbar\omega)^{2}\right]\left[W^{2}-(\hbar\omega)^{2}\right]}f\Delta\mu_{ex}$$

(2.4)

W is the energy of the transition in joules, and is obtained directly from the electronic spectrum in a specified solvent. To be strictly accurate, this value should be for the molecule in the gas phase, otherwise the value of λ_{max} in the lowest polarity solvent should be used.

$\hbar\omega$ is the fundamental (LASER) photon energy, and is 1.868×10^{-19} J (or 1.17eV) for a Nd/YAG laser at 1.064 μm.

f is the oscillator strength and is the fraction of electrons involved in the transition. Chako *et al* [46] have estimated that for a solute in solution, giving a narrow band-width, the oscillator strength is given by:

$$f_{solution}=\frac{Cm\nu^{2}\eta}{\pi e^{2}N}\int\varepsilon\,d\nu$$

(2.5)

For a gas, the correction factor, η, which is the refractive index of the solution, becomes unity so

$$f_{gas}=\frac{Cm\nu^{2}}{\pi e^{2}N}\int\varepsilon\,d\nu$$

(2.6)

If f is calculated so that the molecules in solution act as if they were in a gas then :

$$f = \frac{9\eta}{\left(\eta^2 + 2\right)^2} \frac{Cmv^2}{\pi e^2 N} \int \varepsilon \, dv$$

(2.7)

where η is the refractive index of the solution; e is the charge of an electron (1.602×10^{-19} C); m is electron mass (9.109×10^{-31} Kg); C is the speed of light (3×10^8 mS^{-1}); N is Avogadro's number (6.02×10^{23}); v is the frequency of the transition in Hz of the λ_{max} of the band in a "transparent" solvent; $\int \varepsilon \, dv$ is in Hz, and was calculated directly from the area under the electronic spectrum curve, and was calibrated for 4-nitroaniline having an oscillator strength of 0.51 in hexane.[162] Nitrobenzene has a literature value of f = 0.193 (for band = 251.5nm)[46] and by the method outlined above, nitrobenzene was calculated to have f = 0.17 for the same band.

$\Delta\mu_{ex}$ is the change in the dipole moment on excitation to a specified energy level, and is in Cm. The various models used for the calculation of $\Delta\mu_{ex}$ from electronic spectra have been surveyed by Koutek, [117] and has proposed the following refined equation:

$$\Delta E = \frac{-2\mu_g \Delta\mu}{4\pi \varepsilon_0 a^3}\left[A''\right] - \frac{\left(\mu_{ex}^2 - \mu_g^2\right)}{4\pi \varepsilon_0 a^3}\left[B''\right]$$

(2.8)

where A" and B" are constants for each solvent used, and are given by:

$$A'' = \left[\frac{X + Y - 2\varepsilon_s - 1}{X - Y + \varepsilon_s + 2} - \frac{\eta_s^2 - 1}{\eta_s^2 + 2}\right] \qquad \text{and} \qquad B'' = \left[\frac{\eta_s^2 - 1}{2\eta_s^2 + 2}\right]$$

$$\text{where } X = 0.5\varepsilon_s \text{Ln}\varepsilon_s \text{ and } Y = 3\left(\varepsilon_s - 1\right)\left(\text{Ln}\varepsilon_s\right)^{-1}$$

Terms: μ_g is the ground state dipole, Cm; μ_{ex} is the excited state dipole moment, Cm; ε_s is the solvent dielectric constant; ε_0 is 8.85×10^{-12} Fm^{-1}; a is the molecular cavity radius, determined by calculation of molecular volume from density, m; $\Delta\mu$ is the dipole change on excitation, Cm; ΔE is the energy change on going from a LOW to HIGH solvent polarity giving a negative number for RED shifts; η_s is the solvent refractive index.

Equation (2.8) is only valid for a system that changes from gas phase to solution. The measurement of electronic spectra in the gas phase is difficult, and so by measuring the electronic spectra in two solvents with differing polarity, the gas phase terms may be eliminated. It is assumed that changes in μ_g , μ_{ex} and a^3 are small with respect to the change in solvent, and that variations in $\Delta\mu$ $(= \mu_{ex}-\mu_g)$, are also constant within the error of the calculation. So for two solvents, defined with subscripts 1 and 2, the change in excitation energies is given by:

$$\Delta E_2 - \Delta E_1 = P^* \left\{ \frac{1}{4\pi\varepsilon_0 a^3} \right\} \left\{ \left[2\Delta\mu\mu_g \left(A_1'' - A_2'' + B_1'' - B_2'' \right) \right] + \Delta\mu^2 \left(B_1'' - B_2'' \right) \right\} \tag{2.9}$$

Terms: $\Delta E_2 - \Delta E_1$: The difference in the λ_{max} values for the two solvents, calculated in Joules, the value of ΔE is negative for red shifts with a change from low to high "polarity". ε_0 : 8.85 x 10^{-12} Fm^{-1}. a^3 : The molecular cavity radius - determined by calculation from either the density of the material, or from CNDOVSB calculations, in metre units. $\Delta\mu/\mu_g$: The dipole change and the ground-state dipole, quoted in Cm, where 1Debye = 3.33 x 10^{-30} Cm. ε_s : The solvent dielectric constant. η : The solvent refractive index. P^* is the calibration factor, and for 4-nitroaniline, is equal to 1.55 x 10^{22}.

Table 2.3 shows a comparison between cited literature values for the excited state dipole moments and those calculated from solvatochromism data.[130]

Table 2.3 Density, molecular cavity radius and measured excited state dipole moments of reference compounds, and comparison with cited literature values.[162]

Compound	Density, gcm^{-3}	a , 10^{-10}m	$\Delta\mu_{ex}$, 10^{-29}Cm	L.V. $\Delta\mu_{ex}$, 10^{-29}Cm
p-Nitroaniline	1.424	3.38	4.49	4.10
o-Nitroaniline	1.442	3.36	1.62	3.33
m-Nitroaniline	1.43	3.37	2.38	4.03
Nitrobenzene	1.196	3.44	1.09	1.69

Table 2.4 summarizes the results for some simple organic compounds.

2.4.2 Errors Within the Solvatochromic Method for the Determination of β

Equation (2.4) is only an approximation, and calculates the contribution to β from the electronic transition state taken, and for 4-nitroaniline the charge transfer band contributes 75% of the total β, while for other molecules, this value is lower. The effect of including more excited states in the calculation of β is admirably demonstrated by Morley *et al* [144] where, for polyenes, the initial β value oscillates from +100% to -50% of the final value. In the case of polyphenols, this oscillation is smaller.

There are few reported solvatochromism measurements of β, but Broussoux *et al*[34] have reported that the β value for 4-nitroaniline was 24 x 10^{-40} m^4V^{-1} (5.73 x 10^{-30} cm^5esu^{-1}) which compares to 129 x 10^{-40} m^4V^{-1} (30.9 x 10^{-30} cm^5esu^{-1}) by the calculations outlined here.

The CNDOVSB calculations were performed on molecular structures obtained from or built from structures listed in the Cambridge Structural Database using the VIKING 5.0 molecular modelling package developed by Dr J.O. Morley of ICI, Manchester.[47,108]

Table 2.4 Comparison of the second order hyperpolarizabilities calculated from several sources for some selected organic compounds. The solvatochromism data were obtained by the method described in this Thesis. $\times 10^{-40}$ m^4V^{-1}

Compound:	EFISH (Ref)	CNDOVSB (Ref)	Solvatochromism (±80%)	
Aniline	3.73 (1) 5.15 4.61 6.20	10.2 (2)	--	
Nitrobenzene	8.38	4.52	1.07	Hex
2-Nitroaniline	42.7	25.6	3.77	Hex
3-Nitroaniline	25.1	19.3	3.36	Hex
4-Nitroaniline	49.4 70.8 145 151	55.7	130	Hex
2-Chloro-4-nitroaniline	142 (2)	45.7 (2)	36.0	DCM
2-Methyl-4-nitroaniline	70.0 (1)	57.4	118	DCM

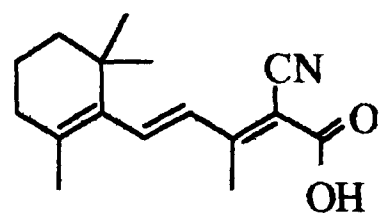
Solvents: HEX, hexane; DCM, dichloromethane. (1) = ref. 47, (2) = ref. 69.

2.4.3 Discussion

It is assumed in these calculations that the most significant, lowest energy transition seen in the electronic spectrum is wholly responsible for the charge transfer on excitation. The minimum oscillator strength being 0.05, and for a conversion to the extinction coefficient see equation (2.7). This assumption is about 75% correct in the ideal case of 4-nitroaniline,[47] but breaks down for more complex molecules such as 2-nitroaniline and 2-chloro-4-nitroaniline. The direction of the charge transfer in 2-nitroaniline is not aligned along the ground state dipolar axis and has an EFISH β value of 42.7 x 10^{-40} m^4V^{-1}. Whereas the value measured by solvatochromism was 3.77 x 10^{-40} m^4V^{-1}, 9% of the

EFISH value which is outside the limits of the experimental error of the EFISH technique.[47,69,143,144]

β-Ionylidenecyanoacetic acid is a compound with 3 double bonds, with a predicted dipole of 2.52 x 10^{-29} Cm (CNDOVSB), and molecular structure:



The molecular cavity radius of 3.96 x 10^{-10} m is determined from the same CNDOVSB calculations, or from knowing the density of the compound. Two electronic spectra are taken in solvents of suitable polarity, the greater the difference the better. In this case in methanol and dichloromethane. For each electronic spectrum, ε_0 values for λ_{max} are calculated. The area of the most significant lowest energy transition in the solvent with lowest polarity (nearest to the gas-phase situation) is measured by cutting out the peak, weighing, and by knowing the mass/area, $\int \varepsilon \, dv$ is calculated which is here equal to 7.35 x 10^{20}. $\Delta E = 8.33 \times 10^{-20}$J, W = 5.6 x 10^{-19} J, $\Delta\mu = 7.10 \times 10^{-29}$Cm, $\nu_{CT} = 84.5 \times 10^{15}$ Hz, f = 0.5 gives a $|\beta|$ of 170 x 10^{-40} m^4V^{-1}, compared to the CNDOVSB model which gave $\beta = 34.4 \times 10^{-40}$ m^4V^{-1}. For a FORTRAN program of the calculation, see Appendix 2.

The difference of 80% between cited literature values and those calculated from solvatochromic data is common. Both values of β suggest that the SHG response of β-ionylidenecyanoacetic acid will be in the order of 10-20 x urea, equivalent to that of 2-methyl-4-nitroaniline.[47]

2.5 Conclusion

This chapter described the design, implementation and calibration of apparatus for measurements of the second harmonic generating efficiency of solids based on the Kurtz powder technique, and a solvatochromic method of determining the magnitude of the second-order hyperpolarizability constant β.

The modified Kurtz powder technique for second harmonic measurements gave reliable and easily reproduced results for materials which had been ground to a standard size (equipment error measured as ± 7%). The method was also efficient for screening a large number of unsized samples. However, the samples must have a degree of asymmetry - either from the structure of the crystal or induced by poling or by a host molecule. The size of the SHG response depends also on the degree of impurity of the sample, from which solvent it has been crystallized, and the nature of the sample (powder or crystalline).

The powder SHG results cannot be taken as a definitive test for non-centrosymmetric compounds as certain centric compounds show a residual SH in the range of 0.5 to 1.5 x urea. The origin of this effect has not been explained but has been ascribed as the result of spontaneous asymmetric polymorphism, surface interactions[99,169] or quadrupole resonance effects. Not all SH signals are caused by a second-order process and this problem can be eliminated by altering the incident power, and noting if the effect on the induced SH was second order or not. The effects caused by luminescence and fluorescence generally occur at high incident powers and give rise to signals which do not decay in the time span of the laser pulse (10-15 ns).

Measurement of the hyperpolarizability constant, β, can only be done reliably using the EFISH technique. However, the range of published results for 4-nitroaniline shows there to be a certain degree of uncertainty with errors quoted to be ±15 to ±20% (see Table 2.3). Furthermore, there is no requirement for the material under test to be in a non-centrosymmetric state, which is also true for the solvatochromism technique described in this chapter. However, unlike the EFISH technique, solvatochromism measurements can only be considered as an approximate indication of the magnitude of β, as solvatochromism results deviate up to 80% from the stated literature EFISH values.

The solvatochromic method has certain advantages; the technique is simple and does not require expensive apparatus; it can be done on any compound which is soluble in a non-polar solvent; and the materials under test do not have to crystallize in a non-centrosymmetric space group.

CHAPTER THREE

Synthesis, Structure and Non-linear Optical Properties of Co-ordination Compounds Based on Pentadionato-Compounds.

3.1 Introduction

In recent years considerable success has been achieved in designing organic materials which display non-linear optical properties.[47] The molecular requirements for maximizing the non-linear properties of organic molecules are well defined and the introduction of appropriate donor and acceptor functional groups into conjugated organic molecules can be achieved using conventional synthetic procedures. There are additional crystallographic requirements. Firstly the molecules must pack in a non-centrosymmetric space group and, secondly for powder samples, they must satisfy phase matching criteria by packing close to a particular inclination to the principal symmetry axis. These requirements are difficult to achieve in practice.[78] Recently, some attempts have been made to transfer these molecular design concepts to coordination and organometallic compounds:

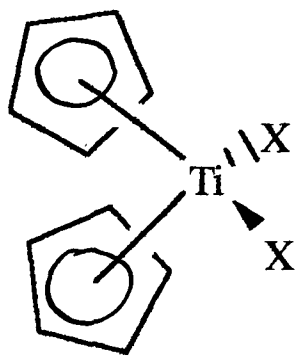
In 1987 the compound (Z)-[1-ferrocenyl-2-(4-nitrophenyl) ethylene] was found to have an SHG efficiency of 62 x urea at 1907 nm.[88] Until this date, very little research had been done into the possibility of using organometallic compounds for second harmonic generation. At the same time Eaton *et al* [75-77] and Anderson *et al* [7] were investigating organometallic inclusion compounds of thiourea with metallo-carbonyls, the most efficient inclusion compound being 3[(η-benzene)tricarbonylchromium)]:1(thiourea) which had an SHG efficiency of 2.3 times urea (@ 1064 nm).

Interest grew and in the following year (1988), many new potential NLO areas were investigated. Tam *et al* [197, 198] looked into polymers composed of Pd(0) and Pt(0) coupled to aromatic hydrocarbons of the form $MX(Ar\text{-}NO_2)(PEt_3)_2$. Frazier *et al* [81] used a palladium centre to synthesize Langmuir-Blodgett films composed of palladium poly-

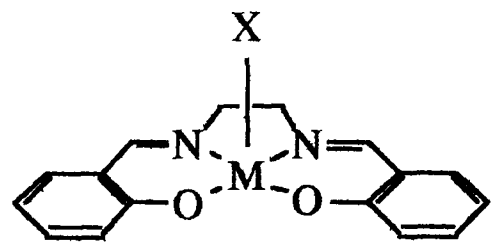
ynes. Other workers were starting to explore alternative metals such as cadmium, mercury, zinc, nickel and lead. Tao *et al* [200] synthesized thio-semicarbazide cadmium chloride monohydrate [$Cd(NH_2CSNNH_2)Cl_2.H_2O$], which showed an efficiency of about five times urea. His work was followed by a series of compounds based on the tri-allylthiourea cadmium and mercury chlorides and thiocyanates, the efficiency of these salts being around three times urea.[201, 221, 223-225]

In 1989 chiral octahedral Mo centres were used to direct the symmetry of (η^5-C_5H_5)Fe(η^5-C_5H_4)- ligands to produce complexes with SHG efficiencies of 123 x urea (at 1906nm).[55] In 1989/90 some effort was made to devise a theoretical model which would explain the optical properties of organometallic compounds.[220,202e]

In 1990 the search for NLO organometallic compounds was extended to polymeric titanium acetylides made up from $(C_5H_5)_2TiX_2$ where X are the bridging -C≡C- groups, and polymeric systems using (SALEN)MX monomers, which bridge through the apical ligand X, where M is Cr, Mn, Fe and Co; some of the polar materials showed weak SHG properties at 1064 nm:[202a]

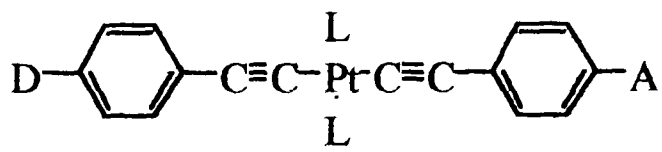


$(C_5H_5)_2TiX_2$



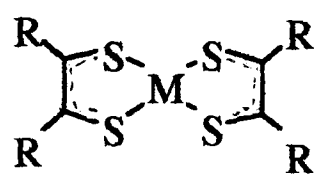
(SALEN)MX

Marder *et al* [202b] investigated platinum acetylenes which were first investigated as polymers by Frazier and Tam, and discovered that all the non-symmetric *trans*-bis(acetylide) complexes so far examined exhibited SHG approximately 0.25 x urea. There was no indication of any interaction from the donor group to the conjugated benzene ring, but there was evidence of metal to ligand charge transfer processes in these complexes:



Polymers of a similar nature to the Pt and Pd analogues described by Frazier and Tam [202d] were synthesized from novel octahedral Rh complexes for $\chi^{(3)}$ active materials while Blau *et al* [21] studied the third order optical properties of metal diacetylides.

Metal dithiolenes, using Ni, Pd or Pt, have been investigated as potential materials for resonance enhanced third order processes such as degenerate four wave mixing, self focussing and two photon absorption:[202c]



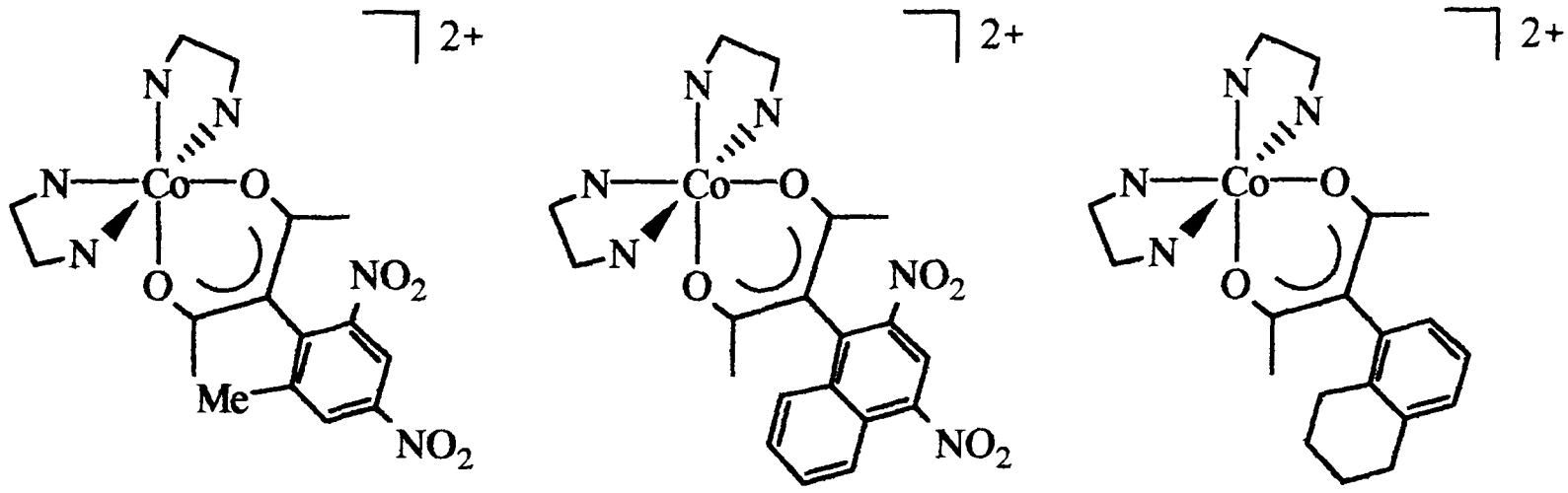
Metal Dithiolene

More recent investigations into the SHG properties of organometallic and coordination compounds are summarised in references 13, 39, 85, 89, 90, 142, 180 and 199.

This Chapter describes the theoretical prediction, synthesis and characterization of substituted metal pentadionato- complexes which represented reasonable target molecules for non-linear optical measurements. These complexes were chosen for the following reasons: (a) thermally stable pentadionato- complexes have been reported for the majority of metals; [40, 173] (b) the pseudo-aromatic nature of the metal pentadionato- ring can provide a range of derivatives *via* electrophilic substitution reactions [59,61] and, (c) a wide range of conjugated pentadionato- ligands can be synthesized.[11,12,16,57,58,174,193]

The complex [(-)-3-(6-methyl-2,4-dinitrophenyl)pentane-2,4-dionato][tris(2-aminoethylamine]cobalt(III) dibromide dihydrate has been resolved into its enantiomers which show optical activity (see Fig. 3.1 compound I).[148-151] The optical activity has been attributed to the restricted rotation of the 2,4-dinitrophenyl- ring and is termed atropisomerism. However, the 2,4-dinitro- ring rotates when in solution and the enantiomer slowly racemizes. If larger substituted naphthalene groups are introduced at the 3- position, the spontaneous racemization does not occur (see Fig. 3.1 compounds II and III).

Fig. 3.1 Chiral octahedral cobalt(III) compounds showing atropisomerism. From refs. 149-151.



I II III

Complexes of the type [3-substituted-pentane-2,4-dionato][tris(2-amino-ethylamine]cobalt(III) dihalides are violet in colour, and show intense electronic absorptions in the region of 532 nm and, therefore, second-harmonic generation measurements done at 1064 nm are not possible. The complex[(-)-3-(6-methyl-2,4-dinitrophenyl)pentane-2,4-dionato][tris(2-aminoethylamine]cobalt(III) dibromide dihydrate crystallizes in the space group $P2_1$ which, under ideal conditions, is one of the best space groups for SHG.[47] The second harmonic generation properties of this complex have not been measured. Some pentadionato- compounds show strong solvatochromic behaviour such as [Cu(tetramethylethylenediamine)(pentane-2,4-dionato)][NO_3].[178,186] It was hoped that the properties of atropisomerism and charge transfer could be combined using suitable pentane-2,4-dionato- ligands coordinated to metals. Such complexes have been prepared and characterized by conventional analytical, spectroscopic and, in some cases, X-ray crystallographic techniques. Their non-linear optical properties have been probed directly on powdered samples using a modification of the Kurtz powder second harmonic generation experiment [118] and indirectly by CNDOVSB calculations and solvatochromism measurements.

3.2 CNDOVSB Calculations on Pentane-2,4-dionato- Ligands

A series of potential synthetic target ligands were built up using the VIKING (5) molecular modelling graphics system from the crystal structure of difluoro(benzoylacetonato)boron [94] and [(-)-3-(6-methyl-2,4-dinitrophenyl)-pentane-2,4-dionato][tris(2-aminoethyl)-amine]cobalt(III) dibromide dihydrate. [148]

Difluoro(benzoylacetonato)boron is essentially planar, with F- atoms projecting out of the molecular plane and belongs to the P_{nam} space group. The predicted structures were then optimized using An Energy and Structure Optimization Program (AESOP), and CNDOVSB calculations performed for the optimized structures. Tables 3.1 A and 3.1 B are a summary of CNDOVSB results for some pentane-2,4-dionate target compounds. The last column in Table 3.1 is the ratio of the second-order hyperpolarizability constant $\beta_{(x)}$, to the molecular volume in $Å^3$. This value is an indication of the potential efficiency in a molecular solid as it takes into account the molecular dilution effect. The compound 4-nitroaniline has $[\beta_{(x)}/Å^3] \times 10^{-40}$ equal to 0.51, and for commercial viability potential compounds should have the quantity $[\beta_{(x)}/Å^3]$ equal to or above this value.

CNDOVSB calculations provide an indication of the magnitude of the molecular hyperpolarizability $\beta_{(x)}$ and shows that for 4-substituted-benzoylacetone compounds the introduction of either an electron donating group (such as MeO-) or an electron withdrawing group (O_2N-) into the molecule will increase the magnitude of $\beta_{(x)}$. Benzoylacetone, (III.1), has $\beta_{(x)} = 10.1 \times 10^{-40}$ while 4-nitrobenzoylacetone, (III.2), has $\beta_{(x)} = 39.8 \times 10^{-40}$ and for 4-methoxybenzoylacetone - enolate, (III.5), $\beta_{(x)} = 52.3 \times 10^{-40}$ m^4V^{-1}. Co-ordination compounds using these ligands were synthesized as part of the research reported in this Thesis.

Table 3.1 B shows the results from CNDOVSB calculations based on more complex pentane-2,4-dionate ligands. Compounds (III.10) to (III.12) were based on the crystal structure of [(-)-3-(6-methyl-2,4-dinitrophenyl)-pentane-2,4-dionato]-[tris(2-aminoethyl)-amine]cobalt(III) dibromide dihydrate were obtained by introducing an sp^3 carbon atom at the 3 position. Geometric isomers were obtained by rotation of the C-C

Table 3.1A

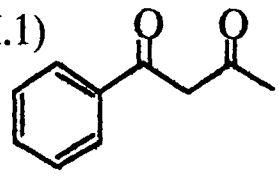
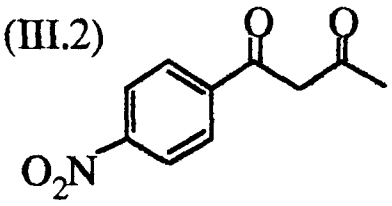
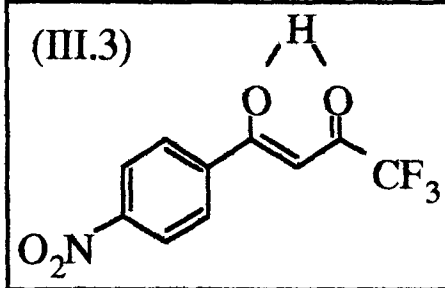
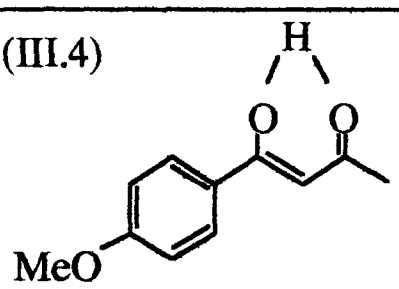
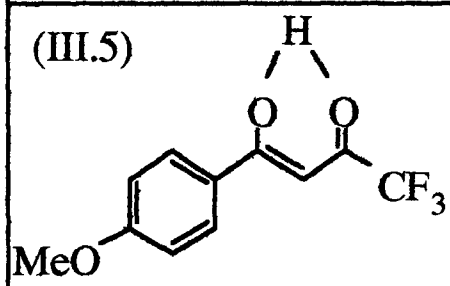
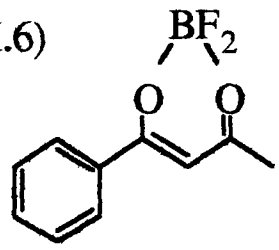
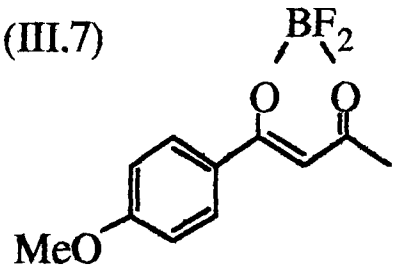
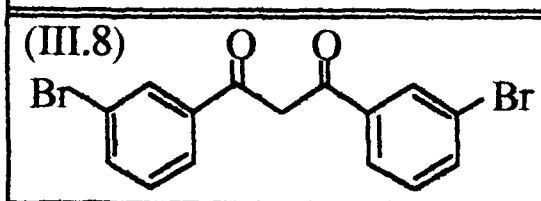
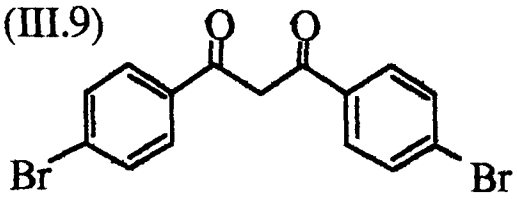
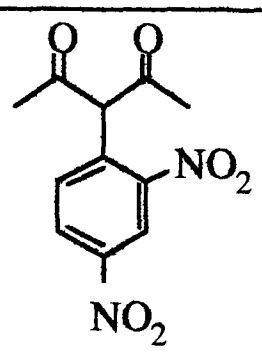
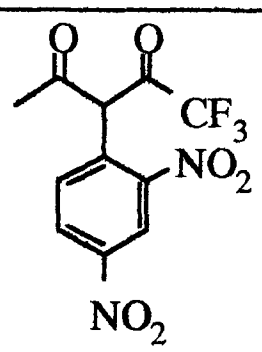
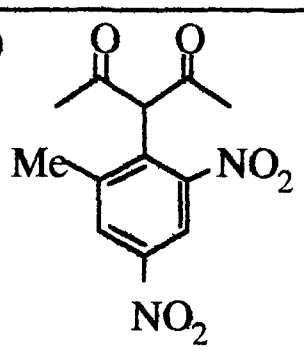
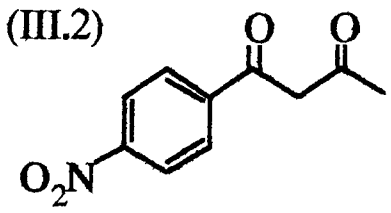
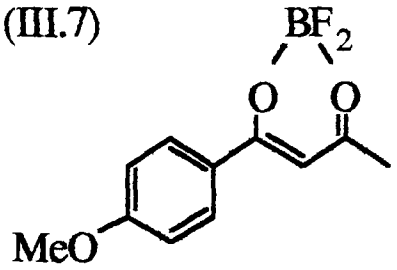
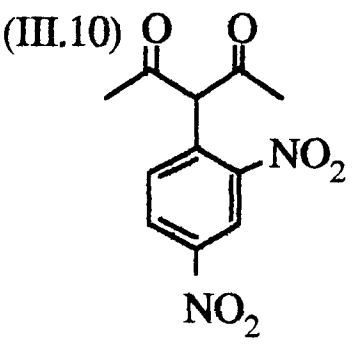
Compound	Molecular Volume, Å cubed	Ground-state dipole moment, debyes	Calculated electronic Transitions and oscillator strengths, nm(f)	$\beta_{(x)} \times 10^{-40}$ m^4 V^{-1}		$\frac{\beta_{(x)}}{Å^3}$
				$\omega = 0$	$\omega =$ 1.17eV	
(III.1) 	144	4.1	322(0.58) 241(0.19) 231(0.17) 211(0.64)	8.0	10.1	0.07
(III.2) 	166	4.4	335(0.56) 249(0.20) 241(0.26)	16.8	39.8	0.24
(III.3) 	172	3.98	339(0.56) 253(0.13)	42.3	62.4	0.36
(III.4) 	170	3.4	321(0.82) 281(0.12) 237(0.11) 231(0.10) 227(0.31)	31.8	52.3	0.31
(III.5) 	174	3.6	321(0.79) 282(0.12) 268(0.12)	26.4	44.0	0.25
(III.6) 	165	9.0	319(0.59) 247(0.13) 236(0.26) 229(0.20) 212(0.51) 208(0.19)	10.9	16.8	0.10
(III.7) 	Trans 189	11.0	326(0.85) 280(0.11) 272(0.10)	27.6	47.3	0.25
	Cis 188	8.2	325(0.86) 280(0.10) 238(0.19)	31.0	53.2	0.28

Table 3.1B

Compound	Molecular Volume, Å cubed	Ground-state dipole moment, debyes	Calculated electronic Transitions and oscillator strengths, nm(f)	$\beta_{(x)} \times 10^{-40}$ m^4 V^{-1}		$\frac{\beta_{(x)}}{Å^3}$
				$\omega = 0$	$\omega =$ 1.17eV	
(III.8) 	251	6.8	354(0.78) 253(0.17) 249(0.25)	20.1	33.9	0.14
(III.9) 	251	2.3	357(0.83) 256(0.23) 251(0.12)	23.5	38.1	0.15
(III.10) 	208	7.4	314(0.06) 271(0.11)	8.8	13.8	0.07
(III.11) 	218	5.9	312(0.06) 272(0.10)	11.3	18.4	0.08
(III.12) 	222	7.8	311(0.05) 280(0.13)	10.9	17.2	0.08

bond, and submitted to AESOP calculations. The final geometries of the modified isomers varied by 2.5 $KcalMol^{-1}$ which is smaller than the accuracy associated with the program. The structure with the lowest energy was chosen for the CNDOVSB calculation. Compounds (III.10) to (III.12) have similar $\beta_{(x)}$ values in the order of 13.8 to 17.2 x 10^{-40} m^4V^{-1}. From the CNDOVSB results, 3-substituted(pentane-2,4-dionates-) (see Table 3.1 B, compounds (III.10) to (III.12)) have lower $\beta_{(x)}$ values than the 4-substituted-benzoylacetone (see Table 3.1.A, compounds (III.1) to (III.7)). The ligand [3-(2,4-dinitrophenyl)pentane-2,4-dione] (III.10) was synthesized and co-ordinated to metals and their NLO properties measured.

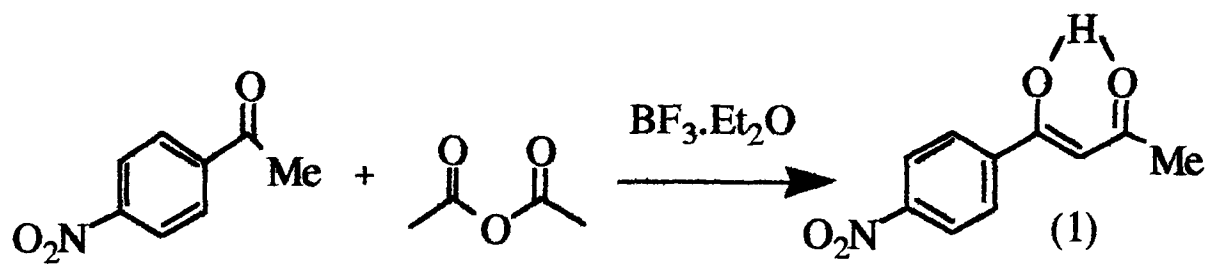
Table 3.2 Comparison of the second-order hyperpolarizability constant β, derived from CNDOVSB calculations and solvatochromism measurements, for three pentane-2,4-dionates.

$\beta_{(x)} \times 10^{-40}$ $m^4 V^{-1}$	CNDOVSB		SOLVATO-CHROMISM
Compound	ω = 0	ω = 1.17eV	Measured as part of this Thesis
(III.2) 	16.8	39.8	32
(III.7) 	31.0	53.2	302
(III.10) 	8.8	13.8	8.8

The solvatochromism results for the measurement of β, for compounds (III.2), (III.7) and (III.10) are compared to the CNDOVSB values in Table 3.2. The magnitudes of β for compounds (III.2) and (III.10) agree well with those calculated by the CNDOVSB. However, the β measured for compound (III.7) from solvatochromism data is almost six times greater than the CNDOVSB value, and may be attributed to both the assumption that the molecular structure chosen for the CNDOVSB calculations is identical to that which exists in solution and that the interaction between the electrons on the pentadionato- ring and the $-BF_2$ group is not the same as that used by the model, and that the solvatochromism method is only approximate.

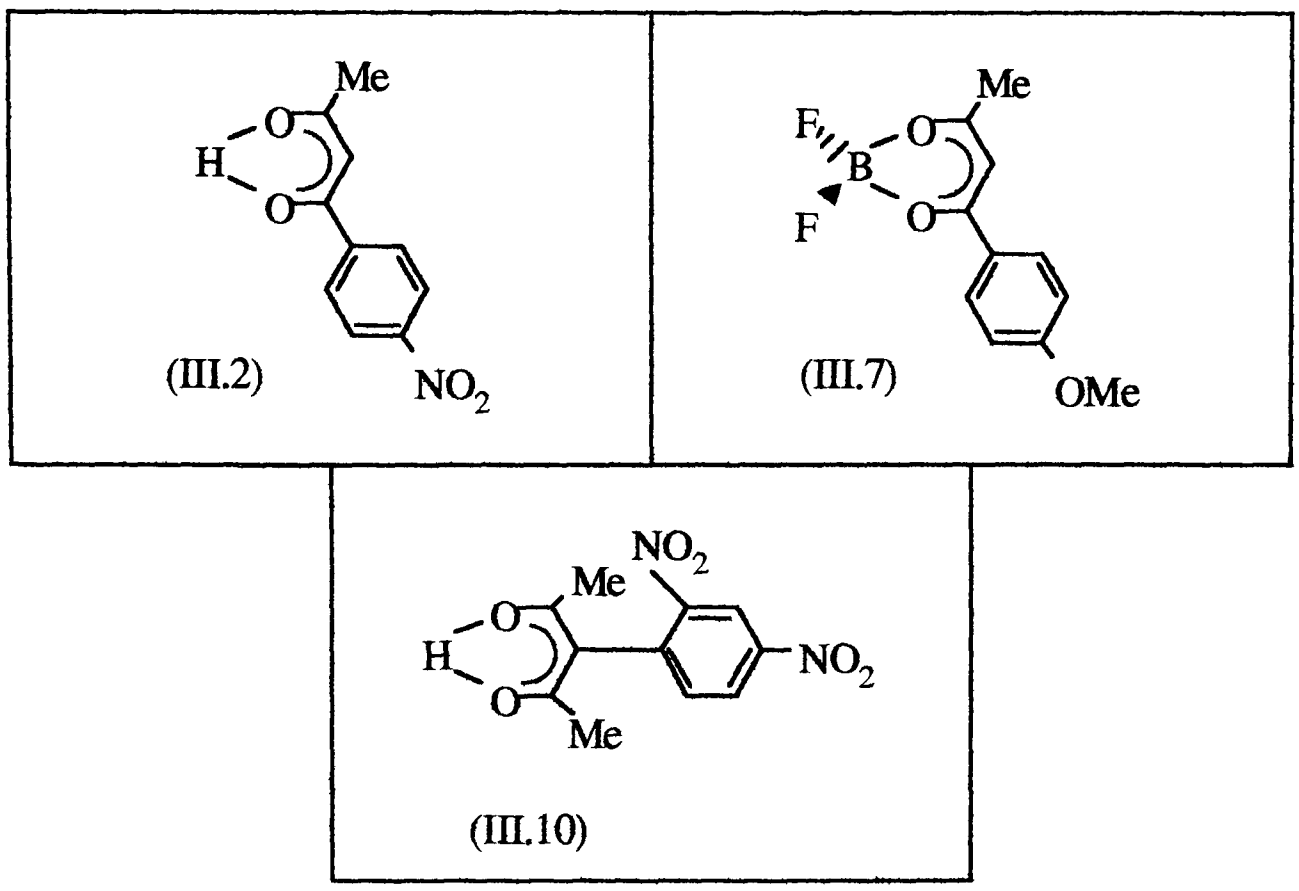
3.3 Results and Discussion

Pentadionato- complexes with substituents at the 3 and 4 positions were made directly from the free ligands, which were formed either in their enol forms or as BF_2 derivatives (see Scheme 3.1). For example, the 4-nitrophenyl derivative (III.2) was synthesized in 29% yield from 4-nitrophenylacetylphenone and acetic anhydride, using $BF_3.Et_2O$ as catalyst, according to the following equation: [132,148]



4-Nitrobenzoylacetone (III.2) is a yellow crystalline compound soluble in the majority of organic solvents and was characterized by elemental analyses as well as infrared and n.m.r. spectral measurements. A characteristic of enolates in solution is that the enolised proton has a ^1H n.m.r. signal around 15 p.p.m., for example compound (III.2) shows a single proton resonance at 15.92 ppm, in $CDCl_3$. The synthesis of the 4-methoxyphenyl derivative (III.7), shown in Scheme 3.1, was similar to that developed for (III.2), but required the addition of a copper(II) ethanoate solution during work-up.

Scheme 3.1 Three pentane-2,4-dionato- ligands synthesized as prospective NLO compounds.

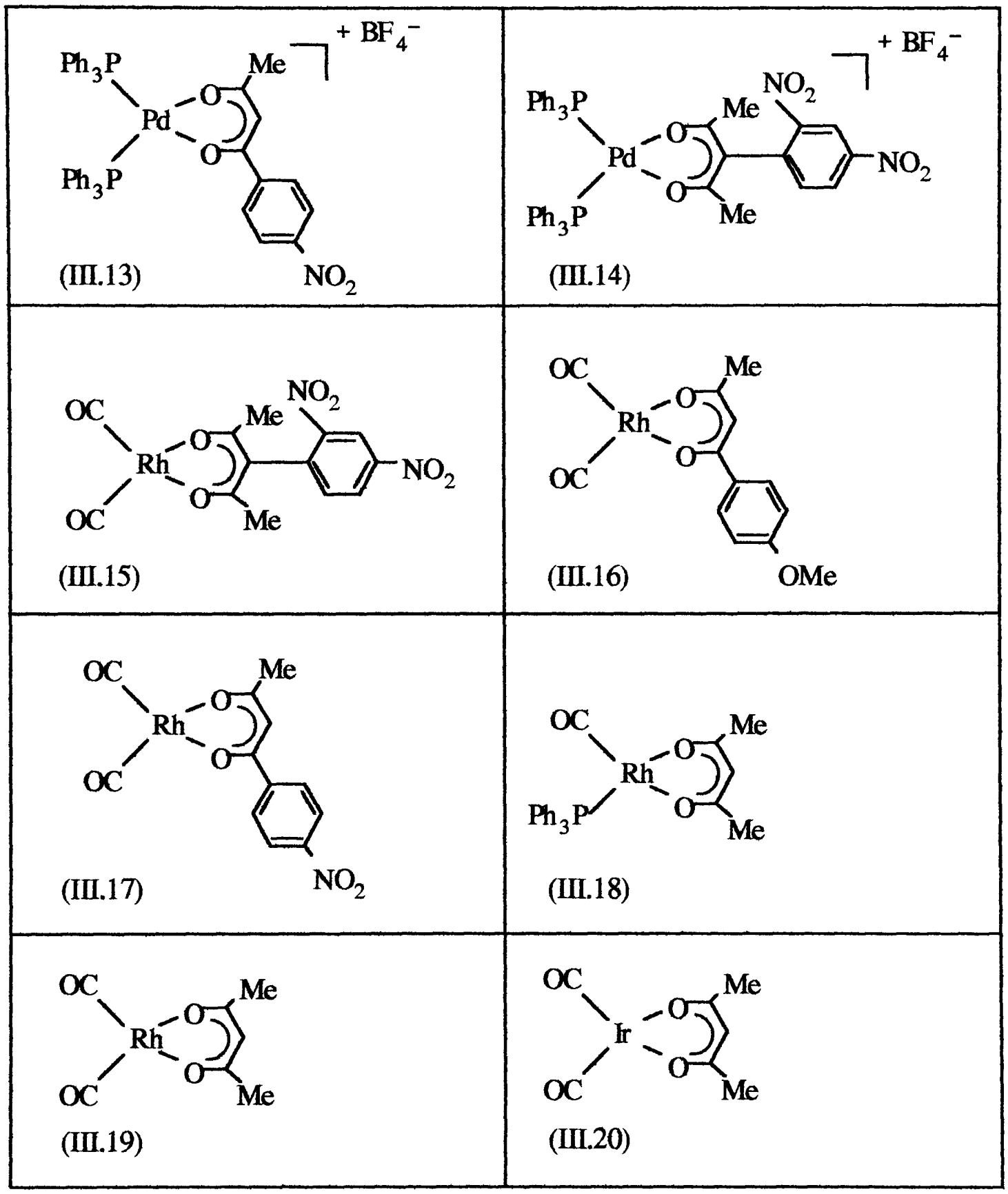


If the reaction was carried out without the copper salt, a dark orange solid resulted, which was found to contain multiple 4-methoxyphenyl rings and methyl groups, and was presumed to be the result of the alternative base catalysed condensation of the starting materials. Compound (III.7) was a dark green crystalline solid, highly soluble in most organic solvents, forming fluorescent green solutions. Reaction of (III.7) with ethanolic NaOH followed by re-acidification to isolate the free acid formed an orange compound identical with the by-product. The crystal structure of difluoro(benzoylacetonato)boron has been reported previously,[94] and a similar structure is assumed for (III.7). The ^{1}H n.m.r. spectrum of (III.7) has a single proton resonance at 6.48 p.p.m., due to the enol proton, and this is similar to the signal of the enol proton in compound (III.2), which is at 6.25 p.p.m.

The 2,4-dinitrophenyl derivative (III.10) was synthesized, by a literature method[148] based on the reaction between 2,4-dinitrofluorobenzene and sodium pentane-2,4-dionate in 85% yield. It is a pale cream crystalline solid and shows the characteristic enolised proton signal at 16.61 p.p.m. Attempts at growing good single crystals of (III.10) for X-ray

crystallographic analysis failed.

Scheme 3.2 Co-ordination compounds derived from pentane-2,4-dionato- ligands.



3.3.1 Palladium compounds (III.13) and (III.14)

The palladium(II) compounds (III.13) and (III.14) were synthesized from *cis*-$PdCl_2(PPh_3)_2$ and the pentane-2,4-dionato- ligand. $AgBF_4$ was added to these reactions

as a halide abstracting reagent. Both are air stable yellow crystalline compounds, with the *cis*- geometry retained. They were synthesized in 47 and 65% yields respectively. The ^{1}H n.m.r. spectra were consistent with the proposed structures, with the enol proton signal of (III.13) occurring at 6.18 p.p.m. Single crystals of (III.13) and (III.14) suitable for X-ray crystallography were grown from the slow diffusion of a 1:1 mixture of tetrahydrofuran and diethyl ether into dichloromethane solutions of the palladium compounds. The synthesis of the 4-methoxyphenyl analogue of (III.13) was attempted using the same conditions, but no palladium complex was identified.

3.3.2 Discussion of the crystal structures of (III.13) and (III.14)

The details of the crystal structure determinations of (III.13) and (III.14) are summarized in Table 3.3, and the relevant atomic coordinates in Tables 3.4 and 3.5. The important structural features of the basic molecular skeletons are illustrated in Figures 3.2 and 3.3, with selected bond lengths and angles listed in Table 3.6. The structures confirm the formulations proposed for the compounds on the basis of spectroscopic data.

For both (III.13) and (III.14) the palladium atom retains the square-planar geometry common to palladium(II) compounds, with the pentane-2,4-dionato- ligands bonded through the oxygen atoms.[115] The Pd-O bond lengths for (III.13) and (III.14) are 2.034(5), 2.046(5), 2.019(2) and 2.033(2)Å respectively, which fall into the range of Pd(II) square planar molecules with Pd-O bonds. The Pd-O bond lengths have been reported to be 1.96(1)Å for bis(pentane-2,4-dionato)palladium(II).[115] The degree of electronic delocalisation can be measured by the length of the C-C bonds in the pentane-2,4-dionato- ring. In bis(pentane-2,4-dionato)palladium(II), the C-C delocalised bonds have lengths of 1.44(2) to 1.40(2)Å, shorter than the normal C-C bond length of 1.52(3)Å but they are not statistically significantly different. In (III.13) the C(38)-C(39) distance is 1.40(1)Å, and in (III.14) the corresponding bond is 1.405(5)Å, thus both pentane-2,4-dionato- rings are delocalised. The C-C bond length between the pentane-2,4-dionato- ring and the phenyl groups are 1.51(1) and 1.502(5)Å respectively showing that the bond order

Fig. 3.2 The crystal structure of [bis(triphenylphosphine)(4-nitrobenzoyl-acetonato)]palladium(II) tetrafluoroborate (III.13).

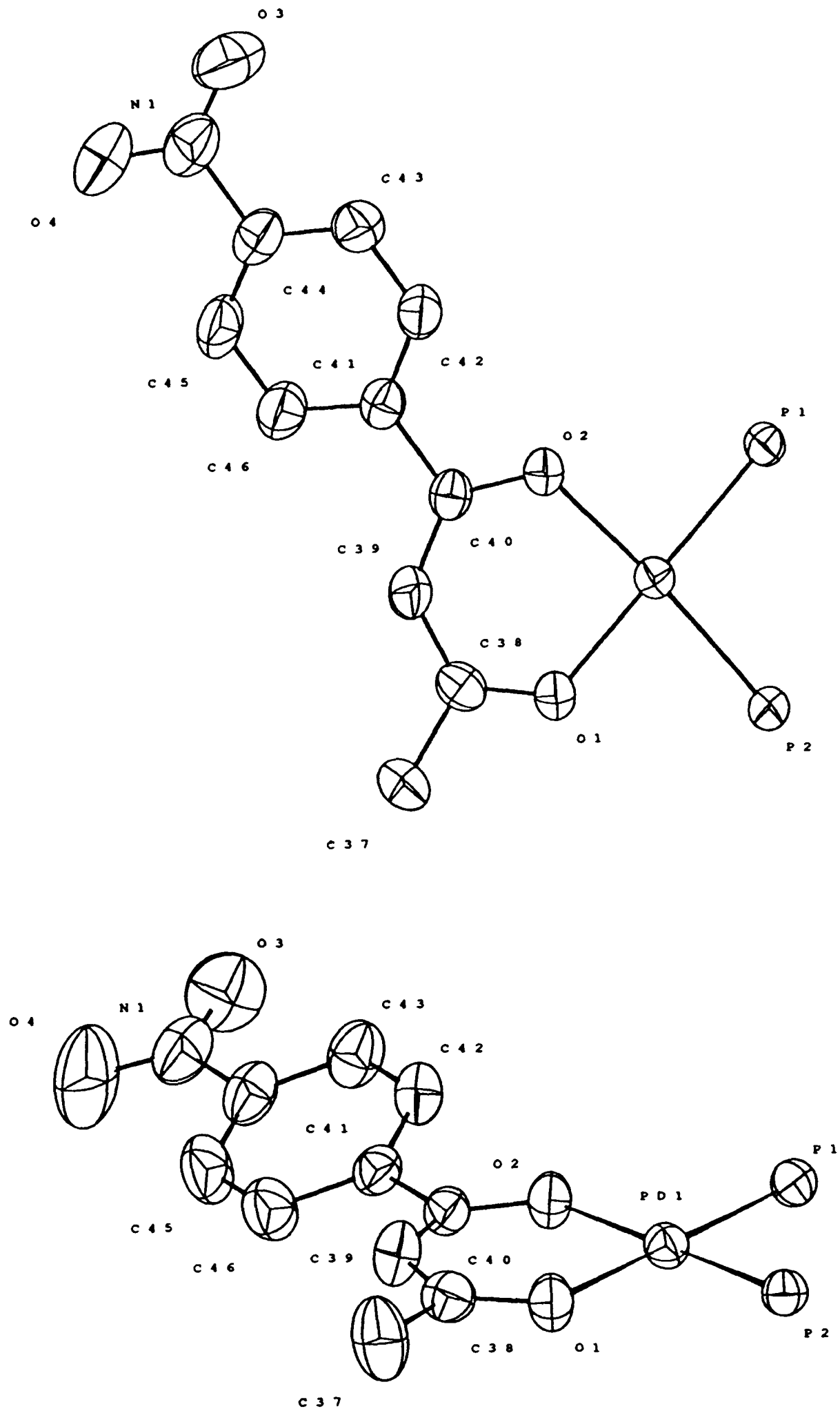
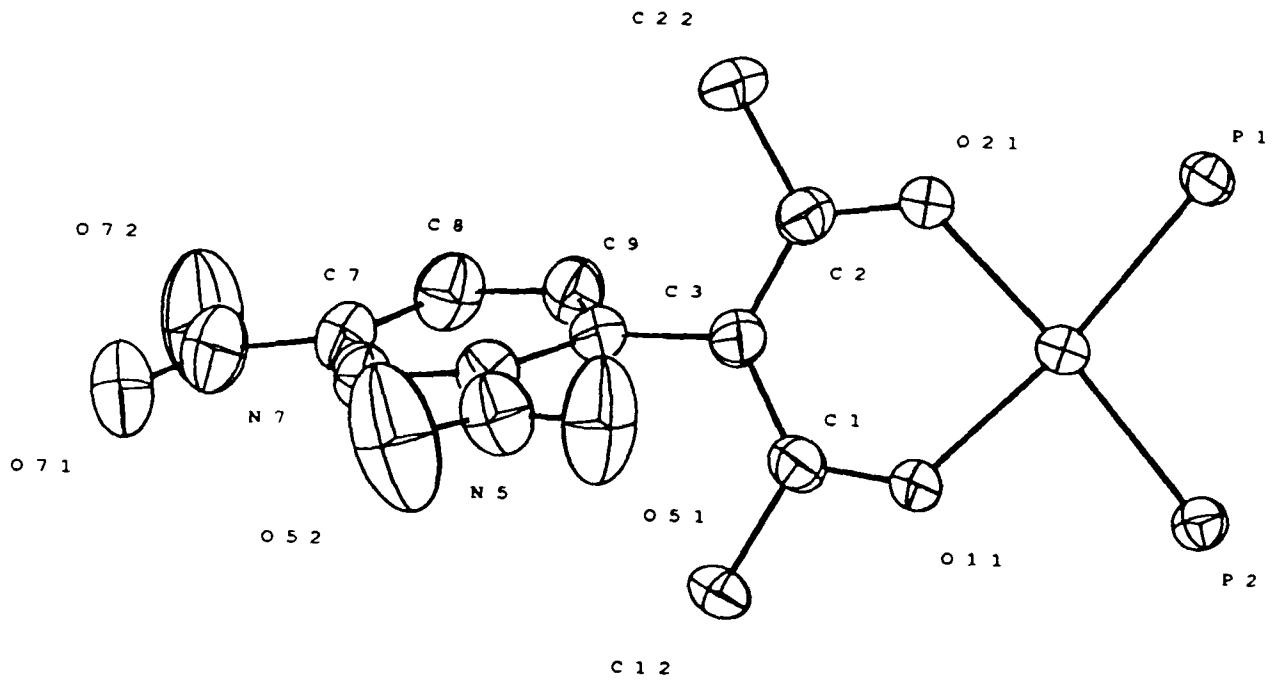
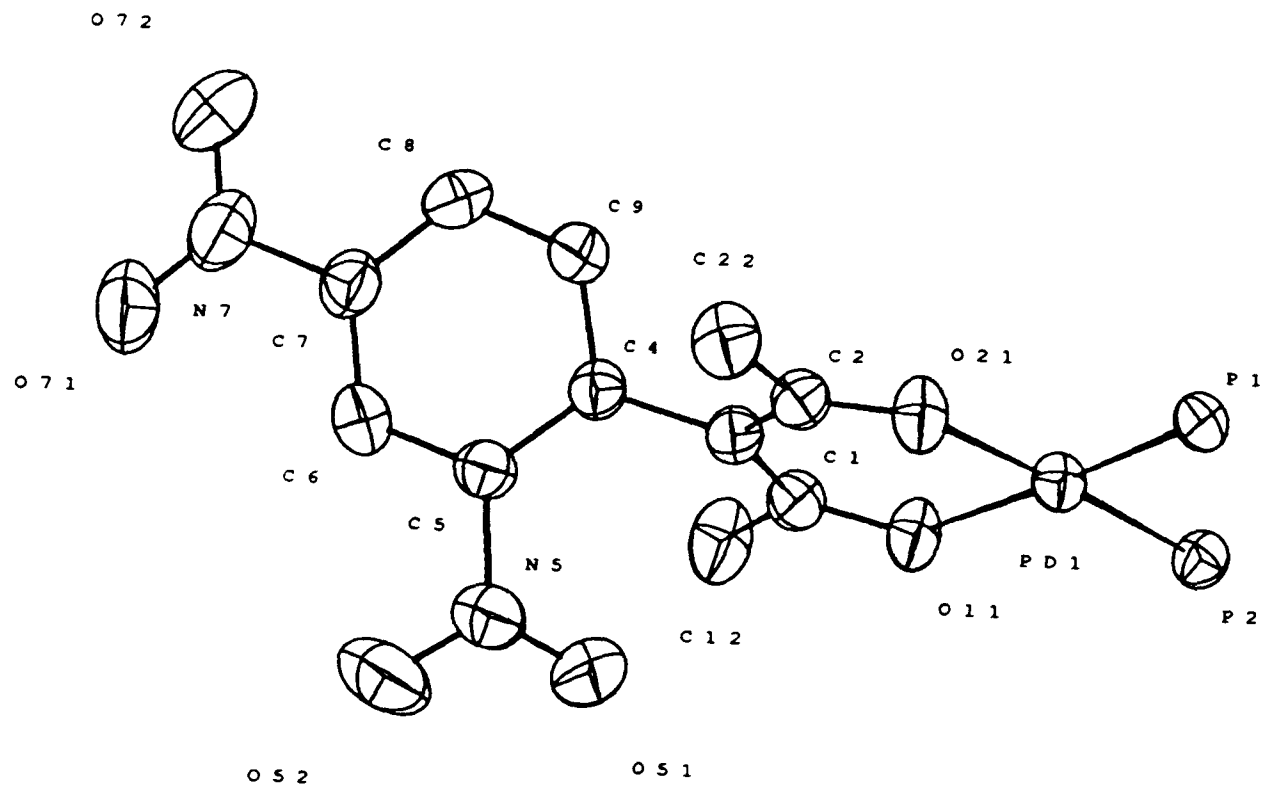


Fig. 3.3 The crystal structure of Synthesis of [bis(triphenylphosphine)(3-{2,4-dinitrophenyl}pentane-2,4-dionato)]palladium(II) tetrafluoroborate (III.14).





is nearer to one than two, and that the conjugation between the pentadionato- ring and the phenyl ring is not extensive. The C-O bond lengths compare well to those reported in the literature.[115] The major difference between (III.13) and (III.14) is that in (III.13) the benzene ring, containing the electron accepting nitro- group, is planar with the pentane-2,4-dionato- ring, and therefore maintains some conjugation with it, while in (III.14) the conjugation is broken between the substituted 2,4-dinitrophenyl- ring and the pentane-2,4-dionato- ring. All nitro- groups remain almost planar to the benzene rings to which they are attached, however, the ortho-nitro group of (III.14) has the greatest deviation from planarity, this effect is common in compounds containing dinitrophenyl- groups.[183]

Table 3.3

Structural details for (III.13) and (III.14).

Compound formula	$C_{46}H_{38}B_1F_4N_1O_4P_2Pd_1$	$C_{47}H_{39}B_1F_4N_2O_6P_2Pd_1$
Formula weight	923.962	982.985
Crystal system	Triclinic	Triclinic
Space group	$P\bar{1}$	$P\bar{1}$
a/Å	10.9954(14)	12.0657(19)
b/Å	13.6922(28)	12.1121(21)
c/Å	14.9637(42)	15.6807(20)
α/degrees	102.933(20)	103.840(12)
β/degrees	92.286(16)	91.227(12)
γ/degrees	98.466(14)	99.596(14)
V/Å^3	2165.5	2185.4
Z	2	2
Dc/g cm^{-3}	1.417(exp. 1.413)	1.491
Linear absorption coefficient:	5.5286	5.550
Data collection:-		
crystal dimensions/mm	0.35 x 0.35 x 0.35	0.30 x 0.28 x 0.28
radiation	Mo Kα	Mo Kα
scan mode	ω - 2θ	ω - 2θ
tmin, tmax/θ	1.5, 22.0	1.0, 25.0
ω-scan width parameters A, B (°) in width = A + Btanθ	0.9, 0.35	0.7, 0.35
Horizontal aperture/mm	3.5	3.5
Min/max h, k, l	-11,11: -14, 14: -15, 15	-8, 14: -14, 14: -18, 18
Total data	9353	8649
Total unique data	5306	7705
total observed data (I>3σI)	4032	5928
Sheldrick merging R-factors,%	1.75	1.77
Absorption correction:-		
type	DIFABS	Φ-scan profile
min/max correction in θ	N/A	1.00, 1.06
Refinement:-		
no. of parameters	632	568
ratio of data:parameters	6.40	10.44
weighting scheme	Unit weights	Unit weights
method of solution	Patterson	Patterson
Final R	4.26	3.16
Final Rw	4.58	3.41

Table 3.4

Positional (x 10^4) and thermal parameters for (III.13) with estimated standard deviations in parentheses.

Atom	x/a	y/b	z/c	U_{eq}[a]	
Pd(1)	4138.9(5)		2990.3(4)	2840.2(4)	314
P(1)	2092(2)		2439(1)	2482(1)	347
P(2)	4498(2)		1806(1)	3644(1)	344
O(1)	5969(4)		3514(4)	3160(3)	420
O(2)	4019(4)		4048(4)	2081(3)	399
O(3)	2702(7)		7053(5)	-792(5)	805
O(4)	4454(7)		8010(6)	-370(6)	903
C(1)	1134(7)		2478(6)	3438(5)	386
C(2)	-138(8)		2227(7)	3309(6)	557
C(3)	-870(1)		2340(8)	4037(8)	689
C(4)	-330(1)		2718(8)	4909(7)	666
C(5)	920(1)		2989(8)	5074(7)	680
C(6)	1654(8)		2871(6)	4333(6)	505
C(7)	1865(7)		1198(6)	1712(5)	403
C(8)	2800(8)		969(7)	1152(6)	521
C(9)	2700(1)		21(8)	553(7)	702
C(10)	1680(1)		-693(8)	504(7)	681
C(11)	740(1)		-475(7)	1038(7)	694
C(12)	830(8)		461(7)	1658(7)	571
C(13)	1403(6)		3254(6)	1874(5)	382
C(14)	1243(8)		4205(7)	2373(6)	488
C(15)	687(9)		4841(7)	1953(7)	589
C(16)	257(9)		4520(8)	1046(7)	623
C(17)	420(1)		3601(9)	542(7)	661
C(18)	1000(9)		2953(7)	951(6)	569
C(19)	5475(7)		966(5)	3029(5)	362
C(20)	5575(8)		36(6)	3230(6)	497
C(21)	6350(1)		-568(7)	2768(7)	639
C(22)	7052(9)		-266(8)	2118(7)	623
C(23)	6969(9)		643(8)	1905(6)	592
C(24)	6182(8)		1267(7)	2350(6)	484
C(25)	3273(7)		944(6)	3971(5)	394
C(26)	2905(8)		1110(7)	4870(6)	534
C(27)	1939(9)		453(9)	5075(8)	671
C(28)	1334(9)		-343(9)	4412(9)	661
C(29)	1685(9)		-519(8)	3536(8)	653
C(30)	2660(8)		122(6)	3309(7)	509
C(31)	5340(6)		2477(5)	4726(5)	345
C(32)	5257(8)		3481(7)	5100(6)	497
C(33)	5830(1)		3987(7)	5942(6)	583
C(34)	6501(9)		3491(8)	6439(6)	585
C(35)	6613(9)		2503(8)	6081(6)	597
C(36)	6039(8)		1994(6)	5227(6)	469
C(37)	7952(7)		4413(7)	3154(7)	629
C(38)	6601(7)		4215(6)	2865(5)	417
C(39)	6137(7)		4775(6)	2292(6)	470
C(40)	4932(7)		4684(5)	1953(5)	366

C(41)	4608(7)	5377(5)	1357(5)	385
C(42)	3566(8)	5090(6)	759(6)	475
C(43)	3255(8)	5711(7)	199(6)	550
C(44)	4013(8)	6615(6)	255(6)	480
C(45)	5037(9)	6924(7)	839(7)	579
C(46)	5343(9)	6311(7)	1404(6)	563
N(1)	3693(7)	7279(6)	-350(5)	609
F(1)	1510(1)	3709(8)	8363(8)	1200(2)
F(2)	2100(1)	2675(8)	7150(7)	1200(2)
F(3)	150(1)	2807(8)	7215(8)	1200(2)
F(4)	1170(1)	2038(8)	8220(8)	1200(2)
F(5)	-170(1)	2660(1)	8040(1)	1200(2)
F(6)	1180(2)	1860(1)	7110(1)	1200(2)
F(7)	1770(2)	2580(1)	8630(1)	1200(2)
F(8)	1540(2)	3590(1)	7620(1)	1200(2)
B(1)	1077(9)	2671(8)	7851(8)	1125(5)
H(21)	-470(7)	2020(6)	2720(6)	690(4)
H(31)	-1720(8)	2120(6)	3930(5)	690(4)
H(41)	-770(7)	2780(6)	5370(6)	690(4)
H(51)	1390(7)	3170(6)	5680(6)	690(4)
H(61)	2540(8)	3100(6)	4410(5)	690(4)
H(81)	3510(7)	1500(6)	1210(5)	690(4)
H(91)	3310(7)	-50(6)	180(6)	690(4)
H(101)	1550(7)	-1340(6)	90(6)	690(4)
H(111)	30(7)	-1010(6)	1040(5)	690(4)
H(121)	170(7)	610(6)	1990(6)	690(4)
H(141)	1470(7)	4390(6)	2950(6)	690(4)
H(151)	580(7)	5440(6)	2300(6)	690(4)
H(161)	-180(7)	4970(6)	730(5)	690(4)
H(171)	180(7)	3280(6)	-90(6)	690(4)
H(181)	1210(7)	2370(6)	600(6)	690(4)
H(201)	5110(7)	-180(6)	3690(6)	690(4)
H(211)	6390(7)	-1120(6)	2930(6)	690(4)
H(221)	7550(7)	-670(6)	1810(6)	690(4)
H(231)	7300(7)	850(6)	1370(6)	690(4)
H(241)	6060(7)	1890(6)	2100(6)	690(4)
H(261)	3340(7)	1680(6)	5260(6)	690(4)
H(271)	1760(7)	570(6)	5650(6)	690(4)
H(281)	730(7)	-720(6)	4500(6)	690(4)
H(291)	1250(7)	-1090(6)	2980(6)	690(4)
H(301)	2970(7)	-40(6)	2710(6)	690(4)
H(321)	4850(7)	3740(6)	4770(6)	690(4)
H(331)	5780(7)	4610(6)	6100(6)	690(4)
H(341)	6820(7)	3790(6)	6980(6)	690(4)
H(351)	7050(7)	2240(6)	6420(6)	690(4)
H(361)	6040(7)	1390(6)	5010(6)	690(4)
H(371)	8320(1)	5010(2)	2990(3)	690(4)
H(372)	8060(1)	4490(3)	3796(7)	690(4)
H(373)	8320(1)	3860(2)	2850(2)	690(4)
H(391)	6670(7)	5150(6)	2110(6)	690(4)
H(421)	3110(7)	4390(6)	720(5)	690(4)
H(431)	2560(7)	5530(6)	-290(6)	690(4)
H(451)	5450(7)	7550(6)	930(6)	690(4)
H(461)	5960(7)	6620(6)	1860(6)	690(4)

Table 3.5

Positional (x 10^4) and thermal parameters for (III.14) with estimated standard deviations in parentheses.

Atom	x/a	y/b	z/c	U_{eq}[a]
Pd(1)	3293(7)	2528.6(8)	2812.2(5)	314
P(1)	3248.5(7)	2363.6(8)	1331.3(6)	331
P(2)	5157.5(4)	2530.7(4)	3048.4(3)	345
B(1)	573(3)	1697(3)	7630(2)	552
C(1)	2255(3)	2615(3)	4517(2)	365
C(2)	902(3)	2470(3)	3266(2)	367
C(3)	1153(3)	2474(3)	4147(2)	359
C(4)	190(3)	2212(3)	4700(2)	362
C(5)	-163(3)	2961(3)	5432(2)	401
C(6)	-990(3)	2601(3)	5952(3)	447
C(7)	-1518(3)	1468(3)	5719(3)	455
C(8)	-1257(3)	707(3)	4985(2)	491
C(9)	-410(3)	1084(4)	4487(2)	436
C(12)	2486(3)	2659(4)	5474(2)	459
C(22)	-289(3)	2422(3)	2932(2)	461
C(111)	2491(4)	3488(4)	1157(3)	389
C(112)	2606(5)	4514(4)	1781(3)	558
C(113)	2037(4)	5383(4)	1683(4)	650
C(114)	1349(5)	5220(5)	953(4)	686
C(115)	1244(4)	4212(4)	310(3)	797
C(116)	1811(3)	3341(3)	407(2)	604
C(121)	2435(3)	988(3)	717(2)	362
C(122)	2398(4)	712(4)	-209(3)	462
C(123)	1714(4)	-282(4)	-683(3)	543
C(124)	1088(4)	-1016(4)	-261(3)	577
C(125)	1145(3)	-774(3)	645(2)	557
C(126)	1812(3)	238(3)	1135(2)	451
C(131)	4521(3)	2528(3)	744(3)	358
C(132)	4950(4)	3559(4)	529(3)	489
C(133)	5940(3)	3654(4)	93(3)	561
C(134)	6496(3)	2732(3)	-131(3)	554
C(135)	6079(3)	1710(3)	85(2)	517
C(136)	5109(3)	1607(3)	523(2)	419
C(211)	5560(3)	1121(3)	2700(3)	389
C(212)	4783(4)	163(4)	2291(3)	483
C(213)	5084(4)	-923(4)	2118(3)	622
C(214)	6157(4)	-1044(4)	2333(3)	619
C(215)	6930(3)	-92(4)	2764(3)	626
C(216)	6640(3)	978(3)	2954(2)	523
C(221)	5557(3)	2888(3)	4224(2)	384
C(222)	5217(4)	2048(4)	4684(3)	470
C(223)	5503(4)	2269(4)	5577(3)	529
C(224)	6133(5)	3324(4)	6003(3)	600
C(225)	6477(4)	4143(4)	5562(3)	679
C(226)	6190(3)	3944(3)	4668(2)	552
C(231)	6084(4)	3592(4)	2623(3)	431
C(232)	5776(6)	4677(4)	2750(3)	574

C(233)	6475(6)	5549(5)	2489(3)	720
C(234)	7454(4)	5343(6)	2105(4)	770
C(235)	7746(3)	4284(4)	1976(3)	777
C(236)	7065(3)	3389(4)	2226(2)	579
F(1)	1335(3)	1808(3)	8298(2)	1063
F(2)	1100(3)	1773(3)	6886(3)	898
F(3)	-39(4)	2529(3)	7892(2)	1093
F(4)	-90(3)	654(3)	7461(2)	1106
N(5)	353(3)	4198(3)	5719(3)	568
N(7)	-2346(2)	1057(2)	6299(1)	615
O(11)	3155(2)	2738(2)	4120(1)	389
O(21)	1613(3)	2529(3)	2682(3)	406
O(51)	1114(4)	4591(3)	5350(3)	799
O(52)	-44(3)	4790(3)	6324(2)	962
O(71)	-2571(4)	1743(3)	6941(3)	697
O(72)	-2774(4)	42(3)	6097(3)	908
H(6)	-1195	3153	6500	860(2)
H(8)	-1640	-65	4842	860(2)
H(9)	-180	490	3952	860(2)
H(11)	1700	2257	5825	860(2)
H(12)	3530	2783	5660	860(2)
H(13)	3073	1958	5633	860(2)
H(21)	-768	2993	3475	860(2)
H(22)	-738	1465	2533	860(2)
H(23)	-315	2833	2273	860(2)
H(112)	3153	4658	2346	860(2)
H(113)	2050	6063	2167	860(2)
H(114)	990	5883	896	860(2)
H(115)	963	4193	-358	860(2)
H(116)	1705	2555	-27	860(2)
H(122)	2928	1325	-519	860(2)
H(123)	1650	-413	-1358	860(2)
H(124)	608	-1750	-638	860(2)
H(125)	650	-1210	956	860(2)
H(126)	1853	438	1806	860(2)
H(132)	4520	4228	731	860(2)
H(133)	6340	4395	-12	860(2)
H(134)	7195	2815	-435	860(2)
H(135)	6510	1033	-83	860(2)
H(136)	4720	870	663	860(2)
H(212)	4035	255	2187	860(2)
H(213)	4505	-1557	1852	860(2)
H(214)	6398	-1798	2215	860(2)
H(215)	7742	-195	2919	860(2)
H(216)	7230	1693	3233	860(2)
H(222)	4748	1248	4387	860(2)
H(223)	5358	1585	5890	860(2)
H(224)	6390	3478	6615	860(2)
H(225)	7035	4948	5904	860(2)
H(226)	6540	4498	4302	860(2)
H(232)	5053	4790	3115	860(2)
H(233)	6212	6398	2679	860(2)
H(234)	8060	5965	1908	860(2)
H(235)	8550	4120	1688	860(2)
H(236)	7365	2568	2092	860(2)

Table 3.6

Important bond lengths (Å) and angles (°) for (III.13) and (III.14), errors in ().

[Bis(triphenylphosphine)(4-nitrobenzoylacetonato)palladium(II) tetrafluoroborate] (III.13)

Atoms	Distance
Pd(1)-O(1)	2.034(5)
Pd(1)-O(2)	2.046(5)
Pd(1)-P(1)	2.268(2)
Pd(1)-P(2)	2.293(2)
O(1)-C(38)	1.271(8)
O(2)-C(40)	1.279(8)
C(37)-C(38)	1.498(10)
C(38)-C(39)	1.400(11)
C(39)-C(40)	1.377(11)
C(40)-C(41)	1.509(10)
C(44)-N(1)	1.485(10)
N(1)-O(3)	1.214(9)
N(1)-O(4)	1.213(9)

Atom	Angle
O(1)-Pd(1)-O(2)	90.88(19)
P(1)-Pd(1)-P(2)	97.49(7)
C(40)-C(41)-C(42)	119.75(66)
C(44)-N(1)-O(3)	117.09(81)

[Bis(triphenylphosphine)(3-(2,4-dinitrophenyl)-pentane-2,4-dionato)palladium(II) tetrafluoroborate] (III.14)

Atom	Distance
Pd(1)-O(11)	2.019(2)
Pd(1)-O(21)	2.033(2)
Pd(1)-P(1)	2.281(1)
Pd(1)-P(2)	2.272(1)
O(11)-C(1)	1.269(4)
O(21)-C(2)	1.274(4)
C(1)-C(12)	1.507(4)
C(2)-C(22)	1.507(5)
C(3)-C(2)	1.407(5)
C(3)-C(1)	1.405(5)
C(3)-C(4)	1.502(5)
C(5)-N(5)	1.479(5)
C(7)-N(7)	1.471(5)
N(5)-O(51)	1.189(4)
N(7)-O(71)	1.201(4)

Atom	Angle
O(11)-Pd(1)-O(21)	88.55(9)
P(1)-Pd(1)-P(2)	98.6(3)
C(2)-C(3)-C(4)	118.07(29)
C(5)-N(5)-O(51)	120.83(34)
C(7)-N(7)-O(71)	118.74(36)

3.3.3 Rhodium Compounds (III.15) to (III.20)

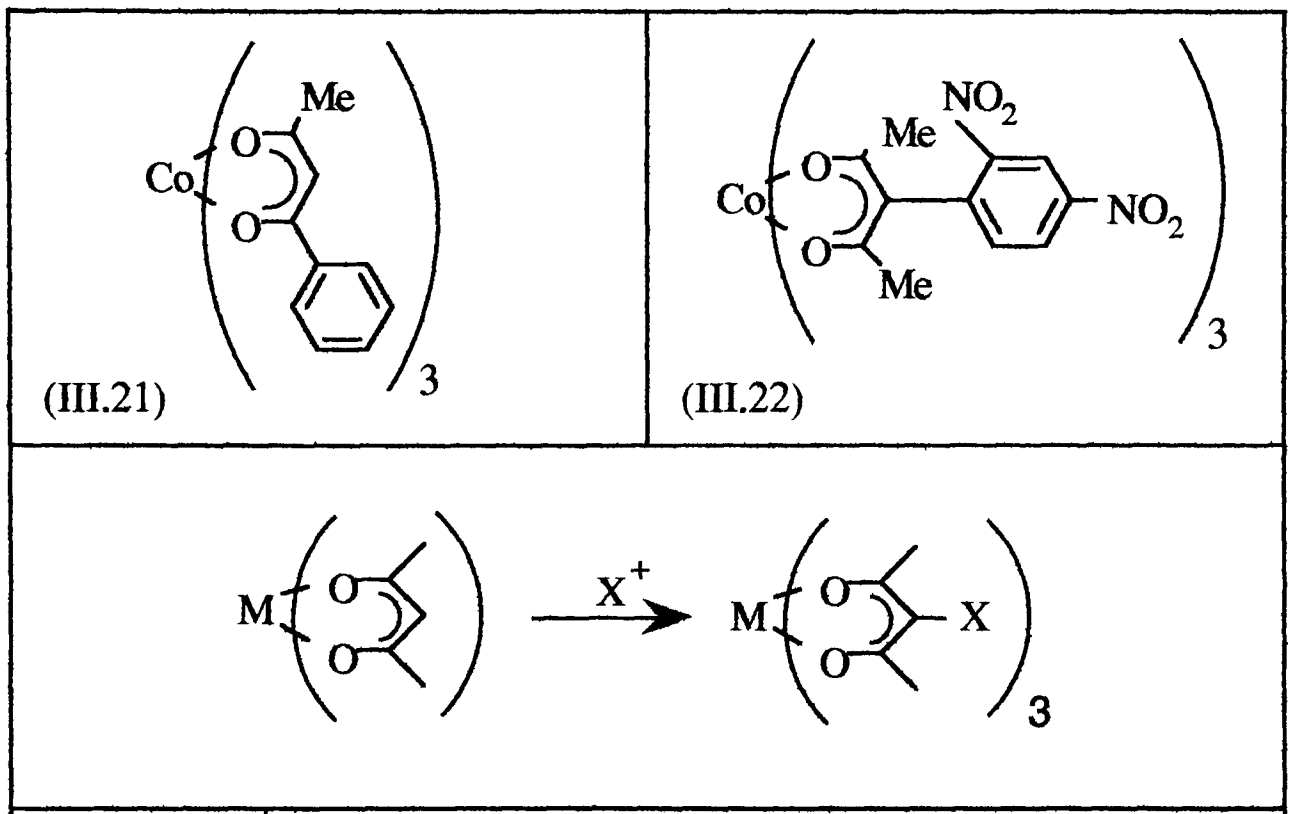
The rhodium(I) compounds (III.15) and (III.16), were synthesized by a modification of the method outlined by Varshavskii *et al.*[205] The ligands were reacted directly with $RhCl_3.3H_2O$, in dimethylformamide. The dimethylformamide acts both as the solvent and the source of CO ligands. The 4-methoxyphenyl- derivative (III.16) is a bright orange solid, while the 2,4-dinitrophenyl- derivative (III.15) is a darker orange. The ^1H n.m.r. spectra of both compounds correspond to the proposed structures, and the enol proton signal of (III.16) occurs at 6.26 p.p.m. Attempts at the synthesis of (III.17) produced a complex brown and yellow mixture of compounds which could not be effectively separated. Compounds (III.18)-(III.20) were synthesized by literature methods.[26,27,205] The rhodium compounds (III.15) to (III.20) were synthesized by Don M. Murphy of this laboratory.

3.3.4 Cobalt(III) and Rhodium(III) Tris-pentane-2,4-dionates

The cobalt(III) pentadionato- complexes (III.21) and (III.22) were made directly from $CoCO_3.H_2O$, the ligand and hydrogen peroxide in aqueous solution (see Scheme 3.3). The octahedral cobalt(III) complexes (III.21) and (III.22) are dark green crystalline solids [25,32] and have been characterized by ^1H n.m.r. spectroscopy. Pentadionato- complexes undergo electrophilic substitution reactions at the 3-position and this route has been used to synthesize the substituted octahedral complexes of cobalt and rhodium(III) shown in Scheme 3.3.[79,80,87] Compounds (III.23) to (27) have Cl, NO_2 and CHO substituents in the 3-position.[56,57,60] All of the cobalt compounds are green, while the

rhodium compound is yellow. These compounds have also been characterized by spectroscopic [62] techniques, and have the physical properties stated in the original publications.

Scheme 3.3 Cobalt(III) and rhodium(III) tris-pentane-2,4-dionates synthesized and tested for SHG.



Compound	Group:	M =	X =
(III.23)		Co	H
(III.24)		Co	Cl
(III.25)		Co	NO_2
(III.26)		Co	2 x H, 1 x CHO
(III.27)		Rh	H

The range of compounds illustrated in Schemes 3.2 and 3.3 demonstrate the ease with which a range of donor and acceptor groups may be introduced into pentadionato-coordination compounds. This is important if a number of such compounds are to be screened for SHG. All the compounds are air stable, and are not light sensitive.

3.4 Second-Harmonic Generation (SHG) Properties of Pentane-2,4-dionato- Compounds

The measured SHG properties of the pentane-2,4-dionato- ligands and complexes synthesized as part of this Thesis are summarized in Tables 3.7 and 3.8. The ligands (III.2) and (III.7) both show some SHG effect, (0.6 x urea) whereas (III.10) has an effectively zero value. These observations may relate more to the centrosymmetric or non-centrosymmetric nature of the space groups which the molecules choose to crystallize in, rather than any molecular properties associated with the donor and acceptor functions on the pentadionato- ligand. Unfortunately, the crystal structures of these ligands have not been reported.

The crystal structures of the palladium complexes (III.13) and (III.14) have been described in this Chapter and unfortunately they both crystallize in centrosymmetric space groups. The SHG properties of these complexes should be zero for symmetry reasons, but nonetheless significant SH signals were observed for both compounds (see Table 3.7). The observation of this signal was reproduced both for samples from the same batch and different syntheses. These observations must result from either the co-crystallization of more than one polymorph, or from the large surface effects associated with fine powders. Other workers have reported similar residual SHG effects for organometallic ferrocenes[13] and organic polymers (see Chapter 2).[209] The remaining complexes (III.15) - (III.19) did not show significant SHG effects.

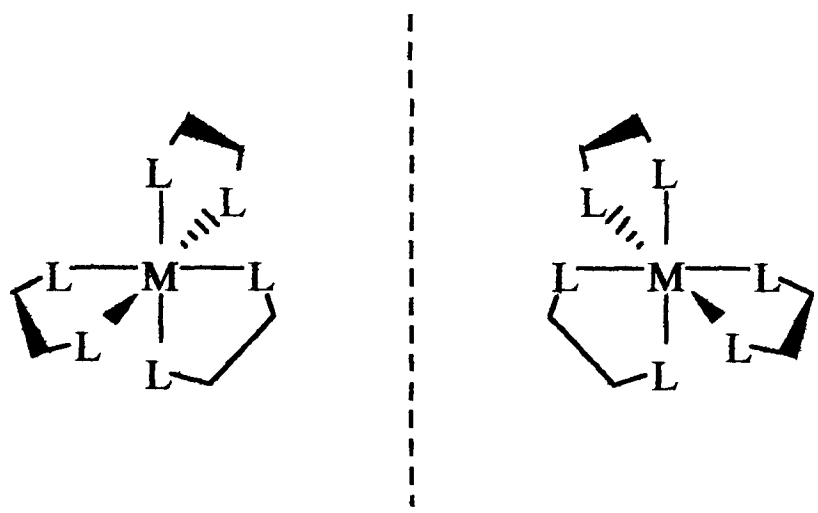
Table 3.7 Measured second-harmonic signals at 1064 nm fundamental laser wavelength; all are a sum of 64 individual laser pulses, and relative to urea.

Compound	Efficiency	Comments	Colour
	Ligands		
(III.1)	0		Colourless
(III.2)	0.56		Yellow
(III.7)	0.67		Dark green
(III.10)	0.01		Pale yellow
	Palladium(II) Compounds		
(III.13)	0.22		Yellow
(III.14)	0.73	Luminesced	Yellow
	Rhodium(I) Compounds		
(III.15)	0.08	Luminesced	Orange-brown
(III.16)	0	Luminesced	Orange
(III.17)	0	Luminesced	Yellow
(III.18)	0	Luminesced	Yellow
(III.19)	0		Red-Green

Table 3.8 Measured second-harmonic generation data for tris-cobalt(III) and rhodium(III) complexes. Incident laser wavelength was 1064 nm, all relative to urea, unless otherwise stated.

Compound	Efficiency	Colour
Tris pentane-2,4-dionato- complexes		
(III.21)	0	Green
(III.22)	0	Dark green
(III.23)	detected (<< 0.02)	Dark green
(III.24)	detected (> III..23)	Green
(III.25)	detected (> III..24)	Dark green
(III.26)	0	Light green
(III.27)	0	Yellow

All the octahedral cobalt(III) and rhodium(III) compounds (III.21) - (27) showed essentially zero SHG effects despite the presence of favourable groups within the molecule. Tris-bidentate octahedral complexes can exist in two propeller-like enantiomers:



It may be concluded that the second-order susceptibilities of tris-pentane-2,4-dionato- compounds vanish because no significant SHG effect is observed. The ligand 4-nitrocatechol has an efficiency of 6 x urea [47] Appendix I, Vol II however, the complex [tris-

(4-nitrocatecholato)tin(IV)][(triethylammonium)$_2$] which has as a slightly distorted octahedra of oxygens surrounding the tin(IV) atom, shows an SHG response of 1.33 x urea @1064 nm.[190] [Tris-(4-nitrocatecholato)tin(IV)][(triethylammonium)$_2$] has been shown to belong to a non-centric space group, Pbca, but the arrangement of enantiomers in a R/L/R/L/R/L array in the crystal structure introduces a point of inversion but the compound still shows residual SHG signals.

Fig.3.2 Schematic diagram of [tris-(4-nitrocatecholato)tin(IV)][(triethylammonium)$_2$].

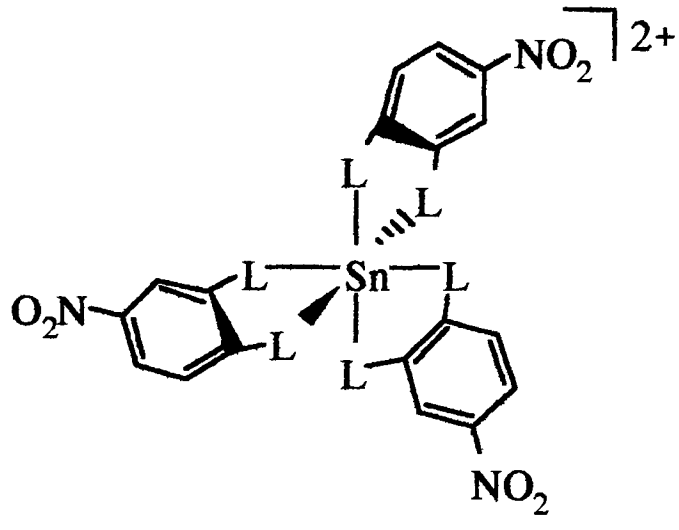


Table 3.9 Electronic spectral data of pentane-2,4-dionato- compounds.

Compound	$\lvert\Delta\lambda_{max}\rvert$	$\Delta\varepsilon_{eff}$	$\lvert\Delta\lambda_{max}\rvert / \Delta\varepsilon_{eff}$
Ligands			
4-Nitroaniline	47	2.05	23
(III.2)	10	2.05	5
(III.7)	0	0.89	0
(III.10)	2	0.89	2
Palladium(II) Compounds			
(III.13)	41	0.83	41
(III.14)	70	0.83	84
Rhodium(I) Compounds			
(III.15)	64	0.89	72
(III.16)	20	1.16	17
(III.18)	14	0.54	26
(III.19)	4	1.16	3
Tris-cobalt(III) Compounds			
(III.21)	99	1.15	46
(III.25)	68	1.98	34
(III.25) cont.	70	0.56	125

Octahedral complexes formed from NLO active ligands loose the non-centrosymmetry required to observe SHG, and thus tris octahedral complexes cannot be used to direct the symmetry of complexes for SHG.

The solvatochromism of the pentadionato- ligands and some of their complexes were also measured, and the data is summarized in Table 3.9. All the compounds showed significant shifts of electronic transition state bands, $|\Delta\lambda_{max}|$ in nm, when the polarity of the solvent was changed. Typically the following solvents were used; hexane, dichloromethane and ethanol. The bands were found to shift up to 99 nm and in the more complex spectra the band shifts were observed using mixed solvent systems. The last column in Table 3.9 gives the value of $|\Delta\lambda_{max}| / \Delta\varepsilon_{eff}$ which is an indication of the solvatochromic behaviour as there are many other factors involved in solvatochromism (see Chapter Two). The compound 4-nitroaniline is included as a point of reference, and the effective dipolar permittivity,[28,170] $\Delta\varepsilon_{eff}$, is used for this comparison following the model of solvatochromism described in Chapter 2. These results suggest that the excitations associated with these bands involve a reasonable change in dipole moment on excitation. The results support the above suggestion that the poor SHG properties observed for these compounds have their origin in the mode of crystallization rather than in the molecular properties.

3.5 Crystal Structure Determination of (III.13) and (III.14)

3.5.1 Data Collection

Suitable crystals of (III.13) and (III.14) were mounted in 0.5 mm Lindemann capillary tubes. Crystal data were collected at room temperature on an Enraf-Nonius CAD4-F automatic diffractometer using molybdenum radiation (Mo-Kα, $\lambda = 0.71069$Å) The unit cell dimensions were calculated from the setting angles of 25 accurately centred reflections in each case.

Data were collected using the $\omega/2\theta$ scan method. Three standard reflections were measured after every 3600 seconds of X-ray exposure time as intensity standards and after every 250 reflections as orientation controls.

3.5.2 Data Reduction

The intensity data were corrected for Lorentz and polarization effects. An empirical absorption correction was applied to (III.14), and equivalent reflections were averaged.

3.5.3 Structure Solution and Refinement

The structures were solved and refined within the CRYSTALS package.[211]

i/ Bis(triphenylphosphine)(4-nitrobenzoylacetonato)palladium(II) tetrafluoroborate (III.13)

The coordinates of the Pd atom in (III.13) were determined from interpretation of a Patterson synthesis. Fourier syntheses were used to ascertain the positions of the remaining non-hydrogen atoms. Following full-matrix least-squares refinement of atomic coordinates and isotropic thermal parameters, DIFABS was applied to unmerged data, which was then remerged.

A difference Fourier synthesis gave the positions of all the hydrogens except those of the methyl group, which were included in geometrically idealized positions. The difference map also showed residual electron density in the region of the anion, indicating disorder. This was modelled as a minor and rigid idealized tetrahedral BF4- ion.

In the final stages of least-squares refinement, the matrix used consisted of 3 blocks. The first block contained the scale factor and a "dummy overall isotropic temperature factor". The second contained the atomic coordinates of all the atoms. There were eight fluorine positions, four in each of the major and minor components of the anion. The third block contained the thermal parameters: anisotropic for the non-hydrogen atoms in the cation, isotropic for the boron atom, a single isotropic parameter for all the hydrogens and another for the fluorine atoms. The bond angles amongst the generated hydrogens and amongst the fluorines of the minor component were restrained to idealized values. The bond lengths in the minor component were restrained to their mean value.

Unit weights were maintained throughout the solution.

ii/ Bis(triphenylphosphine)(3-(2,4-dinitrophenyl)-pentane-2,4-dionato)palladium(II) tetrafluoroborate (III.14)

A Patterson synthesis gave the coordinates of the Pd atom in (III.14) and the remaining non-hydrogen atoms were easily located by further Fourier syntheses. The hydrogen atoms were positioned geometrically. The matrix used for the final cycle of refinement consisted of two blocks. In the first were the coordinates of the non-hydrogen atoms. In the second were the anisotropic thermal parameters for these atoms plus one isotropic thermal parameter for all the hydrogens. Unit weights were employed. Details of the two structures and their solution are summarized in Table 3.3.

3.6 Summary and Conclusions of Chapter Three

This Chapter surveys the use of organometallic and organo- coordination compounds for the generation of second harmonic frequencies from laser light. Limited success has so far been reported especially with substituted ferrocenes which have been shown to be up to 62 times as efficient as the standard urea in frequency doubling.[88]

The use of pentane-2,4-dionato- ligands and their coordination compounds has been introduced as possible NLO active materials. Potential pentanedionato- ligands were investigated by CNDOVSB calculations, and were shown to have a predicted $\beta_{(x)}$ value in the order of 14-53 m^4V^{-1}, equivalent to that of 4-nitroaniline. Three substituted pentane-2,4-dionato compounds were synthesized, and their SHG properties investigated by a modification of the Kurtz powder [118] and solvatochromism techniques. The solvatochromism measurements of $\beta_{(x)}$ approximated to the CNDOVSB results. The SHG efficiency was greatest in difluoro(4-methoxybenzoylacetonato)boron (III.7) at 0.67 times urea.

The NLO properties of complexes synthesized using rhodium(I), cobalt(III) and palladium(II) from substituted pentanedionato- ligands have been described. The single

crystal X-ray structure of bis(triphenylphosphine)(4-nitrobenzoylacetonato)palladium(II) tetrafluoroborate (III.13) and tris(triphenylphosphine)[3-(2,4-dinitrophenyl)-pentane-2,4-dionato]palladium(II) tetrafluoroborate (III.14) were determined. Compounds (III.13) and (III.14) both crystallize in the centric triclinic space group $P\bar{1}$ and give residual SHG responses of 0.22 and 0.73 times urea. Analogous rhodium(I) complexes did not give significant SHG efficiencies. The SHG properties of these complexes do not mirror the expected efficiencies predicted for the ligands alone and this has been shown to be due to the centric nature of the crystal structure in which they crystallize. The possibility of using atropisomerism as a method of introducing chirality by the restricted rotation of the 2,4-dinitrophenyl- group is prevented by the square-planar nature of the Pd(II) atom. However, this does not prevent the use of (III.10) as a ligand to synthesize metal co-ordination compounds with octahedral geometry, or the use of an asymmetric bidentate phosphine ligand in compound (III.14) instead of the two triphenylphosphine ligands which could possibly form a resolvable racemic mixture of isomers analogous to (III.14).

Tris cobalt(III) complexes of substituted pentanedionato- ligands were screened for their NLO properties and were found to have zero SHG efficiencies. Tris bidentate octahedral complexes exist as racemic mixtures of enantiomers which in the case of [tris(4-nitrocatecholato)tin(IV)] dianion has been shown to crystallize in alternating R/L/R/L arrays thus the crystal structure is non-centrosymmetric, but has a point of inversion and therefore zero $\chi^{(2)}$ for symmetry reasons.[190] It is likely that the tris cobalt(III) pentanedionato-complexes have a similar arrangement of R/L isomers leading to near zero SHG efficiencies. Thus tris bidentate complexes alone cannot be used to engineer the correct symmetry to fabricate NLO active materials.

The solvatochromic behaviour of some of the pentanedionato- complexes were studied. Significant shifts in the λ_{max} of the lowest lying, most significant, charge transfer band were observed with solvents of differing polarities.

The centric nature of the ligands and complexes does not permit the investigation of $\chi^{(2)}$ by SHG measurements, but solvatochromism data have suggested that some of the ligands and complexes may have $\beta_{(x)}$ values equivalent to that of 4-nitroaniline.

CHAPTER FOUR

Salts of β-Ionylidenecyanoacetic Acid

4.1 Introduction

Most organometallic and coordination compounds so far tested for second harmonic generation have had efficiencies considerably lower than that of their organic counterparts. The compounds (Z)-[1-ferrocenyl-2-(4-nitrophenyl) ethylene][88] and (E)-[1-ferrocenyl-2-(N-methylpyridinium-4-yl) ethylene iodide][134] have second harmonic generation (SHG) efficiencies of 62 and 220 times urea (at 1907 nm) respectively and are the highest so far reported for organometallic compounds. In the design of coordination compounds for SHG, this lack of success has to be accounted for. One of the reasons for this may be the low π conjugation length associated with simple ligands. In addition, it is more difficult to introduce substituents into co-ordination compounds in order to encourage their crystallization in non-centric space groups.

In the design of inorganic compounds for second harmonic generation the metal may form part of the electronic delocalization network, or simply as a template onto which "electronically active" ligands may be attached.[15] If the template has a tendency to crystallize in a non-centrosymmetric space group, this would have the added advantage of solving the symmetry problem mentioned above. This Chapter describes the design and synthesis of a ligand which has a long conjugation pathway, and its complexation with metal ions.

4.2 Choice of Ligand

4.2.1 Introduction

Metal complexes may be synthesized from a wide range of organic compounds with nucleophilic groups. The nucleophilic site influences the stability of the final complex towards light, heat and dioxygen. The functional site also dictates, to some extent, the

crystal packing in the complex. The length of the conjugated side chains also influences the crystallinity and melting point of the complex. It has been found, as a result of the work described in this Chapter, that ligands made up from long conjugated chains tend to crystallize poorly, and often remain as oils. Crystal formation was encouraged by introducing a polar hydrogen bonding group into the ligand. Ligands which contain a carboxylate group posses the required properties, and are amenable by straight forward synthetic routes.[183]

Long chain carboxylates, with a hydrophilic and hydrophobic end, have been studied as active components for Langmuir-Blogett films. A series of polyene carboxylates have been reported[20,81,102,104,112,131,175,191,192] and measurements of their electric field induced second harmonic generation (EFISH) properties have been published. Tables 4.1 shows EFISH data for selected polyene compounds. It is known that 4-alkoxybenzoic acids show nematic (one dimensional order) and smectic (two-dimensional order with molecular planes perpendicular to crystal layers) liquid crystal phases. These studies have been extended to the nickel and palladium complexes of 4-alkoxydithiobenzoates, which have potential uses as liquid crystals for electro-optic display devices.[3]

Non-linear optical properties of a series of retinol-like compounds have been measured by several workers.[103,112,191,192] Some results have been reported as Patent Applications and so the data are incomplete. Table 4.1 summarizes the results of EFISH measurements on the magnitude of β for some retinol-like molecules, and for one example, compares the EFISH result to that calculated by the CNDOVSB method described in this Thesis. The compound 4-nitroaniline has been used as a reference compound throughout this Thesis, and has a β value of 150×10^{-40} m^4V^{-1}. 4-Nitroaniline has a dipole moment, μ_0, of 4.9 D (1.63×10^{-29} Cm)[163] and therefore $\mu_0\beta$ in the same units as used in Table 4.1 is equal to 735×10^{-40} $m^4V^{-1}D$. Compound A1, retinal (vitamin A aldehyde), is made up of a conjugated chain comprising 5 double bonds and an electron accepting, -CHO, group at one end. The magnitude of $\mu_0\beta$ for A1 is greater than that of 4-nitroaniline, but five times smaller than $\mu_0\beta$ for compounds A2 - A4. This increase in

the magnitude of $\mu_0\beta$ may be due to the shift of the lowest energy electronic transition towards the second harmonic wavelength (532 nm). As the first electronic transition approaches the wavelength of the second harmonic, the system becomes resonant, and β increases exponentially (see Chapter One). The increase in the magnitude of the dipole, or changes in the efficiency of the electron donor or acceptor groups is significantly smaller than the effect on the magnitude of β caused by resonance.

The next section describes the results of CNDOVSB calculations of the magnitude of β done as part of this Thesis on retinol-like molecular structures. The calculations used data obtained from molecular templates built up from known crystal structures. The results from the CNDOVSB calculations were then used as a guide to the potential non-linear optical properties of retinol-like molecules and the results are described in the next Section.

4.2.2 CNDOVSB calculations on retinol-like molecules

The CNDOVSB model for calculating the magnitude of β has been described in Chapter One (Section 1.4).

Table 4.2 summarizes the results of a series of CNDOVSB calculations based on retinol-like molecules. The molecular structures of the compounds shown in Table 4.2 have been built up from crystal structures of β-carotene,[189] *all-trans*-retinal,[93] 3-(1,1,5-trimethyl-5-cyclohexene-6-yl)-propenoic acid,[176] and Vitamin A acetate.[158] Compounds (1) to (5) and (9) have calculated $\beta_{(\omega=1064nm)}$ values lower than that of 4-nitroaniline (β = 150 x 10^{-40} m^4V^{-1}). 4-Nitroaniline has an effective donor- acceptor interaction over a benzene ring while compounds (1) to (9) have only acceptor- groups at one end of the conjugated chain, this will lead to a lower β value for compounds with a similar conjugation length. From Table 4.2 it can be seen that as the length of the electronic chain is increased from 2 in (1) to 5 double bonds in (7), the minimum energy electronic transition (with an oscillator strength of greater than 0.05) tends to a lower wavelength. The hydroxyl- group in compound (9), Vitamin A (Retinol), causes an increase in the

minimum energy transition (from 428 nm for a -COOH group to 394 nm for the -OH group), because the -OH group is not part of the conjugation.

The magnitude of β is also influenced by the torsion angle between the plane of the cyclohexenyl group and the polyene chain. The magnitude of β for compound (7) which is planar is considerably greater than β for compound (8) which has a torsional angle of 60°.

The onset of electronic resonance can be seen in compound (10). As the electronic transition (488nm) approaches the wavelength of the second harmonic (532nm) the magnitude of β increases. β has been calculated at both $\omega = 0$ and $\omega = 1064$ nm (where ω = fundamental laser wavelength) and gives an estimate of the magnitude of β independent of the absorption wavelength. For instance, compound (7) has $\beta_{(\omega_{1064})}-\beta_{(\omega_0)} = 277 \times 10^{-40}$ and compound (10) has $\beta_{(\omega_{1064})}-\beta_{(\omega_0)} = 2550 \times 10^{-40}$ m^4V^{-1} an increase of ten times due to molecular resonance (see Table 4.2).

β-Ionylidenecyanoacetic acid, (2), and its isomer *cis*-β-ionylidenecyanoacetic acid, (3), were thought to be ideal as non-linear optical compounds for three reasons:

1/ The magnitude of β for (2) and (3) were expected to be large enough to be of commercial interest.

2/ The electronic transitions were expected to occur lower than 400 nm which would allow the compounds to be tested for SHG at 1064 nm. Furthermore, compounds which are colourless can be used at diode laser wavelengths, and therefore have direct applications in the electro-optics industry.[177]

3/ Compounds (2) and (3) have been prepared by simple synthetic routes but their electro-optic properties have not been fully investigated. These polyenes therefore were attractive candidates for achieving our aims of synthesizing co-ordination compounds with a ligand possessing a long conjugation pathway.

The first recorded isolation and characterization of β-ionylidenecyanoacetic acid and some of its salts was done by Wittig *et al.*[217] A mixture of *cis*- and *trans*-β-ionylidenecyanoacetic acids and their ammonium salts were prepared and then separated by fractional crystallization. They were characterized by careful degradation into easily

identified fragments. The ammonium salts were synthesized by passing ammonia through a solution of the required acid in benzene/petroleum ether.

There have been no reported metal salts of β-ionylidenecyanoacetic acid. The only reported organometallic compounds derived from Vitamin A like molecules are based on η^4-tricarbonyl-iron bonded to the olefinic chain.[136] This Chapter describes the synthesis and characterization of metal complexes of β-ionylidenecyanoacetic acid.

Recently, there has been some interest in the salts of 2-cyano-(C=C chain)$_n$-carboxylic acids.[193-195] The compound 2-cyano-5-(4-dimethylamino-phenyl)-2,4-pentadienoic acid (below) shows a SH signal of about 1.8 times urea at 1064 nm: [191]

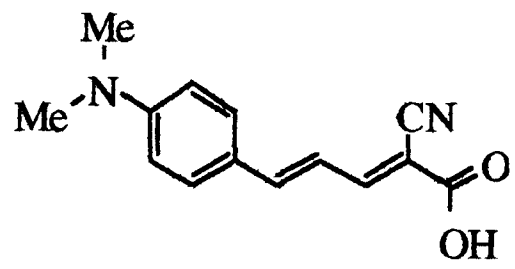
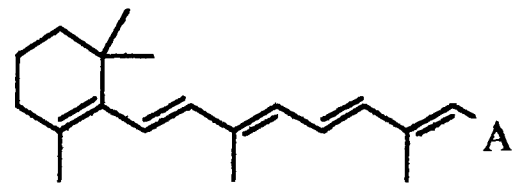
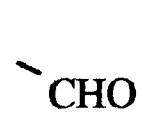
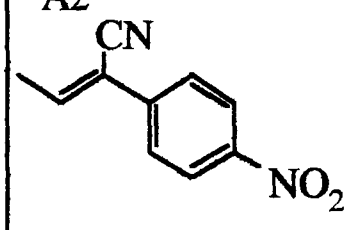
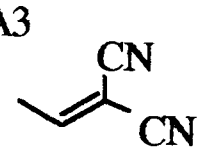
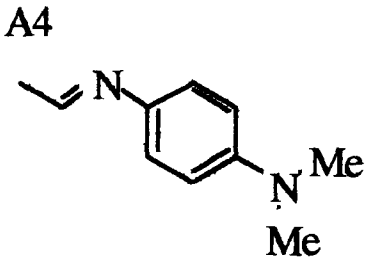


Table 4.1 Second order hyperpolarizabilities of the compounds A1 to A4, and comparisons to CNDOVSB calculations. Taken from refs. 103, 112 and 113.

Compound	λmax/nm	$\mu_0\beta$ (Real)*	$\mu_0\beta$ (Imaginary)	β(CNDOVSB)
A1	380	963	0	1360
A2	480	5900	15000	-
A3	470	5400	6300	-
A4	440	6300	7100	-

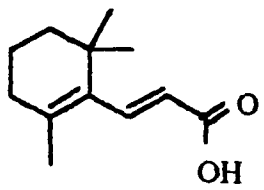
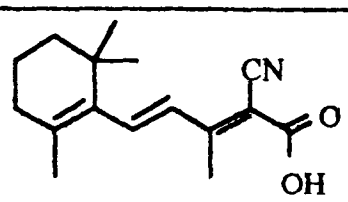
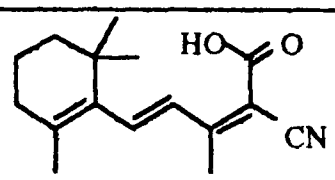
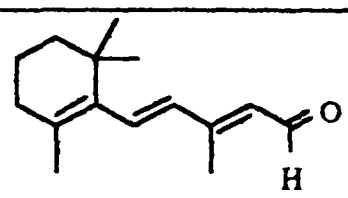
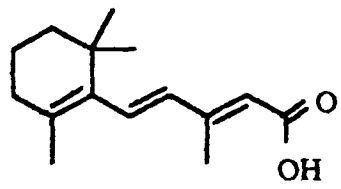
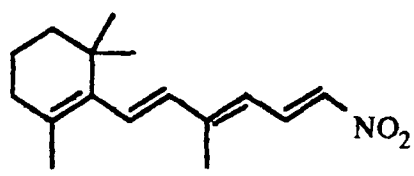
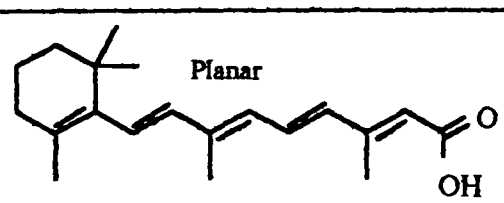
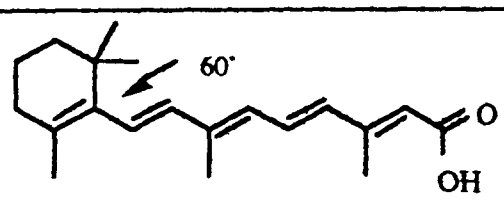
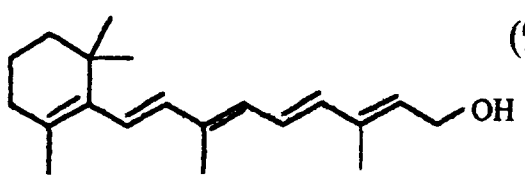
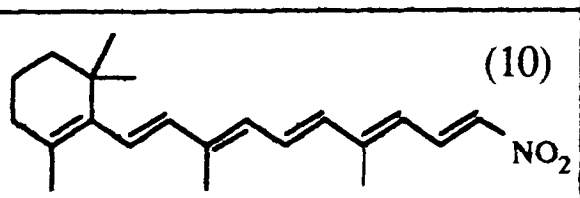
* units are $\mu_0\beta$ in $10^{-40}m^4V^{-1}$.

Where 

A1	A2	A3	A4
			

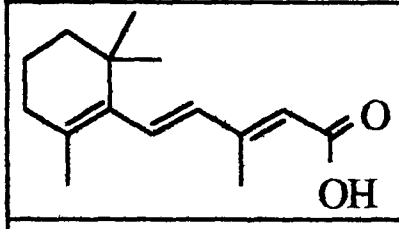
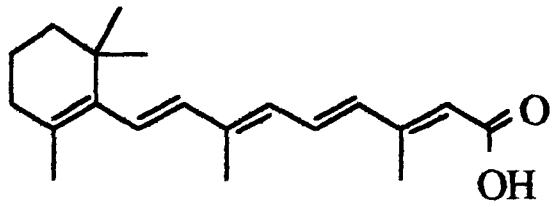
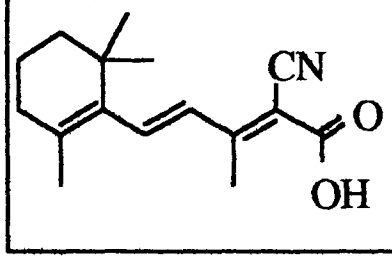
2-Cyano-3-(4-dimethylamino-phenyl)-2,4-pentadienoic acid forms a salt when treated with L-phenylalanine hydrochloride which was reported to give crystals with show strong SHG signals.[131]

Table 4.2 The results of CNDOVSB calculations on specified molecular structures done as part of this Thesis.

	Dipole, D	λ_{max}*	β (ω=0)	β (ω=1064nm)
(1) 	2.95	305	13.3	21.7
(2) 	8.04	375	10.8	50.5
(3) 	8.35	338	10.0	23.5
(4) 	5.63	356	33.1	87.3
(5) 	5.39	363	23.0	79.7
(6) 	8.15	388	87.8	292
(7) 	4.68	428	70.4	347
(8) 	4.04	406	47.8	199
(9) 	2.66	394	9.6	28.1
(10) 	10.28	488	221	2770

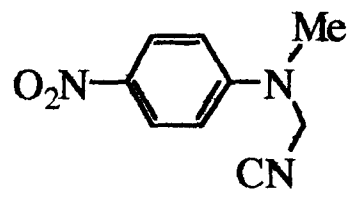
* Where the oscillator strength is greater than 0.05.

Table 4.3 Electronic spectra of 9-trans-β-ionylidene acetic acid, Vitamin A acid(from Planter *et al*, Helv. Chem. Acta, 1962, **45**, 548) and β-ionylidenecyanoacetic acid.

Compound	λ max / nm (ε)		
	EtOH	MeOH	Iso-octane
	258 (4.11) 297 (4.17)		255 (4.11) 300 (4.21)
	325 (4.7) 356 (4.53)		
		210 (3.97) 270 (4.17) 309 (4.31)	DCM 230 273 355

4.3 Synthetic Strategies

A search of the Cambridge Structural Database was made for non-centrosymmetric metal carboxylate complexes. This revealed a narrow class of suitable metals.[19] Simple zinc carboxylates exist as non-centrosymmetric polymeric chains; Capilla *et al* [42] investigated the crystal structure of catena[bis(di-μ-acetato)-zinc(II)], which crystallized in the non-centric space-group Fdd2. This space group has favourable phase matching characteristics and for example the compound:



crystallizes in the space group Fdd2, and has a SHG efficiency of 140 times urea.[47] Clegg *et al* [52-54] made catena[bis(di-μ-propionato-O,O')-zinc(II)], space group $Pna2_1$ and Natarajan *et al*[153] synthesized aquo[bis(o-ethoxy-benzoato)-zinc(II)], space group Pc.

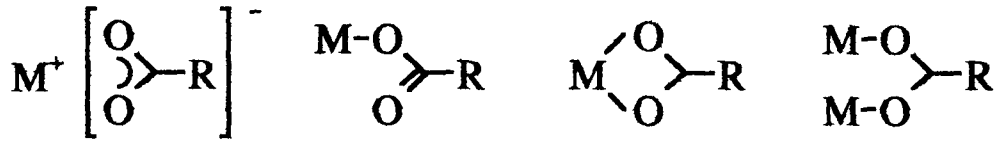
Since all of these zinc carboxylates crystallize in non-centric space groups, it was considered that the more complex zinc carboxylates made from β-ionylidenecyanoacetic acid may also possess this property.

Other transition metal acetates with non-centrosymmetric crystal structures include the diaquo-cadmium diacetate[95] with space group $P2_12_12_1$, and the cyclo[tetrakis(di-μ-acetato)platinum(II)][67] which crystallizes in the $P4_32_12$ space group.

4.4 Vibrational Spectra of Metal Carboxylates

Infrared vibrational spectroscopy is a useful technique in the characterization of metal carboxylates if coupled with data obtained from mass spectrometry, electron spin resonance and magnetic measurements.

The structures of metal carboxylates may be summarized as follows (see Fig. 4.1):



(i) C_{2v} (ii) C_s (iii) C_{2v} (iv) C_{2v}

ionic monodentate bidentate bridging

Fig. 4.1 Possible structures for metal carboxylates and their symmetry relationships.

Structures (i), (iii) and (iv) belong to the point group C_{2v}, while (ii) belongs to the less symmetrical point group C_s. This leads to differences in the vibrational spectra.[44]
The most prominent bands being ν(O-H), ν(C=O) and ν(C-O).

4.4.1 Ionic Carboxylates (i)

The O-C-O angle tends to be in the order of 100-130°, and because of the symmetric nature of the molecule, no C=O stretching modes are seen at 1700 cm^{-1}. Symmetric and antisymmetric CO stretching modes are observed at 1510-1650 and 1280-1420 cm^{-1}. For example, sodium ethanoate shows $\nu(COO)_{sym}$ at 1578; $\nu(COO)_{asym}$ at 1414 cm^{-1}.[139]

4.4.2 Monodentate Carboxylates (ii)

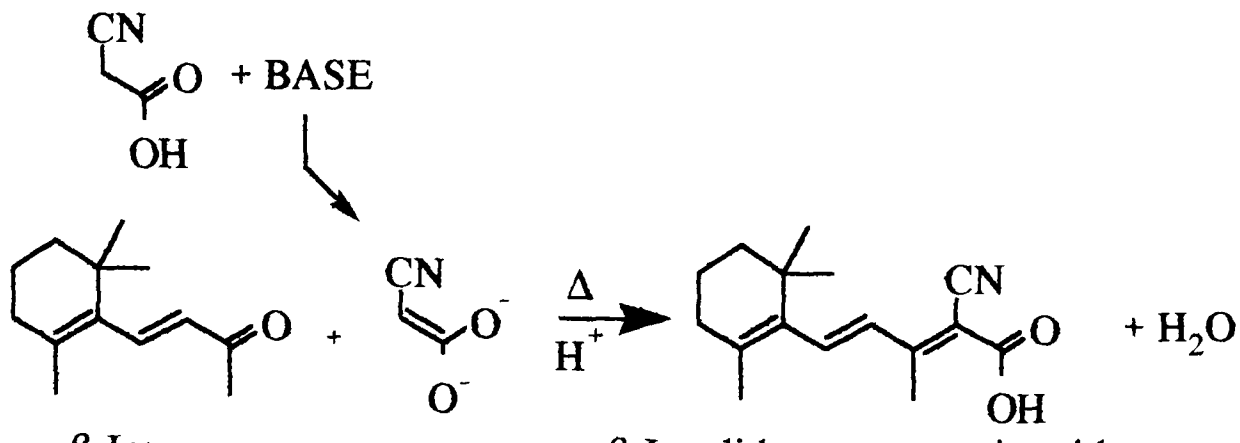
The unidentate carboxylates show an increase in the frequency of the $\nu(COO)_{asym}$ stretch, coupled with a decrease in the frequency of the $\nu(COO)_{sym}$ stretching mode. The spectrum may be complicated by the presence of solvent, e.g. water, which, via hydrogen bonding, leads to a decrease in the frequency of the $\nu(COO)_{asym}$ stretch. An indication of the degree of asymmetry is the parameter $\Delta\nu$ which is the difference between $\nu(COO)_{asym}$ and $\nu(COO)_{sym}$. In cases where carboxylates are monodentate, $\Delta\nu$ tends to be large (in the order of 164 cm^{-1} upwards). $Ni(OAc)_2.3H_2O$ is one of the exceptions It has $\Delta\nu$ equal to 107 cm^{-1}, which is smaller than expected because of the effect of H_2O solvation. In the case of $Li(OAc).2H_2O$ the acetate is monodentate because of the effect of the water molecules with a C-O and CO-M distance of 1.33Å while C=O is 1.22Å. Group 4 compounds have the greatest tendency to form monodentate carboxylate complexes.

4.4.3 Bidentate Carboxylates (iii) and (iv)

It is difficult to ascribe either structure (iii) or (iv) to a particular system because of their similarity. There are several trends that may be described. The $\nu(COO)$ frequency does not differ much from the free ion spectrum, even when co-ordinated to heavy metals. The $\Delta\nu$ for chelating carboxylates, (iii), is in the order of 94 cm^{-1} (e.g. $Zn(OAc)_2.2H_2O$) while bridging acetates, (iv), show a $\Delta\nu$ of around 160 cm^{-1} (e.g. $Zn_4O(OAc)_6$ = 159 and $Cu_2(OAc)_4.2H_2O$ = 185 cm^{-1} (1603-1418 cm^{-1})).

4.5 Preparation and Properties of β-Ionylidenecyanoacetic Acids

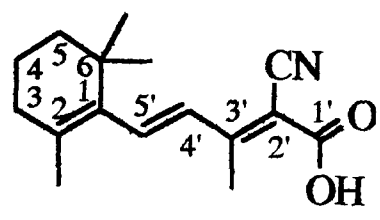
β-Ionylidenecyanoacetic acid was prepared by a modified method reported by Huisman *et al*,[101] as a by product of the synthesis of β-ionylidene acetonitrile. β-Ionone was reacted with the enol- of cyanoacetic acid, catalysed by a mixture of ammonium acetate and acetamide:



β-Ionone β-Ionylidenecyanoacetic acid

The reaction is driven by the loss of water from the reaction mixture by choosing a high boiling point solvent such as toluene, and refluxing the reaction mixture in a Soxhlet apparatus filled with a drying agent. Calcium chloride and 4 Å molecular sieve were both found suitable, the latter giving a cleaner product. The reaction mixture was heated for only two hours to limit the loss of CO_2 and the formation of β-ionylidene acetonitrile.[106,107,111] The reaction mixture was extracted with diethyl ether; the extract was washed with water and then sodium hydroxide solution which removed all the β-ionylidenecyanoacetic acid as the sodium salt. The aqueous sodium ionylidenecyanoacetate/NaOH was acidified with HCl, releasing the free β-ionylidenecyanoacetic acid, which was allowed to crystallize, filtered, dried under vacuum, and recrystallized from tetrachloromethane. The yield of β-ionylidenecyanoacetic acid and β-ionylidene acetonitrile were 19 and 24% respectively. The reaction produces both *cis-* and *trans-* isomers, but the *trans-* isomer is less soluble in tetrachloromethane than the *cis-* isomer, and simple re-crystallizations effected good separation.[184]

Fig. 4.2 Skeletal numbering system for *trans*-β-ionylidenecyanoacetic acid (2-cyano-3-methyl-5-(2,6,6-trimethyl-1-cyclohexen-1-yl)-2,4-pentadienoic acid).

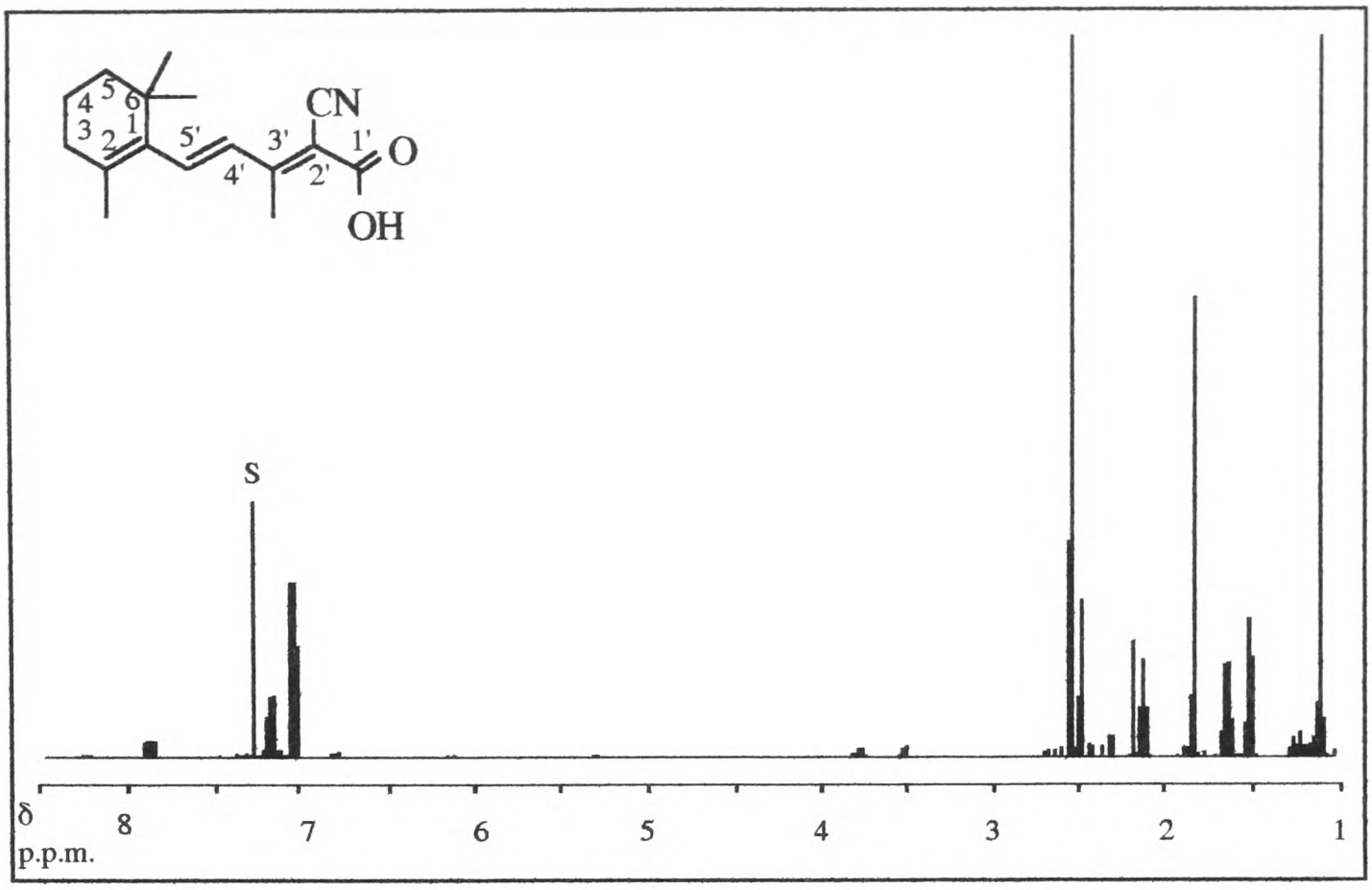


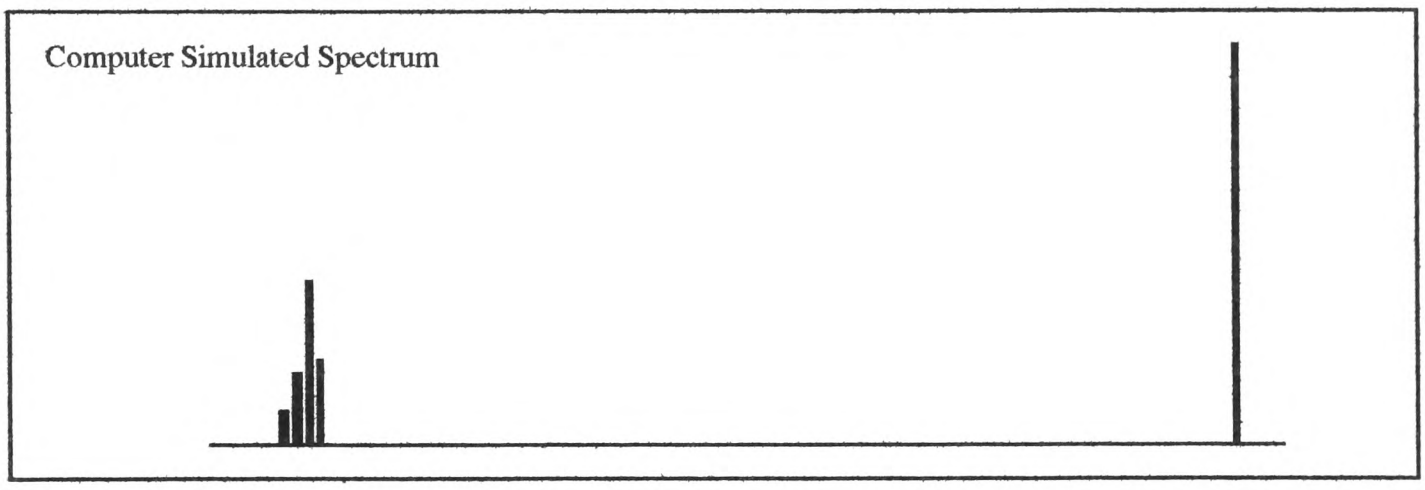
β-Ionylidenecyanoacetic acid is a yellow crystalline compound soluble in toluene, tetrachloromethane, tetrahydrofuran, ether, methanol, ethanol and most other polar organic

solvents. Unlike many organic carboxylic acids, it is insoluble in boiling water. The infrared spectrum was assigned as follows: ν(CN) at 2208 cm^{-1}, the conjugated $\nu(COO)_{asym}$ at 1688 and $\nu(COO)_{sym}$ at 1296 or 1257 cm^{-1}. A strong absorption probably due to the conjugated αβ unsaturated C=C bond was observable at at 1583 cm^{-1}, other assigned bands are given in Table 4.6.

The ^1H n.m.r. spectrum of β-ionylidenecyanoacetic acid (Fig. 4.3) shows the characteristic *trans*-olefinic protons at δ 7.04 (H4') and 7.19 (H5') p.p.m. (for proton assignment see Table 4.4) with a $J_{H,H'}$ coupling constant of 17 Hz. Since the chemical shifts differences are small, the the peaks appear as a second order AB pattern. The insert in Fig. 4.3 shows a computer generated spectrum with the relevant proton coupling constants, and agrees well with the observed spectrum. The H5' resonance shows additional small couplings to the methyl group and methylene H3 protons. The remaining three methyl resonances are observed at δ 2.56 (Me3'), 1.85 (Me2) and 1.11 (2xMe6) p.p.m. The cyclohexenyl ring protons are observed as multiplets at δ 2.13 (H3), 1.65 (H4) and 1.51 (H5) p.p.m.[1] The assignments of the resonances has been discussed by Moss *et al.*[146]

Fig. 4.3 The 500 MHz ^{1}H n.m.r. spectrum of β-ionylidenecyanoacetic acid.





Closer examination of the ^{1}H n.m.r. spectrum of β-ionylidenecyanoacetic acid using COSY (Fig. 4.4) shows the assignment of the resonances and has shown them to be consistent with those for other carotenoids.[146] The two H4 protons of the cyclohexenyl ring are coupled strongly (6.5 Hz) to the H3 and the H5 protons (see Table 4.4). The proximity of the hexenyl ring double bond shifts the H3 resonances down field to 2.13 p.p.m.

Fig. 4.4 The 500 MHz ^{1}H COSY spectrum of β-ionylidenecyanoacetic acid.

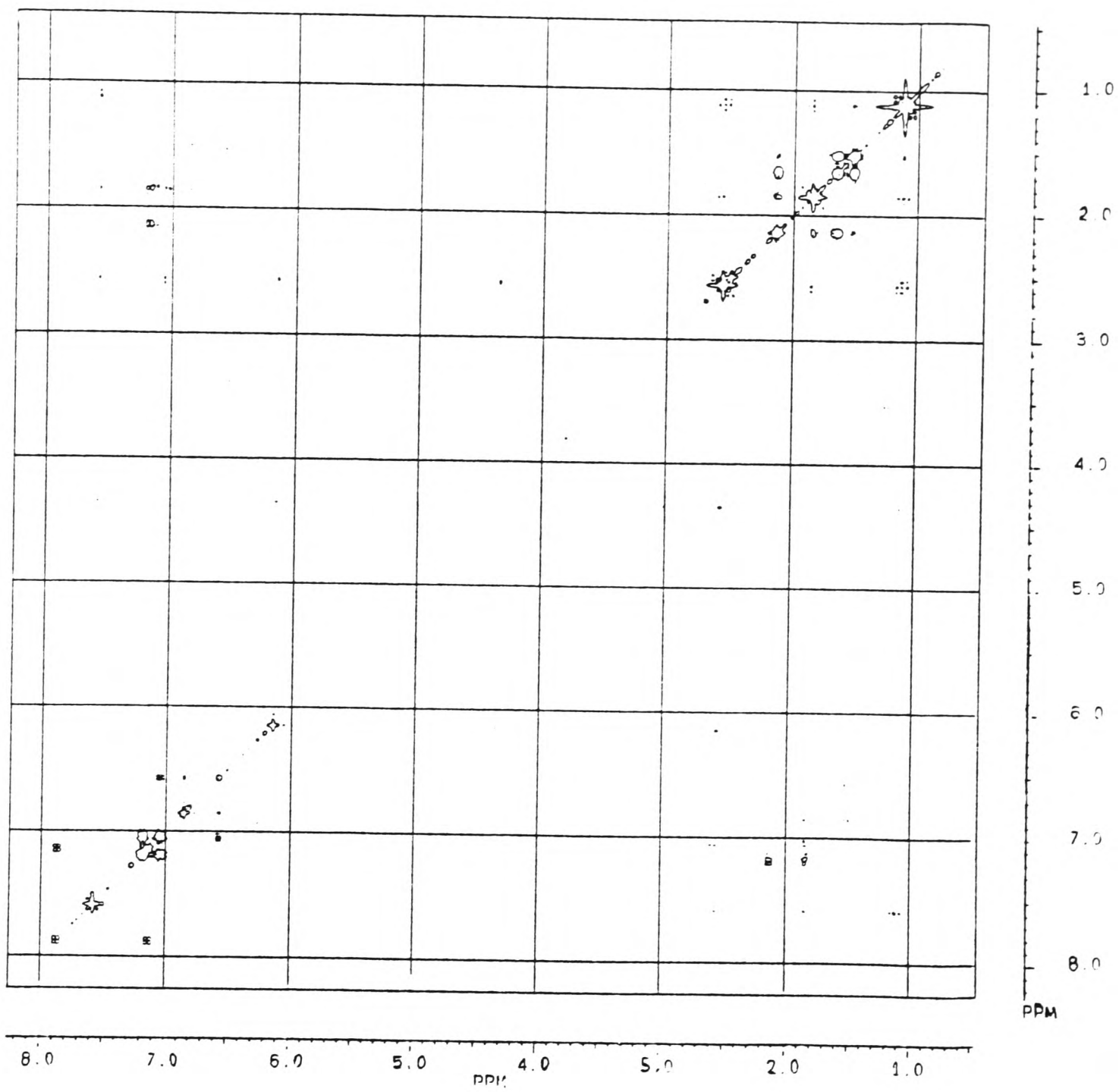
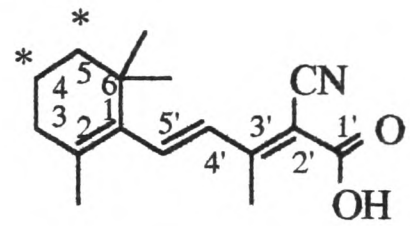


Table 4.4 Proton allocation of COSY β-ionylidenecyanoacetic acid ^{1}H n.m.r.spectra.

										
Me2			1.85							
H3			0.9	2.13						
H4				6.5-7	1.65					
H5			C	<2.7	6.3	1.51				
H4'							7.04			
H5'			0.9	0.9	0.9		17	7.19		
Me6								C	1.11	
Me3'			C				C		C	2.56
Proton Assignment			Me 2	H3	H4	H5	H4'	H5'	Me 6	Me 3'

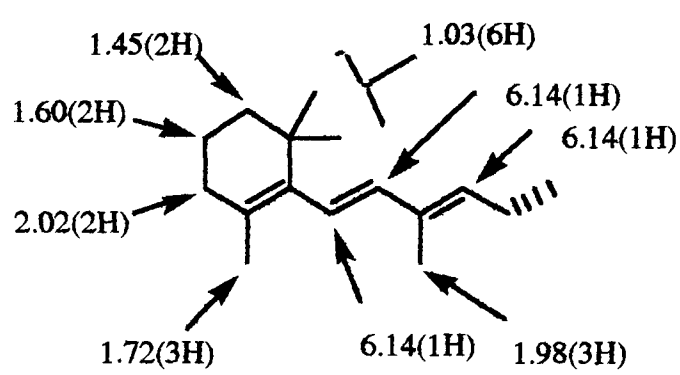
Figures are δ in p.p.m./ coupling constants in Hz..

* Protons are inequivalent because of ring conformations, C = coupling detected and << 0.9 Hz.

The H3 resonances are also coupled weakly (0.9 Hz) to the olefinic proton H5', and this has the same ^{4}J coupling constant observed between H5' and the methyl protons Me2 (0.9 Hz). The olefinic proton H5' shows multiple line splittings, which show up under Gaussian enhancement and are not observed for the H4' proton (See inserts in Fig. 4.4). There is no significant coupling between H4' and any protons on the ring, however

there is a small coupling between H4' and Me3' not seen between H5' and Me3', and so H5' is the olefinic proton nearest the cyclohexenyl ring. The fine structure seen in the resonances of the aliphatic protons H4 and H5 are probably due to an inequivalence in the geminal protons caused by axial and equatorial positions which have been generated by the "locking" action of the double bond in the cyclohexene ring. The resonance of H3 shows the expected triplet, with line broadening (through unresolved line splitting) caused by long range ^{4}J coupling. A comparison of the ^{1}H n.m.r. of β-ionylidenecyanoacetic acid with a half carotinoid structure is shown in Fig. 4.5.[43,172]

Fig. 4.5 The ^{1}H n.m.r. of β-cyclohexenyl- half carotenoid taken from ref. 146. δ values shown in p.p.m. (number of protons).



The mass spectrum of β-ionylidenecyanoacetic acid was measured by both electron impact and FAB methods. The base peak observed in the FAB mass spectrum is the protonated molecular ion corresponding to m/z = 260. The dimeric protonated ion is observed at m/z = 519. The electron impact spectrum does not show the protonated molecular ion, but has m/z = 259 which corresponds to the molecular ion (see Fig.4.6 and Table 4.5A). The fragmentation pattern shows loss of CO_2, Me, and a molecular rearrangement of the cyclohexenyl- ring resulting in the formation of ethene.

Fig. 4.6 The electron impact mass spectrum of β-ionylidenecyanoacetic acid.

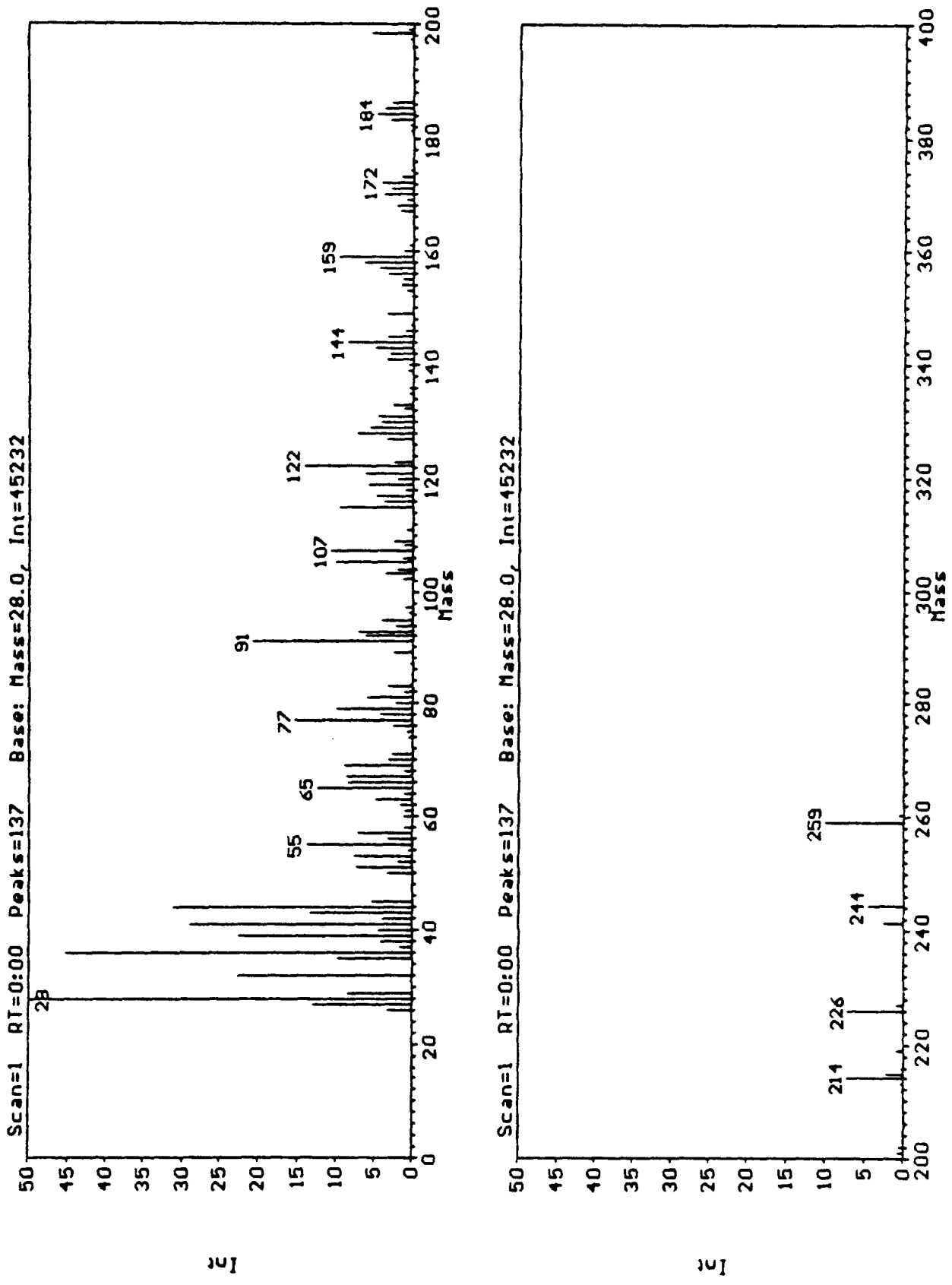
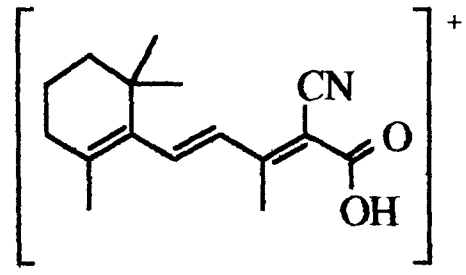


Table 4.5A FAB mass spectrum of *trans*-β-ionylidenecyanoacetic acid.

Molecular ion M^+ = 

m/z	Possible Peak Inference	Fragment Lost from M
519	$[2M+H]^+$	--
260	$[M+H]^+$	--
259	M^+ (EI)	--
244		Me
242		OH
241		H_2O
226		Me + H_2O
214		CO_2
200		CO_2 + Me
186		ethene (Mol. Rearr.) + CO_2
172		Me + CO_2 + ethene (Mol. Rearr.)

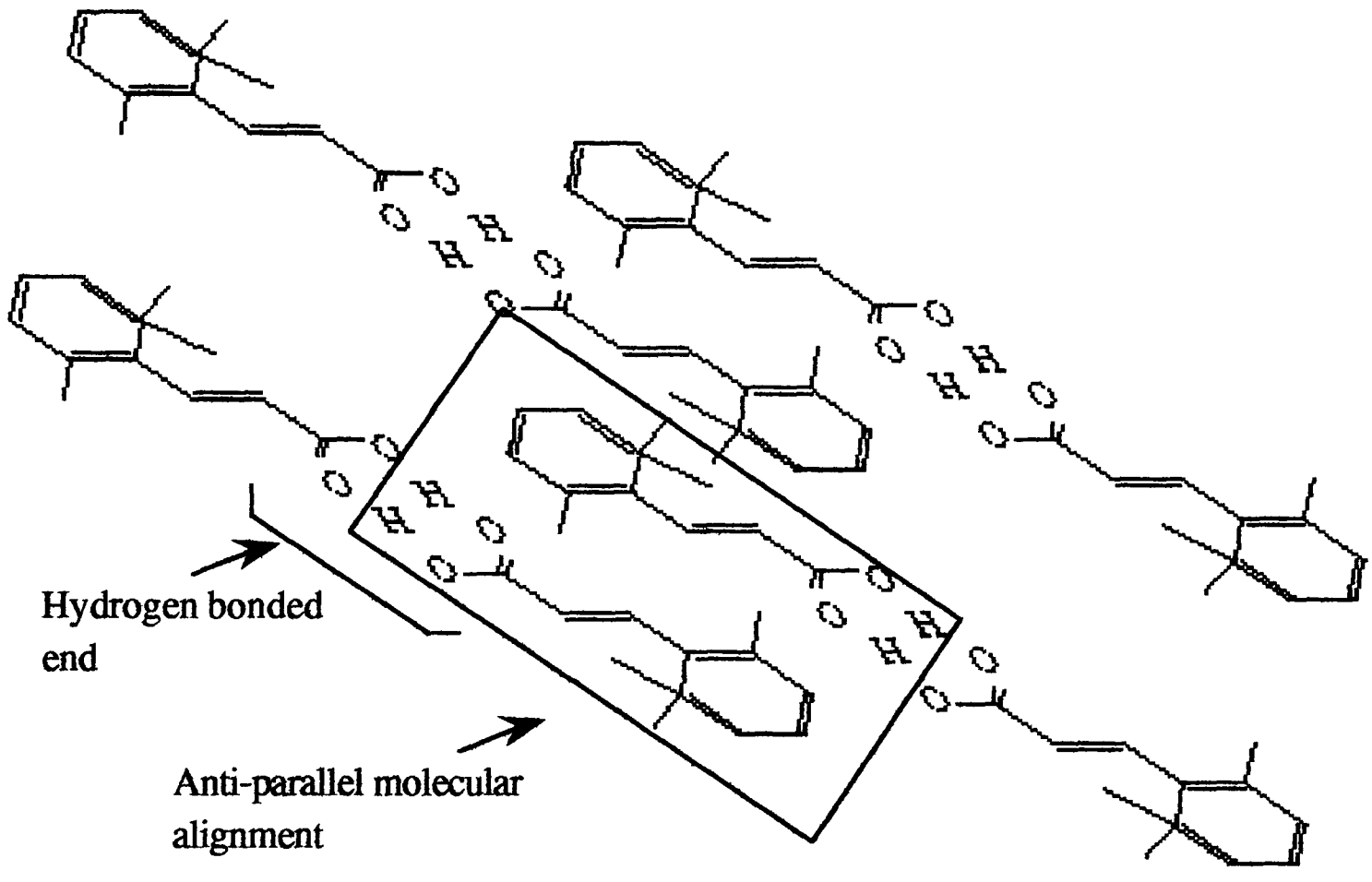
EI signifies only observed in the electron impact mass spectrum.

Table 4.5B FAB mass spectrum fragments (Ion) and relative intensities (R.i.) of silver *trans*-β-ionylidenecyanoacetate, based on Ag = 107, with 1 mass unit resolution.

Ion	m/z	R.i.
$(O_2CR)^+$	260	100
Ag^+	107	75
AgR^+	322	10
$Ag(O_2C)^+$	151	11
$Ag(O_2CR)^+$	**366**	**12**
Ag_2^+	214	6
Ag_2H^+	215	5
Ag_2R^+	428	7
$Ag_2(O_2CR)^+$	473	2.5
$Ag_2(O_2CR)R^{\cdot+}$	687	1
$Ag_2R_2^{\cdot+}$	644	2

The crystal structure of β-ionylidenecyanoacetic acid has not been determined. The structure of 9-*trans*-β-ionylideneacetic acid has been determined. It crystallizes in the centric space group $P2_1/c$,[116] as does the related compound 3-(1,1,5-trimethyl-5-cyclohexene-6-yl)-propenoic acid.[176] In the latter the molecules are arranged end to end so that the carboxylic acid groups hydrogen bond together. The hydrogen bonded dimers are stacked so that the dipoles are anti-parallel, see Fig. 4.7.

Fig. 4.7 Alignment of molecules in 3-(1,1,5-trimethyl-5-cyclohexene-6-yl)-propenoic acid.[176]

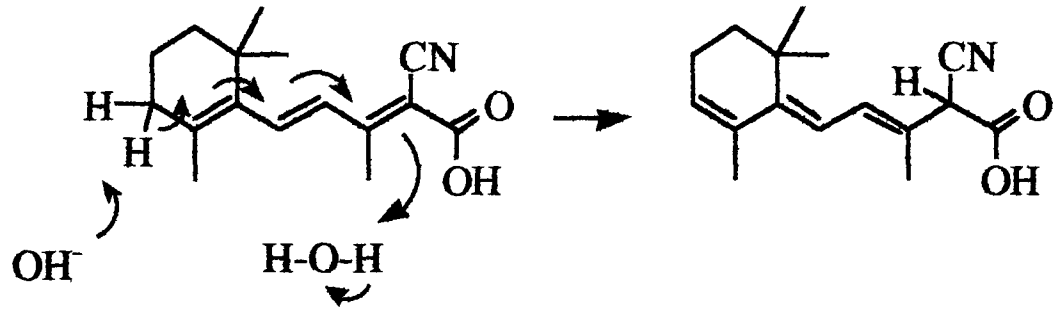


CNDOVSB calculations completed, as part of this research, on the predicted structure of β-ionylidenecyanoacetic acid derived from 3-(1,1,5-trimethyl-5-cyclohexene-6-yl)-propenoic acid, where the cyclohexenyl- ring is trans to the chain, gave $\beta_{CNDOVSB}$ to be 50.48 x 10^{-40} m^4V^{-1}. The electronic spectrum shows the main electronic transition to occur at 355 nm in dichloromethane, and 309 nm in methanol. The solvatochromic shift of 49 nm gives a calculated β value of 170 x 10^{-40} m^4V^{-1} when using the same value for the calculated dipole moment of 2.52 x 10^{-29} Cm. The corresponding β value for 4-nitroaniline and related compounds is in the order of 130 x 10^{-40} m^4V^{-1} leading to an imprecise prediction (imprecise because many other factors have been ignored) that if the correct symmetry is obtained then SHG values of 10-20 times urea should be obtained.

4.6 The Synthesis of Salts of trans-β-Ionylidenecyanoacetic Acid

Salts of *trans*-β-ionylidenecyanoacetic acid made from bases soluble in non-polar organic solvents were prepared cleanly, by adding the base, as liquid or gas (e.g. diethylamine, ammonia) to a solution of *trans*-β-ionylidenecyanoacetic acid in toluene. The salt precipitates from the non-polar solvent.

The reaction of *trans*-β-ionylidenecyanoacetic acid with bases such as lithium, sodium or potassium hydroxide in aqueous methanolic or ethanolic solutions results in the formation of the corresponding salt. If the base is in excess, the solution becomes red, showing that a major change in the electronic spectrum (and therefore the electronic distribution) has occurred. This change was noted by Huisman and Smit,[101,184] in connection with the synthesis of vitamin A acid and related compounds and attributed to the following rearrangement of *trans*-β-ionylidenecyanoacetic acid to retro-ionylidenecyanoacetic acid:[18]



β-Ionylidene cyanoacetic acid Retro-Ionylidene cyanoacetic acid

The *trans*-β-ionylidenecyanoacetic acid reacts with sodium hydrogen carbonate in methanolic water, to form a straw-yellow solution of the sodium β-ionylidene cyanoacetate. This reaction shows that the HCO_3^- ion is not basic enough to induce the rearrangement.

Reaction of the free acid with LiOH, NaOH or KOH solution in water produces a solution of the corresponding salt. If this solution is then carefully neutralized with dilute HCl to a pH of 7, or until the free acid is just about to precipitate, then this solution can be used to synthesize directly other water insoluble metal salts.

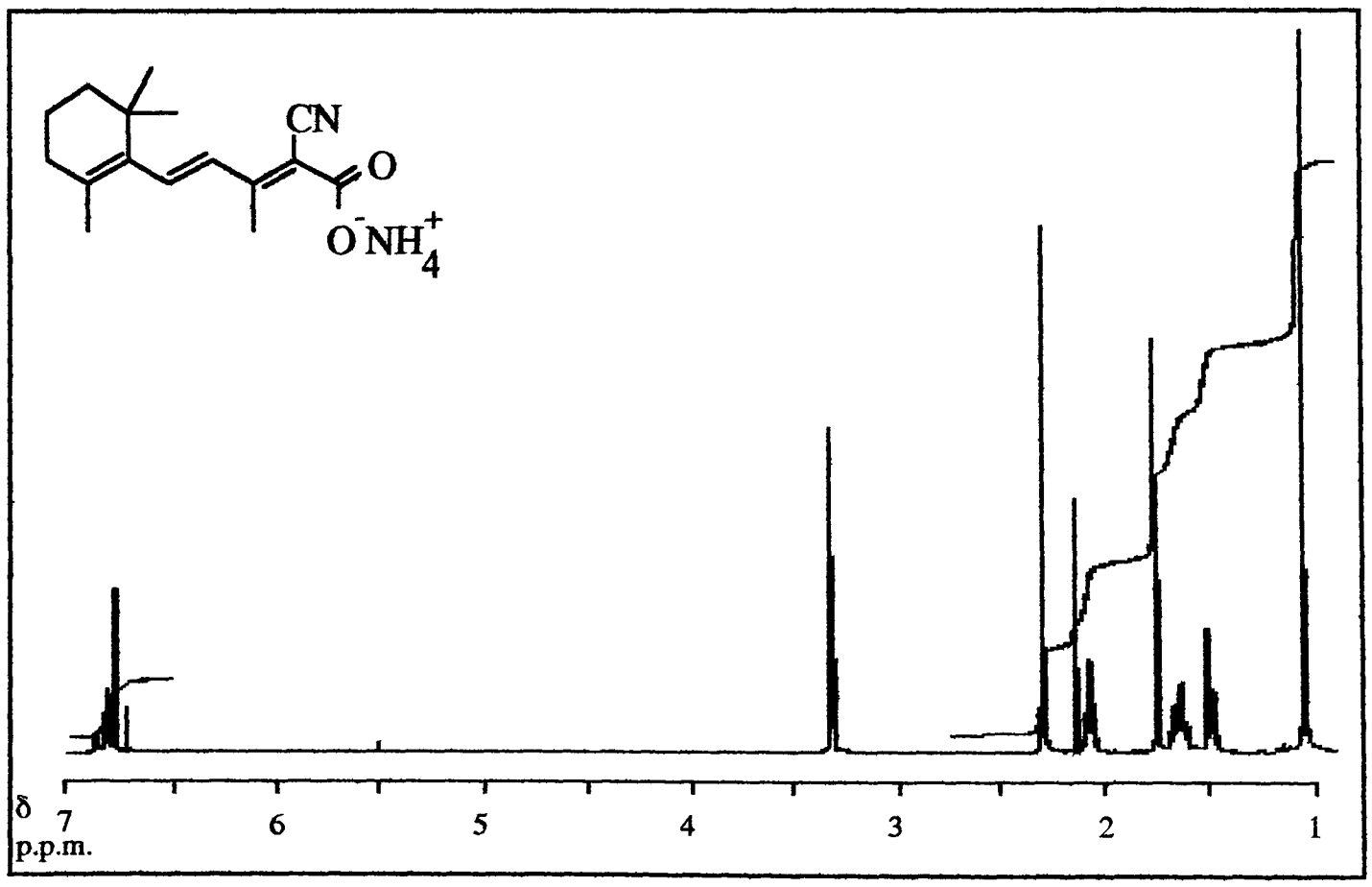
Table 4.6 The infrared spectral data for β-ionylidenecyanoacetic acid, some of its salts, and for comparison, some simple carboxylates.

Key: All values in cm^{-1}. n = Nujol Mull / KBr plates. h = Hexachlorobutadiene / KBr Str. = Stretch. Def. = Deformation.	Compound Number	ν(C=O) asym	ν(C-O) sym	ν(CN)	ν(αβ C=C)	ν(H-C=C-H) def.	ν(CC-H)	ν(O-H) or water	Δν	Phase.	Ref.
General Carboxylates	--	1700	1200-1300								
Ionic Carboxylates	--	1510-1650	1280-1400								
Sodium Ethanoate	--	1578	1414						164		137
Copper Ethanoate	--	1603	1418						185		265
β-Ionylidenecyanoacetic Acid	--	1688	1296 1257	2208	1583	961	931	2619		n	
NH_4L	(IV.1)	1611	1352	2231 2209	1582	966	805	3171	259	n	
Et_2NH_2L	(IV.2)	1625 1602	1354 1336	2195	1576 1544	966	793			n	
Et_4NL	(IV.3)	1648	1404	2129	1488	950		3400	244	n	
CsL	(IV.4)	1605	1350	2214	1580	967	803	3405	255	n/h	
AgL	(IV.5)	1563	1358	2208	masked	965	792	3400	205	n/h	
BaL_2	(IV.6)	1595	masked	2215	1563	976	814 804	3300		n	
ZnL_2	(IV.7)	1620 1598	1400 1360	2210	1587	966	840 896	3200		n	
CuL_2	(IV.8)	1637	1400	2254 2223	1563	972	791	3200	237	n/h	
NiL_2	(IV.9)	1621	--	2210		974		3100		n	

4.6.1 Ammonium *trans*-2-cyano-3-methyl-5-(2,6,6-trimethyl-1-cyclohexen-1-yl)-2,4-pentadienate (ammonium *trans*-β-ionylidenecyanoacetate) (IV.1)

Ammonium *trans*-β-ionylidenecyanoacetate was synthesized by a modification of the route described by Smit.[152] Dry ammonia gas was passed through a solution of *trans*-β-ionylidenecyanoacetic acid dissolved in diethyl ether, ammonium *trans*-β-ionylidenecyanoacetate (IV.1) precipitated out as a fine white solid. Crude (IV.1) was then recrystallized from water, forming colourless cubes. Elemental analyses were consistent with the molecular formula, and no water of crystallization was detected either by a discrepancy in the elemental analyses or by water absorption bands in the infrared spectrum. The infrared spectrum showed two ν(CN) stretches at 2231 and 2209 cm^{-1} with equal intensities (nujol mull, KBr plates, see Table 4.6 for further assignments). The solution infra red spectrum (in ethanol) showed two ν(CN) stretching modes with unequal intensities at 2223 and 2201 cm^{-1}.

Fig. 4.8 The ^1H n.m.r. spectrum of ammonium *trans*-β-ionylidenecyanoacetate.

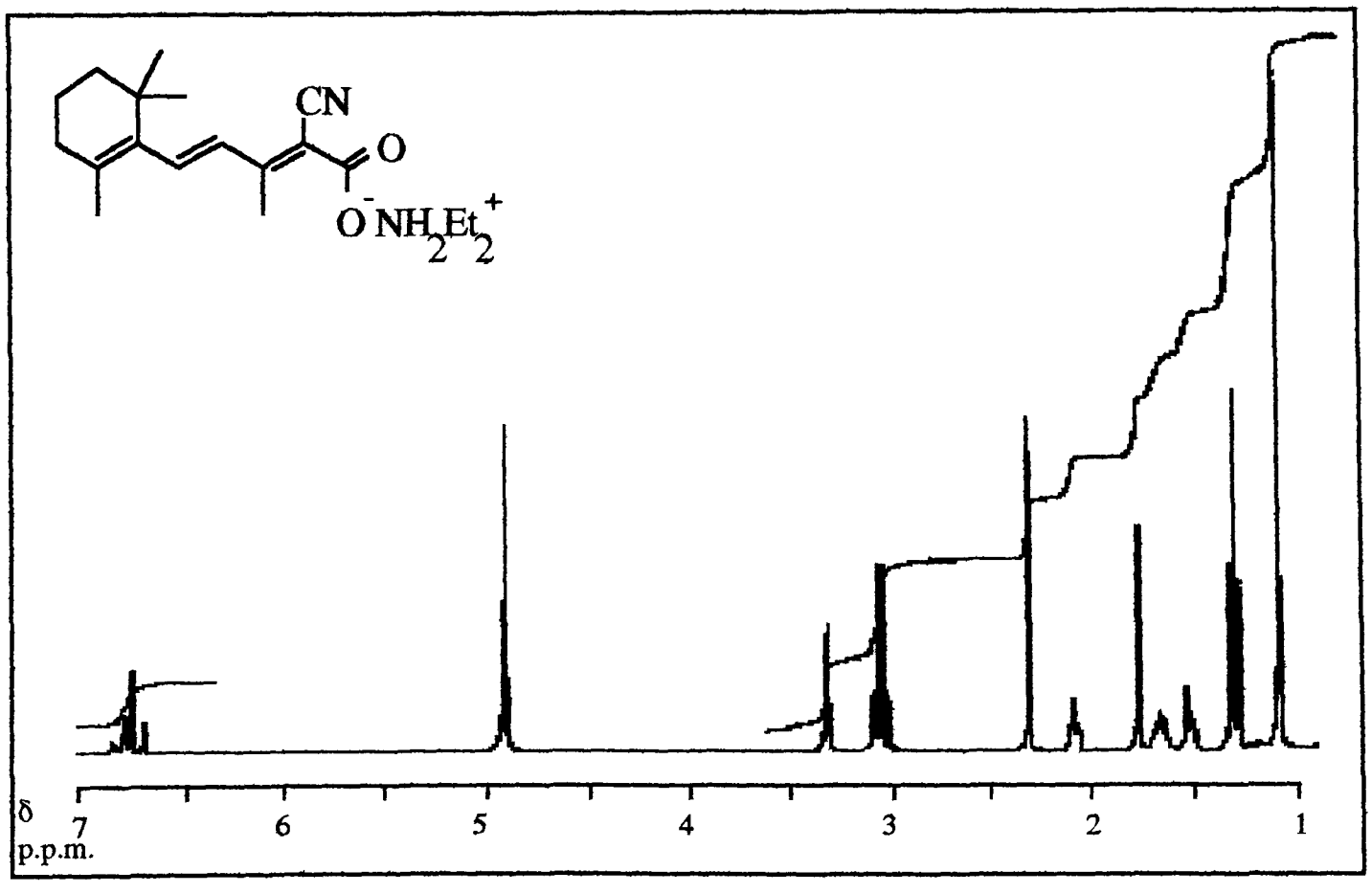


The initial inference was that the two nitrile stretching modes were due to different nitrile environments in the solid state. Unfortunately, two stretches were also observed in solution and this suggests the existence of two different nitrile environments. The ^1H n.m.r. spectra of ammonium *trans*-β-ionylidenecyanoacetate corresponds to that expected for the structure, and corresponds to that of the parent acid (see Fig. 4.8 and Table 4.7). No evidence was observed for the presence of a second isomer.

4.6.2 Diethylammonium *trans*-2-cyano-3-methyl-5-(2,6,6-trimethyl-1-cyclohexen-1-yl)-2,4-pentadienate (IV.2)

A slight excess of diethyl amine was added to a solution of *trans*-β-ionylidenecyanoacetic acid in warm benzene.

Fig. 4.9 The ^1H n.m.r. spectrum of diethylammonium *trans*-2-cyano-3-methyl-5-(2,6,6-trimethyl-1-cyclohexen-1-yl)-2,4-pentadienate (IV.2) in CD_3OD.



The colour of the solution turned from yellow to straw-yellow, and the solution was reduced in volume, and hexane was added to deposit white crystals of diethylammonium *trans*-2-cyano-3-methyl-5-(2,6,6-trimethyl-1-cyclohexen-1-yl)-2,4-

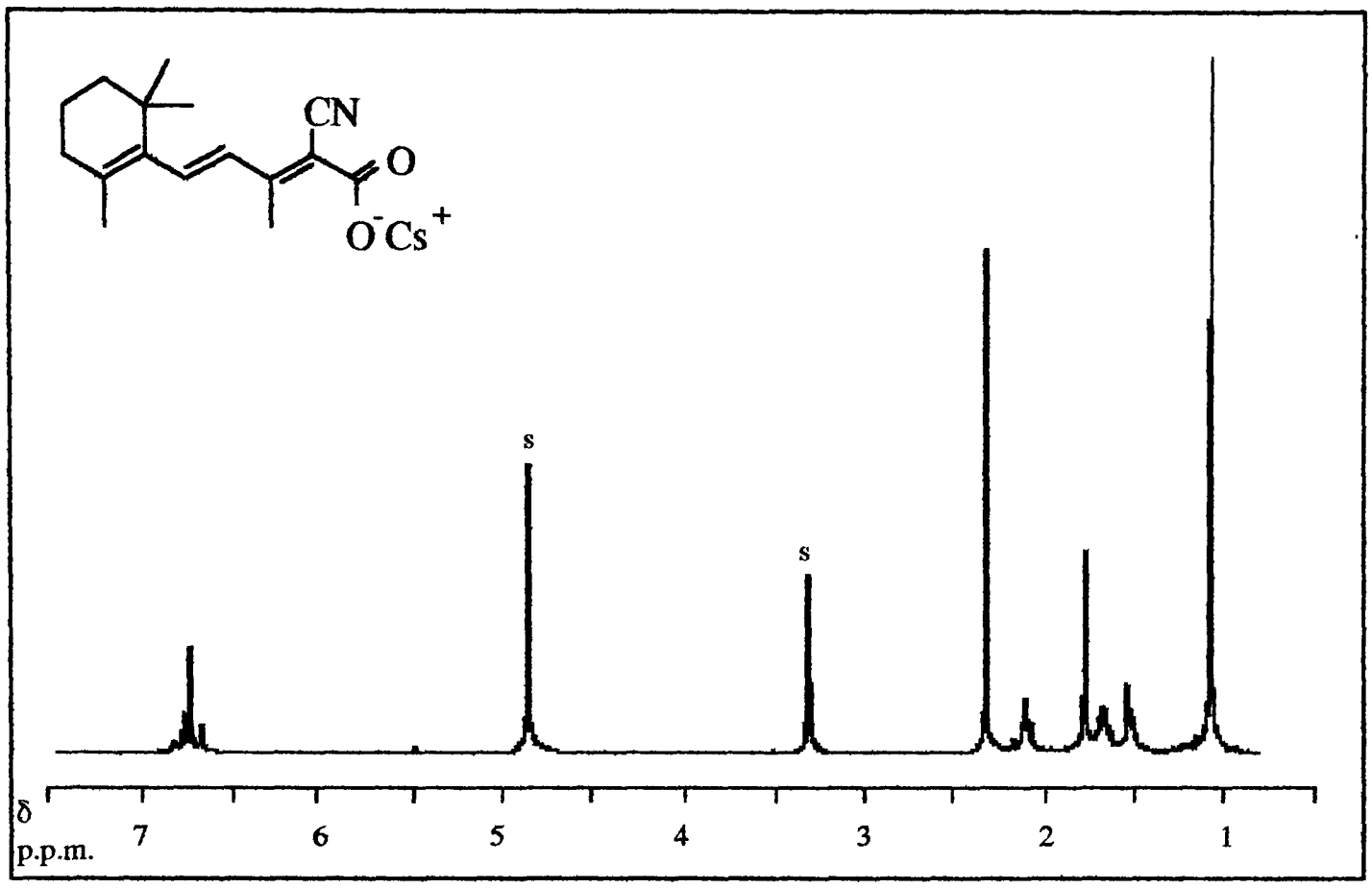
pentadienate (IV.2). Recrystallization from benzene resulted in fine white crystals of (IV.2) in 68% yield. Elemental analyses were consistent with the proposed molecular formula. The infrared spectrum of (IV.2) showed a ν(CN) stretching mode at 2195 cm^{-1} with a less intense band at 2222 cm^{-1}, for other infrared data see Table 4.6.

The ^{1}H n.m.r. spectrum gave the expected Me resonances at δ 1.07, 1.77 and 2.31 p.p.m (see Fig. 4.9 and Table 4.7). The olefinic resonances showed that the usually broader signals due to the 5'H were at 6.81 p.p.m. while The 4'H proton gave a typical signal at δ 6.72 p.p.m. The coupling constant between the 4'H and the 5'H was 16 Hz which is typical of a *trans*- structure. The diethylammonium cation gave the expected triplet at δ 1.29 p.p.m. and quartet at δ 3.04 p.p.m. both with a $^{3}J_{H,H'}$ of 7.5 Hz.

4.6.3 Tetraethyl *trans*-2-cyano-3-methyl-5-(2,6,6-trimethyl-1-cyclohexen-1-yl)-2,4-pentadienate (IV.3)

Equimolar solutions of *trans*-β-ionylidenecyanoacetic acid and tetraethylammonium hydroxide in methanol were reacted to form a violet-red solution. Evaporation of solvent left a red-dichroic oil insoluble in pentane, but reacted violently with tetrachloromethane to form a black deposit. The black solution was filtered through Kieselghur G, and all tetrachloromethane evaporated off, leaving an amber deposit. The amber deposit was dissolved in ethanol, from which on cooling, off-white, hygroscopic crystals formed. The crystals were filtered off, washed with cold ethanol, and dried under nitrogen. The i.r. spectrum showed a broad ν(CN) stretch at 2129 cm^{-1}, with other broad ν(OH) stretches at 3400 cm^{-1} due to water of crystallization. The impure salt was not studied further.

Fig. 4.10 The ^1H n.m.r. spectrum of caesium *trans*-2-cyano-3-methyl-5-(2,6,6-trimethyl-1-cyclohexen-1-yl)-2,4-pentadienate (IV.4) in CD_3OD, s = water and acetone solvents.



4.6.4 Caesium *trans*-2-cyano-3-methyl-5-(2,6,6-trimethyl-1-cyclohexen-1-yl)-2,4-pentadienate (IV.4)

Silver nitrate was added to a solution of the lithium salt β-ionylidenecyanoacetic acid formed by reacting *trans*-β-ionylidenecyanoacetic acid with LiOH in methanol/water, to precipitate out [2-cyano-3-methyl-5-(2,6,6-trimethyl-1-cyclohexen-1-yl)-2,4-pentadienato]silver(I) as a cream coloured solid. The precipitate was isolated, washed with water and methanol, and carefully dried. Caesium bromide was added to a suspension of *trans*-[2-cyano-3-methyl-5-(2,6,6-trimethyl-1-cyclohexen-1-yl)-2,4-pentadienato]silver(I) in aqueous ethanol. AgBr precipitated out leaving a clear solution, which was filtered, and the filtrate reduced to dryness. The resulting pale cream solid was recrystallized from hot acetone. Caesium *trans*-2-cyano-3-methyl-5-(2,6,6-trimethyl-1-cyclohexen-1-yl)-2,4-pentadienate (IV.4) crystallized out as fine white needles. The crystals were filtered off and dried. After removal of solvent the sample was no-longer crystalline.

Table 4.7 ^{1}H n.m.r spectral data for β-ionylidenecyanoacetate compounds.

Values of δ in p.p.m.	Compound Number	2 x Me6	Me2	Me3'	2 x H5	2 x H4	2 x H3	H5'	H4'	3J(H4', H5') / Hz	Solvent
HL	--	1.11	1.84	2.56	1.5	1.6	2.1	7.19	7.04	22	$CDCl_3$
NH_4L	(4.1)	1.06	1.77	2.31	1.53	1.65	2.09	6.81	6.72	16	CD_3OD
Et_2NH_2L	(4.2)	1.07	1.77	2.31	1.5	1.6	2.09	6.81	6.72	16	CD_3OD
CsL	(4.4)	1.08	1.77	2.32	1.54	1.68	2.10	6.82	6.73	18	CD_3OD
AgL	(4.5)	1.02	1.73	2.47	1.45	1.59	2.04	6.85	6.78	16	$CDCl_3$
BaL_2	(4.6)	1.08	1.77	2.36	1.5	1.6	2.10	6.85	6.74	16	CD_3OD
ZnL_2	(4.7)	1.09	1.79	2.45	1.54	1.65	2.11	6.95	6.81	16	CD_3OD
CuL_2	(4.8)	0.88	1.4	2.0	1.25	1.33	1.6	⇐ 6.4 ⇒		*	$CDCl_3$
NiL_2	(4.9)	* Too Broad to Measure - Paramagnetic Molecules									$CDCl_3$
NH_4L'	(4.10)	1.06	1.75	2.24	1.5	1.6	2.09	6.72	7.40	16	CD_3OD
BaL'_2	(4.11)	1.07	1.76	2.27	1.5	1.6	2.15	6.75	7.55	16	CD_3OD
ZnL'_2	(4.13)	1.06	1.81	2.40	1.5	1.6	2.10	7.88	6.96	16	CD_3OD

The elemental analyses of the amorphous white solid did not agree well with the values calculated for the molecular formula. A large water absorption at 3405 cm^{-1} in the infrared. spectrum explained the deviation of the elemental analyses from the calculated value. Some of the water of crystallization could be removed by drying the sample in a vacuum at 50-70°C for two days, resulting in a 0.8% increase in the carbon content and

corresponding 0.1% decrease in the hydrogen content. The i.r. spectrum of the dried sample still showed appreciable amounts of water which could not be removed by further drying under vacuum (equivalent to 0.33 molecules of water to each molecule of (IV.4)). Compound (IV.4) is soluble in water, methanol and acetone, but insoluble in diethyl ether.

The infrared spectrum of (IV.4) showed ν(C≡N) absorbance at 2214 cm^{-1}, while the conjugated $\nu(COO)_{asym}$ band was observed at 1605(s) and $\nu(COO)_{sym}$ at 1350(s) cm^{-1}. The α,β unsaturated ν(C=C) band was at 1580(m) cm^{-1}, and was weaker than the conjugated ν(COO) stretches (see Table 4.6).

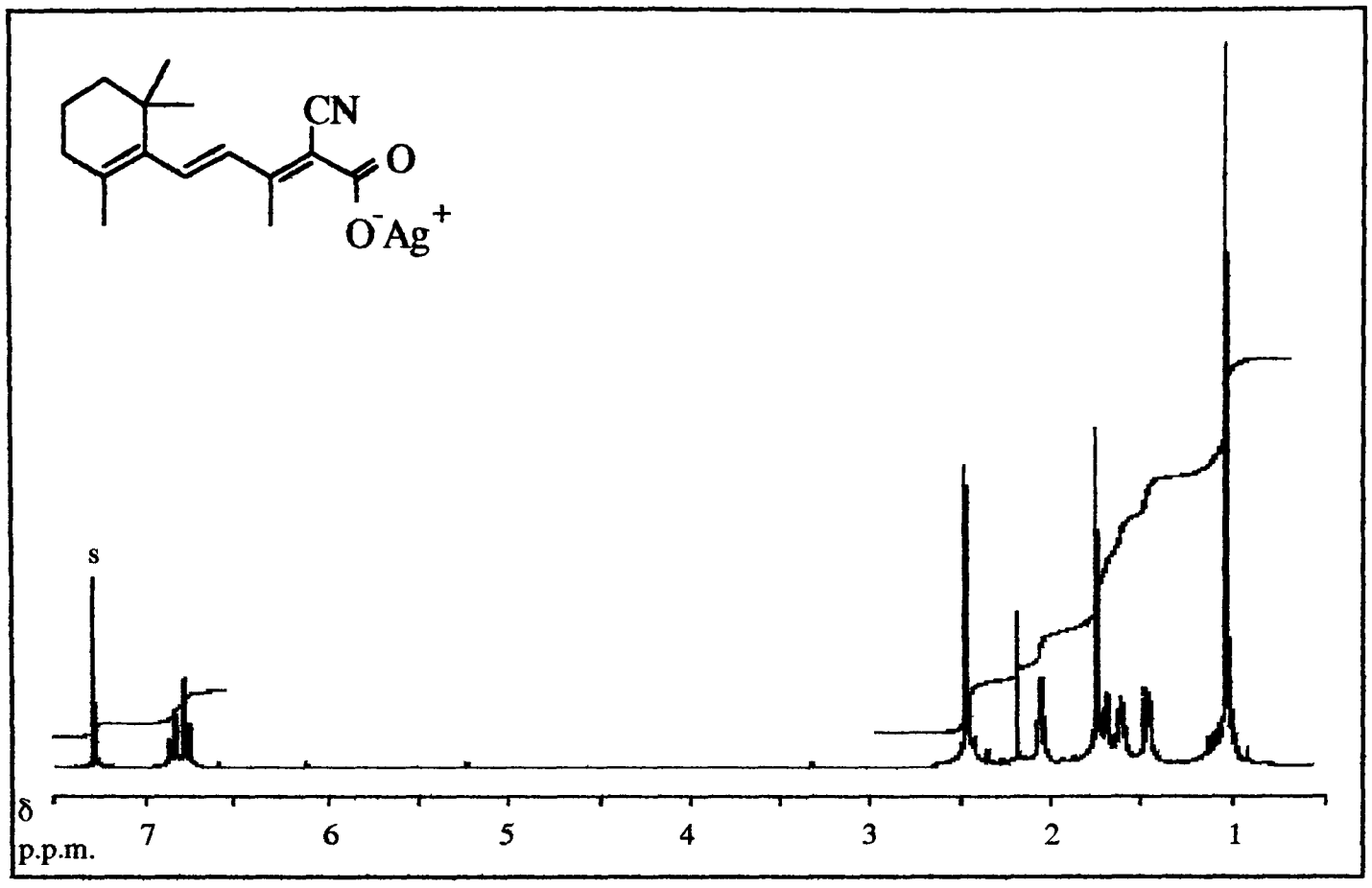
The ^1H n.m.r spectrum of (IV.4) in CD_3OD corresponded exactly to the expected spectrum (see Fig. 4.10 and Table 4.7). The *trans-* olefinic protons 5'H and 4'H gave doublets at δ 6.82 and 6.73 p.p.m. similar to other β-ionylidenecyanoacetic acid salts with a *trans-* $^3J_{H,H'}$ coupling constant of 18 Hz. The 5'H signals showed a similar broadening seen in the spectrum of the free acid. This broadening was shown to be due to small couplings of less than 0.9 Hz between H5' and Me2. The remaining methyl- and alkyl- resonances correspond to those noted for the parent acid.

4.6.5 *Trans*-[2-cyano-3-methyl-5-(2,6,6-trimethyl-1-cyclohexen-1-yl)-pentadienato]silver(I) (silver *trans*-β-ionylidenecyanoacetate) (IV.5)

Methanolic silver nitrate reacted with a neutral aqueous alcoholic solution of sodium or lithium β-ionylidenecyanoacetate, to form a buff coloured precipitate. After the precipitate was washed and dried, the silver β-ionylidenecyanoacetate was obtained as a fine powder, in 88% yield. It decomposed slowly in direct light, but could be stored indefinitely in the dark.

It dissolved in trichloromethane and dichloromethane, but was insoluble in hexane, acetone, water, methanol and ethanol and had a tendency to retain solvents, which could not be readily removed *in vacuo*. Attempts at recrystallization from chlorinated solvents resulted in oils, and those solutions were also found to decompose slowly with time.

Fig. 4.11 The ^{1}H n.m.r. spectrum of silver β-ionylidenecyanoacetate (IV.5).



The infrared spectrum showed ν(C≡N) at 2208 cm^{-1}, and conjugated ν(COO) at 1563 cm^{-1} which was 125 cm^{-1} lower than the free acid at 1688 cm^{-1}. The broad absorption due to water at 3400 cm^{-1} was not affected by repeated drying in a good vacuum at 50-70°C (see Table 4.6).

The ^{1}H n.m.r. spectrum of (IV.5) in $CDCl_3$ differed from that of the parent acid in that the *trans*- olefinic protons at δ = 6.85 (H5') and 6.78 (H4') p.p.m. had been shifted up-field (see Fig. 4.11 and Table 4.7). H5' showed a slight broadening probably due to the combined ^{4}J coupling of the Me2 and H3 groups as seen in β-ionylidenecyanoacetic acid. The remaining methyl- and alkyl- resonances corresponded to those present in the parent acid.

The shift in the electronic spectrum, giving rise to the colour change of yellow to white on going from the free acid to the silver salt, suggests that a large change in the electron delocalization has taken place.

The FAB mass spectrum showed the parent ion at m/z = 366/368, with the isotope distribution of 50:50 $^{107}Ag/^{109}Ag$. Mehrotra *et al*[139] have stated that silver acetates are dimeric in the solid phase (by mass spectrum), with the base peak being $Ag_2(O_2CR)^{+}$.[2]

The mass spectrum of the silver β-ionylidenecyanoacetate showed a small peak due to $Ag_2(O_2CR)^+$ m/z = 473/475/477 but these peaks were less intense than that of the peak due to $Ag(O_2CR)^+$. Loss of CO_2 from $Ag(O_2CR)^+$ gave a peak at m/z 322/324, while the peak at m/z = 260/262 was due to loss of Ag^+, the Ag^+ ion being observed at m/z = 107/109. A peak at m/z = 413/415 which has one silver atom associated with it was not identified (for fragmentation pattern see Table 4.5B). Fragmentation assignments follow those in ref. 2 for silver acetate. The mass spectra of silver carboxylates so far investigated show no peak due to $Ag(O_2CR)^+$.[2] The mass spectrum of silver *trans*-β-ionylidenecyanoacetate described above has a peak due to the $Ag(O_2CR)^+$ ion, and therefore suggests that silver *trans*-β-ionylidenecyanoacetate is monomeric in the solid phase.

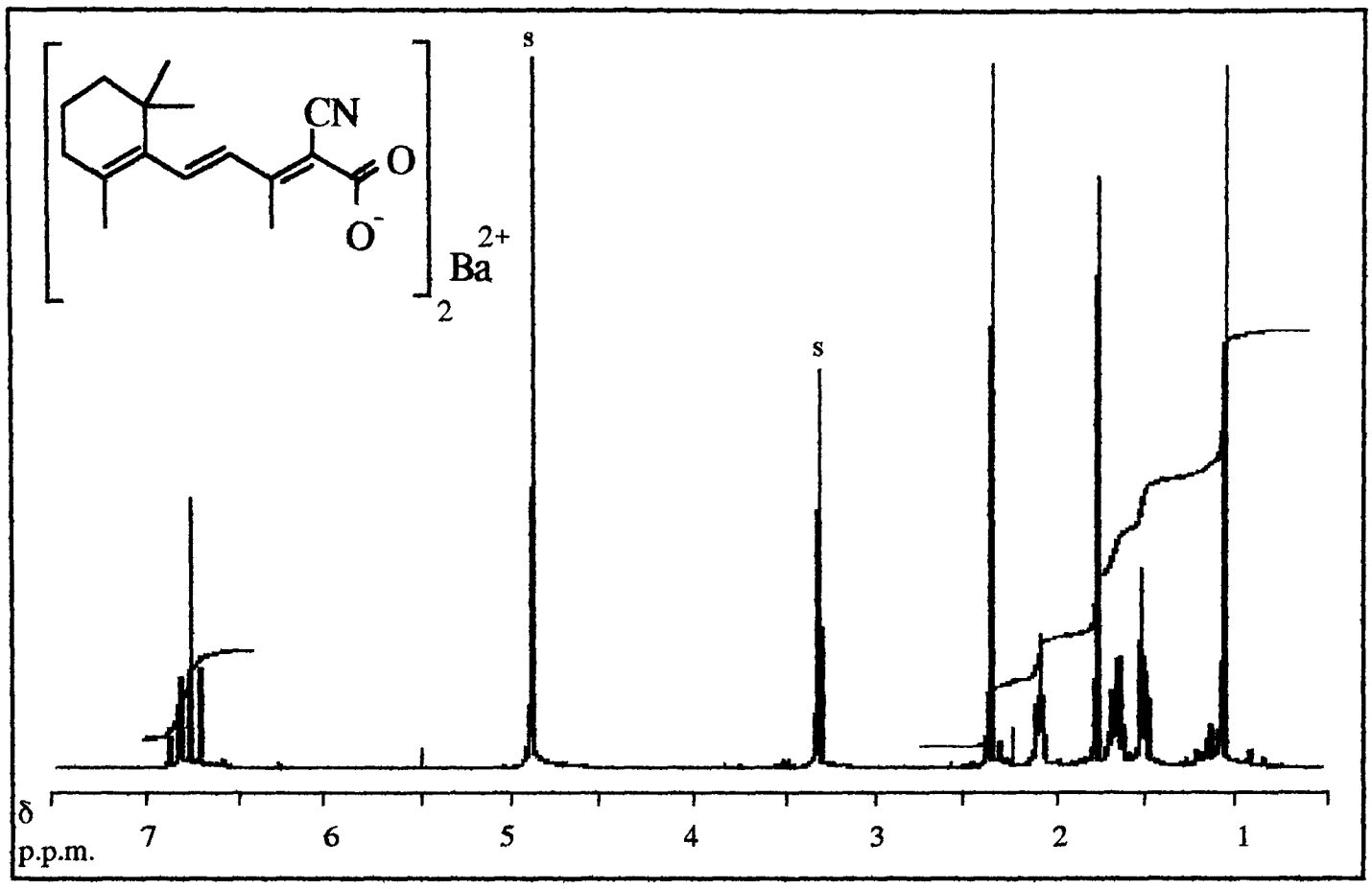
4.6.6 Barium *trans*-2-cyano-3-methyl-5-(2,6,6-trimethyl-1-cyclohexen-1-yl)-2,4-pentadienate (IV.6)

An aqueous solution of barium nitrate was added to sodium β-ionylidenecyanoacetate to precipitate out barium *trans*-2-cyano-3-methyl-5-(2,6,6-trimethyl-1-cyclohexen-1-yl)-2,4-pentadienate as a white solid. The white solid was redissolved in hot boiling water, and fine white crystals (in 26% yield) formed on cooling. Unfortunately, crystals suitable for X-ray diffraction studies could not be grown.

The elemental analyses indicated the presence of 3 waters of crystallization. The infrared spectrum showed a broad water absorption band at 3300 cm^{-1}, and an intense water resonance (with an integration which approximates to 6H) was observed in the ^1H n.m.r. spectrum at δ 4.9 p.p.m.

The infrared spectrum showed a weak ν(CN) stretch at 2215 cm^{-1}, while the strong ν(αβ-unsaturated COO) absorbed at 1595 cm^{-1} typical of the asymmetric stretch. However, the symmetric stretch, normally seen around 1350 cm^{-1} was absent. The less intense absorption due to the unsaturated carbonyl C=C bond was observed at 1563 cm^{-1}, in a position typical for this functional group.

Fig. 4.12 The ^{1}H n.m.r. spectrum of barium *trans*-2-cyano-3-methyl-5-(2,6,6-trimethyl-1-cyclohexen-1-yl)-2,4-pentadienate (IV.6).



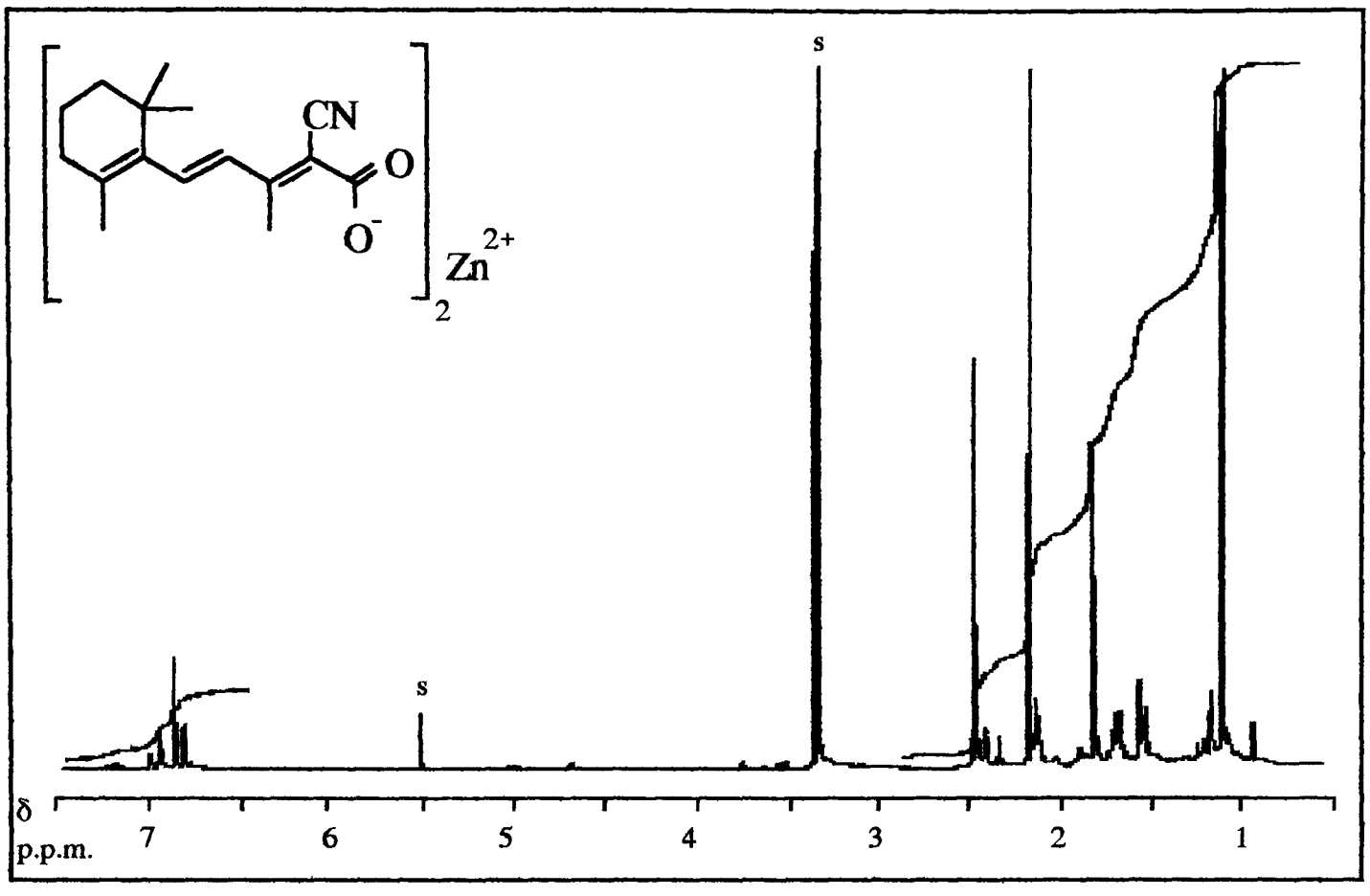
s at 3.3 p.p.m. due to partially duterated CD_3OD, s at 4.9 p.p.m. due to water.

The ^{1}H n.m.r. spectrum of (IV.6) has signals due to the H4' and H5' olefinic protons occur at δ = 6.74 and 6.85 p.p.m. with $^{3}J_{H,H'}$ coupling of 16 Hz, typical of *trans*- geometry of the C4' and C5' bond (in CD_3OD). The H5' doublet is broadened by coupling to protons due to Me2 and C3, as seen in β-ionylidenecyanoacetic acid. The remaining signals closely resemble those of β-ionylidenecyanoacetic acid (see Fig. 4.12 and Table 4.7).

4.6.7 *Trans*-[2-cyano-3-methyl-5-(2,6,6-trimethyl-1-cyclohexen-1-yl)-2,4-pentadienato]zinc(II) (IV.7)

The reaction of zinc(II) carbonate with *trans*-β-ionylidenecyanoacetic acid in an aqueous methanolic solution, under reflux, produced a pale yellow precipitate of *trans*-[2-cyano-3-methyl-5-(2,6,6-trimethyl-1-cyclohexen-1-yl)-2,4-pentadienato]zinc(II) (IV.7). The solid was filtered off, and washed with cold methanol, to remove any unreacted β-ionylidenecyanoacetic acid.

Fig. 4.13 The ^1H n.m.r. spectrum of *trans*-[2-cyano-3-methyl-5-(2,6,6-trimethyl-1-cyclohexen-1-yl)-2,4-pentadienato]zinc(II) (IV.7) in CD_3OD. S, residual solvents.



Impure (IV.7) was formed in 58% yield. Compound (IV.7) synthesized by this route was soluble in hot tetrachloromethane, and tetrahydrofuran, but insoluble in methanol, diethyl ether, acetone, hexane and water. If crude (IV.7) was dissolved in tetrahydrofuran, and the excess solvent removed by evaporation, the resulting solid was soluble in methanol and diethyl ether. The impure compound was purified by slow cooling of a water/ethanol solution of the zinc compound. The pale yellow crystals were unsuitable for single crystal X-ray crystallographic analysis.

Compound (IV.7) was also synthesized by the reaction in aqueous solution between sodium β-ionylidenecyanoacetate and zinc(II) chloride. The amorphous yellow powder of (IV.7) was insoluble in cold methanol, ethanol, acetone, and diethyl ether and soluble in hot tetrachloromethane and tetrahydrofuran.

The elemental analyses of (IV.7) synthesized above did not correspond to the expected molecular formula. The elemental analyses gave an empirical formula of $Zn_2C_{48}H_{60}N_3(3.7H_2O)$, which is equivalent to two zinc atoms and exactly three carboxylic acid groups. It is documented that zinc acetate may be distilled under vacuum,

to form crystals of the basic zinc acetate. The basic zinc acetate has a molecular formula $[Zn_4O(OCOMe)_6]$, with a zinc to carboxylate ration of 2:3. The basic zinc acetate is composed of a central oxygen atom surrounded by a tetrahedron of zinc atoms. Each zinc atom is bridged across each edge by the acetate ligands.[139] It is proposed that the zinc acetate of β-ionylidenecyanoacetic acid has a similar structure. Differences in the solid infrared spectrum should result, and if this geometry is retained in solution, the ^1H n.m.r. spectrum should show subtle differences from that of the other ionic β-ionylidenecyanoacetates.

The infrared spectrum of (IV.7) showed a water absorption at 3200 cm^{-1} typically seen in compounds with water of crystallization. The nitrile stretch was observed at 2210 cm^{-1}. The following absorptions were allocated as follows: $\nu(COO)_{asym}$ bands were seen at 1620 and 1598 cm^{-1}; $\nu(COO)_{sym}$ were seen as weak band at 1400 and 1308 cm^{-1} (see Table 4.6). The infrared data suggests either the mixing of modes of vibration common in carboxylates or that two different types of carboxylates are present in the solid phase. This observation is in agreement with the infrared data published for $ZnO(O_2CCH_3)_6$ having bridging asymmetrical and symmetrical COO stretches at 1639/1600 and 1489/1441 cm^{-1} respectively. While $Zn(O_2CCH_3).(H_2O)_2$ has only chelated carboxylates with asymmetrical and symmetrical ν(COO) stretches at 1550 and 1456 cm^{-1} respectively.

The ^1H n.m.r. spectrum of (IV.7) in the high field region shows that the cyclohexenyl ring is intact and all resonances in the region 1-3 p.p.m. are similar to those of the parent acid. The olefinic resonances have been shifted downfield in comparison with all the other salts. The H5' signal was observed at δ 6.95 (compared to 6.8) and H4' signal was at δ 6.81 p.p.m. (compared to about 6.7 p.p.m.), see Fig. 4.13 and Table 4.7. The unusual deviation of the olefinic proton signals from H4' and H5' can be explained by the change of the molecular structure from [Zn(β-ionylidenecyanoacetate)$_2$] to [Zn_4O(β-ionylidenecyanoacetate)$_6$]. The unusual shift in the olefinic protons cannot be explained by the electronegativity of the Zn atom in comparison to the other cations, however, the

introduction of an extra oxygen atom would effectively increase the "electronegativity" of the "Zn" atoms and therefore induce a downfield olefinic proton shift.

4.6.8 *Trans*-[2-cyano-3-methyl-5-(2,6,6-trimethyl-1-cyclohexen-1-yl)-2,4-pentadienato]copper(II) (IV.8)

Copper(II) sulphate was added to an aqueous solution of *trans*-[2-cyano-3-methyl-5-(2,6,6-trimethyl-1-cyclohexen-1-yl)-2,4-pentadienato]sodium, *trans*-[2-cyano-3-methyl-5-(2,6,6-trimethyl-1-cyclohexen-1-yl)-2,4-pentadienato]copper(II) (IV.8) precipitated out as a bright green solid quantitatively. The precipitate was isolated, and dried. In this state (IV.8) was hydrated as shown by a strong water absorption in the infrared spectrum and the presence of water in the ^1H n.m.r. spectrum. The amount of water was estimated from the elemental analyses as 3.5 moles of water per mole of copper salt. A sample of (IV.8) was dried for 3 days at 50-70°C in a vacuum, and the elemental analyses had changed only slightly. The dried sample gave a magnetic moment of 1.57 μ_B (based on the the dimer with an RMM of 1160) which is comparable to the moment of 1.49 μ_B given by binuclear $Cu_2(OAc)_4.2H_2O$,[45,97] and lower than the spin-only value value for mono-nuclear carboxylates of 1.73 μ_B (1 e).[139] It has been observed that Cu(II) compounds have moments ranging from 1.9 to 2.2 μ_B depending on whether they are tetrahedral or octahedral. The octahedral complexes have magnetic moments at the lower end, while the tetrahedral complexes have magnetic moments nearer 2.2 μ_B. Conclusions based solely on magnetic measurements must be treated with caution.[70]

The infrared spectrum showed the water of crystallization as a broad band at 3200 and a shoulder at 1606 cm^{-1}. The other band assignments were: ν(CN) at 2254 and 2223 cm^{-1} and the strong $\nu(COO)_{asym}$ stretch at 1637 cm^{-1} and the $\nu(COO)_{sym}$ stretch at 1400 cm^{-1} (see Table 4.6). In comparison, the antisymmetric and symmetric stretches for dimeric copper(II) acetate are at 1603(s) and 1418(vs) cm^{-1}, giving a $\Delta\nu$ of 185, while that of copper(II) *trans*-β-ionylidenecyanoacetic acid (IV.8) being 237 cm^{-1}. These data are ambiguous so cannot be used to decide if copper(II) *trans*-β-ionylidenecyanoacetic acid

(IV.8) exists as a dimer in the solid state.

Trans-[2-cyano-3-methyl-5-(2,6,6-trimethyl-1-cyclohexen-1-yl)-2,4-pentadienato]copper(II) (IV.8) is soluble in ethanol, methanol, acetone, dichloromethane and tetrahydrofuran, but insoluble in hexane and water. Attempts at recrystallization by conventional means from the above solvents only resulted in green oils. Crystals were obtained by slow diffusion of hexane into a tetrahydrofuran solution of the copper salt, but were unsuitable for single crystal X-ray analysis.

The ^{1}H n.m.r. spectrum showed the result of paramagnetism on the proton signals, and as the signal broadening was considerable, no useful data were obtained.

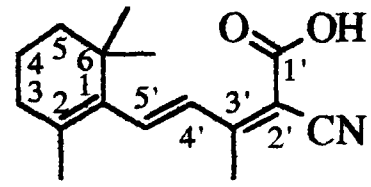
The low resolution FAB mass spectrum of *trans*-[2-cyano-3-methyl-5-(2,6,6-trimethyl-1-cyclohexen-1-yl)-2,4-pentadienato]copper(II) was poor and showed a weak peak corresponding to the monomer at m/z = 581. However, no peak corresponding to the dimeric species was observed at m/z = 1162. The fragmentation pattern corresponded to loss of CO_2 from the ligand ion which gave a peak at m/z = 216. The mass spectrum does not disprove the observations made from the magnetic and infrared spectra because of the poor quality mass spectrum which was obtained. The evidence outlined here is ambigouos and cannot be used to ascertain if *trans*-[2-cyano-3-methyl-5-(2,6,6-trimethyl-1-cyclohexen-1-yl)-2,4-pentadienato)copper(II) exists as a monomer or dimer in the solid state.

4.8 The Synthesis of Salts of *Cis*-β-Ionylidenecyanoacetic Acid

4.8.1 Ammonium *cis*-2-cyano-3-methyl-5-(2,6,6-trimethyl-1-cyclohexen-1-yl)-2,4-pentadienate (IV.10)

The synthesis of ammonium *cis*-2-cyano-3-methyl-5-(2,6,6-trimethyl-1-cyclohexen-1-yl)-2,4-pentadienate (IV.10) was done by a modification outlined by Smit.[184] The collected mother liquors from several preparations of *trans*-β-ionylidenecyanoacetic acid were re-dissolved in toluene. Dried ammonia gas was passed through the solution to precipitate out crude ammonium *cis*-[2-cyano-3-methyl-5-(2,6,6-trimethyl-1-cyclohexen-1-yl)-2,4-pentadienate] (IV.10). The white solid was re-crystallized from water, and analyzed correctly. No solvent of crystallization was detected.

Fig. 4.14 Skeletal numbering system for *cis*-β-ionylidenecyanoacetic acid, *cis*-[2-cyano-3-methyl-5-(2,6,6-trimethyl-1-cyclohexen-1-yl)-2,4-pentadienoic acid].



The infrared spectrum of (IV.10) showed the nitrile stretch at 2204 cm^{-1}, similar to the nitrile stretch of the *trans*- isomer but in the case of the *cis*-isomer only one stretching mode was observed. The *cis*- conjugated ν(COO) bands (at 1592 and 1359 cm^{-1}) were similar to that of the *trans*- isomer, typical of ionic carboxylates. Other clearly defined bands were equivalent to the *trans*- compound (see Table 4.8).

The ^{1}H n.m.r. spectrum of (IV.10) showed the same resonances as that for the *trans*- isomer in the high field region (δ 1-4 p.p.m.), but there was a dramatic shift to lower field of the two olefinic protons H4' and H5' and a less pronounced shift of the adjacent 3'Me (see Fig.4.14 for proton assignments). The *trans*- isomer showed H4' and H5' signals at 6.7 and 6.8 p.p.m. The corresponding protons in the *cis*- isomer showed signals at 7.40 and 6.72 p.p.m. so the difference in proton signals was 0.1 p.p.m. in the

trans- isomer to 0.68 p.p.m in the *cis*- isomer (see Fig.4.15 and Table 4.9). The H5' proton was identified by the slight broadening of the doublet by long range couplings to Me2 and H3.

Fig. 4.15 The ^{1}H n.m.r. spectrum of ammonium *cis*-[2-cyano-3-methyl-5-(2,6,6-trimethyl-1-cyclohexen-1-yl)-2,4-pentadienate] (IV.10).

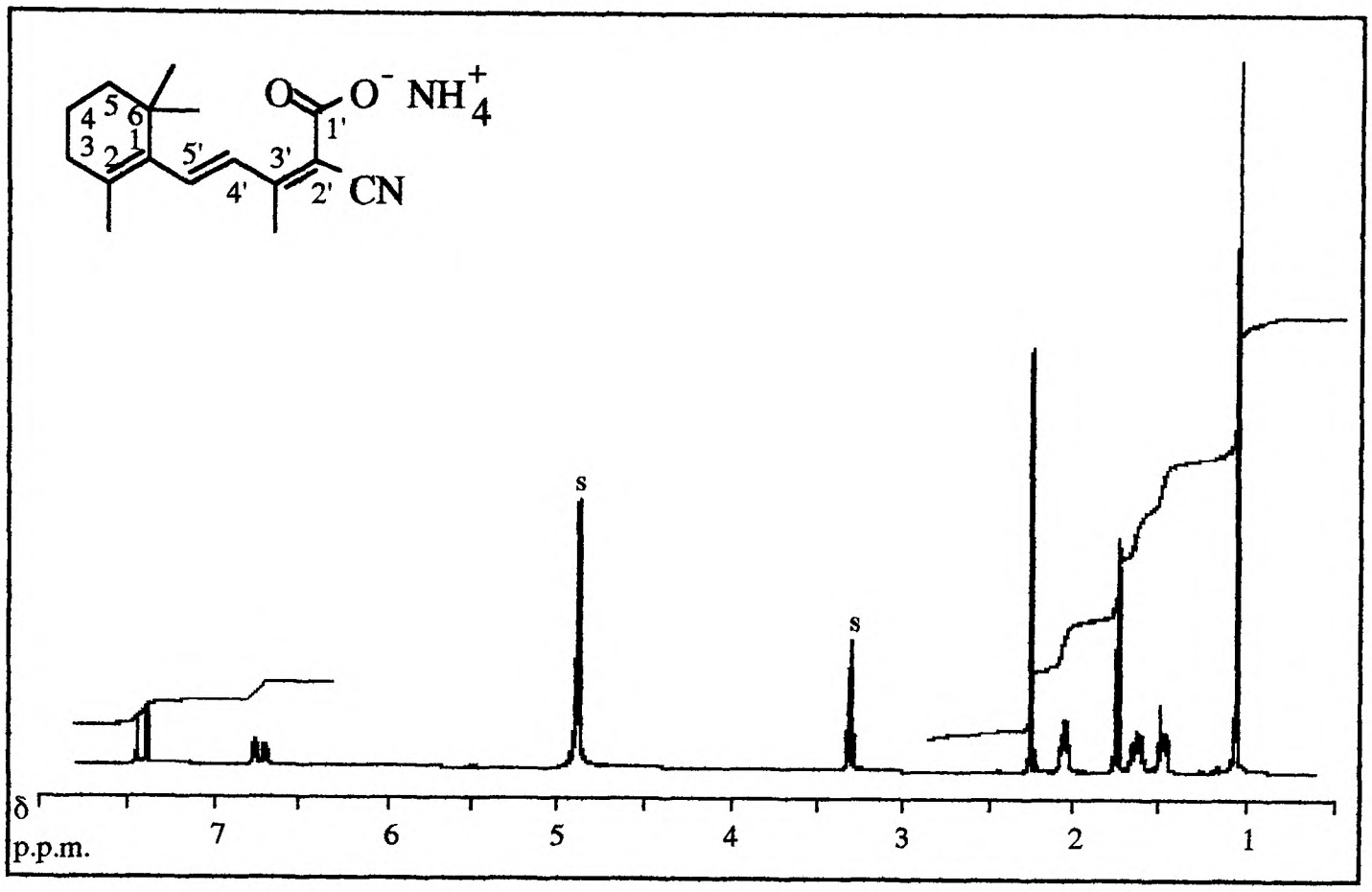


Table 4.8 Infrared data for *cis*-β-ionylidenecyanoacetate compounds.

	Compound Number	ν(C=O) asym	ν(C-O) sym	ν(CN)	αβ C=C	H-C=C-H def.	CC-H	O-H or water	Δν	Phase.
NH_4L'	(4.10)	1592	$^{1359}_{1416}$	2204	1550	974	802	3300	233	n
BaL'_2	(4.11)	1592	1378	2206	1560	988	801	3401	214	n
CuL'_2	(4.12)	1634	1397	$^{2245}_{2211}$	1588	976	791		237	n
ZnL'_2	(4.13)	1620	1401	$^{2211}_{2245}$	1588	980	798	3413	221	n

Key: All values in cm^{-1}, n = nujol mull / KBr plates, h = hexachlorobutadiene / KBr, str = stretch, def. = deformation. L' = *cis*-β-ionylidenecyanoacetic acid.

There is no significant change in the electronic spectrum to suggest a corresponding alteration in the degree of electronic delocalization. The H4'-H5' coupling constant of 16.3 Hz is typical of the *trans*- H-C-C-H group. On the basis of the n.m.r. evidence the electronic environments along the triene chain have been considerably altered, but all the other properties (increased solubility in non-polar organic solvents, no electronic spectrum change) suggest that the overall dipole has been lowered. It is possible that the change in the electronic environment of the 4'H may be due to the near proximity of the carboxylic acid group to this proton which as been induced by the *cis*- structure of the molecule.

The electron impact mass spectrum did not give the M^+ ion, or any of the expected fragments. The probe temperature was raised to 390°C, at which temperature the ammonium salt vaporized and a base peak at m/z = 44 , due to $CO_2^{\cdot+}$, showed that the compound had decomposed.

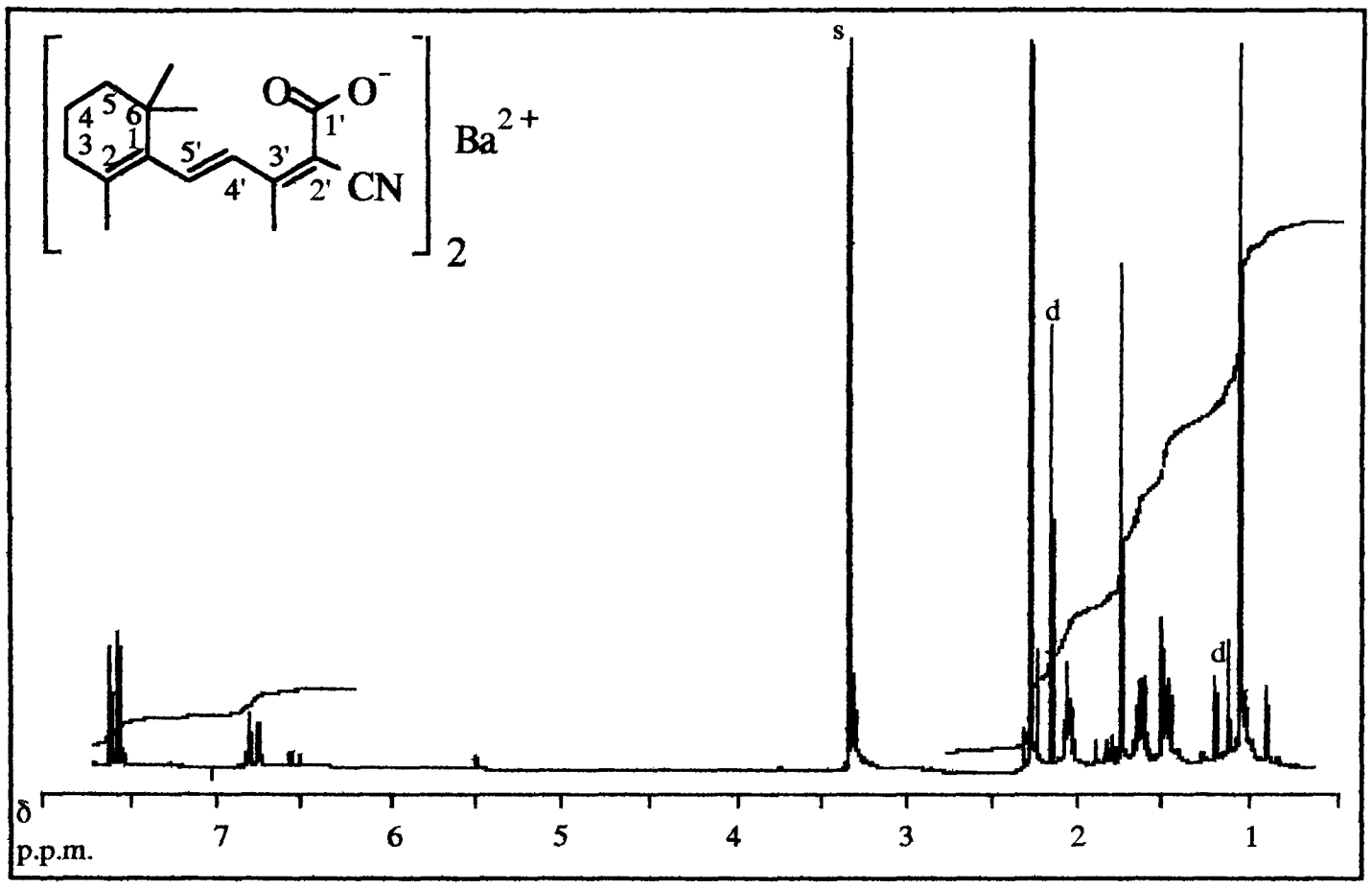
4.8.2 Barium *cis*-2-cyano-3-methyl-5-(2,6,6-trimethyl-1-cyclohexen-1-yl)-2,4-pentadienate (IV.11)

A barium nitrate solution was added to an aqueous solution of the ammonium *cis*-β-ionylidenecyanoacetate to precipitate out the barium salt. Barium *cis*-2-cyano-3-methyl-5-(2,6,6-trimethyl-1-cyclohexen-1-yl)-2,4-pentadienate (IV.11) was recrystallized as fine white needles from boiling water. Elemental analyses suggested that (IV.11) crystallized with five waters of crystallization.

The infrared analysis of (IV.11) showed water of crystallization to be present as a broad band at 3401 cm^{-1} and was little different from the *trans*- isomer (see Table 4.8).

The ^1H n.m.r. spectrum of (IV.11) was similar to that of the ammonium salt, and showed all the expected resonances for the proposed structure (see Table 4.7 and Fig. 4.16).

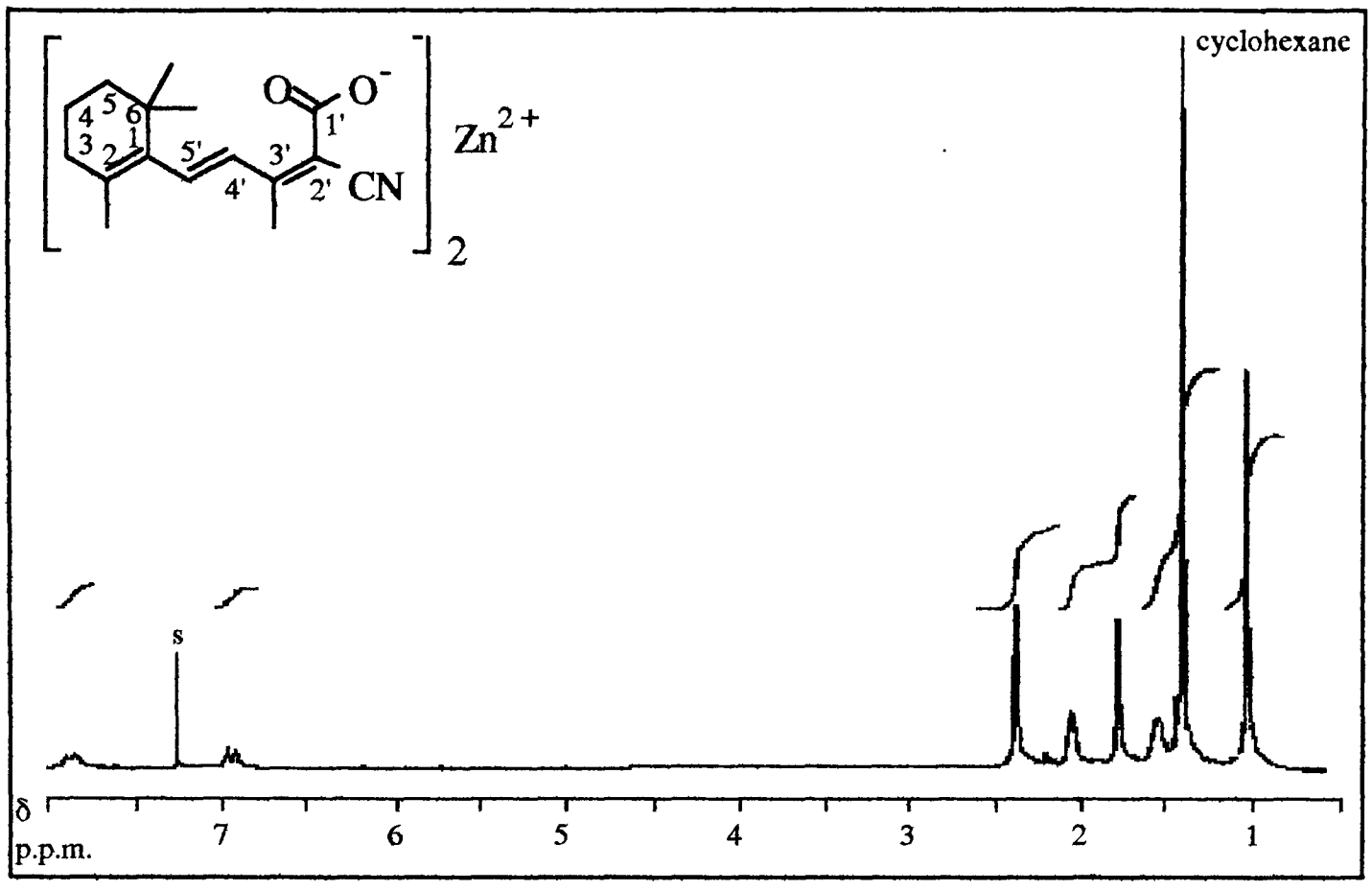
Fig. 4.16 The ^1H n.m.r. spectrum of barium *cis*-2-cyano-3-methyl-5-(2,6,6-trimethyl-1-cyclohexen-1-yl)-2,4-pentadienate (IV.11) in CD_3OD. S, solvents, d-unallocated signal.



4.8.3 *Cis*-[2-cyano-3-methyl-5-(2,6,6-trimethyl-1-cyclohexen-1-yl)-2,4-pentadienato]copper(II) Dihydrate (IV.12)

The copper salt of *cis*-β-ionylidenecyanoacetic acid was synthesized from the ammonium salt as a light blue powder, soluble in acetone but insoluble in water. The elemental analyses suggested two waters of crystallization which was detected by a broad water band in the infrared spectrum.

Fig. 4.17 The ^{1}H n.m.r. spectrum of *cis*-[2-cyano-3-methyl-5-(2,6,6-trimethyl-1-cyclohexen-1-yl)-2,4-pentadienato]zinc (IV.13) in $CDCL_3$. S, solvent.



4.8.4 *Cis*-[2-cyano-3-methyl-5-(2,6,6-trimethyl-1-cyclohexen-1-yl)-2,4-pentadienato]zinc.cyclohexane dihydrate (IV.13)

The zinc salt was prepared in the same manner as that for the copper(II) salt. When *cis*-[2-cyano-3-methyl-5-(2,6,6-trimethyl-1-cyclohexen-1-yl)-2,4-pentadienato]zinc (IV.13) is precipitated out of water it forms an emulsion, which eventually coats the vessel sides as a yellow oil. The yellow oil was soluble in methanol, tetrahydrofuran, tetrachloromethane, iso-propyl ether and hot cyclohexane. The crude sample of (IV.13) was recrystallized from cyclohexane at 4°C to form bright yellow crystals. The elemental analyses gave the ratio of zinc to β-ionylidenecyanoacetate to be 1:2 (when N=2). The number of carbon atoms was in excess by 6, and the number of hydrogen atoms by 12, which suggests that the yellow crystals contained one mole of cyclohexane of crystallization per mole of zinc carboxylate. The presence of the cyclohexane of crystallization showed up in the ^{1}H n.m.r. spectrum as a broad singlet at δ 1.43 p.p.m. with an area corresponding to 12 protons. Water of crystallization was present as shown

by the i.r. and ^{1}H n.m.r. spectra. Calculations indicate two moles of water per mole of zinc.

The ^{1}H n.m.r. spectrum of (IV.13) was similar to that of the *cis*- ammonium salt (see Fig. 4.17). The olefinic proton shifts due to H4' and H5' are at δ 6.96 and 7.88 p.p.m. The signals are reversed from those of the *cis*- ammonium salt and depends on the observation that the signals from H5' are always broader than those of the H4'. This reversal is equivalent to the behaviour of the *trans*- zinc salt.

Cis-[2-cyano-3-methyl-5-(2,6,6-trimethyl-1-cyclohexen-1-yl)-2,4-pentadienato]-zinc.cyclohexane dihydrate (IV.13) was a hygroscopic solid which rapidly absorbed water from the air, which was observed as a broad band in the infrared spectrum at 3413 cm^{-1}. There are only two ν(COO) bands in (IV.13) with Δν = 221. The two ν(COO) bands are similar to the *trans*- isomer (Δν = 220) but no secondary bands were observed (see Table 4.8).

4.8.5 Other Metal Salts of β-Ionylidenecyanoacetic Acid

Attempts were made to synthesize the cadmium(II), lead(II) and cerium(IV) salts of β-ionylidenecyanoacetic acid. Precipitates were formed when ammonium *trans*-β-ionylidenecyanoacetate reacted with aqueous solutions of $CdCl_2$, $Pb(NO_3)_2$, and $Ce(SO_4)_2$. The cadmium salt could only be isolated as a pale yellow oil, soluble in most organic solvents except for hexane. Elemental analyses of the lead and cerium salts showed that there were of a non-stoichiometric nature. No further analytical data were obtained for these salts, however, SHG measurements were made on those solids which were isolated.

4.8.6 Summary

A variety of the salts of β-ionylidenecyanoacetic acid were synthesised and, in most cases, characterised by spectroscopic and elemental analyses. The physical properties of the salts varied considerably depending on the nature of the cation.

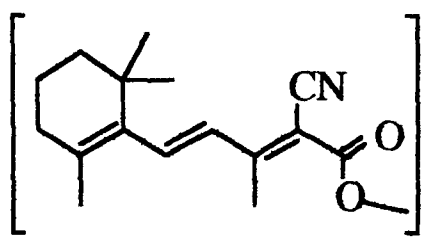
4.9 Second Harmonic Generation Properties of Salts Derived from β-Ionylidenecyanoacetic Acid

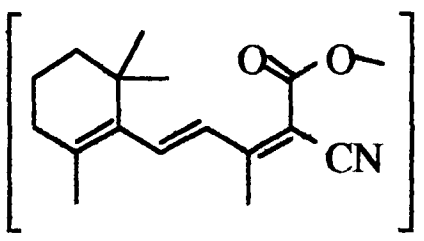
Table 4.9 shows the measured SHG efficiencies of salts derived from β-ionylidenecyanoacetic acid compared to that of urea at 1064 nm. The β-ionylidenecyanoacetic acid salts of Ba^{2+}, Ni^{2+} and $H_2NEt_2^+$, showed signals of 0.18, 0.19 and 0.12 x urea respectively, which is comparable to that of the parent acid, β-ionylidenecyanoacetic acid (0.12 x urea). The observed SHG efficiencies for the Ba^{2+}, Ni^{2+} and $H_2NEt_2^+$ salts indicate that the crystal structures are probably centrosymmetric, and that the SHG signals observed could be the result of minor asymmetry induced by surface or resonance effects as discussed in Chapter 2. However, quadrupole effects will not give rise to this low level of SHG, because the power of the incident radiation required to observe quadrupole effects is higher than that used for this measurement (the SHG efficiencies of these salts were measured at 0.57 mJ per pulse, while with this apparatus luminescence has been observed to occur at power levels in excess of 1 mJ per pulse).

The SHG efficiencies reported here are in the order of 0.15 x urea, which is considerably lower than that predicted from the molecular structure of the ligand. However, the SHG levels measured here are not far short of those reported by Anderson *et al*[7] for organometallic inclusion compounds which crystallize in non-centrosymmetric crystal structures. The inclusion compound $(thiourea)_3$: (1,3-cyclohexadiene)$Fe(CO)_3$ gave an SHG signal of 0.4 x urea, and crystallized in the non-centrosymmetric space group $Pna2_1$, as light yellow rectangular plates.[7]

The remaining salts all had SHG responses around 0.1 x urea or less and therefore have insignificant SHG. In all cases, except for the Ce^{4+} salt, the β-ionylidenecyanoacetic acid salts are of the correct colour for testing at an incident wavelength of 1064 nm. Compounds that are red or brown absorb at 532 nm (green) and so unless the compound is an extremely efficient frequency doubler the observed SHG powers will be zero.

Table 4.9 Second harmonic data for β-ionylidenecyanoacetic acid salts, measured at 1064 nm incident wavelength on unsized powders. Lu = luminesced, **** = not measurable, ****** = not measured.

L = 

L' = 

Compound	SHG x Urea	Colour
HL	0.12	Yellow
AgL	0.006	Cream
CsL	0, Lu	White
NH_4L	******	Colourless
Et_4NL	0	Colourless
H_2NEt_2L	0.12	White
NH_4L'	0.03, Lu	White
BaL_2	0.19	White
CoL_2	0, Lu	Red
NiL_2	0.18	Light green
CuL_2	0.063	Blue
ZnL_2	0.048	White
"PbL_2"	0	White
"CdL_2"	****	Colourless oil
"CeL_4"	0	Red brown

4.10 Summary and Conclusion

Chapter Four has described the search for a possible NLO active ligand, its synthesis, characterization, derivatization and testing for the non-linear optical (NLO) process, second harmonic generation (SHG).

A systematic survey of the literature revealed that work on metal polyenes had

achieved some success in NLO. The compound *trans*-β-ionylidenecyanoacetic acid, 2-cyano-3-methyl-5-(2,6,6-trimethyl-1-cyclohexen-1-yl)-2,4-pentadienoic acid, was chosen as a suitable ligand with the required electronic conjugation. The molecular structure of this ligand could also be altered by simple synthetic routes. The second order hyperpolarizability constant, β, was calculated using the CNDOVSB method for *trans*-β-ionylidenecyanoacetic acid, and related compounds, and were found to be promising. The second order hyperpolarizability constant, β, for *trans*-β-ionylidenecyanoacetic acid was calculated by CNDOVSB to be 50.48 x 10^{-40} m^4V^{-1}, and from solvatochromism data to be 170 x 10^{-40} m^4V^{-1}. The corresponding β value for 4-nitroaniline is in the order of 130 x 10^{-40} m^4V^{-1}, which is of commercial interest.

For compounds to show second harmonic generation, they are required to crystallize in a non-centrosymmetric crystal structure and possible synthetic methods of imposing non-centrosymmetry on *trans*-β-ionylidenecyanoacetic acid using metals were discussed.

Several salts of *trans*-β-ionylidenecyanoacetic acid and *cis*-β-ionylidenecyanoacetic acid were synthesized, characterized and tested for their SHG properties. It was hoped that the carboxylate salts of Zn(II), Cd(II) and Cu(II) might show SHG since the acetates of these metals have been shown to crystallize in non-centrosymmetric space groups. The Cd(II) salt of *trans*-β-ionylidenecyanoacetic acid could only be isolated as a yellow oil, and so could not be tested for SHG. The Zn(II) and Cu(II) salts of *trans*-β-ionylidenecyanoacetic acid were tested for SHG, and gave efficiencies of 0.048 and 0.063 x urea, considerably lower than the predicted SHG (about 10 x urea) efficiency if the carboxylates crystallized in non-centrosymmetric space groups.

The maximum SHG efficiency was unexpectedly found to be given by the Ba(II) salt of *trans*-β-ionylidenecyanoacetic acid with an efficiency of 0.19 x urea.

In the search for non-linear compounds which show second harmonic generation, the use of metal ions to direct the symmetry of prospective organic carboxylates has been shown to be of limited success. The metal salts of larger organic ligands required for NLO have been assumed to crystallize in the same way as their lower homologues. This

assumption, in the case of the salts of *trans*-β-ionylidenecyanoacetic acid, has been shown to be incorrect. Furthermore, the physical properties of the pure salts prevents the growth of good optical crystals and are therefore not suited to SHG generation. The high solubility of the β-ionylidenecyanoacetic acid salts in organic solvents makes them suitable for inclusion into potential NLO organic polymers.

The introduction of non-centrosymmetry into *trans*-β-ionylidenecyanoacetic acid is discussed in Chapters Five and Six.

CHAPTER FIVE

Palladium and Platinum Complexes of β-Ionylidenecyanoacetic Acid

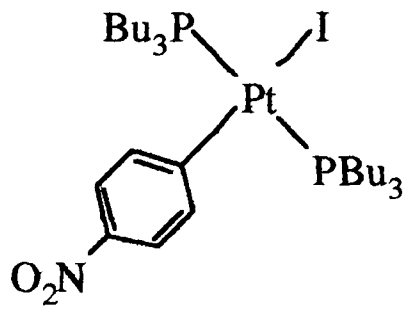
5.1 Synthesis of Palladium and Platinum Carboxylates

5.1.1 Introduction

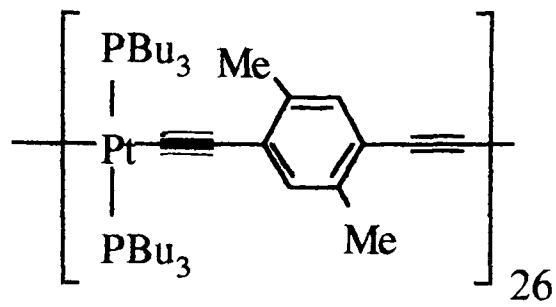
This Chapter describes the synthesis, characterization and NLO testing of platinum(II) and palladium(II) complexes containing oxygen co-ordinated β-ionylidenecyanoacetate. Platinum(II) and palladium(II) carboxylate complexes were chosen as metal templates because they are known to crystallize in non-centrosymmetric crystal lattices and so increase the probability that the novel platinum(II) and palladium(II) compounds synthesized here would crystallize in a non-centrosymmetric manner.

A new class of platinum based organometallic compounds have been investigated by Tam *et al*[197,198] which showed some second harmonic generation properties. The square-planar platinum(II) and palladium(II) compounds of the form $[MXR(PEt_3)_2]$, where X is a halogen and R is an aromatic halide, tend to crystallize in non-centrosymmetric space groups. The complex *trans*-[PtI(4-nitrophenyl)$(PEt_3)_2$], (V.1), space group $C_{mc}2_1$, a pale yellow solid packed with a herring bone structure in the crystal gave an SHG efficiency of 5-8 x urea. This has been the largest SH signal measured for compounds based on palladium or platinum so far reported.

Platinum(II) monomers of the type shown in Fig.5.1 were synthesized and their second and third order non-linearities measured.[202h] The SHG efficiencies of the centrosymmetric Pt(II) acetylides were in the order of 0.003 x urea, while the compounds which crystallized in non-centrosymmetric space groups had SHG efficiencies of 0.3 x urea.

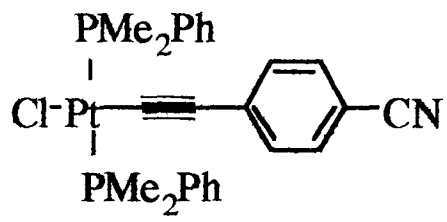


(V.1)

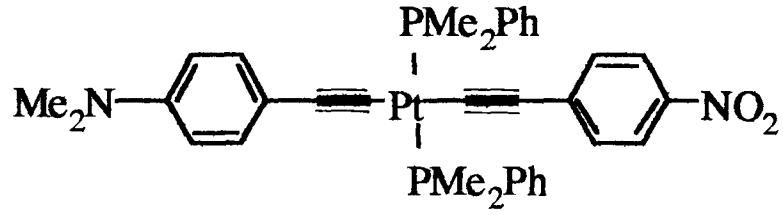


(V.2)

Fig. 5.1 Two examples of monomeric platinum(II) acetylides with space group and SHG efficiencies, taken from ref. 202h.



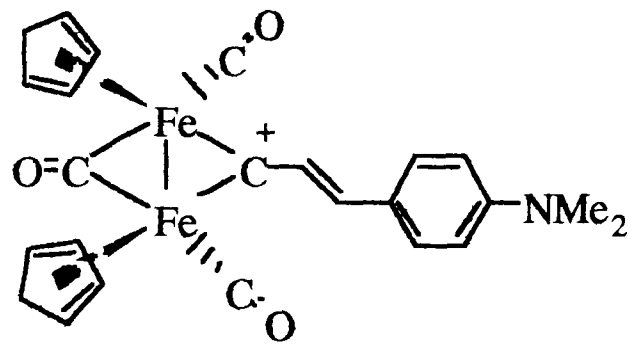
Space Group $P\bar{1}$
0.003 x urea



Space Group C2/c
0.3 x urea

Guha *et al* [81,89,90] have investigated the third-order hyperpolarizabilities of platinum poly-ynes based on linking phenyl and 2,5-dimethylphenyl groups between acetylenes, see (V.2). The combination of non-centrosymmetric crystal structures and long chain ligands should lead to ideal compounds for SHG purposes. The use of the metal as part of the electronic delocalization network has been observed to give rise to either intense ligand to metal and/or metal to ligand charge transfer bands.[84] Attempts have been made to use diiron alkenylidyne complexes where the bridging carbon atom attached to the iron atom acted as an electron acceptor. The donor group (such as dimethylaminophenyl) was situated at the end of a conjugated chain and the series of compounds reported gave no second harmonic signals except for $\{(\eta\text{-}C_5H_5)_2Fe_2(CO)_2(\mu\text{-}CO)(\mu\text{-}(E)\text{-}C\text{-}CH{=}CH\text{-}$

C_6H_4-(p)-$N(CH_3)_2\}^+BF^-$, (V.3), which gave a response of 0.77 x urea @ 1.9 μm. No compounds containing Pt or Pd have been reported to act in this way.



(V.3)

However, a single crystal X-ray analysis demonstrated that the crystal structures belonged, unambiguously, to the centrosymmetric space group $P2_{1/n}$.[13] The paradox that centrosymmetric compounds can show SHG has been discussed previously in Chapter 2.

This Chapter describes the synthesis, and testing for SHG properties, of complexes of the type $Pd/PtX_m(OCOR)_nL_2$ (X = halogen, L = phosphine, n/m = 1, m=2 or n=2 with n/m=0). Complexes of this type have a greater tendency to crystallize in non-centrosymmetric space groups, they are easy to manipulate by simple synthetic methods, and the electro-optic properties of these complexes have not been previously investigated.

The carboxylates of palladium, platinum and rhodium compounds derived from ethanoic, propanoic and benzoic acids have been described by Stephenson *et al.*[188] Diacetatoplatinum(II) exists as brown crystals made by the reaction of platinum(II) nitrate with glacial acetic acid. The propionate, benzoate, trifluoroacetate and pentafluoropropionate have also been reported.[67] The acetate and propionate complexes exist as trimers in solution (benzene). In the solid phase, the platinum acetates form platinum squares with the platinums in octahedral environments.

Stephenson *et al*[188] synthesized palladium carboxylates with L= PPh_3, $AsPh_3$, $OSMe_2$, Et_3N, and Et_2NH. Diacetatobis(triphenylphosphine)palladium(II) was synthesized from diacetatopalladium(II) and triphenyl phosphine in benzene. The complex was reported to be lemon-yellow in colour, and decomposed in warm benzene, to give a red solution, turning finally to brown, depositing palladium metal. The compound also decomposed in alcohols. The carboxylates were not isolated because of this decomposition.

Nyman *et al*[157] attempted the synthesis of monomeric palladium acetates by reaction of the Pd(0) pre-cursor, $Pd(PPh_3)_4$, with ethanoic acid, to form bis(triphenylphosphine)diacetatopalladium(II). The monomeric palladium carboxylates, as was noted by Stephenson *et al*, tended to decompose in alcoholic solvents.

The carboxylates of platinum are far more stable than their palladium analogues.[139] The diacetate cyclo[tetrakis(di-μ-acetato)platinum(II)] which crystallizes in the non-centrosymmetric space group $P4_32_12$ is a purple solid, and consists of platinum tetramers.[67] Initial attempts to synthesize monomeric adducts with nitrogen and phosphorus donors had failed. $[Pt(CO_3)(PPh_3)_2]$ reacts with ethanoic and benzoic acids to yield the bis adducts.[157] These complexes appeared to crystallize with a half molecule of solvent per molecule of complex, except in the case of diethyl ether.

The synthesis of monomeric platinum carboxylates was achieved by the reaction between platinum(II) acetate and silver carboxylate.[218] By this method $[Pt(RCOO)_2]$ where RCOO = a series of complex carboxylates (e.g. benzoate, butyric, trimethyl acetic, lauric, stearic, cinnamic acids) were synthesised. The crystal structure of monomeric diacetatoplatinum(II) has been reported by Appleton *et al*.[9]

The use of silver as a halide abstracter was briefly reported by Cheney *et al*.[49] $[Pt_2Cl_2L_2]$ was reacted with silver acetate or silver benzoate, in acetone, in the dark for 24 hours (L = o-(t-butyl-o-tolylphosphine)). The complexes were then crystallized from cyclohexane / dichloromethane and crystallized with 1/2 or 1 mole of hydrocarbon of crystallization per molecule of platinum, respectively. They were found to be bridged (via carboxylate) binuclear compounds, with the hydrocarbons trapped within the lattice. Other authors have reported similar reactions.[96]

Mixed complexes, of the general type $MPd(O_2CCH_3)_4.xCH_3COOH.yH_2O$, where M=Ca, Sr, Ba, x=4, y=0; Mn, Ni, Cd, x=y=0; Co,Zn, x=y=2; Cu, x=y=0 and Pd, x=2, y=0, have also been reported.[139]

5.1.2 The Vibrational Analysis of Platinum and Palladium Halides

A simple preliminary diagnosis of the types of M-Cl bonds present, is achieved by far infrared analysis of nujol mulls between caesium chloride plates. The stretching frequencies of M-Cl groups indicate whether the groups are *cis*-or *trans*-. Duddell[71] has surveyed the vibrational Raman and infrared spectra of many Pt and Pd compounds, Table 5.1 shows selected results. Cheney *et al*[49] agree with these results, and have used them as a diagnostic tool to assign the structures of many compounds.

Table 5.1 Some vibrational frequencies of selected Pt-Cl, Pt-P, Pd-Cl, and Pd-P bonds, in differing environments. All values are in cm^{-1}, s = strong, v= very, m = medium, w = weak, sh = shoulder.

Bridged compounds: $M_2X_4L_2$

M-X terminal ν(Pt-Cl) 347s, 341ms, ν(Pd-Cl) 346s

M-X bridged trans to X ν(Pt-Cl) 330wm, 322sh, ν(Pd-Cl) 294m

M-X bridged, trans to L ν(Pt-Cl) 260s, ν(Pd-Cl) 256s

M-L ν(Pt-P) 393s, ν(Pd-P) 382m

Trans- compounds: MX_2L_2

MX_2 ν(Pt-Cl) 339s, ν(Pd-Cl) 355vs

ML_2 ν(Pt-P) 346s, ν(Pd-P) 410m

Cis- compounds: MX_2L_2

MX_2 $\nu(Pt\text{-}Cl)_{asym}$ 280vs, ν(Pd-Cl) 271s

MX_2 $\nu(Pt\text{-}Cl)_{sym}$ 304vs, ν(Pd-Cl) 284s

ML_2 $\nu(Pt\text{-}P)_{asym}$ 427m, ν(Pd-P) 366m

ML_2 $\nu(Pt\text{-}P)_{sym}$ 442w, ν(Pd-P) 390vw

For example, $[PtCl_2(diphos)]$, has ν(Pt-Cl), 280m and 315m cm^{-1}, confirming that it has *cis*- Pt-Cl bonds.

5.2 The Syntheses and Characterization of Platinum and Palladium - β-Ionylidenecyanoacetate Complexes

5.2.1 Introduction and Synthetic Strategies

Complexes of platinum(II) and palladium(II) were synthesized from the conjugated polyene carboxylate, β-ionylidenecyanoacetic acid, and phosphorus donor ligands. The platinum(II) and palladium(II) centres were used as templates, which were expected to have a high probability of packing in a non-centrosymmetric crystal structure, which is one of the requirements necessary for second harmonic generation.

The introduction of β-ionylidenecyanoacetate into a platinum complex was successfully attempted by two general methods. Firstly, by halide abstraction using silver ions, and, secondly, by the reaction of β-ionylidenecyanoacetic acid with carbonatobis(triphenylphosphine)platinum(II).

Reactions with different stoichiometries were attempted in order to synthesize unsymmetric, square-planar complexes of platinum(II) and palladium(II) with β-ionylidenecyanoacetic acid (L = β-ionylidenecyanoacetate) :

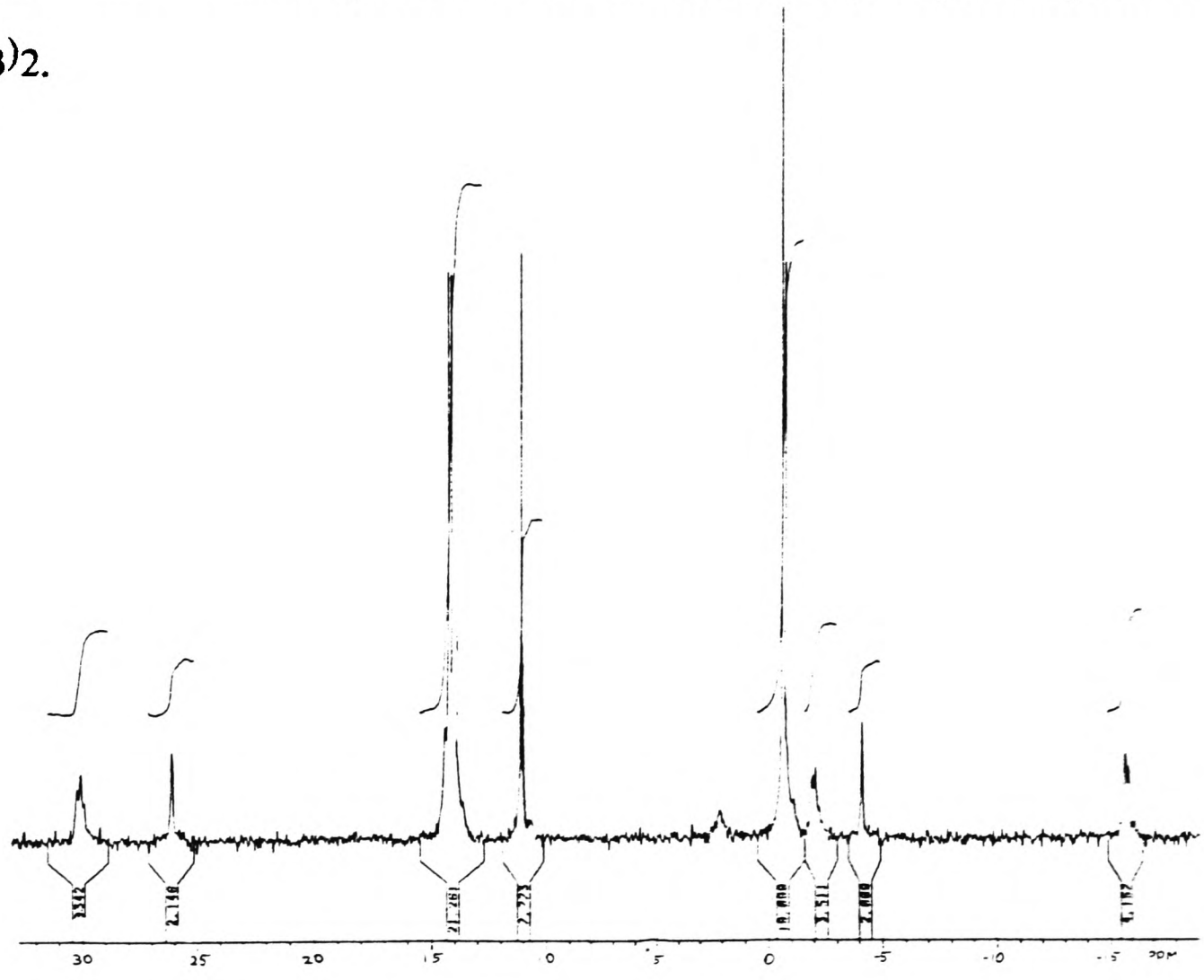
Section	Starting Materials				Compd. Number	Expected Products
5.2.2	*cis*- $PtCl_2(PPh_3)_2$	+	1AgL	⇒	(V.4)	$PtCl_1L_1(PPh_3)_2$
5.2.3	*cis*- $PdCl_2(PPh_3)_2$	+	2AgL	⇒	(V.5)	$PdL_2(PPh_3)_2$
5.2.4	$PtCl_2$(diphos)	+	2 AgL	⇒	(V.6)	PtL_2(diphos)
5.2.5	$PtCl_2$(diphos)	+	1AgL	⇒	(V.7)	$PtCl_1L_2$(diphos)
5.2.6	*cis*- $PtCO_3(PPh_3)_2$	+	2HL	⇒	(V.8)	$PtL_2(PPh_3)_2$

5.2.2 The Synthesis of Chloro(*cis*-{2-cyano-3-methyl-5-(2,6,6-trimethyl-1-cyclohexen-1-yl)-2,4-pentadienato})[bis(triphenylphosphine)]platinum(II), PtCl(β-ionylidenecyanoacetate)$(PPh_3)_2$ (V.4)

The reaction of *cis*-$[PtCl_2(PPh_3)_2]$ with one equivalent of silver β-ionylidenecyanoacetate in dichloromethane precipitated AgCl, which was filtered off, and the solvent removed. The off-white solid froth deposit was crude PtCl(β-

ionylidenecyanoacetate)$(PPh_3)_2$ (V.4). The *cis*- isomer was concentrated by precipitation using hexane as co-solvent from a toluene solution of both isomers. The pale yellow *trans*- isomer, being more soluble, remained in solution. The mixture was further purified by chromatography using a silica-gel column. The eluted product was re-examined by thin layer chromatography, and found to still be a mixture, despite their resolution on the column.

Fig. 5.2 The ^{31}P n.m.r. spectrum of *cis* and *trans* PtCl(β-ionylidenecyanoacetate)-$(PPh_3)_2$.



The ^{31}P n.m.r. spectrum of PtCl(β-ionylidenecyanoacetate)$(PPh_3)_2$ showed *cis*- and *trans*- isomers in a ratio of 6:1 (see Fig. 5.2). The ^{31}P n.m.r. spectrum of the *cis*- isomer showed doublet resonances at δ 14.030 p.p.m. ($^1J_{Pt-P}$ = 3882 Hz, $^2J_{P,P'}$ = 17 Hz with peak areas of 1:4:1), coupled to δ 0.789 p.p.m. ($^1J_{Pt-P}$ = 3658 Hz, and $^2J_{P,P'}$ = 17 Hz, peak areas of 1:4:1). The *trans*- isomer showed a singlet at δ 10.98 p.p.m., and associated platinum satellites ($^1J_{Pt-P}$ = 3680 Hz, with peak areas of 1:4:1). Elemental analyses were satisfactory for $PtCl_1$(β-ionylidenecyanoacetate)$_1(PPh_3)_2$ with some

precipitation from solution during the Pt analysis leading to a low platinum metal assay. The mass spectrum gave m/z = 1014, and a fragmentation pattern corresponding to $PtCl_1(\beta\text{-ionylidenecyanoacetate})_1(PPh_3)_2$ (see Table 5.2).

Table 5.2 Fragmentation pattern for $PtCl_1(\beta\text{-ionylidenecyanoacetate})_1(PPh_3)_2$

Molecular ion, $M^+ = [Pt(PPh_3)_2Cl(\beta\text{-ionylidenecyanoacetate})]^+$	
m/z	Fragments Lost From M
1014	--
977	Cl
933	CO_2 + Cl
755	β-ionylidenecyanoacetic acetate
718	β-ionylidenecyanoacetic acetate + Cl
456	β-ionylidenecyanoacetic acetate + Cl + PPh_3

The ^1H n.m.r. spectrum in $CDCl_3$ solution, showed that proton resonances due to the cyclohexenyl- ring were essentially the same as those of the free ligand, but did show the presence of two isomers with proton resonances shifted upfield by 0.05 p.p.m. The two series of resonances were not of equal abundance. The downfield series were six times as intense as the upfield series which was consistent with the ^{31}P n.m.r. spectrum. From the ^{31}P n.m.r. evidence the *cis-* isomer, being more abundant, has all the proton resonances shifted downfield, compared to the *trans-* isomer which may be associated with the presence of opposing ligands in the *trans-* isomer. Traces of toluene gave a methyl signal at 2.18 p.p.m. and phenyl protons ortho- to the methyl group gave a doublet of doublets, partially obscured by the triphenylphosphine signals, at δ 7.32 p.p.m. ($^3J_{H,H'}$ = 7.3 Hz, $^4J_{H,H''}$ = 2 Hz). The olefinic resonances appear to have collapsed into one signal, *cis-* at 6.623 p.p.m. and *trans-* at 6.597 p.p.m. This collapse of the olefinic protons in (V.4) will be discussed in Section 5.3.

The ^1H n.m.r. spectrum also shows that there are *cis-* and *trans-* isomers by the

existence of two rather than one *ortho*-phenyl proton signal groups due to the triphenylphosphine ligands.

The infrared spectrum shows the ν(CN) stretch at 2204(w) cm^{-1}, and as in Pt(β-ionylidenecyanoacetate)$_2$(PPh$_3$)$_2$, the ν(COO)$_{asym}$ stretch was unusually high at 1645(m) cm^{-1}. The vibrations associated with the -C=C- chain are very weak or absent, which, as stated above, leads to the conclusion that some interaction is occurring between the conjugated C=C double bond and the platinum atom. Further evidence for *cis*- and *trans*- isomers was given by the presence of ν(Pt-Cl) stretching modes at 310 and 320 cm^{-1}.

Final consideration of all the evidence suggests that the reaction has produced a mixture of *cis*- and *trans*- isomers of PtCl$_1$(β-ionylidenecyanoacetate)$_1$(PPh$_3$)$_2$ in a ratio of 6:1. Although attempts were made to separate the isomers by crystallization and chromatography this proved to be unsuccessful perhaps because of isomerization in solution resulting from the presence of the labile RCO_2^- ligand.

5.2.3 The Synthesis of Di{[*cis*-2-cyano-3-methyl-5-(2,6,6-trimethyl-1-cyclohexen-1-yl)-2,4-pentadienato]bis(triphenylphosphine)}palladium(II), Pd(β-ionylidenecyanoacetate)$_2$(PPh$_3$)$_2$ (V.5)

[PdCl$_2$(PPh$_3$)$_2$], as a suspension, was reacted with two mole equivalents of freshly precipitated silver β-ionylidenecyanoacetate in trichloromethane. Silver chloride precipitated out as a heavy grey solid, leaving a clear yellow solution. Hexane was used to precipitate out crude Pd(β-ionylidenecyanoacetate)$_2$(PPh$_3$)$_2$ (V.5) from the reaction mixture as a yellow powder. Compound (V.5) was purified by recrystallization from hexane/trichloromethane solution to form yellow crystals. Elemental analyses were satisfactory for [Pd(β-ionylidenecyanoacetate)$_2$(PPh$_3$)$_2$].CHCl$_3$ and no palladium metal precipitated from solution during the palladium analysis.

Table 5.3 The positive and negative FAB mass spectra of [Pd(β-ionylidenecyanoacetate)$_2$(PPh$_3$)$_2$].CHCl$_3$.

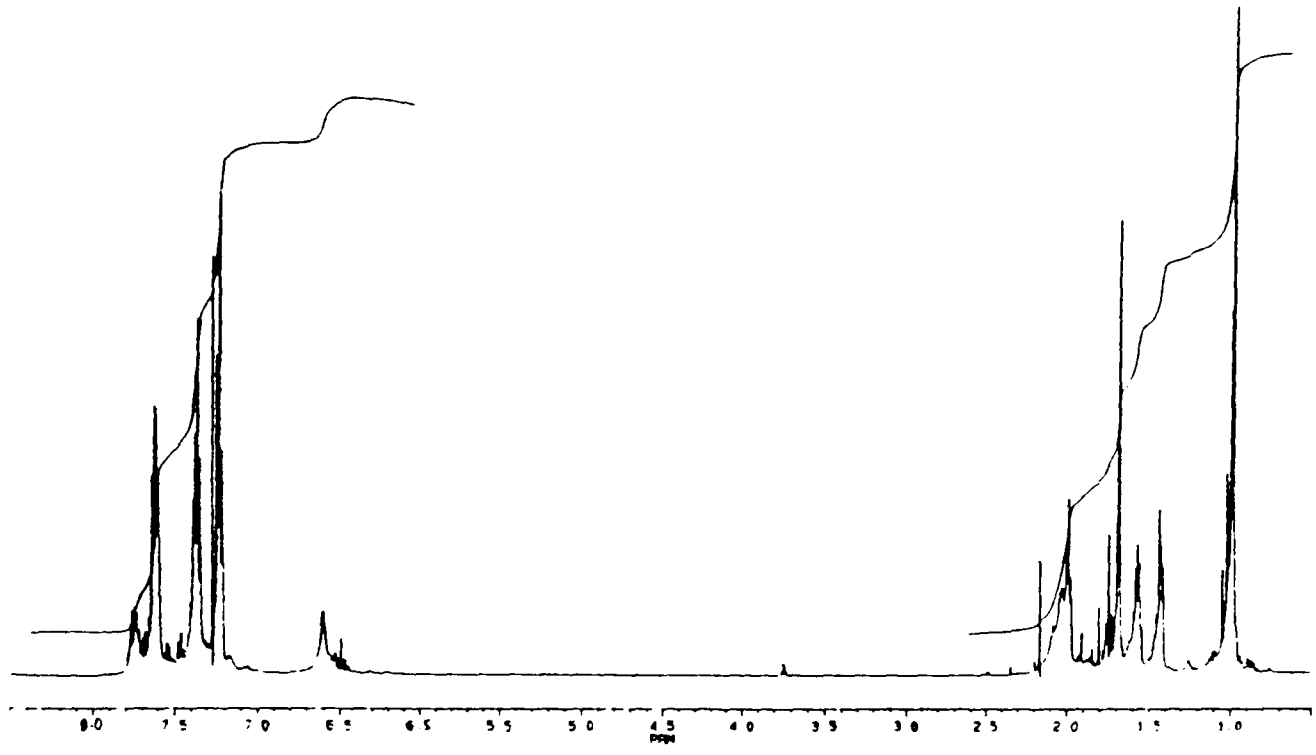
Positive FAB mass spectrum data		
m/z	R.i.	Possible Inference
2296	0.1	$[M]_2^{+\cdot}$
2039	0.25	$[M]_2^{+\cdot}$ - (β-ionylidenecyanoacetate)
1776	1.5	$[M]_2^{+\cdot}$ - 2(β-ionylidenecyanoacetate)
1515	0.5	$[M]_2^{+\cdot}$ - 2(β-ionylidenecyanoacetate) and PPh_3
1147	0.5	$[M]^{+\cdot}$
996	0.9	n/a
889	4.5	$[M]^{+\cdot}$ - (β-ionylidenecyanoacetate)
738	4.0	$[M]^{+\cdot}$ - (β-ionylidenecyanoacetate) and 2 x Ph
630	10	$[M]^{+\cdot}$ - 2(β-ionylidenecyanoacetate)
583	5.5	$[M]^{+\cdot}$ - (β-ionylidenecyanoacetate) and PPh_3 and CO_2
524	5.0	n/a
367	1.7	$[M]^{+\cdot}$ - 2(β-ionylidenecyanoacetate) and PPh_3
262	30	$[PPh_3]^{+\cdot}$

Negative FAB mass spectrum data		
m/z	R.i.	Possible Inference
1146	2.0	$[M]^{-\cdot}$ - H
886	1.4	$[M]^{-\cdot}$ - (β-ionylidenecyanoacetate)
621	2.0	$[M]^{-\cdot}$ - 2(PPh_3)
580	2.1	$[M]^{-\cdot}$ - 2(PPh_3) - CO_2
533	2.0	$[M]^{-\cdot}$ - 2(PPh_3) - 2 x CO_2
411	10	n/a
259	20	(β-ionylidenecyanoacetate) + H
258	100	[β-ionylidenecyanoacetate]$^{-\cdot}$
214	20	[β-ionylidenecyanoacetate]$^{-\cdot}$ - CO_2
152	20	n/a
122	9.5	n/a

The positive FAB mass spectrum of (V.5) shows the presence of a very weak dimeric species corresponding to [Pd(β-ionylidenecyanoacetate)$_2$(PPh$_3$)$_2$]$_2^{+\cdot}$ at m/z = 2296. A strong fragmentation pattern was observed corresponding to the loss of [β-ionylidenecyanoacetate] and triphenylphosphine from the dimer. The monomer ion at m/z = 1147 has a greater intensity than the dimer, but is still less abundant than the fragmentation ions signals (see Table 5.3). The negative FAB mass spectrum shows ion fragments due to loss of acidic protons from the β-ionylidenecyanoacetate group. The base peak m/z = 258 was due to the β-ionylidenecyanoacetate anion (see Table 5.3). The ^{1}H n.m.r. spectrum in $CDCl_3$ solution was similar to that of PtCl$_1$(β-ionylidenecyanoacetate)$_1$(PPh$_3$)$_2$. The positions of the resonances due to Me6, Me2, H5, H4 and H3 were unaltered but the signal due to Me3', expected to be at around δ 2.3 p.p.m. had become broader, and shifted to coincide with the signal due to H3 at 2.0 p.p.m. (c. 10H) (see Fig. 5.3) The olefinic protons gave a very broad single signal at 6.6 p.p.m. (4H), with no sign of the typical coupling between *trans*-H-C=C-H protons. The broadening of the signals due to the olefinic protons will be discussed in Section 5.3. Evidence of *trans*- and *cis*- Pd(II) isomers in (V.5) was given by the presence of two different sets of signals due to the phenyl- ring protons of the triphenylphosphine ligand (see Fig. 5.3).

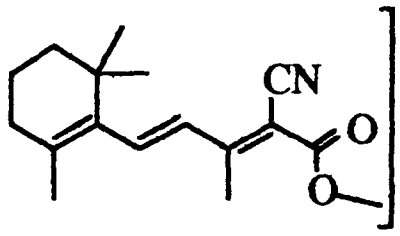
The vibrational data summarized in Table 5.4 shows that the $\nu(COO)_{asym}$ stretch for (V.5) was similar to that for PtCl(β-ionylidenecyanoacetate)(PPh$_3$)$_2$. In the case of (V.5) $\Delta\nu$ was 221 cm^{-1} which is similar to those observed for other compounds derived from β-ionylidenecyanoacetic acid.

Fig. 5.3 The ^1H n.m.r. spectrum of Pd(β-ionylidenecyanoacetate)$_2$(PPh_3)$_2$.



In summary, the analytical and spectroscopic data surveyed here for the major products from the reaction of [$PdCl_2(PPh_3)_2$] with two mole equivalents of silver β-ionylidenecyanoacetate, are consistent with a mixture of *cis*- and *trans*-di{*cis*[2-cyano-3-methyl-5-(2,6,6-trimethyl-1-cyclohexen-1-yl)-2,4-pentadienato]bis(triphenylphosphine)}-palladium(II).$CHCl_3$, [Pd(β-ionylidenecyanoacetate)$_2$(PPh_3)$_2$].$CHCl_3$, (V.5).

Table 5.4 Infrared data for compounds (V.4) to (V.8).

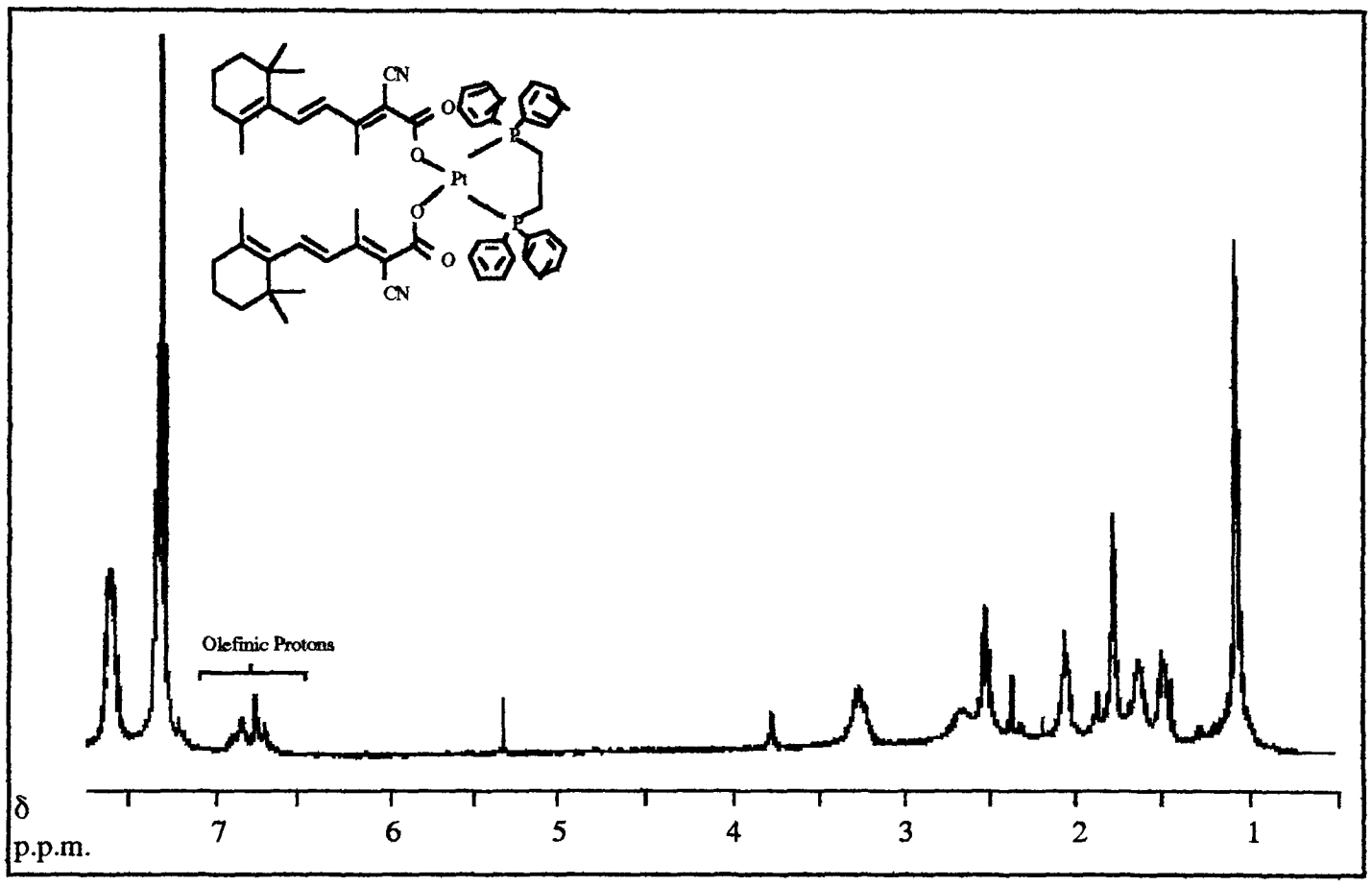
L = 	Compound Number	ν(C=O) asym	ν(C-O) sym	ν(CN)	ν(αβ C=C)	ν(H-C=C-H) def.	ν(CC-H)	Δν (CO_{2a} - CO_{2s})	ν(Pt-P) sym/asym	ν(Pt-Cl)	Unidentified band
Pt(diphos)L_2	(V.6)	1610	1439 1360	2200	1560	969	803	>171	536 483	-	1340
"Pt(diphos)Cl_1L_1"	(V.7)	1630	1440 1360	2204	-	998	-	>190	540 490	-	1350
"Pt(PPh_3)$_2L_2$"	(V.8)	1634	1350 1310	2205	1558	-	842	>284	530 500	310 320	1310
Pt(PPh_3)$_2Cl_1L_1$	(V.4)	1645	1438	2204	1550	-	835	207	531 500	-	1308
Pd(PPh_3)$_2L_2$	(V.5)	1655	1434	2203	1587	970	832	221	-	-	1303

Key: All values in cm^{-1}, L = *trans*- β-ionylidenecyanoacetic acid.

5.2.4 The Synthesis of Di-{*cis*[2-cyano-3-methyl-5-(2,6,6-trimethyl-1-cyclohexen-1-yl)-2,4-pentadienato]-(bis(diphenylphosphino)ethane)}platinum(II), Pt(β-ionylidenecyanoacetate)$_2$(diphos), (V.6)

Cis-[dichlorobis(diphenylphosphino)ethaneplatinum(II)] was chosen as the starting material because the bidentate phosphine ligand (diphos) would prevent the formation of the *trans*- isomer. $PtCl_2$(diphos), as a suspension in $CHCl_3$, was reacted with two mole equivalents of freshly precipitated silver β-ionylidenecyanoacetate. Silver chloride precipitated out as a heavy grey solid, leaving a clear yellow solution.

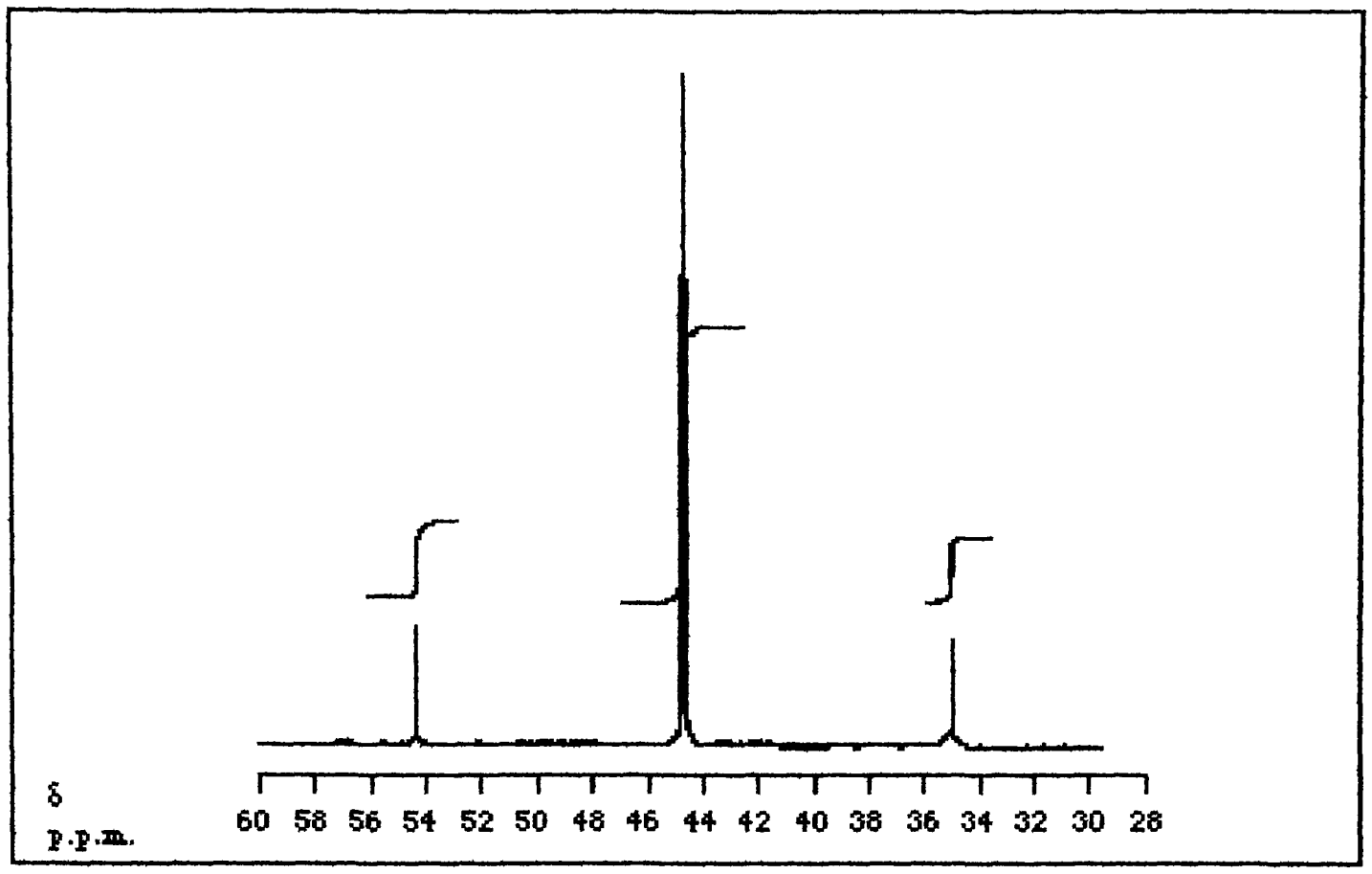
Fig. 5.4 The ^{1}H n.m.r. spectrum of Pt(β-ionylidenecyanoacetate)$_2$(diphos) in $CDCl_3$.



This yellow solution was found to be very light sensitive, and on exposure to sunlight, decomposed and precipitated out platinum metal. An off-white solid was isolated on removal of the solvent. The solid residue was soluble in benzene, toluene, dichloromethane, trichloromethane and acetone but insoluble (melted to an oil) in hot hexane and cyclohexane. The off-white solid was extracted using a toluene/dichloromethane mixture, and a semi-crystalline light-yellow solid was obtained by

slow evaporation of the extract at -20°C.

Fig. 5.5 The ^{31}P n.m.r. spectrum of Pt(β-ionylidenecyanoacetate)$_2$(diphos) in CH_2Cl_2.



The ^{31}P n.m.r. spectrum (in CH_2Cl_2) of the isolated solid thought to be Pt(β-ionylidenecyanoacetate)$_2$(diphos), showed there to be only one product present which gave a signal at 1:4:1 multiplet at δ 44.71 p.p.m. with ^{195}Pt(I=1/2; 33.6% abundance) satellites with a measured $^1J_{Pt-P}$ coupling constant of 2350 Hz (see Fig. 5.5). It is normal for Pt(II) compounds with a *cis*- geometry to have a $^1J_{Pt-P}$ coupling constant of around 3000 Hz and those with a *trans*- geometry to have a larger $^1J_{Pt-P}$ coupling constant in the region of 3300-3400 Hz.[29-31] Appleton *et al*[8] measured the coupling constants of square planar platinum complexes and the effect of altering one of the ligands. A coupling constant of 2350 Hz as observed in (V.6) is not typical of oxygen or nitrogen co-ordinated ligands but is similar to the coupling constants observed for carbon-platinum bonded ligands. The coupling constant is also very different from that in (5.7).

The ^1H n.m.r. spectrum in $CDCl_3$ solution had characteristic signals due to the (diphos) and (β-ionylidenecyanoacetate) ligands in the ratio of 1(diphos):2(β-ionylidenecyanoacetate) (see Fig. 5.4). The signals due to the phenyl- groups of the

(diphos) ligand occur as complex multiplets at δ 7.6 and 7.3 p.p.m. The compound $PtCl_2$(diphos) showed the same phenyl- proton signals at 7.6 and 7.9 p.p.m. (in CD_3CN). The methylene protons in $PtCl_2$(diphos) occur as two overlapping triplets (because of the combined $^3J_{H,H'}$ with $^2J_{H,P}$ coupling of 19 Hz) at δ 2.45 p.p.m. however those in Pt(β-ionylidenecyanoacetate)$_2$(diphos) occur as a broad triplet at 3.24 p.p.m. The proton n.m.r. spectrum showed signals due to residual tetrahydrofuran and dichloromethane solvents. The olefinic protons H4' and H5' occur at δ 6.71 (d, $^3J_{H,H'}$ = 16 Hz) and 6.85 p.p.m (broad doublet, $^3J_{H,H'}$ = 16 Hz) which are typical signals due to the *trans*-geometry of the H-C=C-H bond of the β-ionylidenecyanoacetate anion. The remaining proton signals corresponded to the proposed structure of the β-ionylidenecyanoacetate anion (see Fig. 5.4).

Elemental analyses confirmed the ratio of the two ligands to be 1(diphos):2(β-ionylidenecyanoacetate). The percentage platinum in the complex could not be obtained accurately because platinum metal precipitated out during the assay. Traces of chlorine (about 1.1(4)% max, 1.11; min, 1.17) were due to dichloromethane solvent trapped within the solid, typical of platinum(II) carboxylate complexes.[49,157]

The vibrational spectra of palladium(II) and platinum(II) carboxylates have been investigated by Stephenson *et al.*[188] It was found that diacetatoplatinum(II) showed $\nu(COO)_{asym}$ and $\nu(COO)_{sym}$ vibrational modes at 1562 and 1429 cm^{-1}, with a $\nu(COO)_{def}$ band seen at 689 cm^{-1}. Correlations between the vibrational spectra of palladium(II) and platinum(II) carboxylates must be avoided as the complexes are not isomorphous. However, comparisons between the difference of the asymmetric and the symmetric stretching modes have been shown to be an effective analytical tool. In general monomeric chelated *trans*-palladium(II) carboxylates show $\Delta\nu = 150\ cm^{-1}$, while trimeric (or dimeric) carboxylates having bridging and chelating groups have a $\Delta\nu = 250\ cm^{-1}$. Di-{*cis*[2-cyano-3-methyl-5-(2,6,6-trimethyl-1-cyclohexen-1-yl)-2,4-pentadienato]-bis-(diphenylphosphino)ethane}platinum(II), (V.6), contains a broad band assigned to the $\nu(COO)_{asym}$ stretching mode at 1610 cm^{-1}, and the $\nu(COO)_{sym}$ stretching modes appear at 1439, 1360 and 1340 cm^{-1}. Multiple $\nu(COO)_{sym}$ stretches have been observed for

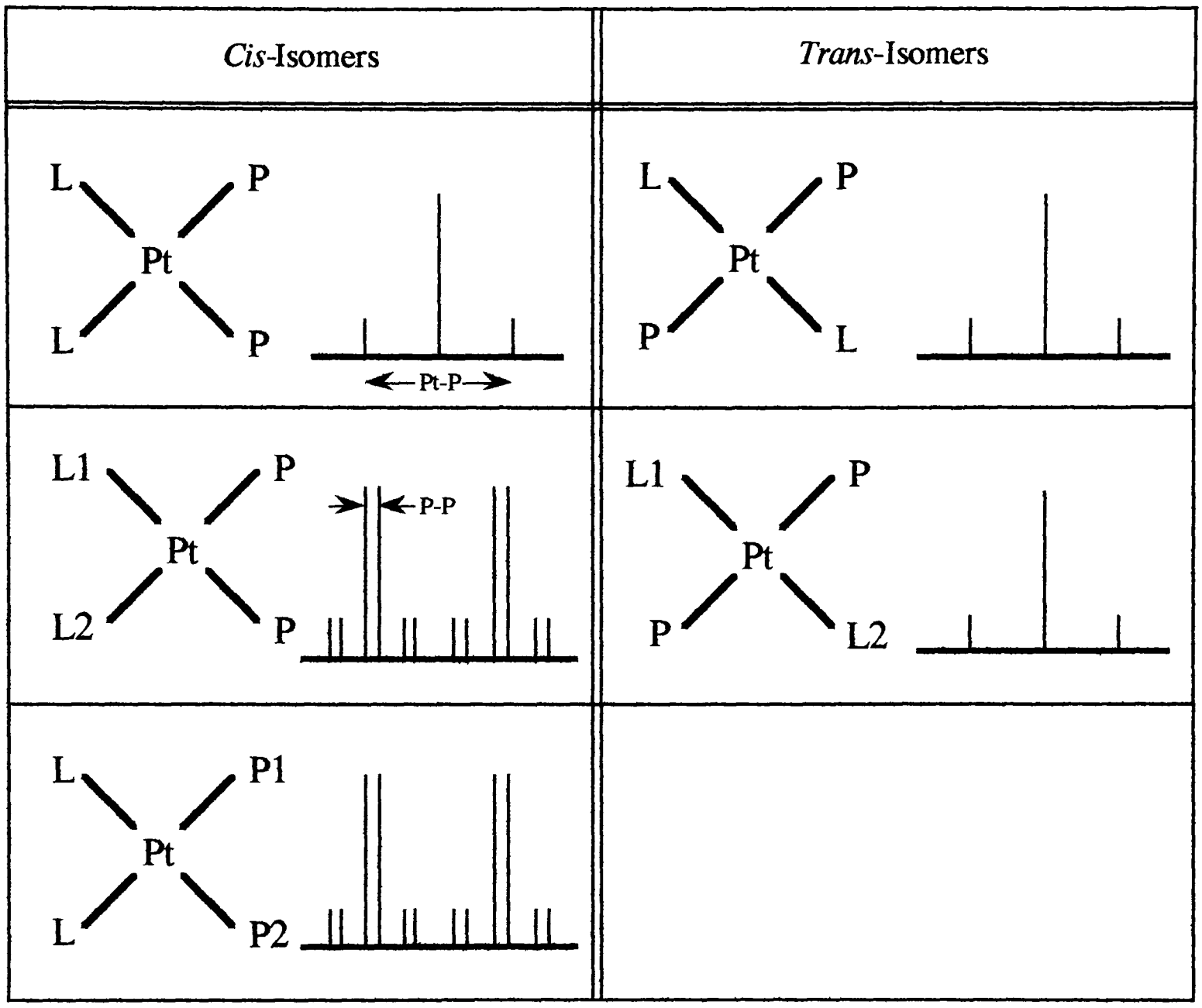
palladium(II) acetates[188] and have been attributed to mixed terminal/bridged COO groups. However, in the case of di-{*cis*[2-cyano-3-methyl-5-(2,6,6-trimethyl-1-cyclohexen-1-yl)-2,4-pentadienato]bis(diphenylphosphino)ethane}platinum(II), (V.6), the (diphos) ligand locks the platinum(II) square planar molecule into the *cis*- configuration which prevents the formation of multinuclear species connected by bridging carboxylates.

The analytical data summarized above leads to the conclusion that the compound synthesized corresponds to monomeric di-{*cis*[2-cyano-3-methyl-5-(2,6,6-trimethyl-1-cyclohexen-1-yl)-2,4-pentadienato]bis(diphenylphosphino)ethane}-platinum(II).0.5CH_2Cl_2. There are some aspects of the spectroscopic data which remain unresolved, in particular, the magnitude of the ^1J(Pt-P) coupling constant. Confirmation of the structure by single crystal X-ray structural analysis was not possible because of the difficulties associated with growing suitable single crystals.

5.2.5 <u>The Attempted Synthesis of Monochloro-[*cis*-{2-cyano-3-methyl-5-(2,6,6-trimethyl-1-cyclohexen-1-yl)-2,4-pentadienato}bis(diphenylphosphino)ethane]-platinum(II), PtCl(β-ionylidenecyanoacetate)(diphos) (V.7)</u>

$PtCl_2$(diphos), as a suspension in dichloromethane, was reacted with <u>one mole equivalent</u> of freshly precipitated silver β-ionylidenecyanoacetate in dichloromethane. Silver chloride precipitated out as a heavy grey solid, leaving a clear yellow solution. The solvent was removed under reduced pressure, leaving an off-white froth-like solid. The off-white solid was extracted with trichloromethane, and thin layer chromatographic analysis suggested that only one product was present. Crystals could not be grown by the usual methods because of the high solubility in the solvents CH_2Cl_2, $CHCl_3$ and tetrahydrofuran.

Fig. 5.6 Theoretical ^{31}P n.m.r. spectra of *cis*- and *trans*- square planar platinum(II) isomers.



The ^{31}P n.m.r. spectrum showed that the solid product contained four P environments in the ratio of 100:69:45:37. The ^{31}P n.m.r. spectrum shows no P-P coupling and therefore the *cis*- square planar Pt(II) geometry is retained and both the ligands are equivalent (see Fig. 5.6). The coupling constants of the four signals observed in (V.7) at δ 38.75 ($^{1}J_{Pt-P}$ = 3618); 29.04 ($^{1}J_{Pt-P}$ = 3656); 37.35 ($^{1}J_{Pt-P}$ = 3760); 26.26 p.p.m. ($^{1}J_{Pt-P}$ = 3808 Hz). None of these corresponded to the signal observed for *cis*-Pt(β-ionylidenecyanoacetate)$_2$(diphos) (δ 44.71 p.p.m. ($^{1}J_{Pt-P}$ = 2350 Hz) described in the previous section. The ^{31}P n.m.r. Pt-P coupling constants are in the correct region for other literature values for *cis*- Pt(II) square planar geometry. The compound *cis*-[bis(acetato)bis(triphenylphosphine)]platinum(II) was reported to show the

triphenylphosphine signal at +5.56 p.p.m. (CH_2Cl_2) with $^1J_{Pt-P}$ of 3823 Hz.[105a] Other compounds of this series discussed in Section 5.2.3 (compound (V.4)) have Pt-P coupling constants for β-ionylidenecyanoacetate complexes measured at 3680 Hz for *cis*- and 3882 Hz for the *trans*- isomer. It is difficult to propose structures for these compounds without considering a variety of products resulting from H migration in the ligand. The ^1H n.m.r. spectrum data for (V.7) shows two characteristic multiplets due to the P-phenyl groups of the (diphos) ligand at δ 7.6 and 7.9 p.p.m. The corresponding shifts observed for the starting material $PtCl_2$(diphos) are at 7.6 and 7.9 p.p.m. which demonstrates that (V.7) has a *cis*- Pt(II) square planar geometry. The corresponding resonances for the P-phenyl protons in Pt(β-ionylidenecyanoacetate)$_2$(diphos) are at δ 7.3 and 7.6 p.p.m.

The the ^1H n.m.r. spectrum (in $CDCl_3$) shows that the ratio of β-ionylidenecyanoacetate to (diphos) was 2:1. However, satisfactory elemental analyses for this formulation could not be obtained. The proton n.m.r spectrum also showed four Me3' environments, and a series of *trans*-olefinic protons in the 6.2 to 6.6 p.p.m. region, which could be attributed to proton migration processes.

The infrared spectrum had a single weak ν(CN) band at 2208 cm^{-1}, and a very broad absorption at 1650 cm^{-1} attributed to the $\nu(COO)_{asym}$ stretching mode. The $\nu(COO)_{sym}$ stretch was either 1440 or 1360 cm^{-1}, the latter being in the correct region. The compound *cis*-[bis(acetato)bis(triphenylphosphine)platinum(II) was reported to show the $\nu(COO)_{asym}$ stretching mode at 1636 and the $\nu(COO)_{sym}$ stretch at 1370 cm^{-1}.[105a] The intensities of the ν(COO) and ν(CN) bands are normally retained in the metal salts (see previous section) but their low intensities in these compounds suggest that there is now less electronic conjugation through the β-ionylidenecyanoacetate ligand. There are several bands in the region expected for symmetrical ν(COO) vibrations. There were no Pt-Cl stretching modes at 280 and 310 cm^{-1}, which would have indicated a *cis*- Pt(II) geometry. $PtCl_2$(diphos) has ν(Pt-Cl) at 280, 290 and 315 cm^{-1} (Nujol mull, CsI plates). The $\nu(Pt-P)_{asym}$ and $\nu(Pt-P)_{sym}$ stretching modes which are normally seen in *cis*- Pt(II) compounds at 427 and 442 cm^{-1} respectively, were observed for (V.7) at 490 and 540 cm^{-1} corresponding to the Pt-P bands in $PtCl_2$(diphos) seen at 490 and 540 cm^{-1}. The Pt-P vibrations of *trans*- Pt(II) compounds exist at 346 cm^{-1}. Unusually, no strong

conjugated C=C band was observed in the region of 1580 cm^{-1}, furthermore, the out of plane vibration due to the deformation of the H-C=C-H group was no-longer present. This change in the C=C group coupled with the observation that the olefinic C-H stretches have increased in frequency suggests that there could be some Pt to C=C interactions within the molecule. These observations are discussed further in Section 5.3.

In summary the reaction between $PtCl_2$(diphos) and one mole equivalent of silver β-ionylidenecyanoacetate produced a mixture of four compounds which retain the *cis*-geometry around the Pt centre. The two carboxylate ligands were equivalent as shown by the ^{31}P n.m.r. spectrum. The four compounds could not be separated by chromatography or recrystallization. The analytical data summarized here does not correspond to the expected product, PtCl(β-ionylidenecyanoacetate)(diphos) (V.7) but to Pt(β-ionylidene-cyanoacetate)$_2$(diphos).CH_2Cl_2. The spectroscopic data suggests the possibility of products resulting from ligand rearrangements but the spectra are too complex to be readily interpreted.

5.2.6 The Attempted Synthesis of {*Cis*[2-cyano-3-methyl-5-(2,6,6-trimethyl-1-cyclohexen-1-yl)-2,4-pentadienato]$_2$bis(triphenylphosphine)}platinum(II), Pt(β-ionylidenecyanoacetate)$_2$(PPh_3)$_2$ (V.8)

A dichloromethane suspension of [Pt(CO_3)(PPh_3)$_2$] and two equivalents of β-ionylidenecyanoacetic acid dissolved in MeOH were refluxed for 5 minutes. The colour changed from yellow to a lighter yellow. The solvent was removed under reduced pressure. The residue was re-dissolved in trichloromethane, and then hexane was added to precipitate out a pale cream solid, (V.8).

Pt(β-ionylidenecyanoacetate)$_2$(PPh_3)$_2$ was soluble in acetonitrile, diethyl ether, methanol, toluene and trichloromethane, but insoluble in hexane. Elemental analyses corresponded to the expected molecular formula, however platinum metal precipitated out of solution during the platinum assay, and so the result was lower than the theoretical percentage.

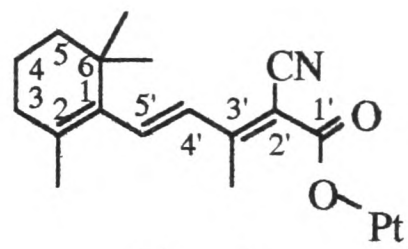
The infrared spectrum included the ν(CN) stretching mode at 2205 cm^{-1}. The

$\nu(COO)_{asym}$ stretching mode was observed at 1634 cm^{-1} which is unusually high. The remainder of the bands were similar to those seen for (V.7) except for another band at 1310 cm^{-1} allocated to the $\nu(COO)_{sym}$ stretching mode. The band at 1310 cm^{-1} appeared in palladium(II) and platinum(II) carboxylates which contain the triphenylphosphine group. This has been observed in this study and was reported previously by Stephenson *et al.*[188] The conjugated C=C and vibrations related to H-C=C-H were not present in (V.8). The same was seen for compound (V.7).

The ^1H n.m.r. data of the products indicated that mixtures of compounds had resulted from the reaction. Furthermore, the spectroscopic data suggested that isomerization of the ligand by a retro- shift had occurred. Some structural characterization of the complex mixture was attempted using COSY ^1H n.m.r. spectral data (collected on a Brucker 500 MHz instrument, in $CDCl_3$ solution). The spectrum showed only superficial similarities to that of β-ionylidenecyanoacetic acid (see Section 4.6), which suggested the formation of products resulting from the retro- shift.

The most obvious couplings seen in the COSY spectrum of β-ionylidenecyanoacetic acid were those between H5' and Me2 and H5' and H3 (see Table 4.4). The same couplings were seen in the COSY spectrum of Pt(β-ionylidenecyanoacetate)$_2$(PPh_3)$_2$ (see Table 5.5). There were considerable differences, however, in the chemical shifts of these protons in the complexes compared to the free acid (see Fig. 5.7).

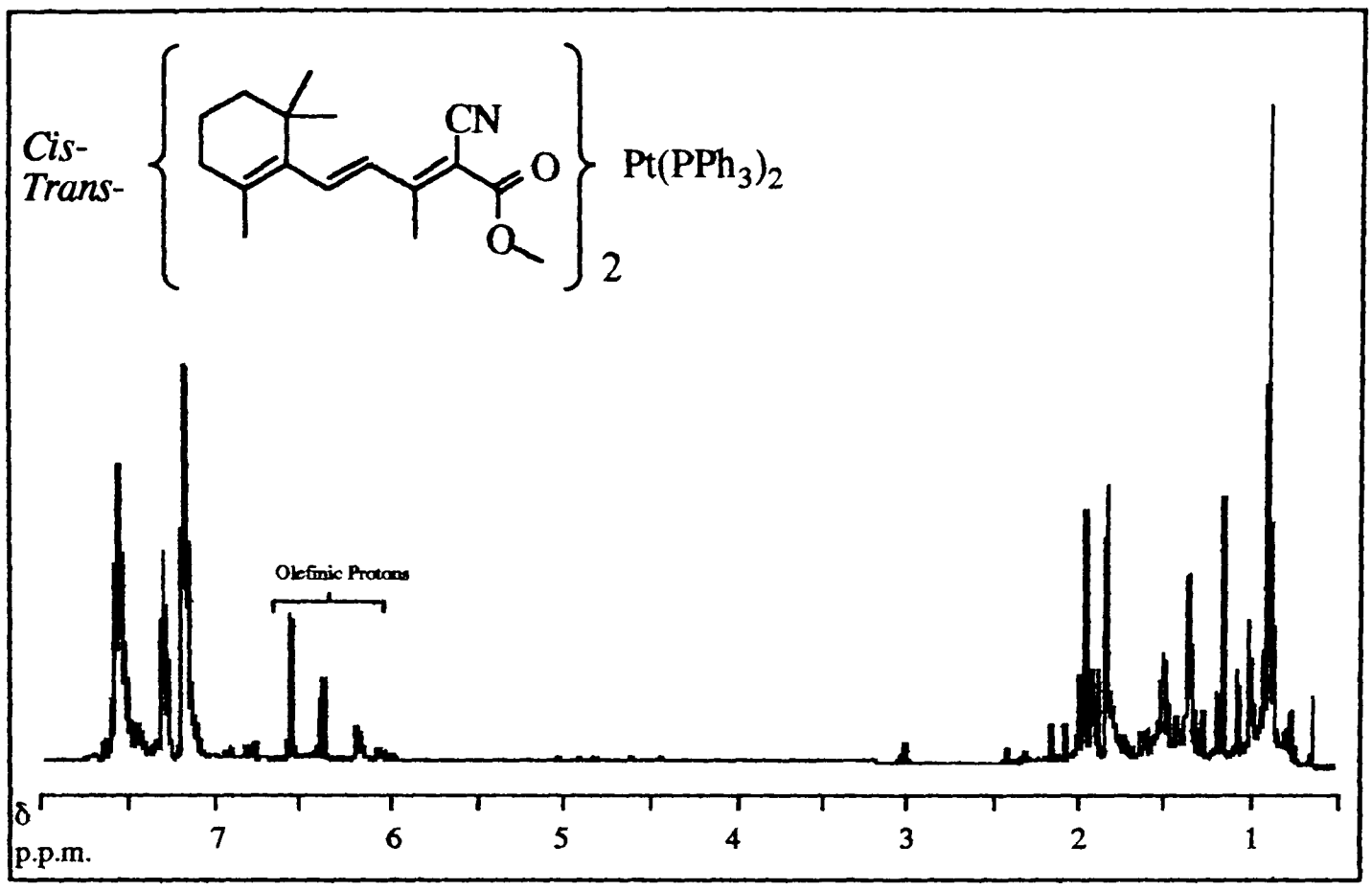
Table 5.5 COSY data for Pt(β-ionylidenecyanoacetate)$_2$(PPh$_3$)$_2$ (V.8).

						 Ligand				
Me2			1.26							
H3				1.89						
H4				8	1.58					
H5					8	1.43				
H4'							6.42			
H5'			C	C			12.2	6.22#		
Me6									0.99	
Me3'										na
Proton Allocation			Me 2	H3	H4	H5	H4'	H5'	Me 6	Me 3'

Figures are δ in p.p.m./ coupling constants in Hz.

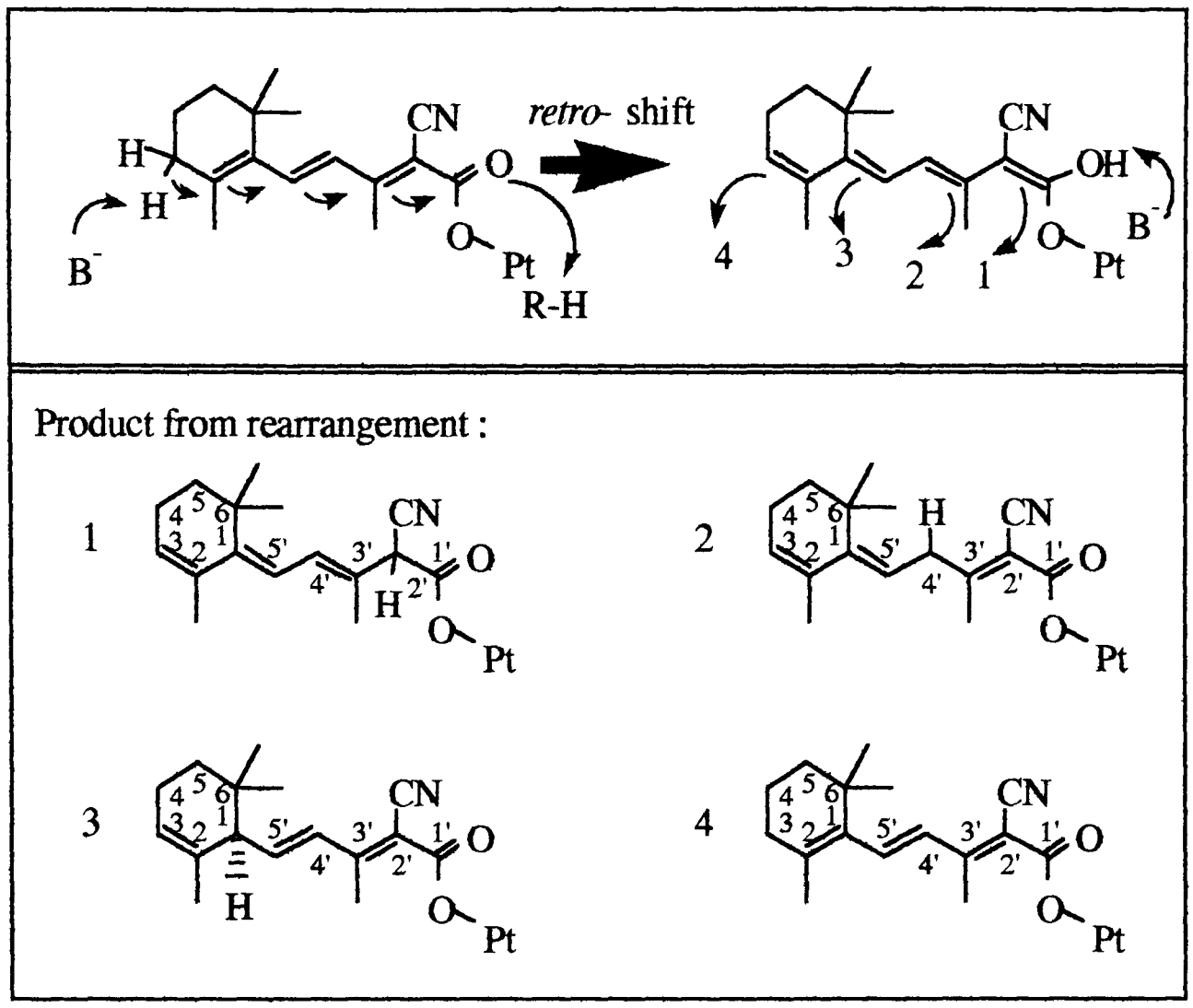
C = coupling of < 1 Hz , # peak is broad due to long range multiple coupling.

Fig. 5.7 The ^1H n.m.r. spectrum of Pt(β-ionylidenecyanoacetate)$_2$(PPh$_3$)$_2$.



Firstly, the broad doublet due to H5' (usually about δ 7.19 p.p.m.) which is normally observed downfield from that of the sharp signal due to H4' (usually about 7.04 p.p.m.), was upfield of H4' (6.42 p.p.m.) at δ 6.22. This inversion in chemical shift has only been observed previously in the case of ammonium *cis*-[2-cyano-3-methyl-5-(2,6,6-trimethyl-1-cyclohexen-1-yl)-2,4-pentadienate] (IV.10). The remaining resonances have all been shifted upfield, notably Me2 (1.26 p.p.m.) is upfield of H4 and H5. The COSY spectrum of the product isolated from the reaction between [PtCO$_3$(PPh$_3$)$_2$], with two equivalents of β-ionylidenecyanoacetic acid has produced a complex mixture of products. Some of the proton coupling maps corresponded to some of the possible structural isomers which form as a result of the *retro*- shift of a proton. Fig. 5.8 shows the four most probable isomers from a reversal of the reaction which forms *retro*-ionylidenecyanoacetate.[159] The COSY spectrum showed the presence of isomers 3 and 4 in Fig. 5.8.

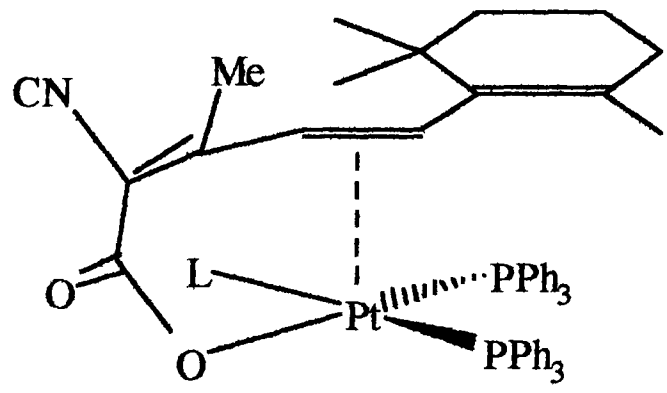
Fig. 5.8 Four isomers formed from the reaction of *retro*-ionylidenecyanoacetate anion with "base".



The ^{1}H n.m.r. spectrum also shows an interesting sharp doublet with a coupling constant of 3 Hz at δ 6.59 p.p.m. The platinum(diphos) compounds (V.6) and (V.7) do not show the same type of signal. The COSY spectrum of (V.8) shows that this peak is coupled to H3 and Me2, and this implies that the doublet at δ 6.59 p.p.m. is due to olefinic protons at H4' and H5'. A similar observation has been made for the other platinum(II) and palladium(II) carboxylate compounds described here which have two triphenylphosphine ligands attached to the metal. These observations are discussed in more detail in Section 5.3.

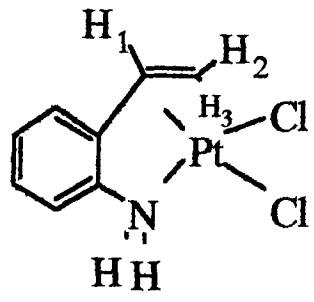
5.3 Possible Evidence for η2-Pt/Pd Bonding in Platinum or Palladium(II) Complexes of β-Ionylidenecyanoacetic Acid and Summary of their Chemical Properties

Unexpected broadening of ^1H n.m.r. spectrum signals and the weakening or complete disappearance of vibrational bands due to the H-C=C-H group which occur in the platinum(II) and palladium(II) complexes (V.7) and (V.8) suggests some form of electronic or molecular interaction. It is proposed here that bonding occurs between the platinum(II) or palladium(II) metal atom and the *trans* olefinic bond of the β-ionylidenecyanoacetate ligand. A possible structure is illustrated below:



Hypothetical platinum(II) to C=C bonding in complexes (V.7) and (V.8).

Cooper *et al*[65] synthesized compound (V.9), and observed that the ^1H n.m.r. shifts of the olefinic ligand were similar to that of styrene.



(V.9)

On co-ordination to the platinum(II) centre, the olefinic protons of (V.9) moved "upfield" (to lower δ). For example, the proton signal shifts for H1 were from δ 6.97 to 5.73 p.p.m. (= 1.4 p.p.m. change) while H2 moved from 5.24 to 4.91 p.p.m. (= 0.33 p.p.m.).[127] Moreover, the *trans*- ^3J coupling constant between H1 and H3 was reduced from 17.2 to 12.7 Hz. The energy of free rotation for C=C bonded to Pt has been estimated to be in the order of 40-65 $kJmol^{-1}$ which would allow the rotation of the C=C

bond at room temperature. This rotation of the C=C bonded to Pt while in solution may explain the reduction in the $^{3}J_{H,H'}$ coupling constant.[5] ^{1}J coupling between the olefinic protons and the Pt(II) was observed to be in the order of 60 Hz (0.2 p.p.m. at 300 MHz). No obvious $^{1}J_{Pt-H}$ coupling was observed in compounds (V.4) to (V.7).

5.4 Second Harmonic Generation Properties of Platinum(II) and Palladium(II) Complexes of β-Ionylidenecyanoacetic Acid

The second harmonic generation (SHG) properties of ungraded samples of platinum(II) and palladium(II) complexes of β-ionylidenecyanoacetic acid and the starting materials are presented in Table 5.6.

The SHG efficiencies of the platinum(II) and palladium(II) complexes (V.4) to (V.8) are of the same order as the efficiencies of the starting materials. The near-zero SHG efficiencies show that there was no non-centrosymmetry present in the crystal structures of the complexes (V.4) to (V.8). The SHG efficiencies measured were smaller than those residual SHG signals which have been observed from compounds which crystallize in a centric space group, but which show SHG due to some form of lattice defect or surface effect (see Chapter Two, Section 2.2.2).

Table 5.6 Second harmonic generation of platinum(II) and palladium(II) complexes of β-ionylidenecyanoacetic acid, and some starting materials.

Compound		Efficiency x urea	Colour
$Pt(diphos)L_2$	(V.6)	not tested	White
"$Pt(diphos)Cl_1L_1$"	(V.7)	0.096	White
"$Pt(PPh_3)_2L_2$"	(V.8)	lu	Pale yellow
$Pt(PPh_3)_2Cl_1L_1$	(V.4)	0.032	White
$Pd(PPh_3)_2L_2$	(V.5)	0.02	Yellow
Cis-$Pt(PPh_3)_2Cl_2$		0.08	White
$Pt(PPh_3)_2CO_3$		lu	White
Cis-$Pd(PPh_3)_2Br_2$		0.00	Yellow
L = β-Ionylidenecyanoacetate			

5.5 Conclusion

Attempts were made to synthesize some palladium and platinum compounds of β-ionylidenecyanoacetic acid. However, their study was made difficult by the occurrence of isomers and the difficulty of separating the products by conventional techniques. The chemistry and physical properties of these complexes were found to be unusual. There was an increase in solubility of these complexes due to the size and nature of the β-ionylidenecyanoacetate ligand.

The second harmonic generation properties of these complexes showed no evidence of the non-centrosymmetric crystal structures typical for related complexes. The use of platinum(II) and palladium(II) metal centers to direct the symmetry of the potentially NLO active carboxylic acid, β-ionylidenecyanoacetic acid, in the search for second harmonic generation, was unsuccessful.

CHAPTER SIX

The Introduction of Chirality Into β-Ionylidenecyanoacetic Acid

6.1 Introduction

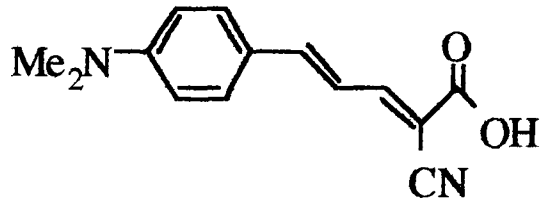
It was observed in 1965 that glass surfaces bearing finger-print smudges emitted ultraviolet light in the region of 340 to 370 nm when excited by light from a 100 W ruby laser.[171] This observation sparked off a series of investigations into the second harmonic generation (SHG) properties of amino acids, peptides and viruses.[68,171] A link had been suggested between the chiral nature of biological systems and non-linear optics. Pasteur was "the first to suggest that the dissymmetric nature of biological systems is hardly accidental but of some fundamental importance in biomechanisms".[167]

Whether or not the observed non-linear effects were due to the amino acids in the finger-prints or to the silica in the glass surface remains unanswered, the fact remains that chiral amino acids are a cheap and simple method of introducing the necessary non-centrosymmetry into molecules and thereby should be of assistance in the search for materials that show second harmonic generation (SHG).

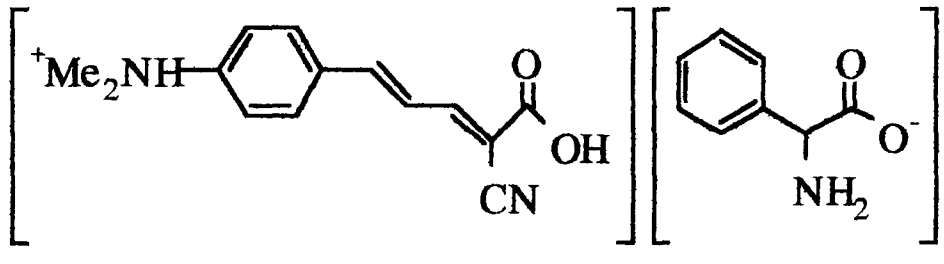
It was found that the general order of efficiencies for bio-organic molecules was proteins @ 0.004 < viruses @ 0.005 < tripeptides @ 0.006 < dipeptides @ 0.05 < amino acids @ 80 (x SiO_2, fundamental 1060 nm).[68] Furthermore, the D-isomer generally showed SHG effects equal to that of the L-isomer and any differences could be ascribed to impurities. Racemic DL-mixtures showed SHG responses 10-20 times lower than the pure enantiomers. There are exceptions, for example DL-alanine crystallizes in a space group without a centre of inversion and is therefore active, with an SHG efficiency of 0.13 x urea.[68,171] These results have been confirmed by more recent work of Agal'tsov *et al.*[4]

The use of amino acids to encourage crytallization in non-centric space groups has been attempted by many authors, sometimes as a last resort.[24] Amino acids, alone, have

already been discussed, leading to materials with a low SHG efficiency.[102] Amino acids have been used to form salts of amines, such as the reaction of (VI.1) with L-phenylalanine.HCl to form the chiral salt (VI.2).[191,192,214] However, the Patent report does not give details of the magnitude of the SHG effect for the salt.



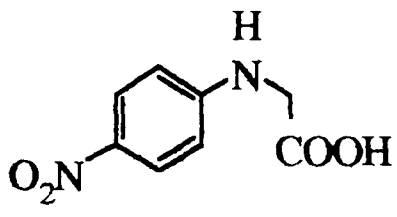
(VI.1)



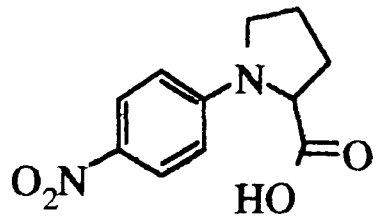
(VI.2)

This reactions destroys the planarity of the Me_2N- group to form the tetrahedral Me_2NH^+ group resulting in the loss of conjugation through the molecule. This should lead to a considerable loss in SHG efficiency because of the decrease in the magnitude of β.

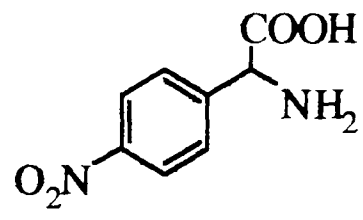
Some functionalised derivatives of amino acids have been synthesized such as 4-nitrohippuric acid (VI.3)[64], N-(4-nitrophenyl)-L-prolinol (VI.4)[100,121] and nitrophenyl alanine (VI.5)[131] which contain conjugated donor-acceptor functions which should give rise to large β. 4-Nitrohippuric acid (VI.3) alone does not show any SHG properties because of symmetry constraints (centrosymmetric space group $C_{2/c}$). However, if 4-nitrohippuric acid is intercalated into a matrix of lithium aluminate, the resulting intercalation compound shows a SHG efficiency of 3.5 x that of hippuric acid alone (2.2 x urea).[64,222]



(VI.3)

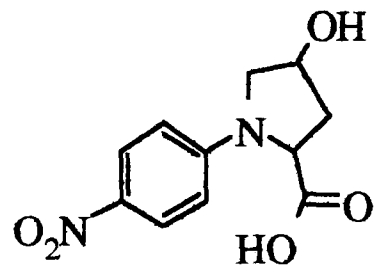


(VI.4)

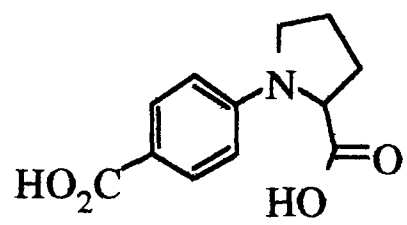


(VI.5)

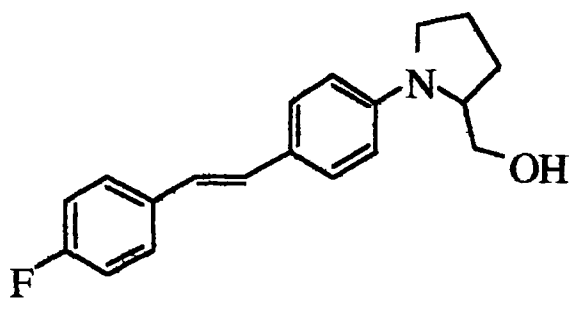
N-(4-Nitrophenyl)-L-prolinol (VI.4) and related molecules give rise to "high" SHG efficiencies. The following series of compounds have also been synthesized and studied.[152]



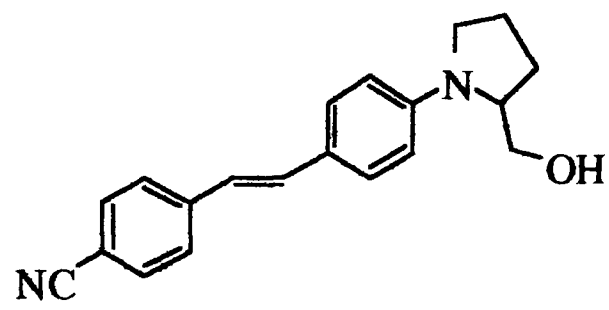
(VI.6)



(VI.7)



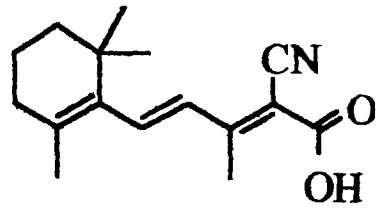
(VI.8)



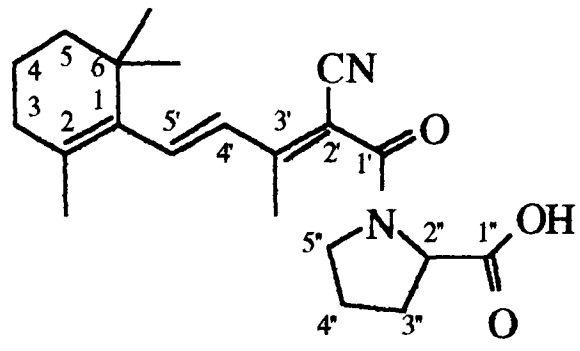
(VI.9)

Compound (VI.6) shows SHG, while compounds (VI.7) to (VI.9) show no SHG. Compounds (VI.6) to (VI.9) have also been orientated by chemically binding them to styrene-based polymers and membranes.[24,100,196]

This Chapter describes the reaction between β-ionylidenecyanoacetic acid;



and the amino acid, L-proline, to form the N bonded derivative;



and the reaction and second harmonic generating properties of the N-bonded derivative and some of its metal salts are discussed.

6.1.1 Metal Salts of L-Proline

Many metal salts of the amino acid L-proline have been synthesized, but their non-linear optical properties have not been reported.

This Chapter investigates the effect of a metal centre on an NLO active ligand. Metal centers with one L-proline group should show SHG, while those with two L-proline groups may or may not show SHG depending on whether or not the L-proline groups mutually cancel each other. The compound {Mo(NO)LCl(3-O-1,2:5,6-di-iso-propylidene-α-D-glucofuranoate)] (where L=$HB(3,5\text{-}Me_2C_3N_2H)_3$) crystallises in the space group $P2_1$ but has an SHG efficiency of only 0.25 x urea, even though the ligand is chiral. The low SHG for this compound has been attributed to there being two molecules per asymmetric unit and so the hyperpolarizabilities are opposed.[55] Copper proline dihydrate crystallizes in the space group $P2_1/n$, with two Cu(II) atoms per unit cell which possesses a centre of inversion through the copper atom.[139] The presence of a centre of inversion in copper proline dihydrate means that SHG responses will not be observed, as effects induced in one L-proline group will cancel those in the second L-proline group.

6.1.2 Optical Activity in the Non-linear Susceptibility

The fundamental paradox in using chirality to overcome symmetry constraints for non-linear optics is that not all chiral or potentially chiral compounds give rise to second order non-linear effects.

Where crystals are composed of a racemic mixture of D and L compounds and possess a center of inversion the compound has a structure which belongs to a centrosymmetric point group. The action of the "inversion centre" reverses the sign of the electronic transition dipole moment, but not the sign of the magnetic transition dipole moment. The upshot of this special class of compound is that SHG can be detected only if the incident radiation is elliptically polarized.[140] Thus R,S-N-acetyl valine exists with a unit cell composed of two R and two S molecules but shows SHG. The measurement requires a good optical quality single crystal since defects and birefringence may cause distortions. Surface effects show up as a constant background. The observed SHG response at 1064 nm for R,S-N-acetyl valine was in the order of 0.003 to 0.02 x urea and quadratic in the fundamental intensity. A distinct comparison with the centrosymmetric materials hexamethylbenzene and 4-dichlorobenzene was made to negate the effects of surface induced SHG.[140] The amino acid, DL-alanine, has a crystal structure with no centre of inversion and therefore has a SHG efficiency of 0.14 x urea, comparable to that of the individual isomers.[171]

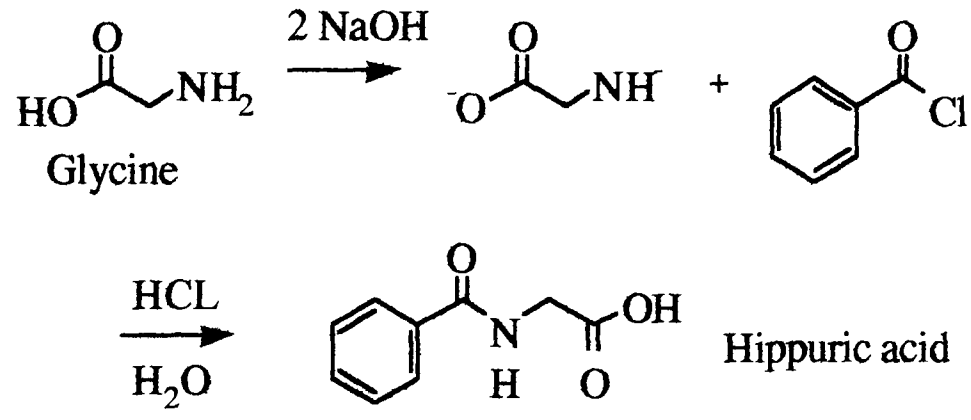
The quadratic response due to the magnetic transition dipole moment is small and gives rise to SHG signals of the same order as those arising from stress defects and surface effects. The detection of the optical activity in $\chi^{(2)}$ could be used as an analytical tool in cases where crystals of optical quality can be grown. However, this technique would not be suitable for general scanning of compounds which are racemic mixtures of chiral compounds, such as the tris(pentane-2,4-dionato)- complexes already discussed in Chapter 3.

6.2 Synthesis of N-Bonded Amino Acid Compounds - The Strategy

The formation of the peptide bond is fundamental in living systems and provides a useful tagging reaction between chiral amino acids and a ligand with a large hyperpolarizability constant, β.

The synthesis of hippuric acid (benzoyl glycine, benzoyl aminoacetic acid, (VI.10))

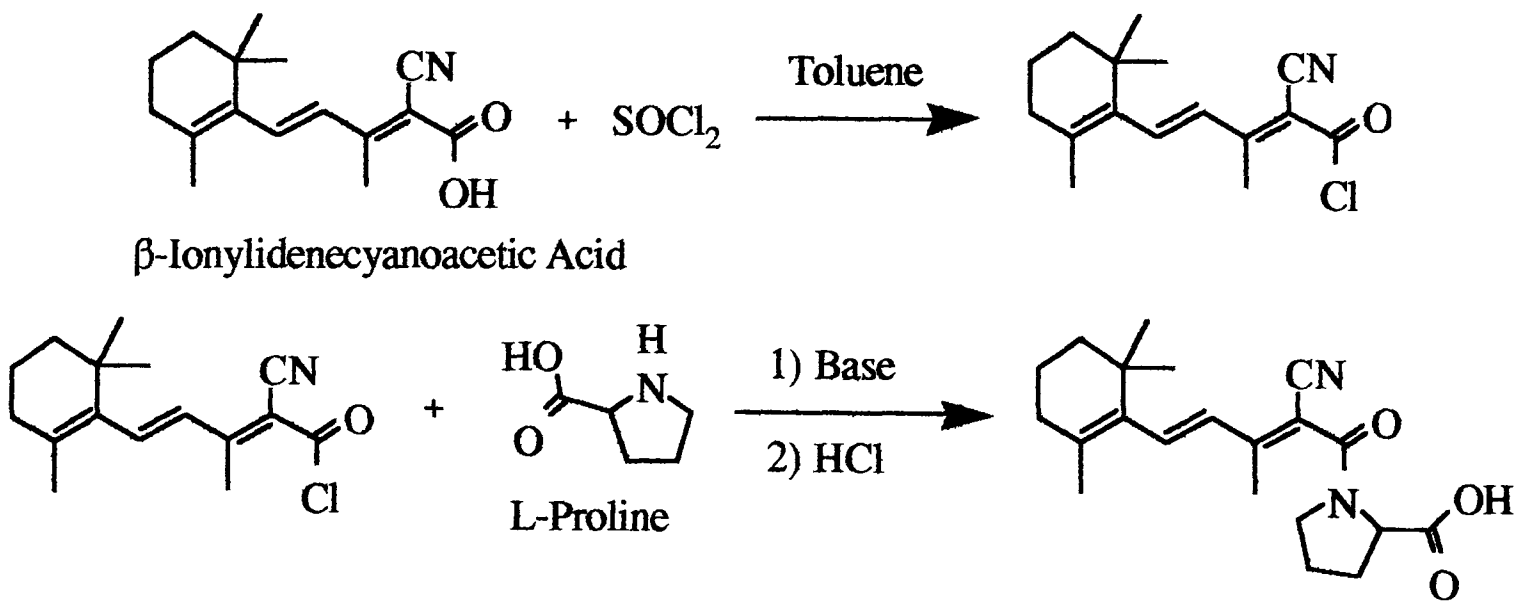
is a simple example of a reaction in which a peptide bond is formed. Hippuric acid (VI.10) can be synthesized by the reaction of the deprotonated salt of glycine (aminoacetic acid), and benzoyl chloride.[206]



(VI.10)

The acyl chloride of β-ionylidenecyanoacetic acid may be formed *in situ* by adding a slight excess of thionyl chloride to a warm toluene solution of β-ionylidenecyanoacetic acid. The toluene/β-ionylidenecyanoacetyl chloride solution can then be reacted with the desired amino acid salt which, after acidification (dil. HCl), and purification, yields N-[2-cyano-3-methyl-5-(2,6,6-trimethyl-1-cyclohexene-1-yl)-2,4-pentadiene-1-one]-L-proline (VI.11) (see Scheme 6.1).

Scheme 6.1 The reaction of β-ionylidenecyanoacetic acid with L-proline.



(VI.11)

N-[2-Cyano-3-methyl-5-(2,6,6-trimethyl-1-cyclohexene-1-yl)-2,4-pentadiene-1-

one]-L-proline (VI.11) retains the carboxylic acid "handle" which can be reacted with metals. Thus the centrosymmetric carboxylic acid, β-ionylidenecyanoacetic acid, has been tagged onto a chiral amino acid, forming a chiral N-bonded compound which should have a non-centrosymmetric crystal structure.

6.3 The Synthesis and Characterization of N-[2-Cyano-3-methyl-5-(2,6,6-trimethyl-1-cyclohexene-1-yl)-2,4-pentadiene-1-one]-L-proline (VI.11)

The acyl chloride derivative of β-ionylidenecyanoacetic acid was reacted with the sodium salt of L-proline in a bi-phase toluene/water system as shown in Scheme 6.1. After extraction and purification N-[2-cyano-3-methyl-5-(2,6,6-trimethyl-1-cyclohexene-1-yl)-2,4-pentadiene-1-one]-L-proline (VI.11), was obtained as a white crystalline solid in 13% yield. The yields were extremely variable and dependent on the time the sodium L-prolinate reacted with the acyl chloride. Optimum results were achieved when the reaction time was 30 minutes.

The infrared spectrum of (VI.11) showed the characteristic nitrile stretching mode at 2208 cm^{-1}. The ν(COO) stretch in L-proline was a broad band at 1620 cm^{-1}, in (VI.11) two strong ν(CO) bands were observed. The band at 1722 cm^{-1} in (VI.11) was at a higher frequency than expected for αβ-unsaturated CO bands, and was allocated to the ν(C=C-CO-N) stretch. Compounds with the C=C-CO-N group show the ν(C=O) stretch shifted to 1745 cm^{-1}.[216] The ν(COOH) vibration in L-proline is at 1620 cm^{-1} and is unchanged in compound (VI.11). The ν(C=C) vibration is seen as a strong absorption at 1602 cm^{-1}. Other sharp bands due to the H-C=C-H group were seen at 967 (def.) and 762 (olefinic C-H) cm^{-1}.

The elemental analyses were consistent with the proposed formula, slight deviations outside the acceptable limits of error were found to be due to traces of β-ionylidenecyanoacetic acid. The residual β-ionylidenecyanoacetic acid resulted from the purification of (VI.11) by crystallization from tetrachloromethane in which β-

ionylidenecyanoacetic acid crystallized out of solution first, and (VI.11) was obtained from the mother liquor which, therefore, contained traces of β-ionylidenecyanoacetic acid.

The ^{1}H n.m.r. spectral data of compound (VI.11) are summarized in Table 6.1 (see Fig. 6.1). The olefinic proton H5' gave a typically broad signal at δ 6.85 p.p.m. and was coupled to H4' at 6.76 p.p.m. ($^{3}J_{H,H'}$ = 16Hz). The coupling constant between H5' and H4' was typical of *trans*- H-C=C-H geometry. The methyl and aliphatic resonances were similar to those of the parent acid. The unique L-proline resonances of the "chiral" proton, H2", was a quartet at 4.60 p.p.m. The $^{3}J_{H,H'}$ coupling of protons attached to carbons making up the proline ring were observed to be inequivalent because of the rigidity of the ring, and are tabulated in Table 6.1.

Fig. 6.1 The ^{1}H n.m.r. spectrum of N-[2-cyano-3-methyl-5-(2,6,6-trimethyl-1-cyclohexene-1-yl)-2,4-pentadiene-1-one]-L-proline (VI.11).

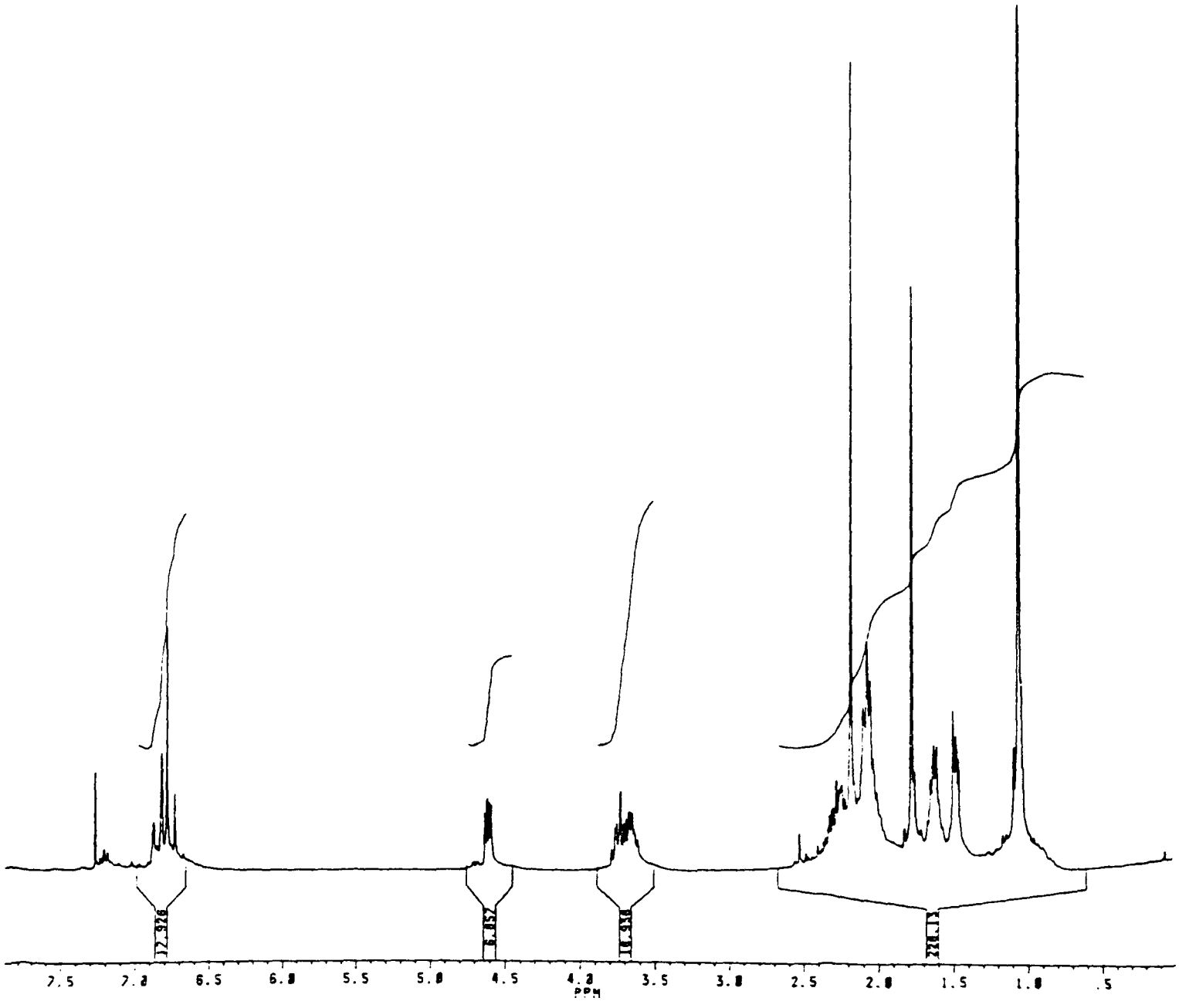
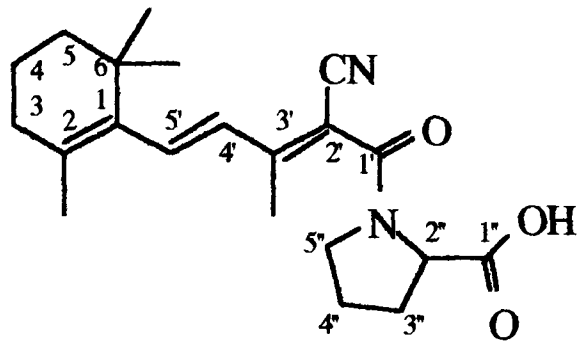


Table 6.1 ^{1}H n.m.r. spectral data for N-[2-cyano-3-methyl-5-(2,6,6-trimethyl-1-cyclohexene-1-yl)-2,4-pentadiene-1-one]-L-proline (VI.11), in $CDCl_3$.



Proton	δ in p.p.m.	Form s/d/t/q/m	Coupled To	Coupling Constant/ Hz
H5'	6.845	d	H4'	16
H4'	6.756	d	H5'	16
Me3'	2.18	s		
H2"	4.60	q	H1" + H3"	4.2 + 8.3
H5"	3.7	m	H4"	
H4"	2.0-	m	H3" + H5"	
H3"	2.2	m	H2" + H4"	
H3	2.05	m	H2 + H4	
H4	1.65	m	H3 + H5	
H5	1.45	m	H4	
Me2	1.78	s		
2xMe6	1.06	s		

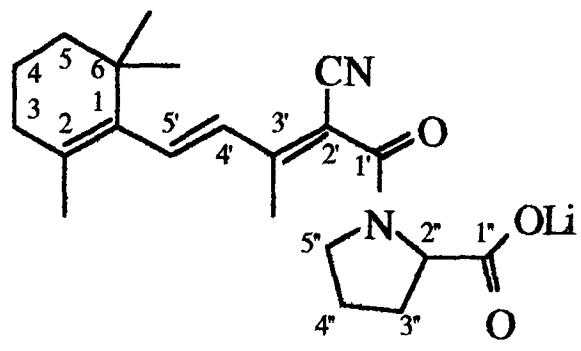
The electron impact mass spectrum of (VI.11) showed only decomposition products.

The analytical data summarized above is consistent with N-[2-cyano-3-methyl-5-(2,6,6-trimethyl-1-cyclohexene-1-yl)-2,4-pentadiene-1-one]-L-proline (VI.11). There was no evidence of bonding in (VI.11) via the oxygen rather than the nitrogen of the L-proline group. The shifted ν(C=O) absorption band of the C=C-CO-N-R group seen in the infrared spectrum, confirms that bonding is via the L-proline nitrogen.

6.4 The Synthesis and Characterization of Metal Salts of N-[2-Cyano-3-methyl-5-(2,6,6-trimethyl-1-cyclohexene-1-yl)-2,4-pentadiene-1-one]-L-proline

6.4.1 The Synthesis and Characterization of [N-{2-Cyano-3-methyl-5-(2,6,6-trimethyl-1-cyclohexene-1-yl)-2,4-pentadiene-1-one}-L-prolinato]lithium (VI.12)

A solution of N-[2-cyano-3-methyl-5-(2,6,6-trimethyl-1-cyclohexene-1-yl)-2,4-pentadiene-1-one]-L-proline (VI.11) in methanol was reacted with a solution of lithium hydroxide in methanol. The methanolic solution of (VI.12) was evaporated to dryness to drive off some of the water. The residue was extracted with diethyl ether in which (VI.12) was soluble. The ether was removed to deposit [N-{2-cyano-3-methyl-5-(2,6,6-trimethyl-1-cyclohexene-1-yl)-2,4-pentadiene-1-one}-L-prolinato]lithium (VI.12) as a deliquescent white solid. [N-{2-Cyano-3-methyl-5-(2,6,6-trimethyl-1-cyclohexene-1-yl)-2,4-pentadiene-1-one}-L-prolinato]lithium (VI.12) was soluble in diethyl ether, tetrachloromethane and benzene. A crude solid could be prepared by precipitation from a benzene solution of (VI.12) using hexane as co-solvent, in which (VI.12) was insoluble. The elemental analyses were satisfactory for the proposed molecular formula of (VI.12) and also showed that some solvent was retained, which could not be removed by vacuum drying for 24 hours at 50°C.



(VI.12)

The vibrational spectrum of (VI.12) had a clear ν(CN) band at 2203 cm^{-1}. The conjugated ν(C=C-CO-N-R) seen in (VI.11) at 1722 cm^{-1} had moved to 1641 cm^{-1}, while the ν(COOH) absorption originally at 1620 cm^{-1} was now completely masked by the ν(C=C-CO-N-R) band. The symmetrical ν(COO) stretch was seen at 1420 cm^{-1},

shifted to a higher frequency than the $\nu(COO)_{sym}$ stretches typical of β-ionylidenecyanoacetic acid (see Table 4.6) which suggested that this ν(COO) stretch is more typical of a non-conjugated COO^- group. The bands due to the H-C=C-H group were similar to those seen in (VI.11). The ν(H-C=C-H) deformation was at 968 cm^{-1} while there were two possible weak olefinic ν(C-H) vibrations at 763 and 788 cm^{-1}. Although the data discussed here is correct for [N-{2-cyano-3-methyl-5-(2,6,6-trimethyl-1-cyclohexene-1-yl)-2,4-pentadiene-1-one}-L-prolinato]lithium exact characterisational data was not obtained from ^1H n.m.r. spectral studies.

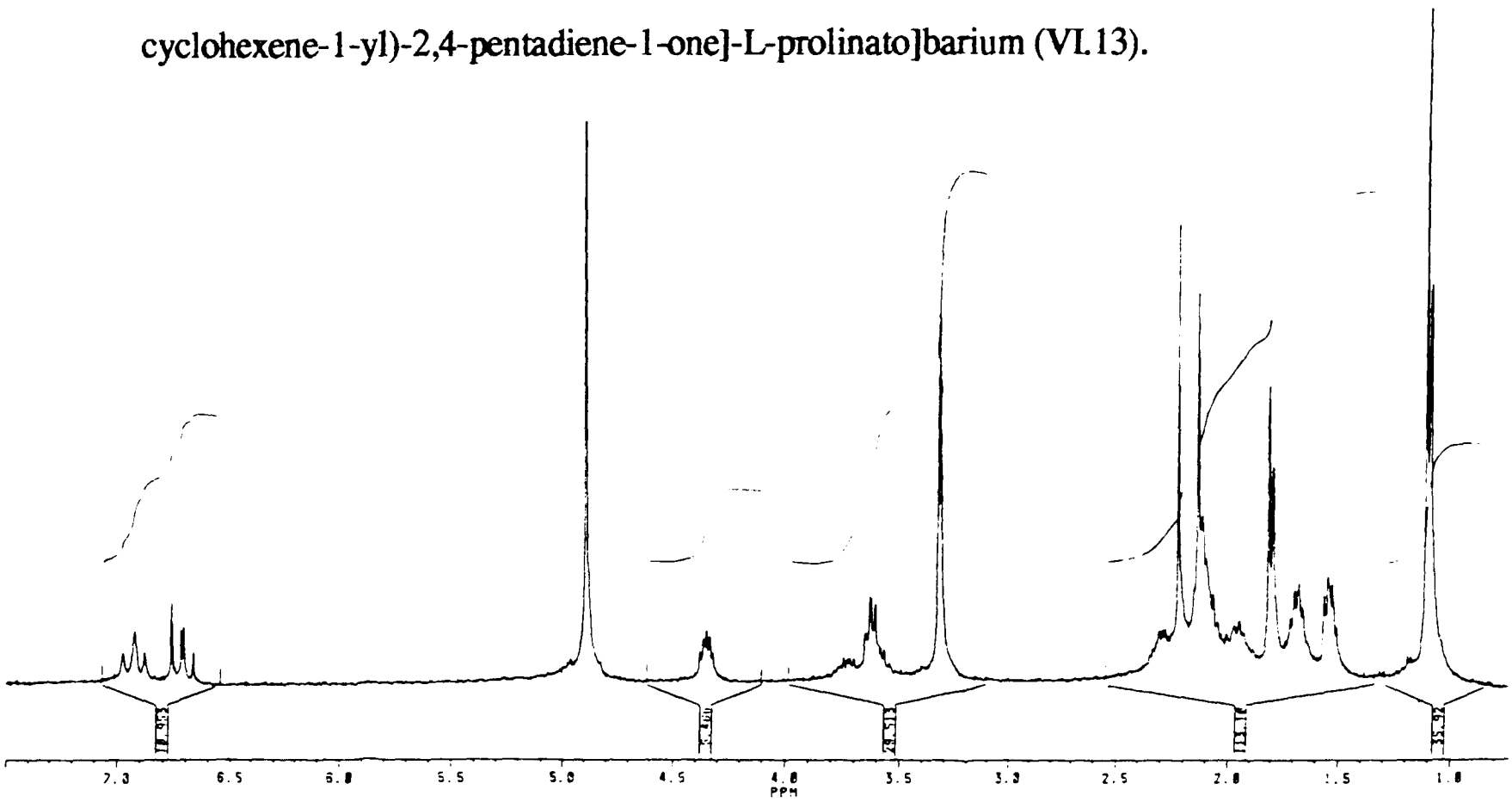
6.4.2 The Synthesis and Characterization of [N-{2-Cyano-3-methyl-5-(2,6,6-trimethyl-1-cyclohexene-1-yl)-2,4-pentadiene-1-one}-L-prolinato]barium (VI.13)

Barium hydroxide was reacted in boiling aqueous solution with (VI.11) to form a thick pasty mass of crude [N-{2-cyano-3-methyl-5-(2,6,6-trimethyl-1-cyclohexene-1-yl)-2,4-pentadiene-1-one}-L-prolinato]barium (VI.13). Compound (VI.13) was purified by recrystallization from hot boiling water, and the first crop was isolated as long white needles in 28 % yield. The white needles analyzed correctly for [N-{2-Cyano-3-methyl-5-(2,6,6-trimethyl-1-cyclohexene-1-yl)-2,4-pentadiene-1-one}-L-prolinato]barium dihydrate (VI.13).

The solution ^1H n.m.r. spectrum (in CD_3OD) shows that the ligands on (VI.13) are in two slightly different environments (see Fig. 6.2). The largest differences can be seen in the olefinic resonances around δ 6.25 p.p.m. and the neighbouring Me3' protons. Tables 6.2A and B present the n.m.r. spectral data for (VI.13).

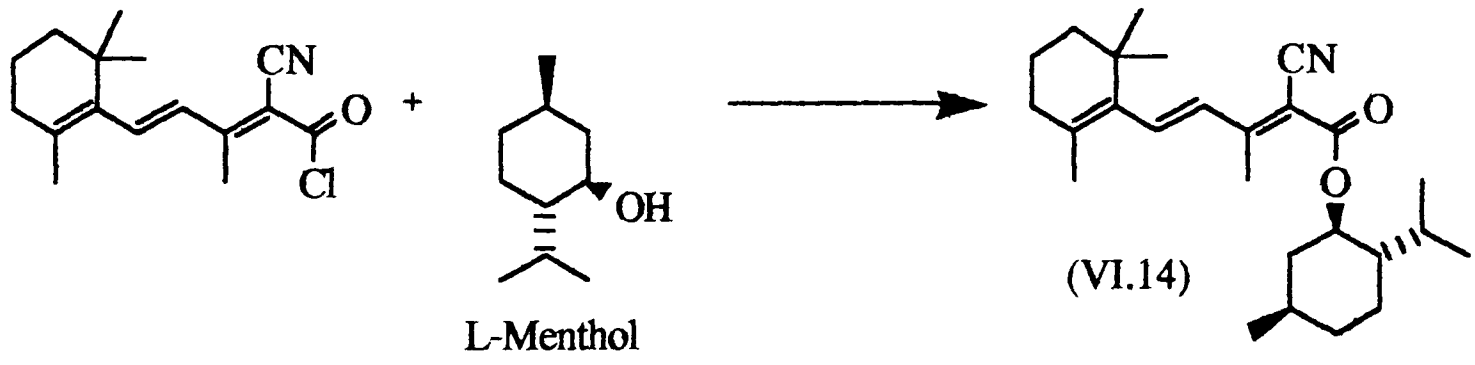
The vibrational spectrum of (VI.13) was similar to that of (VI.12). The main difference was the appearance of a weak band at 1733 cm^{-1} possible due to the secondary amide group. A broad absorption due to water of crystallization was seen at 3400 cm^{-1}.

Fig. 6.2 The ^{1}H n.m.r. spectrum of N-[2-cyano-3-methyl-5-(2,6,6-trimethyl-1-cyclohexene-1-yl)-2,4-pentadiene-1-one]-L-prolinato]barium (VI.13).



6.4.3 The Attempted Syntheses of Other [N-(2-Cyano-3-methyl-5-(2,6,6-trimethyl-1-cyclohexene-1-yl)-2,4-pentadiene-1-one)-amino Acids and Related Compounds

The reaction between the acyl chloride of β-ionylidenecyanoacetic acid and the chiral alcohol L-menthol to form the ester was attempted (VI.14):



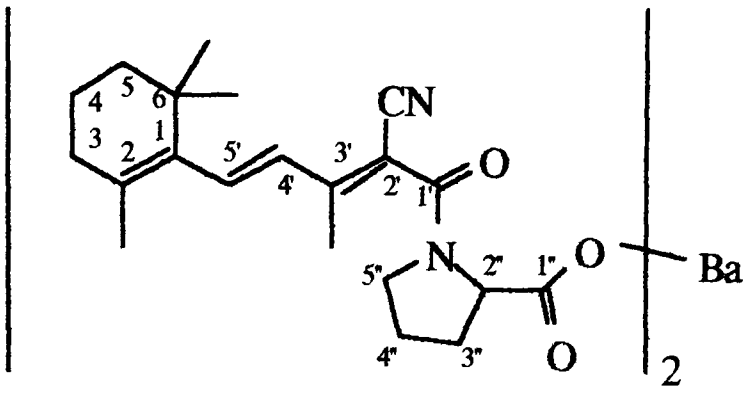
L-Menthol

(VI.14)

The reaction product was a yellow oil smelling strongly of burnt rubber. The product was not analyzed.

An attempt was made to synthesize the N-bonded compounds similar to that formed between β-ionylidenecyanoacetic acid and L-proline using L-phenylalanine and L-aspartic acid. In both cases the amino acids did not react with β-ionylidenecyanoacetyl chloride.

Table 6.2A ^{1}H n.m.r. spectral data for the two series of ligand signals of (VI.13), in CD_3OD. Ligand one, lowest field.



Proton	δ in p.p.m.	Form s/d/t/q/m	Coupled To	Coupling Constant/ Hz
H5'	6.940	d	H4'	12 - broad
H4'	6.733	d	H5'	12.65
Me3'	2.22	s		-
H2"	4.3	q	H1" + H3"	overlapping
H5"	3.6	m	H4"	-
H4"	2.0-	m	H3" + H5"	-
H3"	2.2	m	H2" + H4"	-
H3	2.1	m	H2 + H4	overlapped
H4	1.65	m	H3 + H5	-
H5	1.55	m	H4	-
Me2	1.80	s		-
2xMe6	1.10	s		-

6.5 Summary

The attachment of the chiral amino acid L-proline to β-ionylidenecyanoacetic acid was successful. The product N-[2-cyano-3-methyl-5-(2,6,6-trimethyl-1-cyclohexene-1-yl)-2,4-pentadiene-1-one]-L-proline (VI.11) retained an accessible non-conjugated carboxylic acid group which could be reacted with metals to form salts. The N-(2-cyano-3-methyl-5-(2,6,6-trimethyl-1-cyclohexene-1-yl)-2,4-pentadiene-1-one)-L-prolinato salts of barium and lithium were synthesized and characterized by conventional spectroscopic means. Measurements were made on the second harmonic generation efficiency of these

compounds, and some starting materials and the data are discussed in the next section.

6.6 Second Harmonic Generation (SHG) Studies on N-[2-Cyano-3-methyl-5-(2,6,6-trimethyl-1-cyclohexene-1-yl)-2,4-pentadiene-1-one]-L-proline and its Metal Salts.

Powdered samples of N-[2-cyano-3-methyl-5-(2,6,6-trimethyl-1-cyclohexene-1-yl)-2,4-pentadiene-1-one]-L-proline (VI.11), and the corresponding lithium (VI.12) and barium (VI.13) salts were tested for second harmonic generation as well as the amino acids, L-proline and L-phenylalanine. The results are summarized in Table 6.3.

Table 6.2B ^{1}H n.m.r. spectral data for the two series of ligand signals of (VI.13), in CD_3OD. Ligand two, highest field.

Proton	δ in p.p.m.	Form s/d/t/q/m	Coupled To	Coupling Constant/ Hz
H5'	6.89	d	H4'	12.7 broad
H4'	6.679	d	H5'	12.6
Me3'	2.13	s		-
H2"	4.3	q	H1" + H3"	overlapping
H5"	3.6	m	H4"	-
H4"	2.0-	m	H3" + H5"	-
H3"	2.2	m	H2" + H4"	-
H3	2.1	m	H2 + H4	overlapped
H4	1.65	m	H3 + H5	-
H5	1.55	m	H4	-
Me2	1.79	s		-
2xMe6	1.09	s		-

Table 6.3 Second harmonic generation efficiencies for compounds (3.11) to (3.13) and related compounds, measured at 1064 nm incident laser wavelength, * from ref. 68.

Compound number	Efficiency x urea	Colour
(VI.11)	0.39-0.97	Colourless
(VI.12)	0 lu	White
(VI.13)	0 lu	White
L-Proline	0.5	White
L-Phenylalanine	0.15	White
L-Menthol	0.28	Colourless
Hippuric Acid	1.5*	White

N-[2-Cyano-3-methyl-5-(2,6,6-trimethyl-1-cyclohexene-1-yl)-2,4-pentadiene-1-one]-L-proline (VI.11), which includes the conjugated triene system of β-ionylidene-cyanoacetic acid and a chiral L-proline "tag" showed an SHG efficiency of 0.39-0.97 x urea. L-proline itself gave an efficiency of 0.5 x urea, lower than that of (VI.11), which demonstrated that in (VI.11) a slight but significant contribution to the SHG from the conjugated triene group has been made. The contribution is greater than observed because the triene group also "dilutes" the SHG effect of the L-proline group.

The lithium compound, [N-{2-cyano-3-methyl-5-(2,6,6-trimethyl-1-cyclohexene-1-yl)-2,4-pentadiene-1-one}-L-prolinato]lithium (VI.12), showed no SHG. Compound (VI.12) was expected to show some SHG because the chirality of the L-proline group had been retained. It is possible that, as explained in Chapter One, hydrogen bonding effects are playing a major role in the alignment of molecules within these molecules. Compound (VI.11) can hydrogen bond between the adjacent -OH of the prolinato- groups. compound (VI.12) no-longer has the possibility of hydrogen bonding via this group (now -OLi) and dipole-dipole interactions take over as the major influence on the crystal packing of the molecules. If the dipoles in (VI.12) align themselves anti-parallel, then it is possible that

the electronic changes induced by an applied field (the laser) may be equal and opposite, and therefore cancel each other out. This effect would be equivalent to having a centre of symmetry, and no SHG would be observed.

The barium compound, [N-{2-cyano-3-methyl-5-(2,6,6-trimethyl-1-cyclohexene-1-yl)-2,4-pentadiene-1-one}-L-prolinato]barium (VI.13), showed no SHG. This observation indicates that the responses to the incident laser field of the two "L-prolinato tags" within the ligands which are attached to the same barium atom, cancel each other out.

6.7 Conclusions

This Chapter has described one method by which non-centrosymmetry can be introduced into centrosymmetric compounds. The NLO inactive compound, β-ionylidenecyanoacetic acid has been successfully modified by attaching the chiral amino-acid L-proline onto the molecule to form the N-bonded derivative, N-[2-Cyano-3-methyl-5-(2,6,6-trimethyl-1-cyclohexene-1-yl)-2,4-pentadiene-1-one]-L-proline

(VI.11). Compound (VI.11) showed a SHG efficiency of 0.39 - 0.97 times urea which was greater than that of pure L-proline. NLO active compounds which have a SHG response in the order of urea tend to be coloured (urea, an exception, is colourless). Compounds which are colourless and have an SHG efficiency exceeding that of urea, have a greater usefulness in the laser diode commercial market, and (VI.12) meets both requirements.

The lithium and barium derivatives of (VI.11) both show zero SHG efficiencies indicating that:

1/ Hydrogen bonding has a significant effect on compounds that show SHG.

2/ Unidentate salts of chiral molecules do not always show SHG, possibly because dipole-dipole interactions take over as the predominant factor in the influence of crystal packing. This leads to an electric dipolar response with a centre of inversion, and therefore vanishing second order susceptibility, and zero SHG.

3/ Bidentate salts of chiral molecules may also show zero SHG because of the equal, but opposing responses of the two chiral ligands present within the molecule.

Chapter Six has demonstrated that chiral amino-acids are an effective method of introducing the non-centrosymmetric requirement for SHG into a molecule.

CHAPTER SEVEN

Experimental

7.1 General Details

The reactions were routinely carried out using Schlenk line techniques under pure, dry nitrogen, with dry, oxygen-free solvents. Microanalyses (C, H, N and metals) were carried out by Mr. M. Gascoyne and his staff of this laboratory. Infrared spectra were recorded on a Perkin Elmer FT1710 spectrometer, as either Nujol or hexachlorobutadiene mulls between KBr or CsI disks. ^{1}H and $^{31}P-\{^{1}H\}$ n.m.r. spectra were recorded using a deuterium locked Bruker A.M. 300 spectrometer. Electronic spectra were obtained using a Perkin-Elmer 552 UV-VIS spectrophotometer with 10mm silica cells in solvents which are transparent at the frequencies used. FAB mass spectra were obtained using the SERC mass spectrometry service, Swansea, and low resolution electron impact mass spectra were run by myself.

Starting Materials:

Tetrakis(triphenylphosphine)platinum was synthesized according to the procedure given in ref. 105b.

Cis-[bis(triphenylphosphine)]carbonatoplatinum(II) was synthesized from tetrakis-(triphenylphosphine)platinum, dioxygen and carbon dioxide.[157]

Dichloro(1,5-cyclooctadiene)platinum(II) was synthesized according to the procedure given in ref. 105c.

Dichloro-(diphenyphosphinoethane)platinum(II), and other platinum(II) halide complexes were synthesized from dichloro(1,5-cyclooctadiene)platinum(II) and the relevant phosphine.[105d]

Dichlorobis(triphenylphosphine)palladium(II) was synthesized according to the procedure given in ref. 156e.

7.2 Experimental Details Relevant to Chapter Three

(III.1) *Synthesis of benzoylacetone.*

As described in reference 133, obtained in 30% yield. I.r.: ν(C=O), 1693(s), 1602(s) cm^{-1}. ^1H n.m.r. data: ($CDCl_3$ solution) ketone; δ 2.21 (s, Me); 6.19 (s, 2H); enol; 2.61 (s, Me); 4.11 (s, 1H); either form 7.46 (d, phenyl protons, 8Hz); 7.52 (d, phenyl protons, 8Hz); 7.87 p.p.m. (m, phenyl protons). M/z (electron impact) $M^+ = 162$, fragments; -Me m/z = 147, -phenyl m/z = 105, -COPh m/z = 85, Ph m/z = 77.

(III.2) *Synthesis of 4-nitrobenzoylacetone.*

A mixture of 4-nitroacetophenone (1.65g, 0.01mol), acetic anhydride (2.04g, 0.02mol) and toluenesulphonic acid monohydrate (0.076g, 0.4mmol) was stirred for thirty minutes. Boron trifluoride etherate (2.11cm^3, 2.44g, 0.172mol) was added slowly to the mixture which evolved heat and the solution became amber. The reaction mixture was stirred for a further 16-20 hours at room temperature. The reaction mixture was then quenched with aqueous sodium acetate (5.52 g, 0.04mol, in 10cm^3 of water).

The reaction vessel was fitted with a reflux condenser and the reaction mixture was refluxed for three hours. The solution was cooled, and extracted with three aliquots of 30-60°C petroleum ether and diethyl ether (10cm^3 each). The combined extracts were washed with 5% sodium hydrogencarbonate solution, and finally with water.

The combined organic extracts were then dried over anhydrous sodium sulphate, which left a clear yellow solution. The dried diethyl ether solution was reduced in volume, and yellow crystals formed, crude yield of 4-nitrobenzoylacetone, (III.2), 0.64g (29%). The crude product was purified by sublimation or by conversion into its water soluble sodium salt, and final re-acidification followed by re-crystallization from hot hexane. A sublimed sample gave the following analyses (Found: C, 57.9; H, 4.2; N, 7.1; $C_{10}H_9NO_4$ requires C, 58.0; H, 4.4; N, 6.7%). I.r. : ν(C=O), 1694(w); ν(NO_2)

1519(s), 1346(s) cm^{-1}. N.m.r. data: ^1H ($CDCl_3$ solution) δ 15.92 (s, 1H, remaining enol proton); 8.17 [d of d , 4H, Ph, $^3J(H, H')$ 7.18, $^3J(H, H')$ 8.21 Hz]; 6.25 (s, 1H, enolized proton); 2.28 p.p.m. (s, 3H, CH_3). Electronic spectrum (ethanol solution): λ_{max} 320 (Log ε 4.11), 250(4.02), 201(3.94); (n-hexane solution): 310(4.16), 242(4.11), 197nm (3.82). M/z = 207 ±1 m.u.

(III.7) ***Synthesis of difluoro[4-methoxybenzoylacetonato]boron.***

4-Methoxyacetophenone (1.5g, 0.01mol), was added to dried, fused and degassed 4-toluenesulphonic acid (0.20g), under nitrogen. The mixture became reddish-amber, and was dissolved in acetic anhydride (50cm^3, dried and degassed) when cool. The solution was re-heated to help dissolution, and cooled to room temperature. Boron trifluoride etherate (2.2cm^3) was added slowly, and the reaction mixture was stirred for two days during which the solution became black, with a white suspension. The mixture was then quenched with both a sodium acetate solution (5g in 10 cm^3 water) and a copper acetate solution (2g in the minimum amount of water), a green precipitate was formed, which was filtered off, washed with water, and the residue redissolved in 1:1:1 mixture of petroleum ether (80-100°C), acetone and trichloromethane. The dark solution was dried over sodium sulphate, reduced in volume, and crystallized three times from the above solvent mixture. Dark green crystals of difluoro[4-methoxybenzoylacetonato)boron, (III.7), formed, yield 0.53g (22%) (Found: C, 55.8; H, 4.7; Na, less than 0.1; Cl, 0.4; Cu, 0.1%; $C_{11}H_{11}BF_3O_3$, requires C, 55.05; H, 4.62% the compound also gives a positive flame test for copper - indicating BF_2 - the exception). I.r. : ν(CO) 1606(m), 1567(s), 1511(s), ν(BF) 1267(s), 1190(s), 1130(s), 1092(s) cm^{-1}. N.m.r. data: ^1H ($CDCl_3$ solution), δ 8.06 [d, 2H, Ph, $^3J(H, H')$ 8.45Hz]; 7.00 [d of d, 2H, Ph, $^3J(H, H')$ 9.63, $^4J(H, H')$ 2.00 Hz]; 6.48 (s, 1H, C-H enol proton); 3.93 (s, 3H, OMe); 2.38 p.p.m. (s, 3H, CH_3). Electronic spectrum (ethanol solution): λ_{max} 349(Log ε 4.23), 275(3.36), 239(3.67), 204(3.64); (CH_2Cl_2 solution): 349, 280, and 242nm .

(III.10) ***Synthesis of 3-(2,4-dinitrophenyl)pentane-2,4-dione.***

Freshly prepared sodium acetoacetonate (0.67g, 5.49mmol) was dissolved at room temperature in dry, degassed acetone ($50cm^3$). 2,4-Dinitrophenyl fluorobenzene (1.00g, $0.67cm^3$, 5.37mmol) was added to the acetone solution, and the mixture refluxed for five hours. On adding the fluorobenzene, the solution went violet, but quickly turned brown. At the end of the reflux, the reaction mixture was diluted with dichloromethane ($50cm^3$), filtered, and the filtrate was reduced to dryness, forming an amber resin. This was extracted with warm 1M sodium hydroxide solution ($10cm^3$), and the extract filtered carefully. The red filtrate was then neutralized with 1M hydrochloric acid, and at the end point a cream solid separated out. The solid was filtered off, washed well with water, then cold ethanol, and the crude 3-(2,4-dinitrophenyl)pentane-2,4-dione, (III.10), was dissolved in trichloromethane, dried over anhydrous sodium sulphate, filtered, reduced to dryness, and recrystallized from ethanol forming very pale yellow crystals, yield 0.69g (47%) (Found: C, 49.3; H, 3.8; N, 10.4; $C_{11}H_{10}N_2O_6$ requires C, 49.6; H, 3.8; N, 10.5%). I.r. : ν(CO) 1614(s) , 1712(s) ; ν(NO_2) 1536(vs), 1348(vs) cm^{-1}. N.m.r. data: ^1H ($CDCl_3$ solution) δ 16.61 (s, 1H, enolized proton); 8.81 [d, 1H, Ph, ^4J(H, H') 2.4Hz]; 8.52 [d of d, 1H, Ph, ^3J(H, H') 7.89, ^4J(H, H') 2.35Hz]; 7.64 [d, 1H, Ph, ^3J(H, H') 8.52Hz]; 1.87p.p.m. (s, 6H, 2Me). Electronic spectrum (ethanol solution): λ_{max} 270 (Log ε 4.09), 235(4.07), 203(4.06); (CH_2Cl_2 solution): 268(4.15), 230(4.10) nm.

(III.13) ***Synthesis of [bis(triphenylphosphine)(4-nitrobenzoylacetonato)-]palladium(II) tetrafluoroborate.***

Cis-$Pd(PPh_3)Cl_2$ (0.24g, 0.342mmol), $AgBF_4$ (0.1316g, 0.676mmol), and 4-nitrobenzoylacetone (0.070g, 0.338mmol), were mixed dry under nitrogen, and CH_2Cl_2 ($10cm^3$) was added to initiate the reaction. The reaction mixture was stirred overnight at room temperature, and formed a heavy white solid (AgCl), suspended in a clear yellow solution. The mixture was filtered, and the residue was washed with CH_2Cl_2, and the

filtrate and washings were combined, reduced to dryness, to leave a spongey yellow solid. The solid was extracted with hot hexane, and diethyl ether, to remove un-reacted starting materials and the residue was dissolved in tetrahydrofuran, filtered, and the yellow solution layered with diethyl ether. After twelve hours, yellow-green crystals had been deposited, these were isolated, and recrystallized from dichloromethane solution, by slow diffusion of a 1:1 mixture of tetrahydrofuran and diethyl ether into the dichloromethane layer. Yellow crystals of [bis(triphenylphosphine)(4-nitrobenzoylacetonato)]palladium(II) tetrafluoroborate formed, (III.13), yield 47% (Found: C, 60.2; H, 4.2; N, 1.6; Pd, 11.1. $C_{46}H_{38}BF_4NO_4P_2Pd$, requires C, 59.8; H, 4.2; N, 1.5; Pd, 11.5%). I.r.: $\nu(NO_2)$, 1560(s) and 1520(s) cm^{-1}. N.m.r. data: ^1H (CD_2Cl_2 solution): δ 7.89 [d, 2H, ^3J(H, H') 9.1Hz]; 7.4(m, 30H, Ph); 6.97 [d, 2H, Ph, ^3J(H, H') 9.08Hz]; 6.18 (s, 1H, enol proton); 1.70p.p.m. (s, 3H, CH_3). Electronic spectrum (CH_2Cl_2 solution): λ_{max} 238, 260, 290 and 350; (acetone solution): 324 and 350nm (extinction coefficients not accurate for these solvents).

(III.14) ***Synthesis of [bis(triphenylphosphine)(3-{2,4-dinitrophenyl}-pentane-2,4-dionato)]palladium(II) tetrafluoroborate.***

$AgBF_4$ (0.3583g, 1.84mmol), *cis*-$Pd(PPh_3)Cl_2$ (0.649g, 0.925mmol) and 3-(2,4-dinitrophenyl)pentane-2,4-dione (0.229g, 0.863mmol) were mixed dry, under nitrogen. Dry, degassed CH_2Cl_2 ($10cm^3$) was added, forming an amber-yellow solution with the silver tetrafluoroborate in suspension. The mixture was stirred at room temperature, and darkened quickly. After twelve hours, a heavy grey precipitate had formed (AgCl), with an amber supernatant liquid. The mixture was filtered, and the residue washed with CH_2Cl_2, the filtrate and washings were combined, reduced to dryness at 50°C, forming a sponge-like yellow solid. This yellow solid was carefully broken up, extracted with hexane and diethyl ether to remove excess starting materials, and the residue was then dissolved in tetrahydrofuran, and layered with diethyl ether. Yellow-orange crystals of bis[(triphenylphosphine)(3-{2,4-dinitrophenyl}pentane-2,4-dionato)]palladium(II) tetrafluoroborate formed, (III.14), yield 0.59g (65%) (Found:

C, 57.4; H, 4.1; N, 2.8; Pd, 10.7; $C_{47}H_{39}BF_4N_2O_6P_2Pd$ requires C, 57.4; H, 4.0; N, 2.9; Pd, 10.8%). I.r. : $\nu(NO_2)$, 1558(s), 1540(s) cm^{-1}. N.m.r. data: $^1H(CD_2Cl_2$ solution): δ 8.62 [d, 1H, Ar, ^4J(H, H') 2.04Hz]; 8.54 [d of d, 1H, Ar, ^3J(H, H') 8.548, ^4J(H, H') 2.04Hz]; 8.13 [d, 1H, Ar, ^3J(H, H') 8.47 Hz]; 7.4 (m, 30H, Ph); 1.19 p.p.m. (s, 6H, 2Me). Electronic spectrum (acetone): λ_{max} 325; (dichloromethane): 255, 235nm.

(III.15) ***Synthesis of [di(carbonyl)(3-(2,4-dinitrophenyl)pentane-2,4-dionato)]rhodium(I).***

$RhCl_3.3H_2O$ (0.2g, 0.76 mmol) was dissolved in degassed dimethyl-formamide ($15cm^3$) to yield a deep red solution. Solid 3-(2,4-dinitrophenyl)-pentane-2,4-dione (0.2g, 0.76 mmol) was added, and the solution refluxed under N_2 for 45 minutes, during which time the solution acquired a slightly yellow tinge. The solution was allowed to cool to room temperature and water ($30cm^3$) was added which precipitated out a yellow solid which was filtered off and dried *in vacuo*. The yellow solid was extracted with benzene, to give a yellow solution, which, on removal of solvent, deposited a brown crystalline solid. Recrystallization from toluene yielded orange-brown crystals of [di(carbonyl)(3-(2,4-dinitrophenyl)pentane-2,4-dionato)]rhodium(I), (III.15). Yield 0.15g (25%) (Found:C, 36.0;H, 2.4;N, 6.4; Rh, 21.1. $C_{13}H_9N_2O_8Rh_1$ requires C, 36.5; H, 2.6; N, 6.6; Rh, 24.2 %). I.r. : ν (CO), 2080(s), 2006(s); $\nu(NO_2)$, 1580(m), 1538(m); ν(Ph), 1580, 1523 cm^{-1}. N.m.r. data: ^1H (CD_2Cl_2 solution), δ 8.73 [d, 1H, ^4J (H, H') 2.1Hz], 8.477 [d of d, 1H, ^3J (H, H') 85.5 , ^4J (H, H') 2.4Hz], 7.60 [d, 1H ^3J (H, H') 85.5 Hz], 1.81p.p.m. (s, 6H, $2CH_3$). Electronic spectra (Ethanol solution): λ_{max} 257, 212; (CH_2Cl_2 solution): 321, 258nm.

(III.16) ***Synthesis of [di(carbonyl)(4-(4-methoxyphenyl)butane-2,4-dionato)]rhodium(I).***

The method is identical to that of the synthesis of (III.15). $RhCl_3.3H_2O$ (0.1g, 3.8mmole), was reacted with difluoro[4-methoxyphenyl-benzoylacetonato]boron (0.1g,

0.42mmol), and the extracted product was re-crystallized from hexane and then CH_2Cl_2, gave [di(carbonyl)(4-(4-methoxyphenyl)butane-2,4-dionato)]rhodium(I), (III.16), as an orange crystalline powder, yield 0.083g (62%) (Found: C, 44.1; H, 3.3. $C_{11}H_{11}O_5Rh_1$ requires C, 44.6; H, 3.1%). I.r. : ν(CO), 2080, 2067, 2010; ν(C=C), 1614, 1584, 1533, 1503; ν(C-O-C), 1171 and 1108cm^{-1}. N.m.r. data: ^1H (CD_2Cl_2 solution), δ 7.86 [d, 2H, Ph, ^3J(H, H') 8.85Hz]; 6.92 [d, 2H, Ph, ^3J(H, H') 8.55Hz]; 6.26 (s, 1H, enol proton); 3.84 (s, 3H, OCH_3); 2.18 p.p.m. (s, 3H, CH_3). Electronic spectra (CH_2Cl_2 solution): λ_{max} 226; (hexane solution): 206nm.

(III.17) ***Attempted Synthesis of [di(carbonyl)(4-(4-nitrophenyl)butane-2,4-dionato)]rhodium(I).***

As for (III.16).

(III.18) ***Synthesis of [di(carbonyl)bis(triphenylphosphine)]rhodium(I).***

From reference 205.

(III.19) ***Synthesis of [di(carbonyl)(pentane-2,4-dionato)]rhodium(I).***

From reference 26.

(III.20) ***Synthesis of [di(carbonyl)(pentane-2,4-dionato)]iridium(I).***

From reference 27.

(III.21) ***Synthesis of tris[benzoylacetonato]cobalt(III).***

The synthesis of tris[benzoylacetonato]cobalt(III) was a modification of the method for the synthesis of tris[pentane-2,4-dionato]cobalt(III).[37] Cobalt(II) carbonate (as $CoCO_3.xCo(OH)_2.yH_2O$, 0.5 g) was suspended in benzene (20 cm^3) and benzoylacetone (0.31 g) was added to the suspension. The reaction mixture was refluxed for 30 minutes. Hydrogen peroxide (16 cm^3 of 10% aqueous solution) was added to the refluxing suspension, and carbon dioxide was evolved. The reaction mixture was cooled, and the

green benzene solution filtered off. The filtrate was first dried with anhydrous sodium sulphate and then evaporated to dryness under reduced pressure, and the residue extracted with dichloromethane. Tris(benzoylacetonato)cobalt(III) (III.21) was obtained as dark green crystals from the green dichloromethane extract, by slow addition of diethyl ether, in 21% yield. (Found : C, 66.1; H, 5.1; $C_{30}H_{27}O_6Co$ requires C, 66.4; H, 5.0%). Electronic spectra (benzene solution): λ_{max} 355, 275; (dichloromethane solution): 454, 270 nm.

(III.22) ***Synthesis of tris[4-(2,4-dinitrophenyl)butane-2,4-dionato]-cobalt(III).***

The synthesis of (III.22) was identical to that of (III.21). Cobalt(II) carbonate (0.25 g) was reacted with 3-(2,4-dinitrophenyl)pentane-2,4-dione (III.10) (0.15 g, 0.66 mmol) to gave tris[4-(2,4-dinitrophenyl)butane-2,4-dionato]cobalt(III), (III.22), as dark green crystals. Compound (III.22) was recrystallized from ethanol, yield 6%. (Found: C, 46.0; H, 3.1; N, 9.7; Co, 6.1. $C_{33}H_{27}N_6O_{18}Co_1$ requires C, 46.4; H, 3.1; N, 9.8; Co, 6.9%).

(III.23) ***Synthesis of tris[pentane-2,4-dionato]cobalt(III).***

Taken from reference 37. (III.23) is sometimes referred to as tris[2,4-pentanediono]cobalt(III).

(III.24) ***Synthesis of tris[pentane-3-chloro-2,4-dionato]cobalt(III).***

Taken from reference 56. Tris(pentane-2,4-dionato)cobalt(III) was synthesized in 23% yield, as a pale green solid. (Found: C, 38.8; H, 3.9. $C_{15}H_{18}O_6Cl_3Co_1$ requires C, 39.2; H, 3.9%). N.m.r. data: ^1H ($CDCl_3$ solution), δ 2.44 p.p.m. (s, 6Me).

(III.25) ***Synthesis of tris[3-nitro-pentane-2,4-dionato]cobalt(III).***

From reference 63. Tris[3-nitro-pentane-2,4-dionato]cobalt(III) was synthesized in 44% yield, as a dark green solid. (Found: C, 37.1; H, 3.7; N, 8.7. $C_{15}H_{18}N_3O_{12}Co_1$

requires C, 36.7; H, 3.7; N, 8.7 %.) I.r.: $\nu(NO_2)$, 1568(s), 1519(s), 1342(s) cm^{-1}. N.m.r. data: ^1H ($CDCl_3$ solution), δ 2.54 p.p.m. (s, 6Me). Electronic spectra (benzene solution): λ_{max} 560, 390, 208; (acetone solution): 550, 322, 208; (methanol solution): 550, 258, 252, 208 nm.

(III.26) ***Synthesis of [bis(3-formyl-pentane-2,4-dionato)(pentane-2,4-dionato)]cobalt(III).***

From reference 63. [Bis(3-formyl-pentane-2,4-dionato)(pentane-2,4-dionato)]-cobalt(III) was synthesized in 27% yield as a green solid. (Found, after recrystallization from methanol: C, 51.8; H, 6.2. $C_{16}H_{21}O_7Co_1$ requires C, 50.0; H, 5.5 %, the carbon analysis was out of the acceptable range and had to be supported by further evidence). I.r. as given in Reference. N.m.r. data: ^1H ($CDCl_3$ solution), δ 2.21 (s, Me); 2.67 (s, 2Me); 5.53 (s, enol proton, 2H); 10.15 p.p.m. (s, formyl proton). M.p. = 178-179°C (L.v. 171.5-173.5°C).

(III.27) ***Synthesis of tris[pentane-2,4-dionato]rhodium(III).***

Taken from reference 74. Tris[pentane-2,4-dionato]rhodium(III) was synthesized in 50% yield, as a yellow solid. (Found: C, 44.9; H, 5.6. $C_{15}H_{21}O_6Rh_1$ requires C, 45.0; H, 5.3%)

7.3 Experimental Details Relevant to Chapter Four

Synthesis of β-ionylidenecyanoacetic acid.

β-Ionylidenecyanoacetic acid was prepared by a modification of the method reported in references 101 and 145. Freshly distilled β-ionone (19.2 g, 0.1 mol) was mixed with cyanoacetic acid (10.2 g, 0.1 mol), acetamide (0.5 g), and ammonium acetate (0.5 g) in glacial acetic acid (20 cm^3) and stirred for 1 hour. Reagent grade toluene was added to increase the volume to 150 cm^3, and the amber coloured mixture refluxed using a Soxhlet apparatus filled with 100 cm^3 of activated 4 Å molecular sieve, for three days.

Sand was used to prevent excessive bumping, and the whole apparatus was flushed with nitrogen during the reflux. Any solvent lost during the reflux was made up by adding further quantities of dry toluene.

After three days, the reaction mixture was cooled, and added to water (200 cm^3). The mixture was extracted with diethyl ether (3 x 50 cm^3) to remove all the organic materials from the aqueous layer. The diethyl ether extract was then washed with water (3 x 100 cm^3), then with aqueous sodium hydroxide (100 cm^3, 1M), the NaOH washings being retained. The diethyl ether layer then contained unreacted β-ionone and β-ionylidene acetonitrile, after removal of diethyl ether, and distillation, β-ionylidene acetonitrile was obtained in 24 % yield.

Acidification of the aqueous NaOH washings with dilute hydrochloric acid (1M) precipitated out crude β-ionylidenecyanoacetic acid, as a yellow semi-crystalline sludge. The crude β-ionylidenecyanoacetic acid was isolated and recrystallized from toluene to give 4.9 g (19 %) of β-ionylidenecyanoacetic acid as bright yellow crystals. β-Ionylidenecyanoacetic acid decomposed slowly and had to be kept under dinitrogen. The gaseous decomposition products smelt of bitter almonds (HCN) and manipulations were therefore performed in an efficient fume hood. (Found: C, 74.4; H, 8.7; N, 5.3. $C_{16}H_{21}NO_2$ requires C, 74.2; H, 8.2; N, 5.4 %.) I.r.: see Table 4.6. N.m.r. data: ^1H ($CDCl_3$ solution), see Fig. 4.3 and Table 4.4. Electronic spectra (methanol solution): λ_{max} 309 (log ε 4.31) , 270(4.17), 210(3.97); (dichloromethane solution): 355(4.26), 273(3.96), 230(3.68) nm. FAB and EI mass spectra; see Fig. 4.6 and Table 4.5A. M.p. 157°C (dec.).

(IV.1) *Synthesis of ammonium trans-2-cyano-3-methyl-5-(2,6,6-trimethyl-1-cyclohexen-1-yl)-2,4-pentadienate (ammonium trans-β-ionylidenecyanoacetate)*

Ammonium *trans*-β-ionylidenecyanoacetate was synthesized by a modification of the method described by Smit.[184] Dry ammonia gas was passed through a solution of trans-β-ionylidenecyanoacetic acid dissolved in diethyl ether, ammonium *trans*-β-

ionylidenecyanoacetate precipitated out as a fine white solid. The crude ammonium *trans*-β-ionylidenecyanoacetate was then recrystallized from water, forming colourless cubes. (Found: C, 69.9; H, 9.3; N, 10.2. $C_{16}H_{24}N_2O_2$ requires C, 69.6; H, 8.7; N, 10.1 %.) I.r.: see Table 4.6. N.m.r. data: ^1H see Fig. 4.8 and Table 4.7.

(IV.2) ***The synthesis of diethylammonium trans-2-cyano-3-methyl-5-(2,6,6-trimethyl-1-cyclohexen-1-yl)-2,4-pentadienate***

A slight excess of diethyl amine (0.9 mmol) was added to a solution of trans-β-ionylidenecyanoacetic acid (0.22g, 0.85 mmol) in warm benzene (25 cm^3). The colour of the solution turned from yellow to straw-yellow. The solvent was removed from the reaction mixture under reduced pressure. The residue (IV.2) was recrystallized from hexane/benzene (1:1) to deposit white crystals of trans-[2-cyano-3-methyl-5-(2,6,6-trimethyl-1-cyclohexen-1-yl)-pentadienato]diethylammonium (IV.2) in 68% yield. (Found: C, 72.3; H, 10.7; N, 8.3. $C_{20}H_{32}N_2O_2$ requires C, 72.3; H, 9.6; N, 8.4 %.) I.r.: see Table 4.6. N.m.r. data: ^1H see Fig. 4.9 and Table 4.7.

(IV.4) ***The synthesis of caesium trans-2-cyano-3-methyl-5-(2,6,6-trimethyl-1-cyclohexen-1-yl)-2,4-pentadienate***

Freshly prepared [2-cyano-3-methyl-5-(2,6,6-trimethyl-1-cyclohexen-1-yl)-2,4-pentadienato]silver(I) (IV.5) (0.202g, 5.5 mmol) was suspended in 95% aqueous ethanol. Caesium bromide (0.12 g) was added in water to the suspension. Silver bromide precipitated out, and was filtered off. The ethanolic filtrate was reduced to dryness and deposited crude (IV.4) as a thick oil. The residue was extracted with hot dry acetone (20 cm^3). Slow evaporation of the acetone solution deposited white crystals of *trans*-[2-cyano-3-methyl-5-(2,6,6-trimethyl-1-cyclohexen-1-yl)-2,4-pentadienato]caesium (IV.4). The crystals were dried at 50-70°C in a vacuum for 2 days. (Found: C, 48.5; H, 5.2; N, 3.5. $C_{16}H_{20}NO_2Cs$ requires C, 49.1; H, 5.1; N, 3.6 %, deviations due to slight traces of water) I.r.: see Table 4.6. N.m.r. data: ^1H (CD_3OD solution) see Fig. 4.10 and Table 4.7.

(IV.5) ***The synthesis of trans-[2-cyano-3-methyl-5-(2,6,6-trimethyl-1-cyclohexen-1-yl)-pentadienato]silver(I) (silver trans-β-ionylidenecyanoacetate)***

β-Ionylidenecyanoacetate (1.3 g) was converted into the sodium salt by reaction with NaOH (0.2 g) in 95% methanol. Silver nitrate (0.85 g) solution was added to the methanolic sodium β-ionylidenecyanoacetate to deposit *trans*-[2-cyano-3-methyl-5-(2,6,6-trimethyl-1-cyclohexen-1-yl)-pentadienato]silver(I) (IV.5) as a pink precipitate. The precipitate was filtered off, washed and dried. Silver β-ionylidenecyanoacetate was obtained as a fine off white powder, in 88% yield. It decomposed slowly in direct light, but may be stored indefinitely in the dark. (Found: C, 51.5; H, 5.6; N, 3.8; Ag, 25.4. $C_{16}H_{20}N_1O_2Ag$ requires C, 52.4; H, 5.5; N, 3.8; Ag, 29.2 %, low carbon analysis due to traces of water which could not be removed) I.r.: see Table 4.6. N.m.r. data: ^1H ($CDCl_3$ solution) see Fig. 4.11 and Table 4.7. FAB mass spectrum see Table 4.5B. Electronic spectrum, dichloromethane solution; λ_{max} 345 (Log ε = 3.98), 325(3.96), 285 nm (4.03).

(IV.6) ***The synthesis of trans-[2-cyano-3-methyl-5-(2,6,6-trimethyl-1-cyclohexen-1-yl)-2,4-pentadienato]barium trihydrate.***

The synthesis of trans-[2-cyano-3-methyl-5-(2,6,6-trimethyl-1-cyclohexen-1-yl)-2,4-pentadienato]barium is typical of the synthesis of other β-ionylidenecyanoacetate salts.

Barium nitrate (0.13 g, 0.5 mmol) was added to sodium β-ionylidenecyanoacetate (from 0.26g of β-ionylidenecyanoacetic acid and sodium hydroxide solution) in water to precipitate out trans-[2-cyano-3-methyl-5-(2,6,6-trimethyl-1-cyclohexen-1-yl)-2,4-pentadienato]barium trihydrate as a white solid. The white solid was redissolved in hot boiling water, and fine white crystals formed on cooling. Yield of *trans*-[2-cyano-3-methyl-5-(2,6,6-trimethyl-1-cyclohexen-1-yl)-2,4-pentadienato]barium trihydrate was 26%. (Found: C, 53.8; H, 6.7; N, 3.9; Ba, 20.8. $C_{32}H_{46}N_2O_7Ba$ requires C, 54.3; H, 6.5; N, 3.9; Ba, 19.4 %) I.r.: see Table 4.6. N.m.r. data: ^1H (CD_3OD solution) see Fig.

4.12 and Table 4.7.

(IV.7) ***The synthesis of trans-[2-cyano-3-methyl-5-(2,6,6-trimethyl-1-cyclohexen-1-yl)-2,4-pentadienato]zinc(II) trihydrate.***

As for the synthesis of (IV.6). Zinc chloride (0.14g) was reacted with boiling sodium β-ionylidenecyanoacetate (from 0.52g of acid) in 94% methanol precipitated *trans*-[2-cyano-3-methyl-5-(2,6,6-trimethyl-1-cyclohexen-1-yl)-2,4-pentadienato]zinc(II) trihydrate (IV.7). The solid was filtered off, and washed with cold methanol, to remove any unreacted β-ionylidenecyanoacetic acid. Impure (IV.7) was formed in 58% yield. The impure compound was purified by slow cooling of a water/ethanol solution of the zinc compound, forming pale yellow crystals of *trans*-[2-cyano-3-methyl-5-(2,6,6-trimethyl-1-cyclohexen-1-yl)-2,4-pentadienato]zinc(II) trihydrate. (Found: C, 60.9; H, 6.6; N, 4.4; Zn, 13.8. $C_{32}H_{46}N_2O_7Zn_1$ requires C, 60.4; H, 7.2; N, 4.4; Zn, 10.3 %) I.r.: see Table 4.6. N.m.r. data: ^1H (CD_3OD solution) see Fig. 4.13 and Table 4.7.

(IV.8) ***The synthesis of trans-[2-cyano-3-methyl-5-(2,6,6-trimethyl-1-cyclohexen-1-yl)-2,4-pentadienato]copper(II) trihydrate.***

Copper(II) sulphate (0.13g) was added to an aqueous solution of sodium β-ionylidenecyanoacetate, to precipitate out *trans*-[2-cyano-3-methyl-5-(2,6,6-trimethyl-1-cyclohexen-1-yl)-2,4-pentadienato]copper(II) trihydrate (IV.8) as a bright green solid. The precipitate was isolated, and dried. (Found: C, 59.8; H, 6.3; N, 4.6. $C_{32}H_{46}N_2O_7Cu_1$ requires C, 60.6; H, 7.3; N, 4.4 %) I.r.: see Table 4.6. Magnetic moment of 1.57 μ_B (based on the the dimer with an RMM of 1160). FAB mass spectrum M^+ at m/z = 581. Electronic spectrum: (dichloromethane solution) λ_{max} 520 (Log ε 2.96), 350(3.77), 290(3.87) nm; (ethanol solution) 313(3.98), 281(4.13), 220(3.98) nm.

(IV.9) ***The synthesis of trans-[2-cyano-3-methyl-5-(2,6,6-trimethyl-1-cyclohexen-1-yl)-2,4-pentadienato]nickel(II) trihydrate.***

The nickel salt of β-ionylidenecyanoacetic acid was synthesized in the same manner as the copper salt (IV.8), as a hydrated pale green solid. (Found: C, 61.6; H, 6.9; N, 4.4. $C_{32}H_{46}N_2O_7Ni_1$ requires C, 61.1; H, 7.3; N, 4.4 %) I.r.: see Table 4.6.

(IV.10) ***The synthesis of ammonium cis-2-cyano-3-methyl-5-(2,6,6-trimethyl-1-cyclohexen-1-yl)-2,4-pentadienate.***

The synthesis of *cis*-[2-cyano-3-methyl-5-(2,6,6-trimethyl-1-cyclohexen-1-yl)-pentadienato]ammonium (IV.10) was done by a modification of the method outlined by Smit.[184] The collected mother liquors from several preparations of *trans*-β-ionylidenecyanoacetic acid were re-dissolved in toluene. Dried ammonia gas was passed through the solution to precipitate out crude *cis*-[2-cyano-3-methyl-5-(2,6,6-trimethyl-1-cyclohexen-1-yl)-pentadienato]ammonium. The white solid was re-crystallized from water. (Found: C, 69.3; H, 8.9; N, 10.0. $C_{16}H_{24}N_2O_2$ requires C, 69.6; H, 8.7; N, 10.1 %) I.r.: see Table 4.8. N.m.r. data: ^1H (CD_3OD solution) see Fig. 4.15 and Table 4.9.

(IV.11) ***The synthesis of cis-[2-cyano-3-methyl-5-(2,6,6-trimethyl-1-cyclohexen-1-yl)-2,4-pentadienato]barium pentahydrate.***

Barium nitrate (0.07g) was added to an aqueous solution of ammonium *cis*-β-ionylidenecyanoacetate (0.15g) to precipitate out *cis*-[2-cyano-3-methyl-5-(2,6,6-trimethyl-1-cyclohexen-1-yl)-2,4-pentadienato]barium.pentahydrate (IV.11). Compound (IV.11) was recrystallized from boiling water as fine white needles. (Found: C, 51.8; H, 6.0; N, 3.8. $C_{32}H_{50}N_2O_9Ba$ requires C, 51.7; H, 6.7; N, 3.8 %) I.r.: see Table 4.8. N.m.r. data: ^1H (CD_3OD solution) see Fig. 4.16 and Table 4.9.

(IV.12) ***The synthesis of cis-[2-cyano-3-methyl-5-(2,6,6-trimethyl-1-cyclohexen-1-yl)-2,4-pentadienato]copper(II) dihydrate.***

The copper salt of *cis*-β-ionylidenecyanoacetic acid was synthesized from the ammonium salt in the same manner as (IV.11) as a light blue powder. (Found: C, 62.5; H, 6.6; N, 4.8; Cu, 9.4. $C_{32}H_{44}N_2O_6Cu$ requires C, 62.4; H, 7.1; N, 4.6; Cu, 10.3 %) I.r.: see Table 4.8. Electronic spectrum: (dichloromethane solution) λ_{max} 522(Log ε 2.35), 361(3.97), 274(3.79), 233(3.91) nm; (ethanol solution) 336(4.22), 276(4.07), 220(3.87) nm.

(IV.13) ***The synthesis of cis-[2-cyano-3-methyl-5-(2,6,6-trimethyl-1-cyclohexen-1-yl)-2,4-pentadienato]zinc.cyclohexane dihydrate.***

The zinc salt was prepared in the same manner as that for the copper(II) salt. Zinc chloride (0.037g, 0.27 mmol) was reacted with ammonium *cis*-β-ionylidenecyanoacetate (0.15g, 0.54 mmol) in water. The supernatant water layer was decanted off, and the yellow oil carefully dried. The yellow oil was redissolved in cyclohexane (3 cm^3), reduced in volume (to 1 cm^3), and allowed to cool to -20°C forming fine yellow crystals of *cis*-[2-cyano-3-methyl-5-(2,6,6-trimethyl-1-cyclohexen-1-yl)-2,4-pentadienato]zinc.cyclohexane dihydrate (IV.13) (the water was absorbed from the atmosphere). (Found: C, 64.9; H, 7.5; N, 4.2; Zn, 9.3. $C_{38}H_{56}N_2O_6Zn$ requires C, 65.0; H, 8.0; N, 4.0; Zn, 9.3 %) I.r.: see Table 4.8. N.m.r. data: ^1H see Fig. 4.17 and Table 4.9.

7.4 Experimental Details Relevant to Chapter Five

(V.4) ***The synthesis of Chloro(cis-{2-cyano-3-methyl-5(2,6,6-trimethyl-1-cyclohexen-1-yl)-2,4-pentadienato})[bis(triphenylphosphine)]-platinum(II), PtCl(β-ionylidenecyanoacetate)$(PPh_3)_2$.***

Cis-$PtCl_2(PPh_3)_2$ (0.6329g, 0.8 mmol) in dichloromethane and reacted with silver β-ionylidenecyanoacetate (0.294g, 8 mmol) dissolved in dichloromethane. After stirring for 30 minutes AgCl was filtered off, and the solvent removed under reduced

pressure, to form an off white solid froth. The solid froth was re-dissolved in toluene, and precipitated out with hexane (used twice the volume of toluene). The white solid was filtered off leaving a yellowish supernatant liquid. The white solid was the cis- isomer. Addition of 3x more hexane caused more white solid to separate out. This was collected and washed with hexane. The combined residues was re-dissolved in tetrahydrofuran, and eluted on a 10 inch long silica-gel column using tetrahydrofuran. The eluted bands were detected by continuous spotting of test samples on a thin layer chromatographic plate. Monochloro-[*bis*-(triphenylphosphine)-*cis*-{2-cyano-3-methyl-5-(2,6,6-trimethyl-1-cyclohexen-1-yl)-2,4-pentadienato}]platinum(II) (V.4) was the third fraction and after reducing the volume of solvent, crystallized in fine yellow needles. Yield 0.21g (26%). (Found: C, 60.4; H, 5.0; N, 1.3; Pt, 14.8 with some precipitation of Pt metal during analysis; and Cl, 3.8. $C_{52}H_{50}Cl_1NO_2P_2Pt$ requires C, 61.6; H, 5.0; N, 1.4; Pt, 19.3 ; and Cl, 3.5%). I.r.: see Table 5.5. N.m.r. data: ^1H ($CDCl_3$ solution) ; δ 7.6 (cis), 7.4 (trans) and 7.2(both) (m, PPh protons); 6.623 (cis) (s); 6.597 (trans) (s); 1.02 (both) (s, Me); 1.4 (m); 1.6 (m); 1.72 (s, Me); 2.0 (t, H); 2.23 p.p.m. (s, Me), with toluene resonances seen at 2.18 (s, Me), 7.32 p.p.m. ($^3J(H,H')$ = 7.3 Hz, $^4J(H,H'')$ = 2 Hz). ^{31}P-{^1H} (dichloromethane solution) (see Fig. 5.2) showed two compounds in the ratio of 6:1, {δ 10.98 [$^1J(Pt\text{-}P)$ = 3680 with peak areas 1:4:1]}; 14.03 p.p.m. [$^1J(Pt\text{-}P)$ = 3882, $^2J(P,P')$ = 17.22 Hz with peak areas 1:4:1]. Mass spectrum M^+ m/z 1014 (see Table 5.3). Electronic spectrum; (dichloromethane solution) λ_{max} 330 (Log ε = 3.53), 230 nm (3.98). Melting point 155-157 °C (dec.).

(V.5) ***The synthesis of di{cis[2-cyano-3-methyl-5-(2,6,6-trimethyl-1-cyclohexen-1-yl)-2,4-pentadienato]-bis(triphenylphosphine)}-palladium(II).$CHCl_3$, Pd(β-ionylidenecyanoacetate)$_2$(PPh$_3$)$_2$.***

Cis-$PdCl_2(PPh_3)_2$ (0.2297g, 3.3 mmol) was reacted with silver β-ionylidenecyanoacetate (0.240g, 6.6 mmol) in trichloromethane ($20cm^3$). A precipitate of silver chloride formed immediately, which was filtered off, leaving a yellow filtrate. Hexane ($10\ cm^3$) was added to the filtrate induce crystallization, which was completed by cooling to -20°C for 12 hours depositing powdery yellow crystals of di{*cis*[2-cyano-3-

methyl-5-(2,6,6-trimethyl-1-cyclohexen-1-yl)-2,4-pentadienato]-*bis*(triphenylphosphine)}palladium(II) (V.5). Yield 0.046g (12%). (Found: C, 65.9; H, 5.8; N, 2.2; Cl, 6.9; Pd, 7.7. $C_{59}H_{65}Cl_3N_2O_4P_2Pd$ requires C, 65.4; H, 5.7; N, 2.2; Cl, 8.4; Pd, 8.4 %). I.r.: see Table 5.5. N.m.r. data: ^1H ($CDCl_3$ solution) see Fig. 5.3; δ 7.6 (cis), 7.35 (trans) and 7.2 (both) (m, PPh protons); 6.6 (broad, 4H); 1.02 (s, 4Me); 1.4 (m, 4H); 1.6 (m, 4H); 1.69 (s, Me); 2.0 (broad m, 4H); 2.99 p.p.m. (masked s, Me). Positive FAB mass spectrum $2M^+$ m/z 2296, M^+ m/z 1147 and negative FAB m.s. m/z 258 due to β-ionylidenecyanoacetate ligand (see Table 5.4). Electronic spectrum; (dichloromethane solution) λ_{max} 340 (Log ε = 4.59), 320(4.60), 235 nm (4.51).

(V.6) ***The synthesis of {di-cis[2-cyano-3-methyl-5-(2,6,6-trimethyl-1-cyclohexen-1-yl)-2,4-pentadienato]-(diphenylphosphinoethane)}-platinum(II), Pt(β-ionylidenecyanoacetate)$_2$(diphos).***

Freshly prepared silver β-ionylidenecyanoacetate (0.44g, 1.2 mmol) in trichloromethane, was added to a suspension of dichloro-bis[diphenylphosphinoethane]platinum(II) (0.4g, 0.6 mmol) in dichloromethane. A heavy grey precipitate (AgCl) formed, stirring was continued for ten minutes. The reaction mixture was not exposed to light. The AgCl was filtered off and the filtrate reduced to dryness *in vacuo* at or below 20°C, depositing a yellow oil. The yellow oil was extracted with 1:9 dichloromethane/toluene mixture (5 cm^3), and the light yellow extract allowed to crystallize at -20°C. Pale yellow crystals of {di-*cis*[2-cyano-3-methyl-5-(2,6,6-trimethyl-1-cyclohexen-1-yl)-2,4-pentadienato]-(diphenylphosphinoethane)}-platinum(II).0.5CH_2Cl_2 (V.6). formed after two months. (Found: C, 65.1; H, 6.3; N, 2.6; Cl (from dichloromethane), 1.1(4); Pt, 10 % - Pt metal precipitated during analysis. Theoretical elemental analyses could not be calculated because of variable solvent inclusion). I.r.: see Table 5.5. N.m.r. data: ^1H ($CDCl_3$ solution) see Fig. 5.4 ; δ 7.6 and 7.3 (m, 4xPPh protons); 3.24 (t, 4H, too broad to measure); 6.71 (d, 2H, $^3J(H,H')$ = 16 Hz); 6.85 (broad doublet, 2H, $^3J(H,H')$ = 16 Hz); 1.05 (s, 4Me); 1.47 (m, 4H); 1.62 (m, 4H); 1.85 (s, 2Me); 2.04 (t, 4H); 2.51 p.p.m. (s, 2Me). $^{31}P-\{^1H\}$

(dichloromethane solution) see Fig. 5.5 ; δ 44.71 p.p.m. (with Pt-P satellites, 1:4:1 ratio, ^1J(Pt-P) = 2350 Hz).

(V.7) ***The attempted synthesis of monochloro-[cis-{2-cyano-3-methyl-5-(2,6,6-trimethyl-1-cyclohexen-1-yl)-2,4-pentadienato}-(diphenylphosphinoethane)]platinum(II), PtCl(β-ionylidenecyanoacetate)(diphos).***

$PtCl_2$(diphos) (0.248g, 3.7 mmol) was suspended dichloromethane. Silver β-ionylidenecyanoacetate (0.45g, 3.7 mmol) dissolved in dichloromethane, was added to the above suspension, and stirred for one hour. AgCl precipitated out, was filtered off, and the clear yellow filtrate reduced to dryness to deposit an off-white solid. The off-white solid was re-extracted with trichloromethane to form a yellow solution. Thin layer analysis of this solution (tetrahydrofuran elutant) indicated that only one product had been formed. (Found: C, 54.0; H, 4.8; N, 1.4; Cl, 6.8(5) %). I.r.: see Table 5.5. N.m.r. data: ^1H ($CDCl_3$ solution) δ 7.6 and 7.9 p.p.m. ^{31}P-{^1H} (dichloromethane solution) showed four compounds in the ratio of 100:69:45:37, {δ 38.75 [^1J(Pt-P) = 3618]; 29.04 [^1J(Pt-P) = 3656]; 37.35 [^1J(Pt-P) = 3760]; 26.26 p.p.m. [^1J(Pt-P) = 3808 Hz]}.

(V.8) ***The attempted synthesis of {bis[cis(2-cyano-3-methyl-5-(2,6,6-trimethyl-1-cyclohexen-1-yl)-2,4-pentadienato)]-bis(triphenylphosphine)}platinum(II), Pt(β-ionylidenecyanoacetate)$_2$(PPh$_3$)$_2$.***

$PtCO_3(PPh_3)_2$ (0.1g, 0.13 mmol) as a suspension in dichloromethane, was reacted with β-ionylidenecyanoacetic acid (0.057g, 0.22 mmol), dissolved in MeOH (10 cm^3), under reflux. The colour of the solution changed from yellow to a lighter yellow. The mixture was stirred for an additional hour, and the solvent removed under reduced pressure. The residue was re-dissolved in trichloromethane, filtered off and layered with hexane which deposited {*cis*[2-cyano-3-methyl-5-(2,6,6-trimethyl-1-cyclohexen-1-yl)-2,4-pentadienato]$_2$-*bis*(triphenylphosphine)}platinum(II) (V.8) as a pale cream solid. (Found: C, 66.2; H, 5.9; N, 2.2; Pt, 9.0 - Pt metal was deposited during analysis. $C_{68}H_{70}N_2O_4P_2Pt$ requires C, 66.1; H, 5.7; N, 2.3; Pt, 15.8 %). I.r.: see Table 5.5.

N.m.r. data: ^1H ($CDCl_3$ solution) see Table 5.2 and Fig. 5.7.

7.5 Experimental Details Relevant to Chapter Six

(VI.11) ***The synthesis of N-[2-cyano-3-methyl-5-(2,6,6-trimethyl-1-cyclohexene-1-yl)-2,4-pentadiene-1-one]-L-proline.***

β-Ionylidenecyanoacetic acid (0.312g, 1.2 mmol) was dissolved in dry toluene (20 cm^3) held at 100°C in a water bath. Thionyl chloride ($SOCl_2$, 0.11 cm^3) was added carefully to the toluene solution of β-Ionylidenecyanoacetic acid in a fume hood. HCl is evolved during the reaction. The yellow toluene solution gradually darkens. After 30 minutes L-proline (0.115g, 1 mmol) in aqueous sodium hydroxide (0.075g NaOH in 0.68g water {10% NaOH}) was added to the toluene solution of β-ionylidenecyanoacetyl chloride. The reaction mixture was pink during the initial addition of the sodium L-prolinate, which gradually became yellow. The reaction mixture was cooled and quenched with water (20 cm^3) and concentrated HCl (7 drops), and the toluene removed under reduced pressure. A yellow oil separated out from the aqueous solution, and the supernatant liquid was decanted off. The yellow oil was carefully washed with water, and dried *in vacuo*. The crude N-[2-Cyano-3-methyl-5-(2,6,6-trimethyl-1-cyclohexene-1-yl)-2,4-pentadiene-1-one]-L-proline was washed with hot pentane (2 x 25 cm^3) to remove unreacted acyl chloride. The yellow residue was first recrystallized from hot tetrachloromethane and the yellow crystals of β-ionylidenecyanoacetic acid which crystallize out first were discarded. The mother liquor was reduced in volume and recrystallized twice from tetrachloromethane to give almost white crystals of N-[2-Cyano-3-methyl-5-(2,6,6-trimethyl-1-cyclohexene-1-yl)-2,4-pentadiene-1-one]-L-proline (VI.11). Yield 13%. (Found: C, 69.3; H, 7.5; N, 7.6. $C_{21}H_{28}N_2O_3$ requires C, 70.8; H, 7.9; N, 7.9 %). I.r.: ν(CN), 2208(w); ν(COO), 1620(br); ν(CC-C=O-N) 1722; ν(C=C), 1602(s); ν(H-C=C-H def.), 967(m); ν(olefinic C-H), 762(w) (olefinic C-H) cm^{-1}. The ^1H n.m.r. results of compound (VI.11) are summarized in Table 6.1 and illustrated in Fig. 6.1. M.p. 160-162°C (dec.).

(VI.12) ***The synthesis of [N-{2-cyano-3-methyl-5-(2,6,6-trimethyl-1-cyclohexene-1-yl)-2,4-pentadiene-1-one}-L-prolinato]lithium monohydrate.***

N-[2-cyano-3-methyl-5-(2,6,6-trimethyl-1-cyclohexene-1-yl)-2,4-pentadiene-1-one]-L-proline (VI.11) (0.085g, 0.24 mmol) in methanol was reacted with a methanolic solution of lithium hydroxide (1.24 cm^3 (2.9 mmol) of a solution of 0.2g Li metal in 150 cm^3 methanol/water 2:1). The methanolic reaction mixture was reduced to dryness to leave a white crystalline solid which was extracted with diethyl ether. The ether was removed from the extract and the residue redissolved in dry benzene. [N-{2-Cyano-3-methyl-5-(2,6,6-trimethyl-1-cyclohexene-1-yl)-2,4-pentadiene-1-one}-L-prolinato]lithium monohydrate (VI.12) was deposited from the benzene solution by the addition of dry hexane. (Found: C, 66.5; H, 7.3; N, 7.0; Li, 1.2. $C_{21}H_{29}N_2O_4Li$ requires C, 66.3; H, 7.6; N, 7.4; Li, 1.8 %). I.r.: ν(CN), 2203(w); ν(CC-C=O-N) 1641; ν(COO), 1420; ν(C=C), 1602(s); ν(H-C=C-H def.), 968(m); ν(olefinic C-H), 763(w) (olefinic C-H) cm^{-1}.

(VI.13) ***The synthesis of [N-{2-cyano-3-methyl-5-(2,6,6-trimethyl-1-cyclohexene-1-yl)-2,4-pentadiene-1-one}-L-prolinato]barium dihydrate.***

Barium hydroxide octahydrate (0.044g, 0.14 mmol) was reacted in boiling aqueous solution with N-[2-cyano-3-methyl-5-(2,6,6-trimethyl-1-cyclohexene-1-yl)-2,4-pentadiene-1-one]-L-proline (VI.11) (0.1g, 0.28 mmol) to form a thick pasty mass of crude [N-{2-cyano-3-methyl-5-(2,6,6-trimethyl-1-cyclohexene-1-yl)-2,4-pentadiene-1-one}-L-prolinato]barium (VI.13). [N-{2-Cyano-3-methyl-5-(2,6,6-trimethyl-1-cyclohexene-1-yl)-2,4-pentadiene-1-one}-L-prolinato]barium dihydrate (VI.13) was purified by recrystallization from hot boiling water, the first crop was isolated as long white needles in 28 % yield. (Found: C, 57.1; H, 6.7; N, 6.2; Ba, 14.5. $C_{42}H_{58}N_4O_8Ba$ requires C, 57.1; H, 6.6; N, 6.3; Ba, 15.5%). I.r.: water 3400; ν(CN), 2204(w); ν(NR), 1733(w); ν(CC-C=O-N), 1613(s); ν(H-C=C-H def.), 968(m) cm^{-1}. The ^1H n.m.r. (in

CD_3OD) results are presented in Table 6.2A and B and illustrated in Fig. 6.2.

REFERENCES

1) N. Acton and A. Brossi, Helv. Chem. Acta., 1980, **63**, 1391.

2) S.K. Adams, D.A. Edwards and R.Richards, Inorg. Chem. Acta., 1975, **12**, 163.

3) H. Adams, A.C. Albeniz, N.A. Bailey, D.W. Bruce, A.S. Cherodian, R. Dhillon, D.A. Dunmar, P. Espinet, J.L. Feijoo, E. Lalinde, P.M. Maitlis, R.M. Richardson and G. Ungar, J. Mater. Chem., 1991, **1**, 843.

4) A.M. Agal'tsov and V.S. Gorelik, Kratk. Soobshch. Fiz., 1989, **2** , 43.

5) T.A. Albright, R. Hoffmann, J.C. Thibeault and D.L. Thorn, J. Am. Chem. Soc., 1979, **101**, 3801.

6) S. Allen and R.T. Murray, Phys. Scr., 1987 (Pub. 1988) **T23** (Trends Phys., EPS-7), 275.

7) A.G. Anderson, J.C. Calabrese, W. Tam, and I.D. Williams, Chem. Phy. Lett., 1987, **134**, 392.

8) T.G. Appleton and M.A. Bennett, Inorg. Chem., 1978, **17**, 738.

9) T.G. Appleton and J.R. Hall, J. Chem. Soc., Chem. Commun., 1983, 911.

10) J.L. Atwood, J.E.D. Davies and D.D. MacNicol (Editors), "Inclusion Compounds", Academic Press, London, 1984 (and references therein).

11) S. Baba, T. Ogura and S. Kawaguch, Japan Inorg. Nucl. Chem. Lett., 1971, 7, 1195.

12) S. Baba, T. Ogura and S. Kawaguch, J. Chem. Soc. Chem. Comm., 1972, 910.

13) J.A. Bandy, H.E. Bunting, M.H.Garcia, M.L.H. Green, S.R. Marder, M.E. Thompson, D. Bloor, P.V. Kolinsky and R.J.Jones, Spec. Publ.- R. Soc. Chem., 1989, **69** (*Org. Mater. Non-linear Opt.*), 225.

14) J.W. Barton, M. Buhaenko, B. Moyle and N.M. Ratcliffe, J. Chem. Soc., Chem. Commun., 1988, 488.

15) M. Barzoukas, M. Blanchard-Desce, D. Josse, J-M. Lehn, and J. Zyss, To be published.

16) H.F. Bauer and W.C. Drinkard, J. Am. Chem. Soc., 1960, **82**, 5031

17) R. Belloli, J. Chem. Educ., 1969, **46**, 640.

18) R.H. Beuteul, D.F. Hinkley and P.I. Pollak, J. Am. Chem. Soc., 1955, 77, 5166.

19) A.B. Blake and L.R. Fraser, J. Chem. Soc. Dalton Trans., 1975, 193.

20) M. Blanchard-Desce, I. Ledoux, J-M. Lehn, J. Malthete and J. Zyss, J. Chem. Soc., Chem. Commun., 1988, **11**, 737.

21) W.J. Blau, H.J. Byrne, D.J. Cardin, and A.P. Davey, J. Mater. Chem., 1991, **1**, 245.

22) N. Bloembergen, "Nonlinear Optics," Benjamin, NY, 1986, Vols. **1** and **2**.

23) N. Bloembergen, Phys. Rev., **174**, 813.

24) E.C. Bolton, G.H.W. Milburn and G.A. Thomson, Chemtronics, 1988, **3**, 215.

25) F. Bonati and G. Wilkinson, J. Chem. Soc., 1964, 3150.

26) F. Bonati and G. Wilkinson, J. Chem. Soc., 1964, 3156.

27) F. Bonati and R. Ugo, J. Organomet. Chem., 1968, **11**, 341.

28) J.E. Brady and P.W. Carr, J. Chem. Phys., 1985, **89**, 5759.

29) J.R. Briggs, C. Crocker, W.S. McDonald and B.L. Shaw, J. Organomet. Chem., 1979, **181**, 213.

30) J.R. Briggs, C. Crocker, W.S. McDonald and B.L. Shaw, J. Chem. Soc., Dalton Trans., 1980, 64.

31) J.R. Briggs, C. Crocker, W.S. McDonald and B.L. Shaw, J. Chem. Soc., Dalton Trans., 1981, 121.

32) D. Bright and J.A. Ibers, Inorg. Chem., 1968, **7**, 1099.

33) S.J. Bross, J. Am. Chem. Soc., 1968, **90**, 506.

34) D. Broussoux, E. Chastaing, S. Esselin, P. Le Barny, P. Robin, Y. Bourbin, J.P. Pocholle and J. Raffy, Rev. Tech. Thomson-CSF, 1989, **20-21**, 151.

35) H. Brunner, Angew. Chem. Int. Ed. Engl., 1971, **10**, 249. (Angew. Chem., 83, 274).

36) B.E. Bryant and W.C. Fernelius, Inorg. Syn., 1957, **5**, 188.

37) E. Bryant, Inorg. Syn., 1950, **5**, 188.

38) A.D. Buckingham and B.J. Orr, Quant. Rev. Chem., 1967, 195.

39) J.C. Calabrese, C. Lap-Tak, J.C. Green, S.R. Marder and W. Tam, J. Am. Chem. Soc., 1991, **113**, 7227.

40) M. Calvin and K.W. Wilson, J. Am. Chem. Soc., 1945, **67**, 2003.

41) Cambridge Structual Database, Cambridge Crystallographic Data Centre, Cambridge, 1990.

42) A.V. Capilla and R.A. Aranda, Cryst. Struct. Commun., 1979, **8**, 795.

43) G. Cardillo, M. Contento, S. Sandri and M. Panunzio, J. Chem. Soc., Perkin Trans. I, 1979, 1729.

44) J. Catterick and P. Thornton, J. Chem. Soc., Dalton Trans., 1977, 1420.

45) J. Catterick and P. Thornton, Adv. Inorg. Chem. Radiochem., 1977, **20**, 291, and references therein.

46) N.Q. Chako, J. Chem. Phys., 1934, **2**, 644.

47) D.S. Chemla and J. Zyss, "Nonlinear Optical Properties of Organic Molecules and Crystals", Academic Press, Orlando, FL, 1987, Vol. **1** and **2** and references therein.

48) C.K. Chen, T.F. Heinz, D. Richard and Y.R. Shen, Phys. Rev. Lett., 1981, **46**, 1010.

49) A.J. Cheney and B.L. Shaw, J. Chem. Soc., Dalton Trans., 1972, 754.

50) A. Citterio, F. Minisci and E. Vismara, J. Org. Chem., 1982, **47**, 81.

51) A. Citterio and F. Ferrario, J. Chem. Research (S), 1983, 308.

52) W. Clegg, I.R. Little and B.P. Straughan, J. Chem. Soc., Dalton Trans., 1986, 1283.

53) W. Clegg, I.R. Little and B.P. Straughan, J. Chem. Soc., Chem. Commun., 1985, 73.

54) W. Clegg, I.R. Little and B.P. Straughan, Acta. Cryst., C(Cryst. Str. Commun.), 1987, **43**, 435.

55) J. Coe, C.J. Jones, J.A. McCleverty, D. Bloor, P.V. Kolinsky and R.J. Jones, J.

Chem. Soc., Chem. Commun., 1989, 1485.

56) J.P. Collman, R.P. Blair, R.L. Marshall and L. Slade, Inorg. Chem., 1963, 2, 576.

57) J.P. Collman, R.A. Moss, S.D. Goldby and W.S. Trahanovsky, Chem. Ind. (London), 1960, 1213.

58) J.P. Collman, R.L. Marshall and W.L. Young(III), Chem. Ind. (London), 1962, 1380.

59) J.P. Collman, R.L. Marshall, W.L. Young, III and C.T. Sears, Jr, J. Org. Chem., 1963, **28**, 1449.

60) J.P. Collman, R.A. Moss, H. Maltz, and C.C. Heindel, J. Am. Chem. Soc., 1961, **83**, 531.

61) J.P. Collman and M. Yamada, J. Org. Chem., 1963, **28**, 3017.

62) J.P. Collman, J. Am. Chem. Soc., 1957, **79**, 3318.

63) J. Collman, R. Marshall, W. Young and S. Goldby, Inorg. Chem., 1962, **1**, 704.

64) S. Cooper and P.K. Dutta, J. Phys. Chem., 1990, **94**, 114.

65) M.K. Cooper and D.W. Yaniuk, J. Organomet. Chem., 1981, **221**, 231.

66) J.F. Corbett, Spectrochem. Acta, 1967, **23A**, 2315.

67) M.A.A.F. de C.T. Carrondo and A.C. Skapski, J. Chem. Soc. Chem. Commun., 1976, 410.

68) M. Delfino, Mol. Cryst. Liq. Cryst., 1979, **52**, 271.

69) V.J. Docherty, D. Pugh and J.O. Morley, J. Chem. Soc., Faraday Trans. I, 1985, **81**, 1179.

70) R.J. Doedens, Prog. Inorg. Chem., 1976, **21**, 209.

71) D.A. Duddell, P.L. Goggin, R.J. Goodfellow, M.G. Norton and J.G. Smith, J. Chem. Soc. A, 1970, 545.

72) A. Dulcic, C. Flytzanis, C.L. Tang, D. Pepin, M. Fetizon and Y.Hoppillard, J. Chem. Phys., 1981, **74**, 1559.

73) W.W. Duley, "Laser Processing and Analysis of Materials." Plenum Press, N.Y., 1983.

74) F.P. Dwyer and A.M. Sargeson, J. Am. Chem. Soc., 1953, **75**, 984.

75) D.F. Eaton, A.G. Anderson, W. Tam and Ying Wang, J. Am. Chem. Soc., 1987, **109**, 1886.

76) D.F. Eaton, A.G. Anderson, W. Tam and Ying Wang, A.C.S. Symposium, 1987, **346**, 381.

77) D.F. Eaton, Tetrahedron, 1987, **43**, 1551.

78) W.C. Egbert, "Advances in Nonlinear Polymers and Inorganic Crystals", Liquid Crystals and Laser Media", Proc. SPIE - Int. Soc. Opt.Eng. , 1987, **824**, 107.

79) R.C. Fay and T.S. Piper, J. Am. Chem. Soc., 1963, **85**, 500.

80) R.C. Fay and T.S. Piper, J. Am. Chem. Soc., 1962, **84**, 2303.

81) C.C. Frazier, Shekhar Guha, Pamela A. Porter, Paula M. Cockerham and Eve A. Chauchard, Proc. SPIE-Int. Soc. Opt. Eng., 1988, **971** (Nonlinear Opt. Prop. Org. Mater.), 206.

82) H. Frinklemann, H. Ringsdorf and J.H. Wendorf, Makromol. Chem., 1979, **179**, 273.

83) H.L. Frish and E. Wasserman, J. Am. Chem. Soc., 1961, **83**, 3789.

84) G.L. Geoffroy and M.S. Wrighton, "Organometallic Photochemistry", Academic Press, NY, 1979.

85) S. Ghosal, M. Samoc and P.N. Prasad, J.J. Tufariello, J. Phys. Chem., 1990, **94**, 2847.

86) R.G. Gillis, Rev. Pure Appl. Chem., 1960, **10**, 21.

87) D.P. Graddon and K.B. Heng, Aust. J. Chem., 1971, **24**, 1059.

88) M.L.H. Green, S.R. Marder, M.E. Thompson, J.A. Bandy, D. Bloor, P.V. Kolinsky and R.J. Jones, Nature, 1987, **330**, 360.

89) S. Guha, C.C. Frazier, W.P. Chen, P. Porter, K. Kang and S.E. Finberg, Proc. SPIE-Int. Soc. Opt. Eng., 1989, **1105** (Mater. Opt. Switches, Isol., Limiters), 14.

90) S. Guha, C. Frazier, P.L. Porter, K. Kang and S.E. Finberg, Opt. Lett., 1989, **14**,

952.

91) T. Hahn (ED), "International Tables for Crystallography", Vol. A: Space-group Symmetry, D. Reidel Pub. Comp., Dordrecht, 1983.

92) D.M. Hall, Prog. Stereochem., 1969, **4**, 1.

93) T. Hamanaka, T. Mitsui, T. Ashida, and M. Kakudo, Acta. Crystallogr., Sect B, 1972, **28**, 214.

94) A.W. Hanson and E.W. Macanlay, Acta. Crystallogr., Sect. B, 1972, **28**, 1961.

95) W. Harrison and J. Trotter, J. Chem. Soc., Dalton Trans., 1972, 956.

96) R.N. Haszeldine, R.J. Lunt, and R.V. Parish, J. Chem. Soc. A, 1971, 3699.

97) W.E. Hatfield, H.M. McGuire, J.S. Pascal and R. Whyman, J. Chem. Soc. A, 1966, 1194.

98) J.B. Heather, R.S.D. Mittal and C.J. Sih, J. Am. Chem. Soc., 1976, **948**, 3661.

99) T.F. Heinz and G.A. Reider, TrAC, Trends Anal. Chem., (Pers. Ed.) 1989, **8(6)**, 235.

100) M.A. Hubbard, N. Miniami, C. Ye, T.J. Marks, J. Yang and G.K. Wong, Proc. SPIE-Int. Soc. Opt. Eng., 1988, **971** (Nonlinear Opt. Prop. Org. Mater.), 136.

101) H.O. Huisman, A. Smit, S. Vromen and L.G.M. Fisscher, Rev. trav. chim., 1952, **71**, 899.

102) Hideji Ikeda, Y. Kawabe and Toshio Sakai, Jpn. Kokai Tokkyo Koho JP 01 19329 (89 19329), 23 Jan 1989, Appl. 87/174846, 15 Jul 1987. (Abstract only)

103) H. Ikeda, T.Sakai and K. Kawasaki, Chem. Lett., 1989, 1285.

104) Hideji Ikeda,Toshio Sakai and Y. Kawabe, Jpn. Kokai Tokkyo Koho JP 02 02, 534 (90 02534), 8 Jan 1990, Appl. 88/145, 906, 15 Jun. 1988. (Abstract only)

105) Inorganic Syntheses: a) A. Dobson *et al*, 1977, **17**, 124. b) R. Ugo, F. Cariati and G. La Monica, 1968. c) D. Drew *et al*, 1972, **13**, 47.

106) O. Isler and P. Schudel, Adv. Org. Chem., 1963, **4**, 115.

107) O. Isler, "Carotinoids", Birkhauser Verlag, Basel, 1971.

108) Y. Itoh, K. Oono, M. Isogai and A. Kakuta, Proc. SPIE-Int. Soc. Opt. Eng., 1989,

1017 (Nonlinear Opt. Mater.), 127.

109) Y.M. Ivanov and G.M. Malakhov (USSR), Nelinein. Spektroskopiya Atomov; Duukhatom. Molekul, M. 1988, 126 (Abstract only).

110) P.D. Kaplan and M. Orchin, Inorg. Chem., 1965, **4**, 1393.

111) P. Karrer, H. Salmon, R. Morf and O. Walker, Helv. Chim. Acta., 1932, **15**, 878.

112) Y. Kawabe, H. Ikeda, T. Saki and K. Kawasaki, Springer Proc. Phys., 1988, **36** (Nonlinear Opt. Org. Semicond.), 120.

113) Y. Kawabe, H. Ikeda, T. Saki and K. Kawasaki, Chem. Lett., 1989, **7**, 1285.

114) D.A. Kleinmann, Phys. Rev., 1962, **128**, 1761.

115) A.N. Knyazeva, E.A. Shugam and L.M. Shkol'nikova, Journal of Structural Chemistry, **11**, 1970, 875. (An English translation of Zn. Strukt. Khim., **11(5)**, 1970, 1938.)

116) B. Koch, Eur. Cryst. Meeting, 1976, 301. (Abstract only).

117) B. Koutek, Coll. Czech. Chem. Commun., 1984, **49**, 1680.

118) S.K. Kurtz and T.T. Perry, J. Appl. Phys., 1968, **39**, 3798.

119) C. Lamberth, Part II Thesis, University of Oxford, 1989.

120) L.A. Laxhuber, B. Rothenhäusler, G. Schneider and H. Möhwald, Appl. Phys. A, 1986, **39**, 173.

121) I. Ledoux, C. Lepers, A. Perigaud and J. Badon, J. Zyss, Opt. Commun., 1990, **80**, 149.

122) I. Ledoux, J. Zyss, J.S. Siegel, J. Brienne and M.J. Lehn, Chem. Phys. Lett., 1990, **172**, 440.

123) B.F. Levine, C.G. Bethea, C.D. Thurmond, R.T. Lynch and J.L. Bernstein, J. Appl. Phys., 1974, **50**, 2523.

124) B.F. Levine and C.G. Bethea, J. Chem. Phys., 1975, **63**, 2666.

125) B.F. Levine and C.G. Bethea, Appl. Phys. Lett., 1974, **24**, 455.

126) B.F. Levine and C.G. Bethea, J. Chem. Phys., 1974 , **60**, 3856.

127) B.F. Levine and C.G. Bethea, R.T. Thurmond, J.L. Berstein, J. Appl. Phys., 1979, **50**, 2523.

128) B.F. Levine and C.G. Bethea, J. Chem. Phys., 1976, **65**, 2439.

129) J.T. Lin, Proc. Int. Conf. Lasers, 1987, 604. (Abstract only).

130) A.E. Lutskii and N.I. Gorokhova, Opt. Spectrosc., 1969, **27**, 917, 499.

131) Y. Manishi, S. Masahiko and T. Shigeaki, Jpn. Kokai Tokkyo Koho JP 63, 112, 545 (88,112,545), 17 May 1988, Appl. 86/256,531, 27 Oct 1986. (Abstract only)

132) C. Mao and C.R. Hauser, "Organic Syntheses", Wiley, New York, 1962, **51**, 90.

133) C. Mao, "Organic Syntheses", Wiley, New York, 1971, **51**, 90.

134) S.R. Marder, J.W. Perry. W.P. Schaefer, B.G. Tiemann, P.C. Groves and K.J. Perry, SPIE Proc. Int. Soc. Opt. Eng., 1989, **1147**, 108.

135) R.H. Martin, Angew. Chem. Int. Ed. Engl., 1974, **13**, 649. (Angew Chem., **86**, 727).

136) R. Mason and G.B. Robertson, J. Chem. Soc. A, 1970, 1229.

137) Mathieson *et al*, Acta. Cryst., 1952, **5**, 599.

138) A.L. McClellan, "Tables of experimental dipole moments", W.H. Freeman and Co., San Francisco.

139) R.C. Mehrotra and R. Bohra, "Metal Carboxylates", Academic Press, 1983.

140) E.W. Meijer, E.E. Havinga and Gl.j.a. Rikken, Phys. Rev. Lett., 1990, **65**, 37.

141) G.R. Meredith, G.J.Van Dusen and D.J. Williams, Macromolecules, 1982, **15**, 1385.

142) Aris Merijanian and H.M. Neumann, Inorg. Chem., 1964, **6**, 165.

143) J.O. Morley and D. Pugh, J. Molecular Electronics, 1989, **5**, 123.

144) J.O. Morley, V.J. Docherty and D. Pugh, J. Chem. Soc., Perkin Trans. 2, 1987, 1351.

145) J.O. Morley and D. Pugh, Spec. Publ. - R. Soc. Chem., 1989, **69** (Org. Mater.Non-linear Optics), 28.

146) G.P. Moss and B.C.L. Weedon, "Chemistry of the Carotinoids" in "The Comparative Biochemistry of Carotenoids," Ed. T.W. Goodwin, 1952, Chapman and Hall, London.

147) D. Murphy, D. Phil Thesis, University of Oxford, 1992.

148) Y. Nakano and S. Sato, Inorg. Chem., 1980, **19**, 3391.

149) Y. Nakano and H. Seki, Chem. Lett., 1976, 611.

150) Y. Nakano, Y. Yoshikana and H. Kondo, J. Am. Chem. Soc., 1984, **106**, 429.

151) Y. Nakano and S. Sato, Inorg. Chem., 1980, **21**, 1315.

152) A. Nakano, K.Yoshino and M. Honma, Jpn. Kokai Tokkyo Koho JP 02,167,529 [90,167,529] (CL, G02F1/35), 27 Jun. 1990, Appl. 88/322, 514, 21 Dec. 1988. (Abstract only)

153) S. Natarajan, D.S.S. Gowda and L. Cartz, Acta Cryst., B, 1974, **30**, 401.

154) J.F. Nicoud, Proc. SPIE-Int. Soc. Opt. Eng., 1988, **971**(Nonlinear Opt. Prop. Org. Mater.), 68.

155) J.F. Nicoud, Spec. Publ. - R. Soc. Chem., 1989, **69** (Org. Mater.Non-linear Optics), 157.

156) J.F. Nicoud, Mol. Cryst. Liq. Cryst., 1988, **156** (Pt A), 257.

157) C.J. Nyman, C.E. Wymore and G. Wilkinson, J. Chem. Soc. A, 1968, 561.

158) W.E. Oberhansli, H.P. Wagner and O. Isler, Acta. Crystallogr., Sect. B, 1974, **30**, 161.

159) W. Oroshnik, G. Karmas and A.D. Mebane, J. Am. Chem. Soc., 1952, **74**, 293.

160) J.L. Oudar and R. Hierle, J. Chem. Phys., 1977, **67**, 446.

161) J.L. Oudar and D.S. Chemla, J. Chem. Phys., 1977, **66**, 2664.

162) J.L. Oudar and D.S. Chemla, J. Chem. Phys., 1974, **66**, 2004.

163) J.L. Oudar and D.S. Chemla, Opt. Commun., 1975, **13**, 164.

164) J.R. Owen and E.A.D. White, J. Mater. Sci., 1976, **2**, 2165.

165) M.S. Paley, Univ. Alabama, Huntsville, AL USA. 1990. Diss. Abstr. Int. B 1990, **51**, 2895. (Not available - abstract only)

166) M.S. Paley, J.M. Harris, H.Looser, J.C. Baumert, G.C. Bjorklund, D. Jundt and R.J. Twieg, J. Org. Chem., 1989, **54**, 3774.

167) L. Pasteur, Compt. Rend., 1860, **51**, 298.

168) I.R. Peterson, "Organic Materials for Non-linear Optics", R. Soc.Chem. Special Publication, **69**, Oxford, 1988.

169) J. Reif, P.Tepper, O. Semmler and E. Matthias, J. Phys. Colloq., 1987, C7-733/C7-735.

170) J.A. Riddick and W.B. Bunger, "Organic Solvents", 3rd ed., Wiley-Interscience, New York, 1970.

171) K.E. Rieckhoff and W.L. Peticolas, Science, 1965, **147**, 610.

172) C.D. Robeson, J.D. Cawley, L. Weisler, M.H. Stern, C.C. Eddinger and A.J. Chechak, J. Am. Chem. Soc., 1955, 77, 4111.

173) A.I. Rubailo, V.P. Selina and Yu.S. Varshavskii, Koord. Khim., 1984, **10**, 1231.

174) A.I. Rubailo, V.P. Selina and Yu.S. Varshavskii, Koord. Khim., 1988, **14**, 957.

175) T. Sakai, Y, Kawabe, H. Ikeda and K. Kawasaki, Appl. Phys. Lett., 1990, **56**, 411.

176) H. Schenk, Cryst. Struct. Commun., 1972, **1**, 143.

177) Y.Q. Shen, W. Gohring, S. Hagen, S. Roth and M. Hanack, J. Molecular Electronics, 1990, **6**, 31.

178) R.E. Sheppard, M.F. Hog, N. Hoblack and C.R. Johnson, Inorg. Chem., 1984, **23**, 3249, and references therein.

179) V.D. Shigonin and G.P. Shipulo, Sov. Phys. -Crystallogr. (Engl. Translation) 1975, **19**, 622.

180) M.I. Sil'vestrova, V.A. Vinogradov, V.V. Shigorin, T.N. Turskaya, G.S. Belikova and Y.V. Pisarevskii, Kristallografiya, 1990, **35**(4), 906. (Abstract only)

181) J. Simon, P. Bassoul and S. Norvez, New Journal of Chemistry, 1989, **13.1**, 113.

182) K.D. Singer and A.F. Garito, J. Chem. Phys., 1981, **75.7**, 3572.

183) S.A. Singham, Part II Thesis, University of Oxford, 1990.

184) A. Smit, Rec. trav. chim., 1961, **80**, 891.

185) V.I. Sokolov and O.A. Rentov, Russ. Chem. Rev., 1965, **34**, 1.

186) R.W. Soucoup and R.S. Schmid, J. Chem. Educ., 1985, **62**, 459.

187) P.D. Southgate and D.S. Hall, J. Appl. Phys., 1972, **43**, 2765.

188) T.A. Stephenson, S.M. Morehouse, A.R. Powell, J.P. Heffer and G. Wilkinson, J. Chem. Soc., 1965, 3632.

189) C. Sterling, Acta. Crystallogr., 1964, **17**, 1224.

190) T.L. Stolberg, D.Phil. Thesis, University of Oxford, 1991.

191) Y. Takeya, H. Matsuzawa and K. Iwata, Eur. Pat. Appl. EP 335, 641, (Cl. C07C121/70), 4 Oct 1989. (Abstract only)

192) Y. Takeya, H. Matsuzawa and K. Iwata, Eur. Pat. Appl. 8/130, 090, 30 May 1988. (Abstract only)

193) Y. Takeya, H. Matsuzawa and K. Iwata, Jpn. Kokai Tokkyo Koho JP 02 77025 (90 77025), 16 Mar 1990, Appl. 88/227,428, 13 Sept. 1988. (Abstract only).

194) Y. Takeya, H. Matsuzawa and K. Iwata, Jpn. Kokai Tokkyo Koho JP 02,134,622 [90,134,622] (CL. G02F1/35, 23 May 1990, Appl 88/286,902, 15 Nov 1988. (Abstract only)

195) Y. Takeya, H. Matsuzawa and K. Iwata, Jpn. Kokai Tokkyo Koho JP 02,134,623 [90,134,623] (CL. G02F1/35, 23 May 1990, Appl 88/286,903, 15 Nov 1988. (Abstract only)

196) Y. Takeya, H. Matsuzawa and K. Iwata, Jpn. Kokai Tokkyo Koho JP 02 78,466 [90,78,466] (CL.B05D1/20), 19 March 1990, Appl. 88/229,797, 16 Sept. 1988. (Abstract only)

197) W. Tam, Y. Yang, J.C. Calabrese; and R.A. Clement, "Nonlinear Optical Properties of Organic Materials", Proc. SPIE - Int. Soc. Opt. Eng., 1988, **971**, 107.

198) W. Tam and J.C. Calabrese, Chem. Phys. Lett., 1988, **144**, 79.

199) W. Tam, J.C. Calabrese, I.D. Williams, Y. Wang and A.G. Anderson, Chem. Mater, 1989, **1**, 128.

200) X. Tao, M. Jiang, D. Xu and Z. Shao, Kexue Tongbao (Foreign Lang. Ed.) 1988, **33**, 651. (Abstract only)

201) X. Tao, N. Zhang, D. Yuan, D. Xu, W. Xu and M. Jiang, Proc. SPIE - Int. Soc. Opt. Eng., 1990, **1337** (Nonlinear Opt. Prop. Org. Mater. 3), 385.

202) a) M.E. Thompson *et al*, b) T.B. Marder *et al*, c) C.S. Winter *et al*, d) H.B. Fyfe, e) C.L. Honeybourne, f) J. Delhalle, g) C.W. Spangler *et al*, h) G. Lesley, in "Organic Materials for Non-linear Optics", at the proceedings of or in R. Soc.Chem. Special Publication, **91**, Oxford, 1990, edited by R.A. Hann and D. Bloor.

203) R.J. Twieg, A. Azena and K.J.Y.Y. Cheng, Chem. Phy. Lett., 1982, **92**, 208.

204) R.J. Twieg and K. Jain, in A.C.S. Symp. Ser., 1982, **233**. Ed D.J. Williams.

205) Y.S. Varshavskii and T.G. Cherkasova, Russian Journal of Inorg. Chem., **12**, 1967, 899.

206) A.I. Vogel, "Practical Organic Chemistry", Longmans, Green and Co., London, 1948.

207) A.I. Vogel, W.T. Cresswell, G.H. Jeffery and J. Leicester, J. Chem. Soc., 1952, 514.

208) J.F. Ward and I.J. Bigio, Phys. Rev. Chem., 1967, 195.

209) T. Watanabe and Seizo Miyata, Proc. SPIE - Int. Soc.Opt. Eng., 1989 (Pub. 1990), **1147** (Non-linear Opt. Prop. Org. Mater. 2, 101.

210) T. Watanabe, K. Yoshinaga, D. Fichou and S. Miyata, J. Chem. Soc., Chem. Commun., 1988, 250.

211) D.J. Watkin, J.R. Carruthers and P.W. Retteridge, 1985 CRYSTALS User Manual, Chemical Crystallography Laboratory, University of Oxford.

212) I. Weissbuch, L. Addadi, M. Lehav and L. Leiserowitz, Science, 1991, **253**, 637.

213) A. Werner, Chem. Ber., **34**, 1901, 2584.

214) R.G. Wilkins *et al* in "Modern Coordination Chemistry," 1960, Interscience, NY, 174.

215) D.J. Williams (ed.), A.C.S. Symp. Ser., 1982, **233**,"Nonlinear Optical Properties of Organic and Polymeric Materials".

216) D.H. Williams and I. Fleming, "Spectroscopic Methods in organic Chemistry", 3rd ed., McGraw-Hill, U.K., 1980.

217) Georg Wittig and H. Hartmann, Chem. Ber., 1939, **72**(B), 1387.

218) D. Wright, Patent Application, Brit. 1214552, Appl. No. 47229/68, 4 Oct. 1968, 19 Sept 1969.

219) J.A. Wyllie, Personal communication from "Technology Catalysts", inc., European Office. Market Research Department, 1990.

220) D. Xu, M.H. Jiang, X.T. Tao, Z. Shao, J.T. Lin and B.H.T. Chai, Proc. SPIE-Int. Soc. Opt. Eng., 1989, **1104** (Growth charact., Appl. Laser Host Nonlinear Cryst.), 188.

221) D. Yuan, Nan Zhang, X. Tao, D. Xu and M. Jiang, Chin. Phys. Lett., 1990, **7**, 334. (Abstract only)

222) F. Zernike and J.E. Midwinter, "Application of Nonlinear Optics", Wiley, NY, 1973.

223) N. Zhang, M.H. Jiang, D.R. Yuan, D. Xu, X.T. Tao and Z.S. Shao, J. Crystal. Growth, 1990, **102**, 581.

224) N. Zhang, M. Jiang, D. Yuan, D. Xu and X. Tao, Chin. Phys. Lett., 1989, **6**, 829. (Abstract only)

225) N. Zhang, M.H. Jiang, D.R. Yuan, D. Xu, Z.S. Shao and X. Tao, Proc. SPIE - Int. Soc. Opt. Eng., 1990, **1337** (Nonlinear Opt. Prop. Org. Mater. 3), 390.

226) J. Zyss and J.L. Oudar, Phys. Rev., 1982, A26, 2028.

227) J. Zyss, D.S. Chemla and J.F. Nicoud, J. Chem. Phys., 1981, **74**, 4800.

228) J. Zyss and G. Berthiern, J. Chem. Phys., 1982, **77**, 3635.

229) J. Zyss and J.L. Oudar, Phys. Rev., 1982, A26, 2076.

APPENDIX ONE

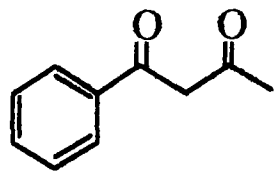
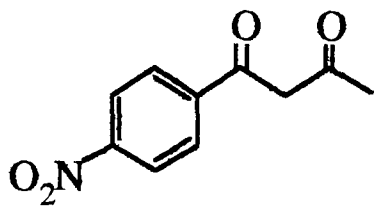
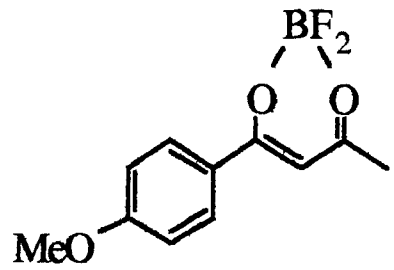
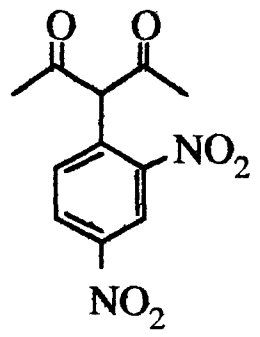
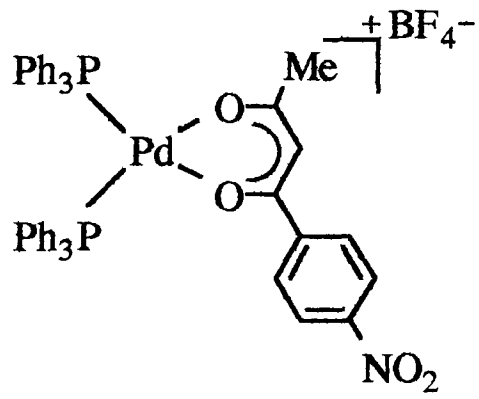
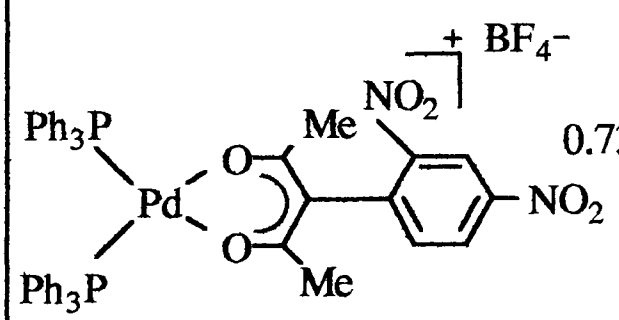
Second Harmonic Generation Data of Powdered Samples

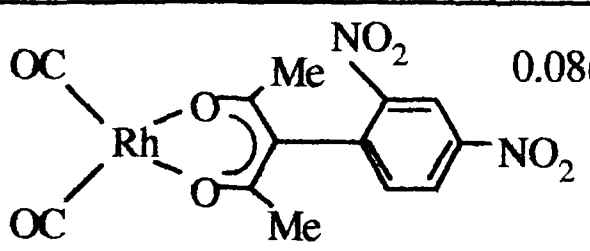
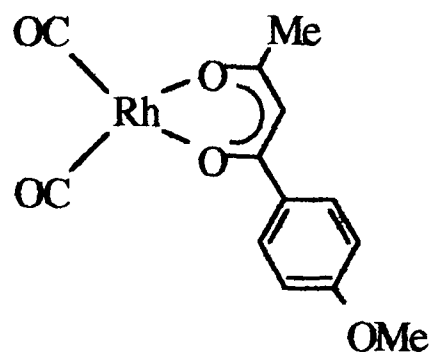
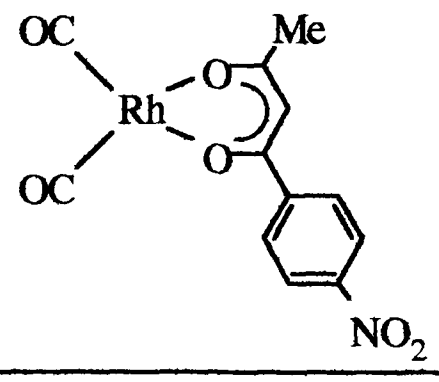
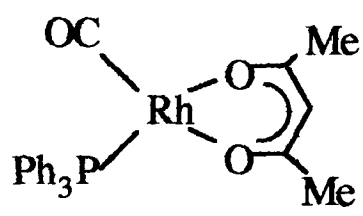
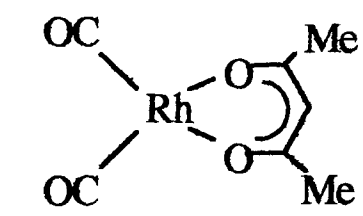
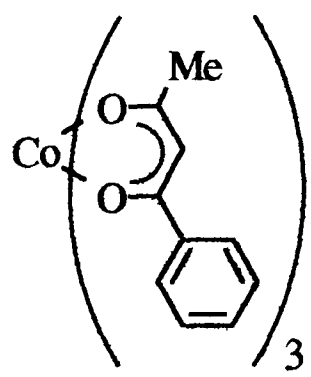
Introduction and Discussion

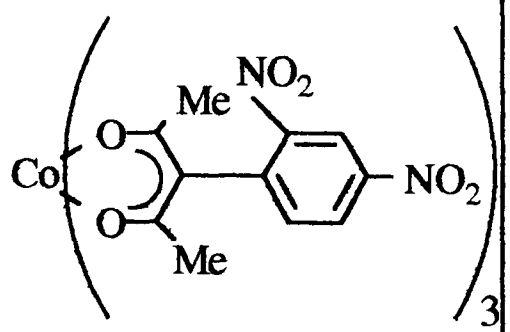
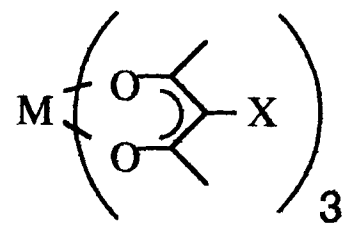
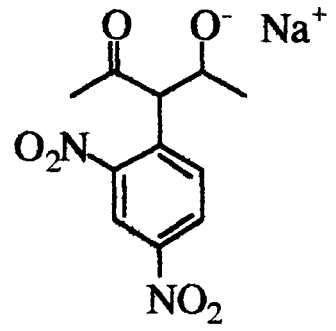
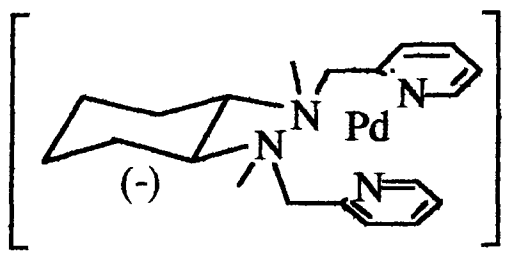
The SHG data presented in this Appendix are a selection of compounds tested by the experimental set-up described in Chapter 2. SHG data on [tris-[catecholato)tin(IV)], and carboranes have been presented in References 147 and 190.

Urea (100 micron mesh) has been used as a standard unless stated otherwise. The variation within the measurement of the urea standards gave rise to an error of ±6%. Placement errors have been measured and estimated to be ±1%, and errors due to optical density filter variation was ±5%. Most of the measurements are the averaged sum of 64 individual laser pulses, and all SHG responses have been observed to be within the time duration of the laser pulse, and therefore exclude other interefering second order processes, such as luminescence (lu).

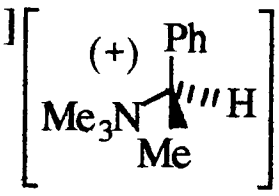
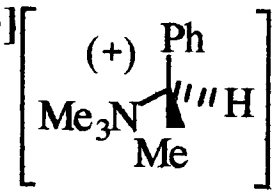
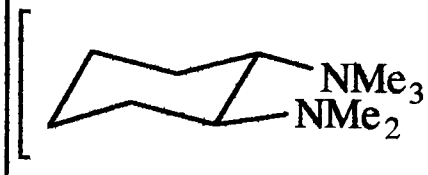
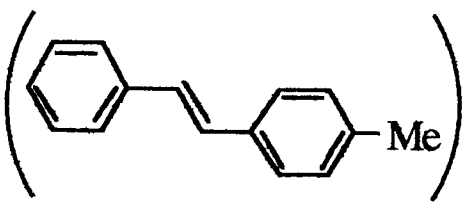
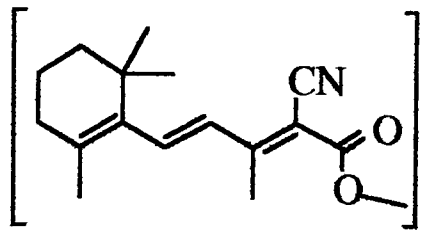
Abbreviations: (lu) = luminescence, u.g. = ungraded (but powdered), (bipy) = 2,2'-dipyridyl, v.s. = very strong.

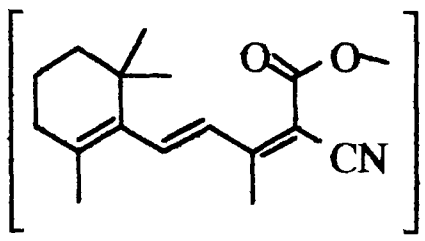
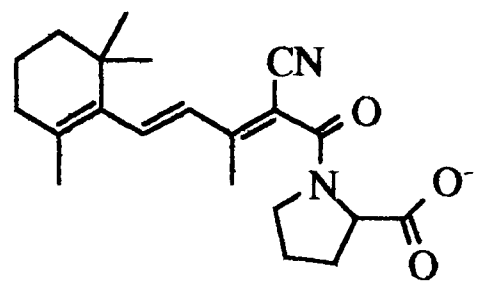
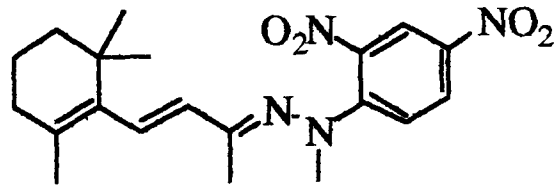
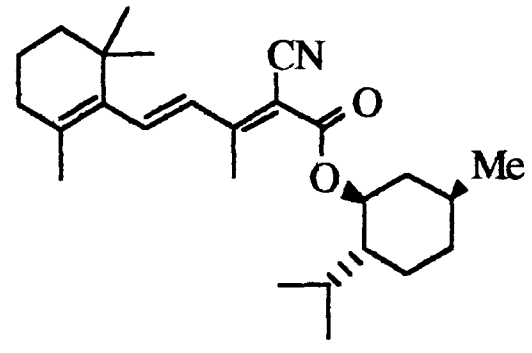
Compound	SHG x Urea	State	Colour	Origin, Number
	0	u.g.	Colourless	(III.1)
	0.56	u.g.	Yellow	(III.2)
	0.67	u.g.	Dark green	(III.7)
	0	u.g.	Pale yellow/ cream	(III.10)
	0.22	u.g.	Yellow	(III.13)
	0.73(1u)	u.g.	Yellow	(III.14)
[Pentane-2,4-dionato]-sodium	0	u.g.	White	Synthesized from NaOH and pentane-2,4-dione.
Bis[pentane-2,4-dionato]-copper(II)	0	u.g.	Blue	Synthesized from [pentane 2,4-dionato]sodium and copper(II) sulphate.

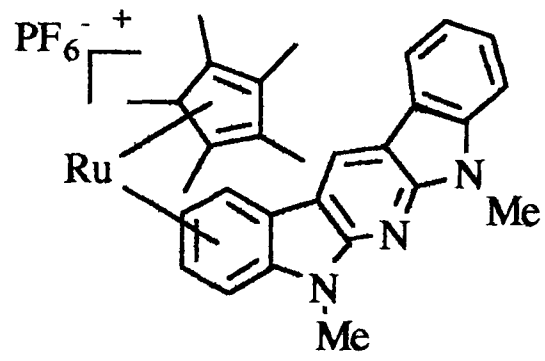
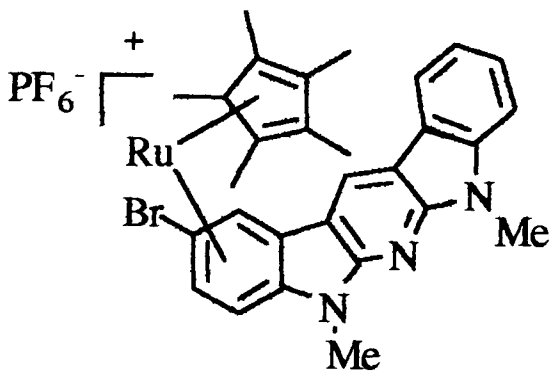
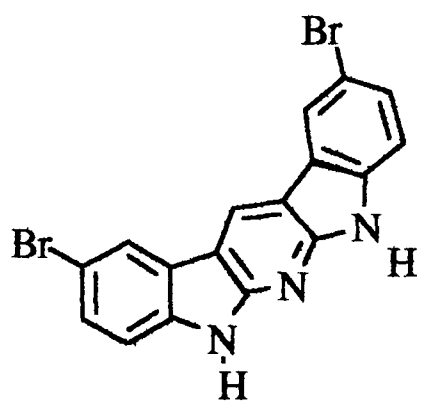
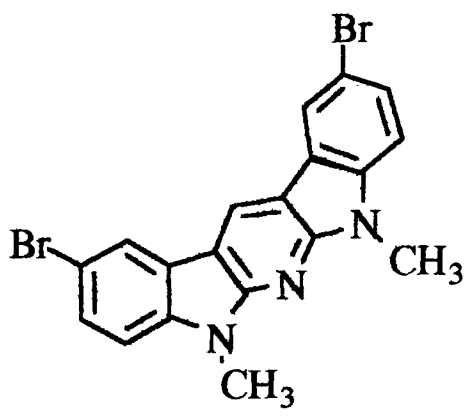
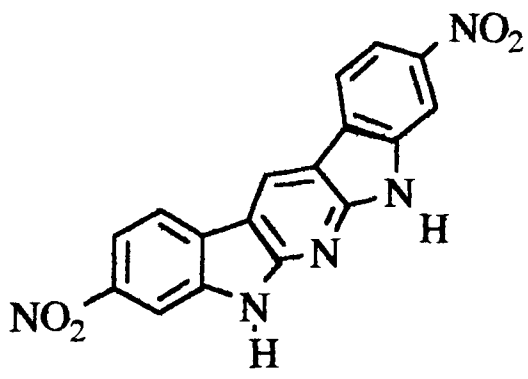
Compound	SHG x Urea	State	Colour	Origin, Number
	0.08(lu)	u.g.	Orange-brown	(III.15)
	0(lu)	u.g.	Orange	(III16)
	0(lu)	u.g.	Yellow	(III.17)
	0(lu)	u.g.	Yellow	(III.18)
	0	u.g.	Red-green	(III.19)
	0	u.g.	Green	(III.21)

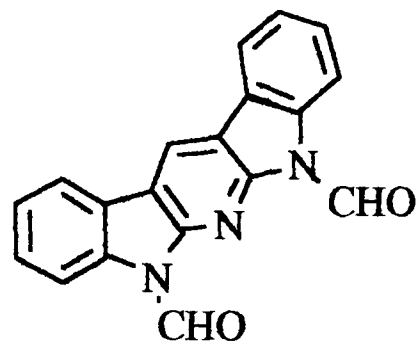
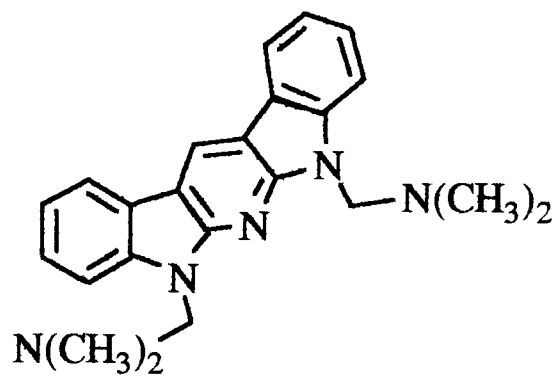
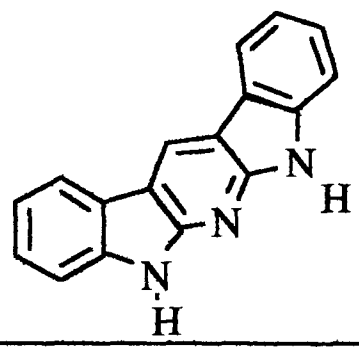
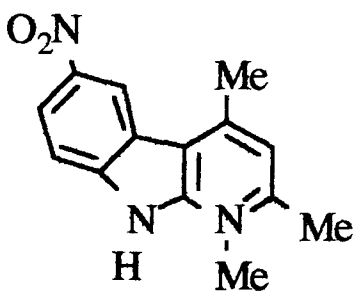
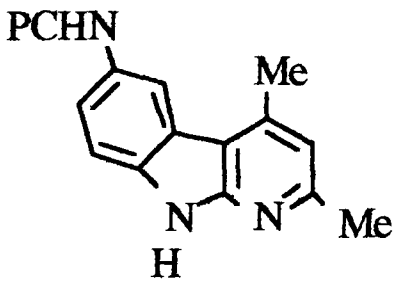
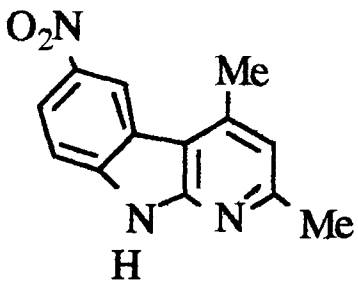
Compound	SHG x Urea	State	Colour	Origin, Number
	0	u.g.	Dark-green	(III.22)
 M= X=				
Co H	<<0.02	u.g.	Dark-green	(III.23)
Co Cl	>(3.23)		Green	(III.24)
Co NO_2	>(3.24)		Dark green	(III.25)
Co 2H, 1CHO	0		Light green	(III.26)
Rh H	0		Yellow	(III.27)
$[Co(en)_2(acac)_2]I_2$	0	u.g.	Red	Synthesized from $[Co(en)_2CO_3]Cl$
	0	u.g.	Red	Synthesized from (III.10) and NaOH.
L-Menthol	0.28	u.g.	Colourless	Lancaster Co.
L-Proline	0.5	u.g.	Colourless	Lancaster Co.
D-Sodium tartrate	0.17	u.g.	Colourless	Lancaster Co.
1,2-Dihydroxybenzene	0	u.g.	Colourless	Aldrich
 $[PF_6]_2$	0.09	u.g.	Cream/ white	W.M. LaidLaw, U. of Oxford

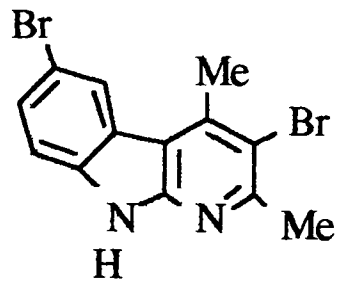
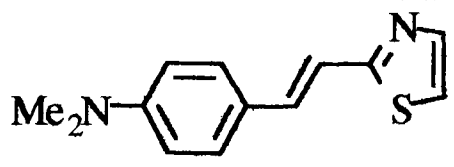
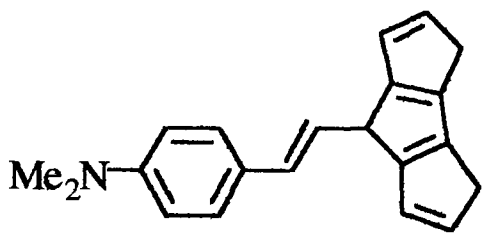
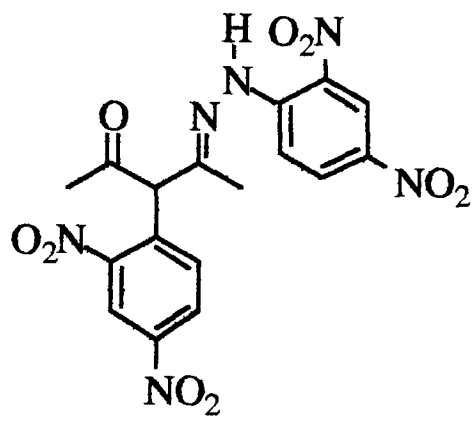
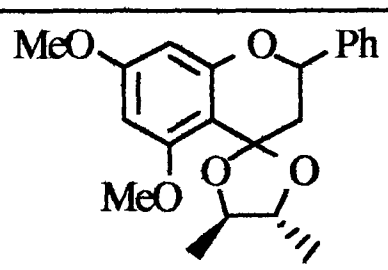
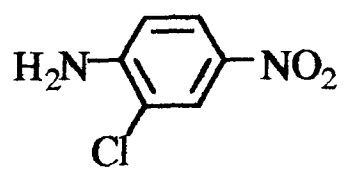
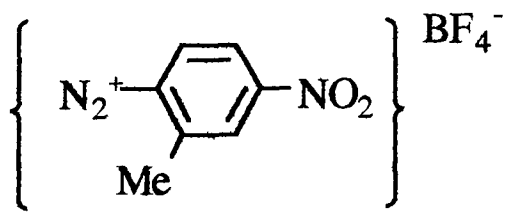
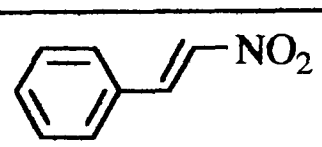
Compound	SHG x Urea	State	Colour	Origin, Number
$[Co(en)_2CO_3]Cl$	0	u.g.	Violet	Inorg. Syn.,14, 64.
$[Co(en)_2CO_3]I_2$	0	u.g.	Violet	Inorg. Syn.,14, 64.
$ReOCl_3(Et_2PhP)_2$	0	u.g.	Green	Synthesis, Ref. 39
$ReOCl_3(PPh_3)_2$	0	u.g.	Yellow	Synthesis, Ref. 39
$ReOCl_3(PPh_2Me)_2$	0(lu)	u.g.	Green	Synthesis, Ref. 39
$ReCl_3(PPh_3)_2(NPh)$	0(lu)	u.g.	Green	Synthesis, Ref. 39
Cis-$(PPh_3)Pd(Br)_2$	0	u.g.	Yellow	See Section 7.
$Zr(HPO_4)_2.H_2O$	0.06(lu)	u.g.	White	M.L.H. Green, U. of Oxford
Quartz	0.29	u.g.	White	Sand
KDP	0·34	100µ	White	Aldrich
ADP	0.37	100µ	White	Aldrich
cis-$Pt(PPh_3)_2Cl_2$	0.08	u.g.	White	See Section 7.
$Pt(PPh_3)_2CO_3$	v.s. lu	u.g.	White	See Section 7.
a-$VO(PO_4).2H_2O$	0.02	u.g.	White	M.L.H. Green, U. of Oxford
$Hg(PPh_3)_2(NO_3)_2$	0.11	u.g.	White	M.L.H. Green, U. of Oxford
$AsB_{10}H_{10}$	0.12	u.g.	White	T. Spalding, Cork U.
$[(NH_3)_5RuNCRu(CN)_3(bipy)][ptol].xH_2O$	0.077	u.g.	Green	W.M. Laidlaw.
$[Ru(bipy)_2(CNMe)_2]I_2$	0.082	u.g.	Yellow	"
$[Ru(bipy)_2(CNMe)_2][ptol]_2$	0	u.g.	Yellow	"
$[(NH_3)_5RuNCRu(CN)_3(bipy)][ptol].xH_2O$	0	u.g.	Green	"
$[Ru(bipy)_2(CNMe)_2][PF_6]_2$	0	u.g.	Yellow	"
$[(NH_3)_5RuNCRu(CN)(bipy)_2]PF_6]_3$	0	u.g.	Green	"
$[(NH_3)_5RuNCRu(CN)_5][Li].3H_2O$	2.16	u.g.	Blue	"
$[(NH_3)_5RuNCOs(CN)_5][Li].3H_2O$	1.3	u.g.	Blue	"
$[(NH_3)_5RuNCRu(CN)_3(bipy)]MeSO_3]$	0	u.g.	Green	"
$[(NH_3)_5RuNCRu(CN)_5]$ [(+) Ph, Me_3N, H, Me] $.xH_2O$ 0.031 x Urea			Blue	"
$[(NH_3)_5RuNCRu(CN)_3(bipy)][CF_3SO_3].3H_2O$	0.10		Green	"

Compound	SHG x Urea	Colour	Origin, Number
$[(NH_3)_5RuNCOs(CN)_5]$ 	0	Blue	W.M. Laidlaw, U. of Oxford.
$[Ru(CN)_4(bipy)]$  $.xH_2O$	0.43	Orange	"
 $[Ru(CN)_4(bipy)].xH_2O$	0	Red	"
$RuCl_2(CO)_2$ 	0.12 (lu)	--	A, Pulham, U. of Oxford.
L = 			
HL	0.12	Yellow	Synthesis, Section 7
AgL	0.006	Cream	(IV.5)
CsL	0(lu)	White	(IV.4)
NH_4L	--	Colourless	(IV.1)
Et_4NL	0	Colourless	(IV.3)
H_2NEt_2L	0.12	White	(IV.3)
BaL_2	0.19	White	(IV.6)
CoL_2	0(lu)	Red	--
NiL_2	0.18	Lt. Green	(IV.9)
CuL_2	0.063	Blue	(IV.8)
ZnL_2	0.048	White	(IV.7)
"PbL_2"	0	White	--

Compound	SHG x Urea	Colour	Origin, Number
"CeL_4"	0	Red/ Brown	--
L' = 			
NH_4L'	0.03(lu)	White	(IV.10)
$Pt(diphos)L_2$	--	White	(V.6)
$Pt(diphos)Cl_1L_1$	0.096	White	(V.7)
$Pt(PPh_3)_2L_2$	lu	Pale yellow	(V.8)
$Pt(PPh_3)_2Cl_1L_1$	0.032	White	(V.4)
$Pd(PPh_3)_2L_2$	0.02	Yellow	(V.5)
L''' = 			
HL'''	0.97	Colourless	(VI.11)
CsL'''	0(lu)	White	(VI.12)
BaL'''_2	0(lu)	White	(VI.13)
	0	Red	Synthesized fromβ-ionone and 2,4-dinitrofluoro-benzene.
	0	Red	Synthesized fromβ-ionylidenecyanoyl chloric and L-menthol.

Compound	SHG x Urea	Colour	Origin, Number
	0.84	--	Helen Phillips, and Dr J. Peach, Dyson Perrins Laboratory, Oxford.
	0(lu)	--	"
	0(lu)	--	"
	1.25	--	"
	0	--	"

Compound	SHG x Urea	Colour	Origin, Number
	0	--	Helen Phillips, and Dr J. Peach, Dyson Perrins Laboratory, Oxford.
	0	--	"
	0	--	"
	0.17	Yellow	"
	0.11	Cream	"
	0.14	Cream	"

Compound	SHG x Urea	Colour	Origin, Number
	0.13	White	Helen Phillips, and Dr J. Peach, Dyson Perrins Laboratory, Oxford.
	1.5	Yellow	"
	0(lu)	--	"
	0(lu)	Red	Synthesized from 3-(2,4-dinitrophenyl)-pentane-2,4,dione and 2,4-dinitrophenyl-hydrazine.
	0.04	White	Dr Prout, Univ. of Oxford.
	1.7	Yellow	Aldrich Ungraded sample
	0	Pale-Red	Synthesized from 4-nitro-6 methylaniline, and fluoroboric acid
	0(lu)	Yellow	Synthesized from benzaldehyde and nitro-methane.

APPENDIX TWO

FORTRAN program for the calculation of β.

```
      implicit double precision (a-h,o-z)
      character*1 ans
      write(*,10)
10     format(' enter delta E (oe) = ', $)
      read(*,*) oe
      write(*,20)
20     format(' enter molecular radius, a = ', $)
      read(*,*) a
      write(*,30)
30     format(' enter static dipole ug = ', $)
      read(*,*) ug
      write(*,40)
40     format(' A1, A2, B1, B2 = ', $)
      read(*,*) aa1, aa2, bb1, bb2
      write(*,50)
50     format(' enter energy of transition w = ', $)
      read(*,*) w
51     write(*,52)
52     format(' do you want to calculate f? ', $)
      read(*,53) ans
53     format(a1)
       if(ans.eq.'y'.or.ans.eq.'Y') goto 58
       if(ans.eq.'n'.or.ans.eq.'N') goto 54
      goto 51
54     write(*,56)
56     format(' enter value for f = ', $)
      read(*,*) f
      goto 82
58     write(*,60)
60     format(' enter refractive index of solution (n0) = ', $)
      read(*,*) sn0
      write(*,70)
70     format(' enter frequency of transition v = ', $)
      read(*,*) v
      write(*,80)
80     format(' enter curve area dv = ', $)
      read(*,*) dv
```

```
      call ff(v,sn0,dv,f)
82      call deltau(a,oe,ug,aa1,aa2,bb1,bb2,ou1,ou2)
      du=ou1
      call beta(f,du,w,s)
      write(*,90) s
90     format(2x,'The beta calculated from delta u1 is: ', D10.2)
      du=ou2
      call beta(f,du,w,s)
      write(*,100) s
100    format(2x,'The beta calculated from delta u2 is: ', D10.2)
      read(*,*)
      stop
      end

      subroutine beta(f,du,w,s)
     implicit double precision (a-h,o-z)
      h=1.054e-34
      e=1.602e-19
      p=1.55e22
      hw=1.868e-19
      s1=p*3*e*h*h/2
      s2=f*du
      s3=(w*w-4*hw*hw)*(w*w-hw*hw)
      s3=w/s3
      s=s1*s3*s2
     return
     end

      subroutine ff(v,sn0,dv,f)
     implicit double precision (a-h,o-z)
      c=3.0e8
      sm=9.1e-31
      pi=3.1415926d0
      e=1.602e-19
      sn=6.022e23
     f1=e*pi*e*sn
     f1=9.d0*c*sm/f1
      f=(sn0*sn0+2)*(sn0*sn0+2)
     f=sn0*f1/f
     ccc=2.0e-20
     ccc=ccc*1.0e-23
     f=ccc*f*v*v*dv
     write(*,10) f
```

```
10      format(2x,'f=',f5.2)
      return
      end

       subroutine deltau(a,oe,ug,aa1,aa2,bb1,bb2,ou1,ou2)
      implicit double precision (a-h,o-z)
       con=4.0*3.1415926*8.85e-12*a*a*a
       C1=-oe*con
       B1=2.*ug*(aa1-aa2+bb1-bb2)
       A1=bb1-bb2
       bbb=b1*b1-4*a1*c1
       bbb=sqrt(bbb)
       ou1=(-b1+bbb)/2.0/a1
       ou2=(-b1-bbb)/2.0/a1
       write(*,10) ou1,ou2
10      format(2x,'delta u1=',D10.2, 2x, 'delta u2=',D10.2)
      return
      end
```

ABSTRACT

Submitted for the Degree of Doctor of Philosophy, Trinity Term 1992
Curt Lamberth, New College, Oxford.

Design of Non-linear Optical Materials Based on Inorganic Compounds

The non-linear optical phenomenon Second Harmonic Generation (SHG) has been a major research area for the past thirty years. This Thesis is concerned with the prediction, synthesis, characterization and testing of inorganic materials which exhibit SHG properties.

Chapter One describes the fundamentals of non-linear optics, and poses the problems, and some of their solutions, confronting the synthetic chemist in the search for new non-linear optical materials. Theoretical predictions of the second order hyperpolarizability constant β using CNDOVSB calculations are discussed. For a material to show SHG, it must possess some degree of non-centrosymmetry (as a surface/layer, crystallize in a non-centrosymmetric space group, be poled by an electric field, or held in an asymmetric host matrix). Furthermore, to have significant NLO effects the compounds must have suitable donor - acceptor functional groups joined by a conjugated molecular system, which must have easily accessible low-lying charge-transfer bands, as well as other less important requirements.

Chapter Two describes the design, implementation and calibration of apparatus for measurements of the SHG efficiency of solids based on the Kurtz powder technique, and a solvatochromic method of estimating approximately the magnitude of the second-order hyperpolarizability constant β.

Novel compounds with potential chirality due to atropisomerism (chirality due to restricted rotation of a group), asymmetric octahedral structures, and asymmetric tetrahedral symmetry of metal centers are discussed in Chapters Three, Four and Five.

Chapter Three surveys the use of organometallic and organo- coordination compounds for SHG. The use of pentane-2,4-dionato- ligands and their coordination compounds has been introduced as possible NLO active materials. Potential

pentanedionato- ligands were investigated by CNDOVSB calculations, and were shown to have a predicted $\beta_{(x)}$ value in the order of 14-53 m^4V^{-1}, equivalent to that of 4-nitroaniline. Three substituted pentane-2,4-dionato ligands were synthesized, and their non-linear optical properties investigated. The solvatochromism measurements of $\beta_{(x)}$ agreed to within experimental error, with the CNDOVSB results. The SHG efficiency was greatest in difluoro(4-methoxybenzoylacetonato)boron at 0.67 times urea. The NLO properties of complexes synthesized from rhodium(I), cobalt(III) and palladium(II) and substituted pentanedionato- ligands have been described. The single crystal X-ray structure of bis(triphenylphosphine)(4-nitrobenzoylacetonato)palladium(II) tetrafluoroborate and tris(triphenylphosphine)[3-(2,4-dinitrophenyl)-pentane-2,4-dionato]palladium(II) tetrafluoroborate were determined. Both compounds crystallize in the centric triclinic space group $P\bar{1}$ and give residual SHG responses of 0.22 and 0.73 times urea respectively. Analogous rhodium(I) complexes did not give significant SHG efficiencies. The SHG properties of these complexes do not mirror the expected efficiencies predicted for the ligands alone and this has been shown to be due to the centric nature of the crystal structure in which they crystallize. Tris cobalt(III) complexes of substituted pentanedionato- ligands were screened for their NLO properties and were found to have zero SHG efficiencies. The solvatochromic behaviour of some of the pentanedionato- complexes were studied. Significant shifts in the λ_{max} of the lowest lying, most significant, charge transfer band were observed with solvents of differing polarities.

Chapter Four describes the search for a possible NLO active ligand, its synthesis, characterization, derivatization and SHG testing. The compound trans-β-ionylidenecyanoacetic acid, 2-cyano-3-methyl-5-(2,6,6-trimethyl-1-cyclohexen-1-yl)-2,4-pentadienoic acid, was chosen as a suitable ligand with the required electronic conjugation. The second order hyperpolarizability constant, β, was calculated using the CNDOVSB method for trans-β-ionylidenecyanoacetic acid, and related compounds. The second order hyperpolarizability constant, β, for trans-β-ionylidenecyanoacetic acid was calculated by CNDOVSB to be 50 x 10^{-40} m^4V^{-1}, and from solvatochromism data to be 170 x 10^{-40}

m^4V^{-1}. Synthetic methods of imposing non-centrosymmetry on *trans*-β-ionylidenecyanoacetic acid using metals are discussed. Several metal and non-metal salts of trans-β-ionylidenecyanoacetic acid and cis-β-ionylidenecyanoacetic acid were synthesized, characterized and tested for their SHG properties. The Zn(II) and Cu(II) salts of trans-β-ionylidenecyanoacetic acid were tested for SHG, and gave efficiencies of 0.048 and 0.063 x urea. The maximum SHG efficiency was found to be given by the Ba(II) salt with an efficiency of 0.19 x urea. In the search for non-linear compounds which show second harmonic generation, the use of metal ions to direct the symmetry of prospective organic carboxylates has been shown to be of limited success. The metal salts of larger organic ligands required for NLO have been assumed to crystallize in the same way as their lower homologues. This assumption, in the case of the salts of trans-β-ionylidenecyanoacetic acid, has been shown to be incorrect. Furthermore, the physical properties of the pure salts prevented the growth of crystals of optical quality and are therefore not suited to SHG generation. The high solubility of the β-ionylidenecyanoacetic acid salts in organic solvents makes them suitable for inclusion into potential NLO organic polymers.

Chapter Five describes the platinum(II) and palladium(II) complexes of β-ionylidenecyanoacetic acid, some of which were successfully synthesized and in most cases characterized by spectroscopic and elemental analyses. The chemistry and physical properties of these complexes were found to be unusual. There was an increase in solubility of these complexes due to the size and nature of the β-ionylidenecyanoacetate ligand. The SHG properties of these complexes showed no evidence of the non-centrosymmetric crystal structures found in related complexes.

Chapter Six describes the use of conventional asymmetric carbon centers to introduce chirality into centrosymmetric compounds. The NLO inactive compound, β-ionylidenecyanoacetic acid has been successfully modified by attaching the chiral amino-acid L-proline onto the molecule to form the N-bonded derivative, N-[2-cyano-3-methyl-5-(2,6,6-trimethyl-1-cyclohexene-1-yl)-2,4-pentadiene-1-one]-L-proline (i). This compound

showed a SHG efficiency of 0.39-0.97 times urea which was greater than that of pure L-proline. The Li and Ba derivatives of (i) both show zero SHG efficiencies indicating that; hydrogen bonding has a significant effect on the magnitude of SHG; unidentate salts of chiral molecules do not always show SHG, possibly because dipole-dipole interactions take over as the predominant factor in the influence of crystal packing. This leads to an electric dipolar response with a centre of inversion, and therefore vanishing second order susceptibility, and zero SHG; bidentate salts of chiral molecules may also show zero SHG because of the equal, but opposing responses of the two chiral ligands present within the molecular unit. Chapter Six has demonstrated that chiral amino-acids are an effective method of introducing the non-centrosymmetric requirement for SHG into a molecule.